TRANSPORTATION RESEARCH
CIRCULAR
Number E-C273 July 2021

TRB Centennial Circular

History and Future Perspectives on Foundation Design for Transportation Structures

The National Academies of
SCIENCES • ENGINEERING • MEDICINE
TRB
TRANSPORTATION RESEARCH BOARD

TRANSPORTATION RESEARCH BOARD
2020 EXECUTIVE COMMITTEE OFFICERS

Chair: Carlos M. Braceras, Executive Director, Utah Department of Transportation, Salt Lake City
Vice Chair: Susan A. Shaheen, Adjunct Professor, Co-Director, Transportation Sustainability Research Center, University of California, Berkeley
Division Chair for NRC Oversight: Chris Hendrickson, Hamerschlag University Professor Emeritus, Carnegie Mellon University, Pittsburgh, Pennsylvania
Executive Director: Neil J. Pedersen, Transportation Research Board

TRANSPORTATION RESEARCH BOARD
2020–2021 TECHNICAL ACTIVITIES COUNCIL

Chair: Hyun-A C. Park, President, Spy Pond Partners, LLC, Arlington, Massachusetts
Technical Activities Director: Ann M. Brach, Transportation Research Board
Richard Bornhorst, Principal, FACTOR, Inc., Silver Spring, Maryland, *Freight Systems Group Chair*
Michael Griffith, Director, Office of Safety Technologies, Federal Highway Administration, Washington, D.C., *Safety and Operations Group Chair*
George Avery Grimes, CEO Advisor, Patriot Rail Company, Denver, Colorado, *Rail Group Chair*
Brendon Hemily, Principal, Hemily and Associates, Toronto, Ontario, *Public Transportation Group Chair*
Nikola Ivanov, Deputy Director, Center for Advanced Transportation Technology Laboratory, University of Maryland, College Park, *Young Members Council Chair*
Pamela Keidel-Adams, Regional Vice President, Kimley-Horn and Associates, Inc., Mesa, Arizona, *Aviation Group Chair*
C. James Kruse, Director, Center for Ports and Waterways, Houston, Texas, *Marine Group Chair*
Jane Lin, Professor, University of Illinois, Chicago, *Sustainability and Resilience Group Chair*
Mark Reno, Principal Engineer, Quincy Engineering, Inc., Rancho Cordova, California, *Highway Infrastructure Group Chair*
Elizabeth Rushley, Lawhon & Associates, Inc., Columbus, Ohio, *Data, Planning, and Analysis Group Chair*
Fred R. Wagner, Partner, Venable, LLP, Washington, D.C., *Legal Resources Group Chair*
Kathryn Zimmerman, Applied Pavement Technology, Inc., Urbana, Illinois, *Policy and Organization Group Chair*

TRANSPORTATION RESEARCH CIRCULAR E-C273

TRB Centennial Circular

History and Future Perspectives on Foundation Design for Transportation Structures

Submitted
December 2020

Transportation Research Board
500 Fifth Street, NW
Washington, D.C.
www.trb.org

TRANSPORTATION RESEARCH CIRCULAR E-C273
ISSN 0097-8515

The **Transportation Research Board** is one of seven major programs of the National Academies of Sciences, Engineering, and Medicine. The mission of the Transportation Research Board is to provide leadership in transportation improvements and innovation through trusted, timely, impartial, and evidence-based information exchange, research, and advice regarding all modes of transportation

The **Transportation Research Board** is distributing this E-Circular to make the information contained herein available for use by individual practitioners in state and local transportation agencies, researchers in academic institutions, and other members of the transportation research community. The information in this E-Circular was taken directly from the submission of the authors. This document is not a report of the National Academies of Sciences, Engineering, and Medicine.

Standing Committee on Foundations of Bridges and Other Structures (AKG70)

Sharid Amiri, Chair
Mohammed Mulla, Vice Chair

Naser Abu-Hejleh
Victor Aguilar-Vidal
Tony Allen
Ben Arndt
Prasenjit Basu
Tejo Bheemasetti
Jan Cermak
Shaoyang Dong
Christopher Dumas
Ken Fishman
Gavin Gautreau
Fei Han
Md. Nafiul Haque
Chad William Harden
Rodrigo Herrera
Bernard Hertlein
Mary Ellen Large
J. Erik Loehr
Nick Machairas
Antonio Marinucci
Masoud Nobahar
Kathryn Petek
Monica Prezzi
Sastry Putcha
Matthew Riegel
Heather Shoup
Timothy Siegel
Hisham Sunna
Gerald Verbeek
Negin Yousefpour
Aaron Zdinak

TRB Staff
Nancy Whiting, *Senior Program Officer*

Transportation Research Board
500 Fifth Street, NW
Washington, D.C.
www.trb.org

Preface

CHAD W. HARDEN
Michael Baker International

Thank you for reading this engineering E-Circular celebrating the Transportation Research Board (TRB) Centennial Anniversary in the year 2020, and its support and influence on the history and standard of practice for foundation design of transportation structures. Much like the many branches of civil engineering, within the topic of foundations of bridges and other structures there are many branches and areas of specialization. Bridge foundations vary from spread foundations to piles, and multiple varieties within pile types such as precast concrete or steel piles, cast-in-place piles, or varieties such as cast and steel shell. However, including foundation type there are hundreds if not thousands of variables to consider in foundation design, which require coordination between civil, structural, and geotechnical engineers as well as state departments of transportation (DOTs), environmental planners, and other stakeholders, and require knowledge of the many design codes and constantly emerging research and design guidance.

To highlight this depth of complexity, consider the first step in selecting a foundation for a bridge as part of a typical project. In the very initial steps of planning, even ahead of engineering, one must understand or estimate the soil type and if this is cohesive or cohesionless or cohesive, the associate pile types that might be suitable for the soil type such as driven piles or drilled methods, and site features or environmental factors such as noise which would preclude specific pile types. Even project delivery method becomes a consideration; in the case of a design–build project the contractor may have a preference for a pile type. Additional considerations include the method and type of soil exploration, drilling method such as standard penetration tests (SPTs) and cone penetrometer tests (CPTs), analysis, and site characterization, and in the case of existing bridges inspection, condition, and load rating are important. Once a foundation type is selected, specific design issues require study including settlement, construction recommendations, pile set-up, pile re-use, soil and pile capacity, and seismic and geo-seismic topics such liquefaction and lateral spreading. Finally, emerging topics such as unmanned aerial vehicles (UAV) and machine learning (ML) continue to shape our industry. To understanding or navigate all these variables and considerations takes years of practice.

This TRB Centennial Circular bring special focus to these constantly evolving variables, research, and engineering considerations, and pay tribute to our industry, leadership, and contributions of TRB as we have grown to understand these issues. Following the 98th Annual Meeting of the Transportation Research Board in January 2019, the idea of a centennial circular was advertised to many committees, members, and friends to participate in the TRB Centennial Celebration, to celebrate our research and project accomplishments with a focus on foundations, and to provide a perspective on the past and future of the field. The writing and review of the Centennial Circular papers included here, have all been accomplished by industry volunteers contributing their time.

It would not be possible to celebrate this milestone without acknowledging in this same year the entire human race has struggled with the worldwide COVID-19 pandemic and related challenges across all dimensions of society. However, through these struggles and challenges, we have also excelled by working together.

In what could never have been imagined, we were horrified by the worldwide COVID-19 pandemic that began to spread rapidly from January to March of 2020. As human life was threatened, all of society voluntarily self-isolated to protect those in at-risk categories, while in parallel we struggled to balance these decisions with other threats to economy, real impacts to mental health and isolation, and quickly trying to understand the science and realities behind the virus. However, at the writing of this introduction, we can observe huge successes in limiting the spread of the virus and communities just beginning a return to normalcy.

Our hearts, hope, and imagination were lifted on May 30, 2020; the United States and the entire world watched the skies and our screens as NASA astronauts piloted the SpaceX Dragon spacecraft successfully into space and on to board the International Space Station (*1*). The DEMO-2 mission marked both the first collaboration with NASA and a commercial partner, the return to space exploration by the United States in over 10 years since the end of the former space shuttle program, and the first steps of the U.S. Artemis program which sets its sights to return American astronauts to the moon by 2024 and establish a lunar presence (*2*), as well as to expand to exploration from "Moon to Mars" with commercial and international partners (*3*).

These events have enormous impact on the human condition, affecting our thoughts, ideas, and quality of life. Along the dimension of quality of life, transportation is a driver in how the events unfold and how we access mobility. Transportation in turn is also changed forever by the events: While use of transportation infrastructure has dwindled during the pandemic, construction workers related to transportation and energy projects, among other worker classifications, were allowed to continue for critical or essential business sectors (*4*, *5*). The successful SpaceX DEMO-2 mission makes space commerce and the idea of space travel as a mode of transportation mobility that much more palpable.

While 2020 permanently shaped our present and future trajectories, as we look to the future we can recognize other events and technologies prior to this year that have and continue to affect transportation use, planning, maintenance and construction. For example, automated vehicles may increase roadway capacity by more than 50%; it is anticipated lanes may reduce and roadway capacity will increase, resulting in a higher demand on existing highway (and bridge) infrastructure, and reduced spending on new highway (and bridge) construction (*6*). Compounding an increase demand on transportation infrastructure, a change in bridge use with "platooning" of truck loads is clear (*7*, *8*). Will existing bridges and foundation support this increased vehicle loading? In the realm of bridge use and maintenance, state transportation departments will need to prepare for a shift in spending from new bridge or widening construction to higher spending on maintenance and inspection, load rating, repair, retrofit, or replacement to extend the life of existing infrastructure.

As an indicator of our rich history, turbulent present, and ever-changing future, the articles included in this Centennial Circular cover a wide spread of topics related to foundation design for transportation structures. Topics from the evolution of our design codes from allowable stress to load and resistance factor design, to next generation tools for seismicity and performance-based design of structures, to machine learning and artificial intelligence. These wide range of topics is an indication of our rich diversity of experience and passions, and the possible depths of just one facet of transportation engineering.

In coordinating this circular, it has been tremendously rewarding to bring authors documenting the forefront of science together with authors of incredible engineering experience, in a medium to connect our history with new branches of engineering. To the future engineers of

America and worldwide, I say embrace a career that is rewarding, satisfying, and which can affect change on the human condition. A career in transportation will empower this opportunity.

This E-Circular would not have been possible without the helpful contribution and time volunteered by the article reviewers. Thank you for supporting this E-Circular.

REFERENCES

1. National Aeronautics and Space Administration. *Launch America*. 2020. Available at https://www.nasa.gov/specials/dm2/.
2. National Aeronautics and Space Administration. *New Space Policy Directive Calls for Human Expansion Across Solar System*. 2017. Available at https://www.nasa.gov/press-release/new-space-policy-directive-calls-for-human-expansion-across-solar-system.
3. National Aeronautics and Space Administration. *What is Artemis?* 2019. Available at https://www.nasa.gov/what-is-artemis.
4. Lazo, L., and K. Shaver. "Work on region's big projects continues amid coronavirus, with construction an 'essential' business." *The Washington Post*, March 28, 2020. Available at https://www.washingtonpost.com/local/trafficandcommuting/work-on-regions-big-projects-continues-amid-coronavirus-with-construction-an-essential-business/2020/03/28/e4af8b38-6dfd-11ea-a3ec-70d7479d83f0_story.html.
5. Official California State Government Website. "Essential Workforce." 2020. Available at https://covid19.ca.gov/img/EssentialCriticalInfrastructureWorkers.pdf.
6. Bowman, J. "How Autonomous Vehicles Will Change the Future of Road Design and Construction." *FMI Quarterly*, September 2016. Available at https://www.fminet.com/fmi-quarterly/article/2016/09/how-autonomous-vehicles-will-change-the-future-of-road-design-and-construction/.
7. Grant, L. "Can Bridges Handle Weight of Platooning Trucks? Engineering Firm Wants to Know." Transport Topics, Arlington, Va., 2018. Available at https://www.ttnews.com/articles/can-bridges-handle-weight-platooning-trucks-engineering-firm-wants-know.
8. Dunne, R. "Truck Size and Weight: What You Need to Know." Presented at 97th Annual Meeting of Transportation Research Board, Washington, D.C., 2018. Available at https://annualmeeting.mytrb.org/Workshop/Details/7682.

PUBLISHER'S NOTE

The views expressed in this publication are those of the authors and do not necessarily reflect the views of the Transportation Research Board of the National Academies of Sciences, Engineering, and Medicine. This publication has not been subjected to the formal TRB peer-review process.

Contents

History of Transition from Allowable Stress Design to Load and Resistance Factor Design and Beyond

VICTOR AGUILAR
Universidad San Sebastián, Chile

ANDRZEJ J. NOWAK
J. BRIAN ANDERSON
Auburn University, Alabama

The Standing Committee on Foundations for Bridges and Other Structures has supported the implementation of the load and resistance factors (LRFD) design philosophy into practice. The committee has contributed by hosting discussions of the advantages, issues, and impact of the implementation of American Association of State Highway and Transportation Officials (AASHTO) Load and Resistance Factor Design (LRFD) into foundation design and other related fields. The background and a historical overview of the development of LRFD in bridge foundations design are presented in this paper. Several National Cooperative Highway Research Program (NCHRP) projects have been of paramount importance on this matter. Milestone research projects are described, and a perspective on the future of the field is drawn. This document is intended to be a roadmap through the most useful material to understand reliability analysis and its application to geotechnical engineering. It is intended to be of interest to those engineers charged with performing reliability-based calibration in need of a starting point. The primary literature and steps followed to develop the current AASHTO LRFD specifications are highlighted. This paper aims to contribute to the understanding and future improvement of the LRFD specifications.

INTRODUCTION

The development of LRFD methodology and the transition from allowable stress design (ASD) to LRFD is an excellent example of the Transportation Research Board (TRB) providing leadership in innovation and progress through research. Research needs within Standing Committee on Foundations for Bridges and Other Structures and other standing committees have led to several NCHRP projects that had an enormous impact on bridge and foundation design practices. The objective of this paper is to serve as a roadmap through the most useful material to understand reliability analysis and its application in geotechnical engineering. A historical perspective is presented, milestone research projects are described, and the background knowledge of reliability analysis is briefly explained. In addition, the primary literature and steps followed to develop the current AASHTO LRFD are highlighted. The implementation of LRFD philosophy in bridge foundations design is described. The advantages, public agencies' involvement, issues, criticism, and future perspectives are also discussed.

Traditionally, the uncertainties in the calculations of loads and resistances were accounted for through a single global factor of safety. This approach is known as ASD and it was followed by AASHTO from 1931 to 1994. This methodology is commonly used in steel building design, wood structures design, and building-related geotechnical designs, among other areas. Later, in the 1960s, a partial factor of safety (individual factors for each load component and type

of resistance) methodology was developed for the concrete industry and eventually was adopted by AASHTO. This design approach includes load factors that amplify each load component (dead, live, wind, snow, earthquake, and so on), accounting for uncertainties associated with them, and the resistance factor that accounts for uncertainties associated with the load-carrying capacity. This methodology is called LRFD. The latest editions of principal design and construction codes follow the LRFD philosophy, for example, steel structures (AISC, 2016), concrete buildings (ACI 318, 2019), masonry buildings (TMS 402, 2013), wood construction (NDS, 2018), loads for buildings [American Society of Civil Engineers (ASCE), 2016], and highway bridges (AASHTO LRFD, 2020).

The transition from ASD to LRFD philosophies, in bridges and foundations, is presented in this paper. Over the past few decades, the Standing Committee on Foundations for Bridges and Other Structures has supported the implementation of the LRFD philosophy into practice by hosting conferences and developing workshops to discuss and work through this topic. The committee has contributed to the implementation of LRFD in foundation design by providing instances for open discussion of the advantages, issues, and impact of the implementation of LRFD. The NCHRP funded several projects to address the LRFD approach with shallow foundations, drilled shafts, driven piles, earth retaining structures, buried structures, soil nailing, geosynthetics, and more.

SAFETY MANAGEMENT BACKGROUND

There are many sources of uncertainty inherent to bridge and foundation design, for example, concrete compressive strength, yield strength, unit weight; soil friction angle and undrained shear strength; and lateral pile capacity will never have exactly the same measured value under the same test conditions. Thus, parameters in design are random variables. The concept of a random variable is closely related to the experimental process. If an experiment is performed repeatedly (with all conditions maintained as precisely as possible) and the measured results are identical, then the variables which are measured are said to be deterministic. However, if the numerical results vary, the item is random (Hart, 1982). Since random variables are inevitable in foundation designs, absolute safety (or zero probability of failure) cannot be achieved. Consequently, structures and foundations must be designed to serve their functions with a finite probability of failure (Nowak and Collins, 2013).

How the engineer treats the uncertainty in a given phenomenon depends upon the situation. If the degree of variability is small, and the consequences of any variability will not be significant, the uncertainty can be ignored by merely assuming that the variable will be equal to the best available estimate. This is typically done with the elastic constant of materials and the physical dimensions of manufactured structural components. If the uncertainty is significant, a conservative estimate of the variable is warranted. This has been done in setting specified minimum strength properties of materials and members. Therefore, some questions arise: how can engineers maintain consistency in their conservatism from one situation to another? For instance, separate professional committees set the specified minimum concrete compressive strength and the specified minimum bending strength of wood (Benjamin and Cornell, 1970). How can engineers maintain consistency in their conservatism within the same construction project? For ex-

ample in a bridge, the specified minimum flexural and shear strength of girders, bent caps, abutments, shallow foundations, and pile foundations should be consistent. Several procedures have been used to achieve a consistent conservatism level and they are described below.

Procedures for Setting Safety Margins

Allowable Stress Design or Working Stresses Design Method

This approach has been used by civil engineers since the early 1800s. It is still common in practice, and it is frequently used as an educational tool when engineering students learn concepts of mechanics of materials and a design problem is presented. Under ASD, the design load effect (Q), which consist of the estimated demand on the component, is compared to the allowable load demand ($Q_{allowable}$), which is the resistance, or strength (R) reduced by a factor of safety (FS).

$$Q \le Q_{allowable} = \frac{R}{FS} \tag{1}$$

At the limit, the FS can be written as follows.

$$FS = \frac{R}{Q} \tag{2}$$

When more than one source of load is acting, the load effect Q is calculated as the direct sum of the best estimation of the separate effects.

Through experience, conventions have developed with regard to what values of a FS are suitable for various situations. Equation 2 tends to give a false impression of certainty. Resistance and loads are random variables. A possible clarification is to name this ratio as the nominal factor of safety (FS_n), which should be the nominal resistance (R_n) over the nominal load effect (Q_n). The term nominal is used for the value used in design.

$$FS_n = \frac{R_n}{Q_n} \tag{3}$$

Another option is to define a central FS as the mean resistance over the mean load effect.

$$\overline{FS} = \frac{\overline{R}}{\overline{Q}} \tag{4}$$

Equation 3 and Equation 4 imply a degree of uncertainty. And clearly, the definition of an appropriate FS requires a probabilistic treatment. A critical drawback of this approach is that all uncertainty is lumped into one global factor, which leads to inconsistent margins of safety for different scenarios. The same FS can imply a very different safety margin in different cases. Consider for example the uncertainty in selecting a design value of friction angle versus undrained shear

strength based on a standard penetration test. The uncertainty in the second case is much more pronounced, but the *FS* applied in design is blind regarding this matter. A detailed probabilistic framework for geotechnical engineering is described by Baecher and Christian (2005).

Target Probability of Failure Method

The method of selecting a target probability of failure, or in other words, a target performance, requires the definition of a performance function (also called limit state function) that represents the margin of safety, which is the difference between the resistance (*R*) and the load effect (*Q*) for a given component or system of interest as expressed in Equation 5 represented in Figure 1. *R* and *Q* are random variables, which means they are uncertain; thus, *g* is also a random variable.

$$g = R - Q \tag{5}$$

In some applications, it is preferred to understand the safety as the resistance-to-load effect ratio, and the limit function is written as below.

$$g = \frac{R}{Q} - 1 \tag{6}$$

For both definitions of *g*, a negative value of the function *g* means failure or unsatisfactory performance.

For Equation 5, the mean (μ) and standard deviation (σ) of *g* relates to the statistics of *R* and *Q* as follows,

$$\mu_g = \mu_R - \mu_Q$$

$$\sigma_g^2 = \sigma_R^2 + \sigma_Q^2 - 2\rho_{RQ}\sigma_R\sigma_Q \tag{7}$$

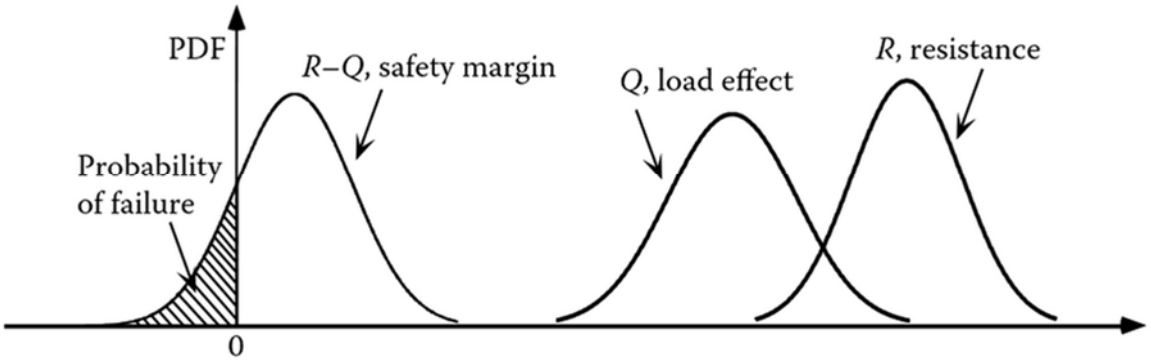

FIGURE 1 Statistical representation of resistance (*R*), load effect (*Q*), and margin of safety (*g*) (Nowak and Collins, 2013).

where ρ_{RQ} is the coefficient of correlation between *R* and *Q*. ρ_{RQ} is one if the variables are perfectly correlated and zero if they are statistically independent.

The performance of a given design is frequently discussed in terms of the reliability index (β), which has been called the safety index in the past. β is defined as a function of the probability of failure, P_F, as follows,

$$\beta = -\Phi^{-1}(P_F) \tag{8}$$

where Φ^{-1} is the inverse standard normal distribution function. When P_F is normally distributed, and *R* and *Q* are statistically independent, the reliability index can also be expressed as follows.

$$\beta = \frac{\mu_g}{\sigma_g} = \frac{\mu_R - \mu_Q}{\sqrt{\sigma_R^2 + \sigma_Q^2}} \tag{9}$$

As above, the reliability index is the number of standard deviations of the mean value of *g* from the critical value of zero. For structural components, *R* and *Q* can be usually considered as independent and uncorrelated. Nonetheless, in geotechnical engineering, the soil is part of the loading and the resistance side. Therefore, the correlation must be determined to use this approach.

This procedure is extended to give separate load factors and resistance factors for use in design and it is the basis of current codes. The LRFD or partial factors of safety is presented as the following design requirement: the total factored nominal load effect being less or equal than the factored nominal resistance,

$$\sum \gamma_i Q_{ni} \leq \phi R_n \tag{10}$$

where Q_{ni} is the nominal value of load component *i*, γ_i is the load factor *i*, R_n is the nominal value of resistance, and ϕ is the resistance factor. Loads and resistance factors are calibrated, so the limit state function meets a beforehand defined target reliability index ($\beta = \beta_T$). Load factors are greater than one to cover for the possibility for overload cases, while resistance factors are lesser than one, so the likelihood of cases where the resistance is lower than predicted is considered. A comprehensive explanation can be found in Nowak and Lind (1979a), Nowak and Lind (1979b), Ellinwood (1980), Nowak and Collins (2013), and examples of applications are presented in Nowak (1999), and Allen (2005), among many others highlighted in this paper.

Minimum Cost of Structural Failure

If the probability of failure of a design can be estimated using the reliability of structures framework, then the total cost of a structure with the inclusion of the cost of failure can be calculated, as well. Thus, the total lifetime cost of a structure can be represented as the sum of the construction cost, routine maintenance costs, failure costs, and repair or demolition costs. The failure costs are associated with the probability of failure and increase quickly as the probability of failure increases. This computation provides an estimate of the optimum probability of failure, which leads to the reliability-based lifetime approach and has demonstrated potential for cost savings and improved efficiency.

Nevertheless, this approach is not widely used yet, it is used mainly in advance research or in the design of critical structures (Nowak and Collins, 2013).

HISTORICAL PERSPECTIVE AND LITERATURE REVIEW

In the first decade of the 1900s, the building design and construction process began to formalize codes and requirements. Those provisions were prescriptive at the time but evolved into a rational design philosophy based on the concept of allowable stresses. AASHTO began issuing the *Standard Specifications for Highway Bridges* that followed ASD methodology in 1931. In the ASD, the uncertainties in the calculations of loads and resistances are accounted for through a single global *FS*. The underlying assumption in this philosophy is an elastic behavior of the structures under loading. This assumption represented major inconsistency in reinforced concrete design where usually sections are cracked under service loads. Thus, in 1956, the concrete industry adopted the strength-based design philosophy, and the first strength-based design specification was introduced in 1963. At the same time, since the publication of Terzaghi's book in 1925, geotechnical engineering has developed a rational approach for design rather than rely only on accumulated practical knowledge. As the structural and geotechnical engineering disciplines progressed, and the computer capabilities allowed engineers to consider several load scenarios in an efficient way, it becomes practical to define several limit states to study safety and performance of designs. A limit state is a condition beyond which a member or system no longer fulfills its intended function. Limit states are defined for strength, serviceability, long-term resistance, and extreme load event. The inclusion of uncertainties in a probabilistic manner to those limit states leads to what is called reliability analysis.

The first mathematical formulations of the structural safety problem can be attributed to Mayer (1926), Streletskii (1947), and Wierzbicki (1936). They recognized the load and resistance parameter are random variables, and therefore, for each structure, there is a finite probability of failure. Their concept was further developed and introduced to the United States by Freudenthal (1947, 1956). The formulations involved convolution functions that were very difficult to evaluate. The practical application of reliability analysis was not possible until the pioneering work of Cornell and Lind in the late 1960s and early 1970s. Cornell (1969) proposed a second-moment reliability index. Hasofer and Lind (1974) formulated a definition of a format-invariant reliability index. An efficient numerical procedure was formulated for calculation of the reliability index by Rackwitz and Flessler (1978). Statistical simulations (such as the Monte Carlo method) were possible thanks to the advance of computers. By the end of the 1970s, the reliability methods reached a degree of maturity, and now they are readily available for applications (Nowak and Collins, 2013).

In 1979, the Ontario Ministry of Transportation released the first edition of the *Ontario Highway Bridge Design Code*, which was the first reliability-based limit state specification in North America. The calibration approach used was developed by Nowak and Lind (1979a, 1979b), and later was used for the calibration of AASHTO LRFD (1994) as described by Nowak (1999). A significant research effort was performed by the National Institute of Standards and Technology, the *NBS Report 577* (Ellingwood et al., 1980), that dealt mainly with buildings and building loads. Nonetheless, the statistical data collected was useful for the calibration of AASHTO LRFD Bridge Code. As U.S. bridge engineers became increasingly more familiar with the Ontario bridge code, the logic in design based on probabilistically calibrated limit states was underlined. Thus, practitioners started to consider whether the AASHTO specifications should be based on a comparable

philosophy. In addition, many revisions that had occurred to the AASHTO specifications led to inconsistencies. In spring 1986, a group of state bridge engineers met in Denver and drafted a letter to the AASHTO Highway Subcommittee on Bridges and Structures indicating their concern that the AASHTO specifications were outdated. In July 1986, a group of state bridge engineers met with the staff of the NCHRP to consider whether a project could be developed to explore the points raised in the Denver letter, and this led to the NCHRP Project 12-28 (Sabol, 1998). This pilot study identified many areas where the bridge design technology and design practice at that time were not reflected in the existing AASHTO specifications. Additionally, it recommended that new specifications be developed based on LRFD format and reliability theories. The project also recommended that a comprehensive commentary be developed. Thus, the bridge subcommittee accepted the recommendations and initiated a second NCHRP Project (NCHRP 12-33) in July 1988 to address the aforementioned issues (Kulicki and Mertz, 2018). The LRFD calibration used the safety implied by the standard specifications as a reference minimum value. It was intended to increase the safety (measured as β) of bridges in 5% to 10% with the new AASHTO LRFD code. Moreover, when the calibrated load and resistance factors were proposed, the live load (LL) factor was arbitrarily increased by the bridge committee to add an extra safety margin. In 1993, at the annual meeting of the AASHTO bridge subcommittee, members voted 41 against 5 to adopt the new *AASHTO Load and Resistance Factor Design Bridge Design Specifications and Commentary* as an alternative to the *AASHTO Standard Specifications for Highway Bridges*. The vote took place after investing over $2 million and after 7 years of concentrated efforts by more than 70 experts in bridge engineering and thousands of hours of review and trial designs from states, industry, consultants, academia, and special agencies. In 1994, AASHTO published the first edition of LRFD in both customary U.S. and SI units (Lwin, 1999).

Since then, bridge superstructures have been designed by using the LRFD method in most states. The transition was perhaps helped by the fact that most structural engineers were somehow familiarized with the LRFD format from their exposure to ACI and AISC codes, which introduced LRFD in 1956 and 1986, respectively. Also, LRFD was available for use in bridge superstructure design since 1973 under the name load factor design (LFD). Before the adoption of LFD into the AASHTO standard as an approved design method for portions of the bridge structure above the foundation, all highway bridge design in the United States was performed using the ASD method. Then, since there were no LFD procedures for foundations, foundations could only be designed using the ASD approach. Engineers who used LFD procedures for bridge superstructures had to work with two sets of loadings, one for the design of the superstructure and one for design of the foundation. The inconsistency of designing the superstructure and substructure under different philosophies required considerable duplication of work and led to inconsistent levels of reliability. NCHRP Project 24-4 was initiated with the objective of developing LFD provisions for foundations. Specification and commentary were developed for shallow foundations, driven piles, drilled shafts, abutments, and other retaining structures (Barker et al., 1991). The resistance factors were determined from fitting ASD and not based on reliability analysis. Practitioners considered those provisions inconsistent with their practice, moreover, foundations were significantly more conservative and costly than before. The effect of various construction techniques on drilled shaft resistance factors was not addressed. In addition, the resistance factors did not account for the variability of the site conditions nor the number of load tests conducted. Also, many accepted design procedures were not supported by the LRFD specifications. Thus, several research projects started with a focus to improve and supplement AASJTP LRFD specification; relevant publications are summarized in Table 1.

TABLE 1 Featured Research Related to the LRFD Development in AASHTO Design Specification for Geotechnical Systems

Findings and Conclusions	Reference
AASHTO LRFD resistance factors were high for some methods (i.e., α-Tomlinson and Meyerhof) and low for others (i.e., Schmertmann SPT) for driven prestressed concrete piles.	McVay et al. (2002)
Developed reliability-based factors for shafts founded in sand, gravel, and rock for several design methods.	Kuo et al. (2002)
Developed resistance factors for the LRFD of deep foundations.	NCHRP Project 24-17 (Paikowsky et al., 2004)
Developed the Washington State DOT pile driving formula and its calibration in LRFD format.	Allen (2005)
Developed resistance factors for axially loaded concrete piles driven into soft soils.	Yoon et al. (2008)
Developed and calibrated procedures and modified the *AASHTO LRFD Section 10: Foundations for the Strength Limit State Design of Shallow Foundations.*	NCHRP Report 651 (Paikowsky et al., 2010)
Recommended revisions to the AASHTO LRFD specifications relating to the distribution of live load to buried structures.	NCHRP Project 15-29 (Nelson et al., 2010)
Proposed LRFD design and construction specifications for soil-nailed retaining structure.	NCHRP Project 24-21 (Lazarte, 2011)
Updated the work done by Paikowsky et al. (2004) with a recalibration of pile resistance with wave equation analysis of piles in initial and restrike conditions.	Smith (2012)
Presented recommendations for the development and sharing of high-quality databases of foundation load tests.	Abu-Hejleh et al. (2015)
Proposed refinements to the design procedures for geosynthetic reinforced soil structures.	NCHRP Project 24-41 (Zornberg et al., 2019)

LRFD IMPLEMENTATION IN GEOTECHNICAL ENGINEERING

The adoption of the AASHTO LRFD in 1994 raised many questions regarding the changes in the design process and its impact on the resultant size of the bridge components and foundations, as well as reinforcement quantities, etc. Several comparisons and design examples were performed to clarify the impact of the new LRFD specifications. Goble (1996) presented an example that indicated the new AASHTO LRFD specifications for driven pile design could be used effectively to produce a more rationally designed foundation. It suggested that modifications should be made to include additional serviceability limit states, and additional research may indicate that changes should be made in some of the resistance factors. Yoon and O'Neill (1997) noticed that resistance factors for foundations do not necessarily directly reflect the variance in site-specific resistance estimates. Their paper described a process whereby resistance factors can be determined from experimental data at a site. An example of that process for driven piles at a specific site in over-consolidated clay was provided. The Federal Highway Administration (FHWA) organized a scanning tour through Canada and Europe that examined geotechnical developments in LRFD methods. The panel agreed that a calibration of the geotechnical load and resistance factors in LRFD code was an urgent need. They stressed the necessity for improving communication among geotechnical, structural, and construction engineers (FHWA, 1999).

The TRB AKG70 committee invited several state structural and geotechnical engineers to participate in a workshop held at the 2008 TRB Annual Meeting. The objective of this workshop was to show various states' experiences in the practical implementation of LRFD in geotechnical and substructure design. Some of the findings are described in Table 2. Due to a lack of experience with the LRFD in the geotechnical area, most state DOTs implemented the specification by designing the bridge superstructures using the LRFD method while still using the ASD method for the bridge foundation design. Abu-Hejleh et al. (2009) prepared a paper to help state DOTs with interpretation and proper integration of AASHTO LRFD design specifications into their design and construction practice for axial compression design of single-driven piles. In an effort to maintain a consistent level of reliability, FHWA and AASHTO set a mandated date of October 1, 2007, after which all federally funded new bridges, including substructures, shall be designed by using the LRFD method (Yoon et al., 2008). Similarly, the FHWA and state DOTs established as a goal that the LRFD standard specifications be used on all new culverts, retaining walls, and other standard structures after 2010. AASHTO, in concurrence with FHWA, set a deadline of October 1, 2010, for full LRFD implementation by all states (Miller and Durham, 2008). However, many AASHTO bridge subcommittee members recognized that there was a general lack of understanding

TABLE 2 Experiences of Public Agencies with AASHTO LRFD Implementation

Agency	Initial Challenges and Problems	Lesson Learned/Action Taken	Reference
Louisiana DOTD	• AASHTO LRFD required deeper borings, CPT soundings, and the use of triaxial strength tests rather than the traditional uniaxial-unconfined compressive strength tests • Issues with the metric unit system and U.S. customary units	• The additional soil borings, or CPT soundings, and testing requirement increase the geotechnical study cost by at least 50 percent • Made available LRFD software tools	D'Andrea and Tsai (2009)
Florida DOT	• -AASHTO LRFD did not include calibration for Florida unique geological formations • -AASHTO LRFD did not include calibration for Florida DOT methods of analyses	• Contract with the University of Florida to develop local calibrations • In-house training for Florida DOT engineers, and consultant engineers • Conversion of documents and software	Lai (2009)
North Carolina DOT	• AASHTO LRFD did not include calibration for North Carolina DOT local geology • AASHTO LRFD did not include calibration for North Carolina DOT's Vesic driven pile design method	• LRFD specifications result in more conservatively foundations • Contract with North Carolina State University to develop local calibrations	Wainaina et al. (2009); Kim and Kreider (2011)
Pennsylvania DOT	• AASHTO LRFD code led to differences with traditional ASD practices	• Performed parametric studies and sample designs to quantify the implication of the LRFD methods • Modified the LRFD specification to fit former ASD local practices • LRFD computer programs were developed • Training sessions for designers of the LRFD specification changes	Miller (2009)

of the calibration process. As a result, Allen et al. (2005) published *Transportation Research Circular E-C079: Calibration to Determine Load and Resistance Factors for Geotechnical and Structural Design* (trb.org) that addresses structural calibration issues raised at an LRFD calibration workshop held after the 2004 TRB Annual meeting. The purpose of that e-circular was to assist structural and geotechnical engineers to better understand the calibration process and what information is required to perform such tasks. In the same line, FHWA disseminated the LRFD approach through presentations, seminars, webinars, and courses (FHWA, 2001; Abu-Hejleh et al., 2011).

LRFD ADVANTAGES, DIFFICULTIES, AND CRITICISMS

AASHTO LRFD is based on sounded principles and a coherent approach for ensuring safety, serviceability, and economy. It was calibrated to produce designs with a consistent and uniform level of safety for a wide range of bridges and its foundations. AASHTO LRFD addresses four limit states: strength, serviceability, fatigue, and extreme events. A rigorous treatment of uncertainties in the design represents a general improvement in professional practice. Other benefits from implementing the LRFD method are consistency in geotechnical and structural components that are now designed under the same philosophy, increased interaction between field inspectors and designers, and improved quality of construction due to the control field testing requirements.

The load and resistance factors developed for the LRFD specifications were calibrated using a combination of reliability theory, fitting to ASD, and engineering judgment. Fitting to ASD was used when the needed data for calibration was not available. In those cases, the level of safety is unknown, and its uniformity may not be achieved. Designers may perceive that without the reliability-based calibration, the adoption of LRFD design is not worthy and it just adds complexity. With time, more and more design methods have been calibrated based on reliability analysis. However, sometimes the data available have been criticized. For example, for pile axial resistance calculation methods, the resistance factors were developed from load test results obtained on piles with diameters of 24 in. or less. In response, the FHWA initiated a project that seeks to research and update FHWA technical references for the design of large diameter open-end piles using the LRFD framework. The outcomes of this project have been discussed in the committee at the 2019 TRB Annual Meeting and in the 2019 AASHTO meeting with great interest.

A concern in the geotechnical community is that resistance factors developed from readily available information and distributed across the country may not reflect their local geology and practices. Many states have local design methods and particular geological formations that were not included in the generalized calibration of the code. AASHTO encourages owner agencies to develop local resistance factors that are calibrated to local geological formations, considering their local practice and experience, and their particular design methods. Several DOTs contracted universities to develop local resistance factors. Another concern is that site-specific conditions, construction quality, and spatial variability have not been included in the calibration. Instead, those sources of uncertainty have been lumped into the soil parameter variation.

Another criticism of the reliability-based design methods is that the calibrations have been performed based on individual element reliability rather than address the complete system reliability. The determination of the system reliability is significantly more complicated and required consideration for the failure mode and correlation among the components of the systems. Correlation is often difficult to quantify because of the amount of data needed. Consider a typical bridge. It

consists of a system of interconnected components including, for instance, deck, girders, bearing supports, bent cap, piers, foundations, abutments, and probably several segments. Different components of the superstructure and its foundation are more vulnerable to a specific type of loading. For example, girders are often controlled by flexure, piers are subjected to a combination of compression and bending moment, bent caps are often controlled by shear force, abutments might be designed for overturning, and either lateral loading or axial loading could control deep foundations design. The failure of a single component might have different consequences. Would the bridge collapse if only one girder fails? Would it even be noticeable if one drilled shaft fails within a group of drilled shafts? How does the flexural failure of a member compared to shear or axial failure? Would the failure of one foundation or abutment lead to a total bridge collapse? Is the failure of one segment of the bridge is as bad as the failure of the whole bridge? A new difficulty arises: How to define appropriate target reliability indices for individual components and the whole system considering their importance, consequences of failure, and mode of failure? It is anticipated that the reliability-related research would address these issues in the future.

Despite the criticisms and the difficulties in the implementation, AASHTO LRFD and reliability-based design have become the accepted practice. It provides a rational framework to deal with uncertainties and manage the safety of transportation infrastructure. It makes possible the inclusion of new material, design method, or new technology, so the safety level is maintained and is consistent with current practices.

FUTURE PERSPECTIVE

The determination of the soil design parameter from subsurface exploration is probably the single most problematic step in geotechnical engineering. The selection of design values should be based on a repeatable chain of reasoning rather than on speculation. In addition, this selection should be consistent with the values used in the calibration of resistance factors. The definition of soil properties for use in design has traditionally been left up to the designer. The LRFD Bridge Code discusses subsurface exploration procedures in Section 10.4. This section of the AASHTO LRFD bridge design specification is currently under review. The goals are improving the consistency of achieving the target reliability and enable designers to acquire appropriate site investigations. A possible outcome of this project is that the resistance factors for foundation design could depend on the number of laboratory tests and site investigations performed.

There are numerous projects related to bridge foundation design and the calibration of load and resistance factors being sponsored by NCHRP, AASHTO, FHWA, DOTs, and other agencies. A comprehensive field load testing and geotechnical investigation program for the development of LRFD recommendations of driven piles on intermediate geomaterials are ongoing. A research project with the objective of developing reliability-based geotechnical resistance factors for axially loaded micropiles and related specifications has been initiated (TRB, 2019).

Today, all DOTs follow AASHTO LRFD code, and some of them combine AASHTO LRFD code with local calibrations. Other geotechnical systems have also updated to the LRFD philosophy; moreover, several calibrations are currently being performed (Table 3).

Reliability analysis provides a logical framework to deal with uncertainties that are inevitable in geotechnical engineering. Therefore, in view of the complexities of describing local geotechnical conditions, it may be preferable to perform a direct reliability-based design including

TABLE 3 Recent Reliability-Based Calibration Efforts

Agency	Calibration Effort	Reference
Arizona DOT	For side-resistance of drilled shafts in cohesionless soils	TRB (2019)
California DOT	For axial resistance of driven piles and drilled shafts	TRB (2019)
Oklahoma DOT	For current methods for design of drilled shafts in weak rock formations	TRB (2019)
Wyoming DOT	For procedures for driven piles on soft rocks	TRB (2019)
Mississippi DOT	Regarding the inclusion of the long-term bearing capacity of driven piles in the LRFD local specifications	TRB (2019)
Florida DOT	Re-evaluating resistance factors for driven piles for local design procedures, as well as developing load and resistance factors for tip grouted drilled shafts	TRB (2019)
Oregon DOT Florida DOT Alabama DOT	Study of analysis methods and reliability-based calibration for drilled shaft foundations under torsional loading	Thiyyakkandi et al. (2016); Li et al. (2017); Aguilar (2018)

the uncertainties in the parameters for the specific problem at hand rather than to rely on a generalized calibrated code.

CONCLUSIONS

Geotechnical designs are part of complex systems that include both structural and geotechnical components. If the structural system is to be designed by the LRFD methodology, then the supporting geotechnical components should too. Thus, reliability-based codes are becoming widespread in geotechnical practice shown by the numerous research efforts oriented to obtain reliability-based design procedures.

Historically, the design methodology for bridges and foundations came from AASHTO. The standard practice for defining a safety margin in the early 1930s was to use one global *FS*. In the 1970s, the development of the partial factors of safety approach that is known as LRFD started. First, LRFD was adopted for superstructure design and later for foundation design, as well. LRFD approach is more suitable for geotechnical applications than ASD since it provides a rational framework to deal with different uncertainty levels. Although initially, the LRFD method for bridge foundation design was gaining prevalence slowly, in the last decade, reliability analysis and probabilistic methods have found extensive application and acceptance in geotechnical engineering. Other geotechnical systems have also followed the LRFD philosophy.

The current AASHTO specifications are still a work in progress, and so updates are anticipated as data availability increases. Practitioners may still suggest a certain level of discomfort with using LRFD method; this may be because they do not agree with the data or data treatment that have been used in past calibration, or because LRFD is not fully transparent to geotechnical engineers that do not have a background on statistical methods of analysis. The number of civil engineers trained in probability theory is limited. The key to a proper understanding and implementation of LRFD in the future lays with universities. The next generations of engineers must understand the details of LRFD to ensure it is not used as a black box. That, in combination with courses on statistical methods for engineers, will guarantee the LRFD method is used appropriately and help the profession to move forward on it.

TRB committees and NCHRP research played a significant role in the development of AASHTO LRFD code and its implementation into the design of bridges' superstructure and substructure. This chapter was intended to be a roadmap through the most useful material to understand reliability analysis and its application to geotechnical engineering. It is of interest to those engineers charged with performing reliability-based calibration in need of a starting point. This paper aims to contribute to the understanding and future improvement of LRFD specifications.

ACKNOWLEDGMENTS

The authors are thankful for the feedback received from the Standing Committee on Foundations for Bridges and Other Structures reviewers. Their contribution completed this literature and historical overview. Special thanks go to Jerry DiMaggio, Tony Allen, and Rodrigo Herrera.

AUTHOR CONTRIBUTIONS

The authors confirm contribution to the paper as follows: study conception and design: Aguilar; data collection: Nowak and Anderson; analysis and interpretation of results: Aguilar and Nowak; draft manuscript preparation: Aguilar, Nowak, and Anderson. All authors reviewed the results and approved the final version of the manuscript.

REFERENCES

AASHTO LRFD. *Bridge Design Specifications*. American Association of State Highway and Transportation Officials, Washington, D.C., 2020.

AASHTO LRFD. *Bridge Design Specifications*. American Association of State Highway and Transportation Officials, Washington, D.C., 1994.

Abu-Hejleh, N., J. DiMaggio, W. Kramer, S. Anderson, and S. Nichols. *Implementation of LRFD Geotechnical Design for Bridge Foundations: Reference Manual* (No. FHWA NHI-10-039). Federal Highway Administration, U.S. Department of Transportation, 2011.

Abu-Hejleh, N. M., M. Abu-Farsakh, M. T. Suleiman, and C. Tsai. Development and Use of High-Quality Databases of Deep Foundation Load Tests. *Transportation Research Record: Journal of the Transportation Research Board, No. 2511*, 2015, pp. 27–36. https://doi.org/10.3141/2511-04.

Abu-Hejleh, P. E., N. Mahmood, J. Dimaggio, and W. K. Kramer. AASHTO Load and Resistance Factor Design Axial Design of Driven Pile at Strength Limit State. Presented at 88th Annual Meeting of the Transportation Research Board, Washington D.C., 2009.

Aguilar, V. Torsional Resistance of Drilled Shaft Foundations. MS thesis. Auburn University, Ala., 2018.

Allen, T. M. *Development of the WSDOT Pile Driving Formula and Its Calibration for Load and Resistance Factor Design.* (WA-RD No. 610.1). Washington State Department of Transportation, Washington, D.C., 2005.

Allen, T. M., A. S. Nowak, and R. J. Bathurst. *TR Circular E-C079: Calibration to Determine Load and Resistance Factors for Geotechnical and Structural Design*. Transportation Research Board, 2005. http://www.trb.org/Publications/Blurbs/156253.aspx

Barker, R. M., J. M. Duncan, K. B. Rojiani, P. S. K. Ooi, C. K. Tan, and S. G. Kim. *NCHRP Report 343: Manuals for the Design of Bridge Foundations*. Transportation Research Board, National Research Council, Washington, DC, 1991.

Baecher, G. B., and J. T. Christian. *Reliability and Statistics in Geotechnical Engineering*. John Wiley & Sons, 2005.

Benjamin, J. R., and A. C. Cornell. *Probability, Statistics and Decision for Civil Engineers*. McGraw-Hill, New York, NY, 1970.

Christian, J., 2018. NCHRP Project 12-55A: Load and Resistance Factors for Earth Pressures on Bridge Substructures and Retaining Walls. Transportation Research Board, National Academy of Sciences. https://apps.trb.org/cmsfeed/TRBNetProjectDisplay.asp?ProjectID=342.

Cornell, C. A., 1969. A probability-based structural code. *Journal Proceedings*, pp. 974–985.

D'Andrea, A. W., and C. Tsai. 2009. TR Circular E-C136: Louisiana Department of Transportation and Development's Experience with LRFD. Transportation Research Board, 2009, pp. 1–9.

Ellingwood, B., T. Galambos, J. G. McGregor, and C. A. Cornell. 1980. *NBS 577: Development of a probability based load criterion for American National Standard A58*. U.S. Department of Commerce, National Bureau of Standards, 1980.

FHWA. Load and resistance factor design for highway bridge substructures. Federal Highway Administration, U.S. Department of Transportation, 2001.

FHWA. FHWA-Hi-98-032 and Geotechnical Engineering Practices in Canada and Europe. Federal Highway Administration, U.S. Department of Transportation, 1999.

Freudenthal, A. M. Safety and the probability of structural failure. *Transactions of the American Society of Civil Engineers*, 1956.

Freudenthal, A. M. The safety of structures. *Transactions of the American Society of Civil Engineers*, Vol. 112, No. 1, 1947, pp. 125–159. https://doi.org/10.1061/TACEAT.0006015.

Goble, G. G. Load and Resistance Factor Design of Driven Piles. *Transportation Research Record: Journal of the Transportation Research Board, No. 1546*, 1996, pp. 88–93. https://doi.org/10.1177/0361198196154600110.

Hart, G. C. *Uncertainty analysis, loads, and safety in structural engineering*. Prentice Hall, 1982.

Hasofer, A. M., and N. C. Lind. Exact and invariant second-moment code format. *Journal of the Engineering Mechanics Division*, Vol. 100, No. 1, 1974, pp. 111–121. https://doi.org/10.1061/JMCEA3.0001848.

Kim, K. J., and C. A. Kreider. *NCDOT Experience in Load and Resistance Factor Design and Construction of Driven Pile Foundations*, 2011.

Kulicki, J. M., and D. R. Mertz. 2018. NCHRP Project 12-33: Development of a Comprehensive Bridge Specification and Commentary. Transportation Research Board, National Academy of Sciences. https://apps.trb.org/cmsfeed/TRBNetProjectDisplay.asp?ProjectID=315

Kuo, C. L., M. C. McVay, and B. Birgisson. 2002. Calibration of Load and Resistance Factor Design: Resistance Factors for Drilled Shaft Design. *Transportation Research Record: Journal of the Transportation Research Board*, No. 108–111, 1808. https://doi.org/10.3141/1808-12.

Lai, P. W. Florida Department of Transportation's Experience with LRFD. *Transportation Research Circular E-C136: Implementation Status of Geotechnical Load and Resistance Factor Design in State Departments of Transportation*, Transportation Research Board, 2009.

Lazarte, C. A. *NCHRP Research Report 701: Proposed Specifications for LRFD Soil-Nailing Design and Construction*. Transportation Research Board, Washington, D.C., 2011. https://doi.org/10.17226/13327.

Li, Q., A. W. Stuedlein, and A. R. Barbosa. Torsional load transfer of drilled shaft foundations. *Journal of Geotechnical and Geoenvironmental Engineering*, Vol. 143, No. 8, 2017, p. 04017036. https://doi.org/10.1061/(ASCE)GT.1943-5606.0001701.

Lwin, M. M. 1999. Why the AASHTO Load and Resistance Factor Design Specifications? *Transportation Research Record: Journal of the Transportation Research Board*, 1999. https://doi.org/10.3141/1688-20.

Mayer, M. *Die Sicherheit der Bauwerke und ihre Berechnung nach Grenzkräften anstatt nach zulässigen Spannungen.* J. Springer, 1926.

McVay, M., B. Birgisson, T. Nguygen, and C. Kuo. Uncertainty in Load and Resistance Factor Design phi Factors for Driven Prestressed Concrete Piles. *Transportation Research Record: Journal of the Transportation Research Board, No. 1808*, 2002, pp. 99–107. https://doi.org/10.3141/1808-11.

Miller, B. Pennsylvania Department of Transportation's Experience with LRFD. *Transportation Research Circular E-C136: Implementation Status of Geotechnical Load and Resistance Factor Design in State Departments of Transportation*, Transportation Research Board, 2009.

Miller, L. J., and S. A. Durham. Comparison of Standard Load and Load and Resistance Factor Bridge Design Specifications for Buried Concrete Structures. *Transportation Research Record: Journal of the Transportation Research Board, No. 2050*, 2008, pp. 81–89. https://doi.org/10.3141/2050-08.

Nelson, C. R., T. J. McGrath, Y. Kitane, G. Li, and D. L. Petersen. *NCHRP Research Report 647: Recommended Design Specifications for Live Load Distribution to Buried Structures*. Transportation Research Board, Washington, D.C., 2010. https://doi.org/10.17226/14377.

Nowak, A. S. *NCHRP Research Report 368: Calibration of LRFD Bridge Design Code*. Transportation Research Board, Washington, D.C., 1999.

Nowak, A. S., and K. R. Collins. *Reliability of Structures*, second edition. CRC Press, 2013.

Nowak, A. S., and N. C. Lind. Practical code calibration procedures. *Canadian Journal of Civil Engineering*, Vol. 6, No. 1, 1979a, pp. 112–119. https://doi.org/10.1139/l79-012.

Nowak, A. S., and N. C. Lind. Practical Bridge Code Calibration. *Journal of the Structural Division*, Vol. 105, No. 12, 1979b, pp. 2497–2510. https://doi.org/10.1061/JSDEAG.0005307.

Paikowsky, S. G., B. Birgisson, M. McVay, T. Nguyen, C. Kuo, G. Baecher, B. Ayyub, K. Stenersen, K. O'Malley, and L. Chernauskas. *NCHRP Research Report 507: Load and Resistance Factor Design for Deep Foundations*. Transportation Research Board, Washington, D.C., 2004.

Paikowsky, S. G., M. C. Canniff, K. Lesny, A. Kisse, S. Amatya, and R. Muganga. *NCHRP Research Report 651: LRFD Design and Construction of Shallow Foundations for Highway Bridge Structures*. Transportation Research Board, Washington, D.C., 2010. https://doi.org/10.17226/14381.

Rackwitz, R., and B. Flessler. Structural reliability under combined random load sequences. *Computers & Structures*, Vol. 9, No. 5, 1978, pp. 489–494. https://doi.org/10.1016/0045-7949(78)90046-9.

Sabol, S. *NCHRP Digest 198: Development of Comprehensive Bridge Specifications and Commentary*. Transportation Research Board, Washington, DC, 1998.

Smith, T. D. Comprehensive Recalibration of Pile Resistance with WEAP Software in Initial and Restrike Conditions for Load and Resistance Factor Design. *Transportation Research Record: Journal of the Transportation Research Board, No. 2310*, 2012, pp. 29–37. https://doi.org/10.3141/2310-04.

Streletskii, N. S. *Foundations of Statistical Account of Factor of Safety of Structural Strength*. State Publishing House for Buildings, Moscow, 1947.

Thiyyakkandi, S., M. McVay, P. Lai, and R. Herrera. Full-scale coupled torsion and lateral response of mast arm drilled shaft foundations. *Canadian Geotechnical Journal*, Vol. 53, No. 12, 2016, pp. 1928–1938. https://doi.org/10.1139/cgj-2016-0241.

Transportation Research Board. Research in Progress. 2019. URL https://rip.trb.org/.

Wainaina, N., K. J. Kim, and C. Chen. North Carolina Department of Transportation's Experience with LRFD. *Transportation Research Circular E-C136: Implementation Status of Geotechnical Load and Resistance Factor Design in State Departments of Transportation*, Transportation Research Board, 2009.

Wierzbicki, W. *Safety of structures as a probabilistic problem*. Przeglad, Technivzny, Polish, 1936.

Withiam, J. L. NCHRP Project 12-55: Load and Resistance Factors for Earth Pressures on Bridge Substructures and Retaining Walls. Transportation Research Board, National Academy of Sciences. 2018. https://apps.trb.org/cmsfeed/TRBNetProjectDisplay.asp?ProjectID=341.

Yang, L., and R. Liang. 2007. Incorporating Long-Term Set-Up into Load and Resistance Factor Design of Driven Piles in Sand. Presented at 86th annual Meeting of the Transportation Research Board, Washington, D.C., 2007.

Yoon, G. L., and M. W. O'Neill. Resistance Factors for Single Driven Piles from Experiments. *Transportation Research Record: Journal of the Transportation Research Board, No. 1569*, 1997, pp. 47–54. https://doi.org/10.3141/1569-06.

Yoon, S., M. Y. Abu-Farsakh, C. Tsai, and Z. Zhang. Calibration of Resistance Factors for Axially Loaded Concrete Piles Driven into Soft Soils. *Transportation Research Record: Journal of the Transportation Research Board*, No. 2045, 2008, pp. 39–50. https://doi.org/10.3141/2045-05.

Zornberg, J. G., A. M. Morsy, B. M. Kouchaki, B. Christopher, D. Leshchinsky, J. Han, B. F. Tanyu, F. T. Gebremariam, P. Shen, and Y. Jiang. *Document 260: Proposed Refinements to Design Procedures for Geosynthetic Reinforced Soil (GRS) Structures in AASHTO LRFD Bridge Design Specifications*. Transportation Research Board, Washington, D.C., 2019. https://doi.org/10.17226/25416.

Seismic Ground Motion Design Criteria for Highway Bridges from the Perspective of Design Engineers

IGNATIUS (PO) LAM
HUBERT LAW
Earth Mechanics, Inc.

BRIAN MARONEY
California Department of Transportation

This paper presents the history and development of criteria for both the design response spectrum method for ordinary, common bridges analyzed by the modal superposition method, and the ground motion time history analysis method and inputs for designing major, important long-span bridges. This paper addresses various challenges encountered by the designers related to implementation of ground motion design criteria.

INTRODUCTION

The authors' experiences with bridges includes new design and retrofit projects in the United States, particularly California Department of Transportation (Caltrans) but also in less seismically active states in the eastern United States. They also are active in both actual projects and professional activities in the development of bridge design guidelines, for example, the Multidisciplinary Center for Earthquake Engineering Research (MCEER) projects for the AASHTO Specifications and Caltrans' Bridge Design Guidelines, and Applied Technology Council (ATC) projects. This paper covers both criteria for design response spectra for ordinary or common bridges analyzed by the modal superposition method, and ground motion time history inputs for designing major and important long-span bridges in time history analyses. This paper addresses various challenges encountered by the designers related to implementation of ground motion design criteria.

AASHTO's and Caltrans' current ground motion design criteria starts with developing an appropriate reference design response spectrum for a given soil–rock condition based on the appropriate attenuation relationship derived from strong motion recordings. The design response spectrum may be determined based on a deterministic or probabilistic approach as described in the following sections. The resulting response spectrum is then used as part of a response spectrum analysis by the bridge engineer, which considers the seismic displacement demand at the natural period of the structure. This is the method appropriate for ordinary, common bridges. The paper will then discuss varying considerations and approaches for long span bridges.

DETERMINISTIC SEISMIC HAZARD APPROACH

Historically, Caltrans led seismic bridge design practice and adopted what is called a deterministic seismic hazard design approach for developing the reference earthquake loading criteria. This

method's main appeal is its simplicity, especially for presenting the approach to nontechnical personnel including managers of governmental agencies as well as the general public.

A deterministic approach requires identification of fundamental geometric seismic sources (earthquake faults) that would affect a project site, including the maximum magnitude associated with the earthquake source and the distance between the source and the site [see item (1) in Figure 1]. Then, an attenuation relationship is used to quantify the amplitude of the design response spectrum at a given structural period [see item (3) in Figure 1]. It is possible that different seismic sources control the spectral amplitude at different period ranges. For example seismic sources with smaller magnitudes from closer distances could control the response spectrum at shorter period ranges, while seismic sources with larger magnitudes would control the response spectrum at longer period ranges. The deterministic approach is simpler in that the method does not require the knowledge of the recurrence relationships (rate of activity) for seismic sources and most geotechnical professionals can conduct the analyses. There is little debate about the calculation procedure associated with the deterministic approach.

Historically, Caltrans would use the median attenuation equation for developing the design response spectrum for ordinary or common bridges in what had been commonly called the maximum credible earthquake (MCE). The MCE approach, as documented by Mualchin and Jones (1992), is well-known to practicing engineers active in seismic design of bridges in California. The authors believe that the wording "maximum" stems from the assumption that an entire fault length will rupture in a design event. However, this will automatically imply that the anticipated demand would have a 50% chance to exceed the design level if indeed the entire fault length is to rupture. For major (long-span) bridges, the historical Caltrans practice would be to design for a response spectrum based on the mean-plus-one sigma (standard deviation) or statistically based on an 84th percentile confidence level in the deterministic based criteria.

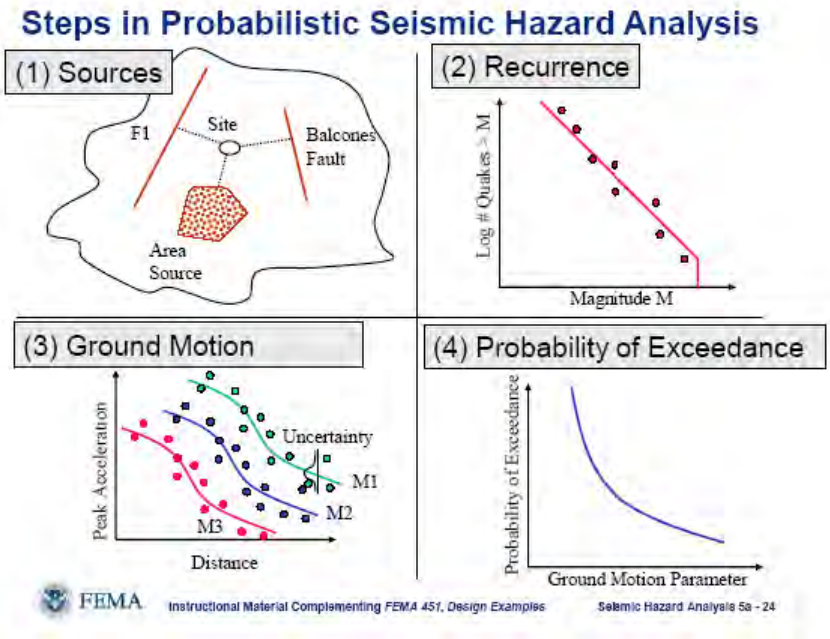

FIGURE 1 Steps in probabilistic seismic hazard analysis. Note that only items (1) and (3) are involved in a deterministic seismic hazard analysis.

Caltrans' method has been called the MCE. The fact that ordinary or common bridges are designed based on a median attenuation relationship led to many criticisms, including that the design level is too low and that the name of MCE is misleading. Even to this day, many mistakenly believe that actual ground shaking will never exceed the MCE spectrum.

PROBABILISTIC SEISMIC HAZARD APPROACH

The Caltrans Toll (long-span) Bridge Seismic Retrofit Program took place from the late 1990s to early 2000s in response to the recommendation for toll bridges outlined in the *Continuing Challenge Report* (Housner, 1995). At that time the Toll Bridge Peer Review Panel introduced a probabilistic earthquake design approach to CT.

Figure 1 illustrates a general procedure for the probabilistic approach which explicitly considers the recurrence relationship [item (2) in Figure 1] to account for seismic source activity, in addition to attenuation relationships which are developed from the statistical analyses of available strong ground motion data. From the authors' experiences, a probabilistic hazard solution tends to be more robust. As an example, if seismologists decided to change the maximum earthquake magnitude assigned to a given fault, such as recently happened to the Hayward fault in San Francisco east bay, the design earthquake will change significantly for the deterministic approach, while a probabilistic approach recognizes that the larger magnitudes would be relatively rare and their implication to the probabilistic hazard solution would be relatively minor. Figure 2 presents a comparison between the probabilistic approach and the deterministic approach conducted for the Carquinez Strait Bridge retrofit project. Eventually, the Toll Bridge Peer Review Panel elected to adopt the largely deterministic approach (based on the 84th percentile attenuation) for anchoring the design level for Caltrans toll bridge seismic retrofit program (Geomatrix, 1995). The comparison indicates that the design ground shaking fits in between a 1,000- and a 2,000-year return period of a probabilistic seismic hazard design approach.

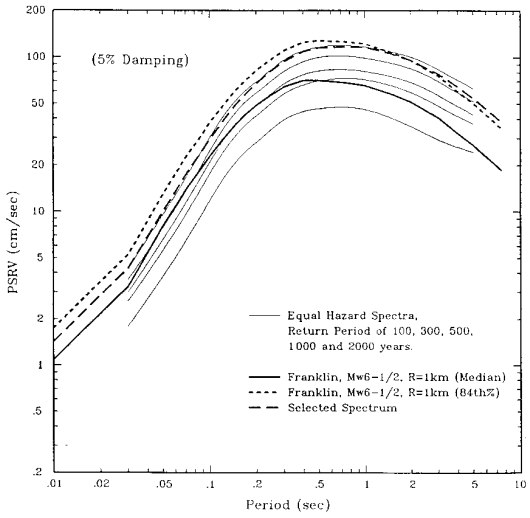

FIGURE 2 Comparison between probabilistic and deterministic rock target spectra from Geomatrix Geohazard Report (1995) for Carquinez Strait Bridge.

RESPONSE SPECTRUM ANALYSIS

A response spectrum (depicting the seismic demand in terms of the acceleration or displacement demand) can be developed by a deterministic approach, or more commonly now with a probabilistic approach. It can be incorporated into the design by a variety of analysis approaches: an equivalent static analysis, equivalent dynamic analysis, and pushover analysis by the bridge engineer. However, the structural and geotechnical engineers must be cognizant of the limitations and intended use of the method, as illustrated with the following experience from the San Francisco–Oakland Bay Bridge (the Bay Bridge).

The Bay Bridge east span comprises four segments (from east to west): (1) shorter span Oakland touch down, (2) long span skyway, (3) the steel self-anchored suspension (SAS) bridge, and (4) the Yerba Buena Island transition structure. The SAS is a steel bridge while the other segments are reinforced concrete structures.

Soil conditions in relation to the bridge segments vary tremendously over the length of the Bay Bridge east span as shown in Figure 3, consisting of soft bay mud of decreasing depth eastward from Oakland to Skyway–SAS interface at E2 Pier. Soft bay mud remains the soil condition at SAS Pier E2. Soil condition at center tower, T1 at SAS consists of varying thickness of thinner bay mud overlying San Franciscan rock. Hard rock is exposed at the western limit of SAS at W2 Pier. The San Franciscan rock extends westward to the entire YBI transition structure.

The drastically varying soil conditions imply different ground motion characteristics and therefore different ways to implement ground motion analysis methods for the project.

For all three segments, with the exception of the SAS, ground motion criteria were generalized into an appropriate design spectra (separate soft bay mud spectra for Oakland touch down and skyway). A rock spectrum was prescribed for the YBI transition structure. Initial design for these three segments were conducted using the conventional response spectrum and displacement pushover analysis approach as usually preferred by designers. However, multiple support ground motion time histories were also furnished for time domain analyses for a final check for the entire bridge.

The response spectrum analysis (RSA) method has the advantage of establishing the seismic demand with relatively little analysis effort. The RSA method allows designers the ability to optimize the design and seismic details. Bridge engineers generally place higher importance in the seismic strategy, seismic performance achieved through design and detailing. Experienced structural designers commonly believe that sophistication in the analysis itself and the exactness of the ground motion criteria (which will always be associated with a great degree of uncertainty) are not as important as implementing appropriate structural detailing to control the bridge to a ductile mode of behavior at overload as opposed to a sudden brittle collapse mode.

The soil conditions at each of the three bridge piers at SAS vary drastically, implying different response spectra at each pier. The SAS is supported by the main cable and suspenders with very different dynamic characteristics than conventional bridges supported by columns and piers. In addition, a RSA solution does not provide adequate information for the design of the hinge pipe beam at the SAS-Skyway interface where drastically different dynamic response characteristics are expected between the two structures. Hence, the RSA method is not appropriate for the design of the SAS and the design was conducted by the time history analysis method.

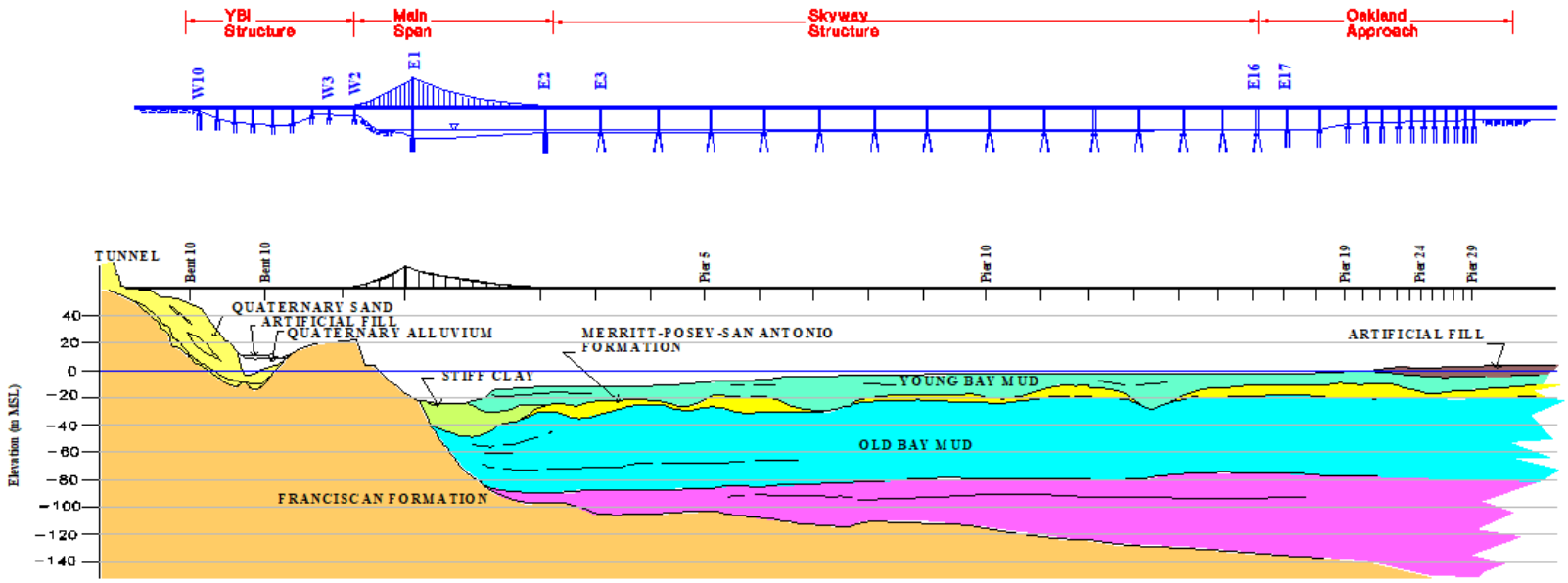

FIGURE 3 Summary of structural types and soil conditions of Bay Bridge east span.

CALTRANS' TOLL BRIDGE EXPERIENCE

After the above geohazard studies conducted for the Caltrans toll bridge program concluded in 1993, the toll bridge structural retrofit contracts commenced in 1995. However, the seismologists in the geohazard study team informed Caltrans and the Peer Review Panel members that the results in their geohazard reports were already outdated due to the realization of a ground motion phenomenon referred to as near-fault forward rupturing directivity effects as observed in several large earthquakes (e.g., 1979 Imperial Valley Earthquake and the 1992 Landers Earthquake). Such ground motion phenomenon will introduce pulse-like long period motions and imply a much higher level of demands for long-span toll bridges. At that time when the seismologists raised the topic of near-fault directivity effects, the subject was not well understood nor documented given that the benchmark near-fault directivity paper was not published until 1997 (Somerville et al., 1997). Despite the need to delay the project schedule and the implication of a higher retrofit cost, Caltrans and the Peer Review Panel accommodated the seismologists to subjectively make increases to the spectral amplitude at longer periods (greater than 2 s) to project near-fault directivity effects. As the toll bridge design and analyses were to be conducted using a time history approach (Geomatrix, 1995), recorded motions with some of the most pronounced long period pulses were selected as startup motions for developing the eventual spectrum-compatible rock motions for input to design analyses.

From Earth Mechanics, Inc. (EMI) and Caltrans' perspective, these debates and controversies had caused disruption to a fast track project schedule. It also resulted in a significant delay to very large design teams assembled for the toll bridge retrofit contracts covering six long-span bridges: (1) Benicia–Martinez, (2) Carquinez Strait, (3) Richmond–San Rafael, (4) San Mateo–Hayward, (5) Vincent Thomas, and (6) San Diego–Coronado bridges. The replacement of East Span San Francisco–Oakland Bay Bridge (SFOBB) was also affected by the controversies.

The near-fault directivity ground motion issue continued to be a controversial topic affecting the Caltrans toll bridge program for the next 20 years. The authors have been involved in all the above mentioned toll bridge projects, including the subsequent replacement of the East Span San Francisco–Oakland Bay Bridge design, the Dumbarton and Antioch Seismic retrofit contracts. EMI served as the lead geotechnical engineer for the East Span Bay Bridge contract and assumed the responsibility for reviewing the work conducted by the project seismologists. The project ground motion criteria team (including the Seismic Peer Review Panel, and Caltrans and EMI personnel involving seismologists, geologists, structural and geotechnical engineers from both Caltrans and EMI) continued to assist Caltrans to deal with the ground motion subject matter and to resolve problems as necessary. The following discusses some of these issues and decisions made which would be useful to readers.

NEAR-FAULT DIRECTIVITY EFFECT

The issue of near-fault directivity effects had originally surfaced much earlier when it was highlighted by late Professor Bruce Bolt in 1991 and first introduced into Caltrans' projects (Geomatrix, 1995). This subject resurfaced again during design of the East Span Bay Bridge which started around 1997. By that time, the subject of near-fault directivity effects had been discussed in Somerville et al. (1997). Somerville et al. proposed some statistics to provide a basis for conducting a

more formal probabilistic seismic hazard analysis and documented a methodology to modify existing conventional attenuation equations to account for such effects. A key figure shown in Figure 4 illustrates the proposed method to amplify long period motions by multiplication factors based on a dependent variable $X\cos(\theta)$ defined for strike–slip faults that was used to quantify the degree of severeness of the near-fault directivity rupturing effect. At the initial assessment of East Span Bay Bridge project, the probabilistic solution with near-fault effects projected an 80% increase in the spectral amplitude at a 3-s period over the reference spectrum which included an earlier vintage of the near-fault directivity effects introduced subjectively for retrofit analyses. Such a large increase obviously would imply a much higher construction cost for the project which led to Caltrans requesting the governor to allocate a Ground Motion Contingency Fund.

From a review of Somerville et al. (1997), authors observed that the proposed ground motion magnification factor shown in Figure 4 was supported by data points plotted to a limited value range of the directivity parameter [$X\cos(\theta)$ value up to 0.8], but the proposed equation was extrapolated to a larger directivity parameter [$X\cos(\theta)$ value up to 1] required for design interest. We pointed out to the seismologists and the Peer Review Panel that the extrapolation was obscured by the log–log plot and that the extrapolation to the range of design interest involved several fold factors above what is supported by data. Realization of this issue led to an intense effort including hiring three groups of seismologists to conduct fault rupturing simulation analyses for a very long fault to answer the question of whether there is ground motion "saturation effects" after the fault has ruptured a certain fault length. Results from this exercise suggested that indeed ground motion "saturation" would occur at a certain point and the findings led to introducing a cap to the Somerville equation as documented by Abrahamson and Silva (1997). The fault rupturing simulation study eventually resulted in about a 30% increase in the spectral amplitude at a 3-s period as opposed to the 80% increase suggested in the initial probabilistic solution. The ground motion design criteria adopted for the East Span Bay Bridge project was documented in a Fugro-EMI Ground Motion Report (Fugro-EMI, 2001).

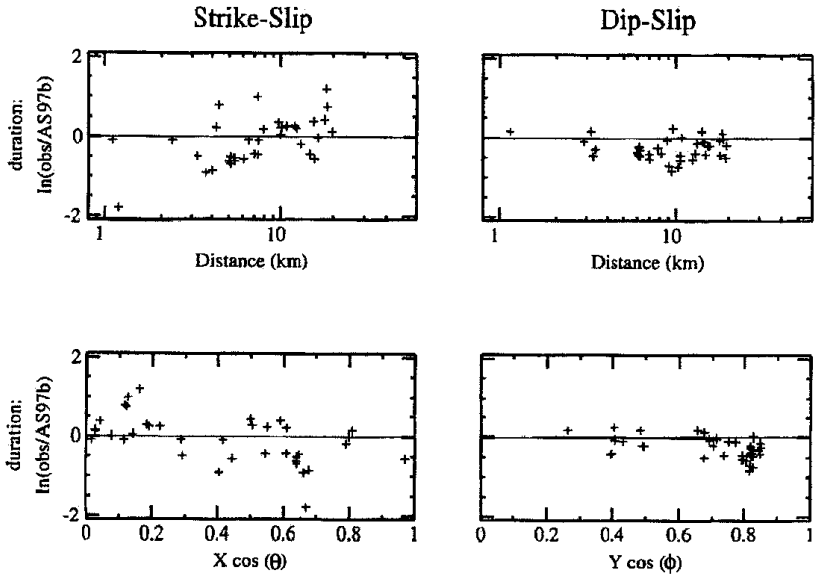

FIGURE 4 Observed versus predicted near-fault directivity strong motion data (Somerville, et al., 1997).

Since the work on the near-fault directivity effects advanced by the East Span Bay Bridge project (Fugro–EMI, 2001), there has been a great deal of advancement in the subject matter, especially the Next Generation Attenuation (NGA–West) activities by Pacific Earthquake Engineering Center (PEER). This major research included collecting an abundance of near-fault strong motion records worldwide and developing ground motion attenuation equations by several groups of seismologists so that there would be independent review and checking among the several teams. The work has been documented by several PEER reports; for example several researchers have advanced the near-fault directivity matter as documented by the PEER report (PEER, 2013) and the pulse-like motion effects on structures by others (Baker, 2007).

The East Span Bay Bridge design has continuously been closely scrutinized by many parties and challenged by political groups including the Legislation Administration Office of California (LAO) as late as 2013 before opening of the East Span Bay Bridge. Therefore, EMI and Caltrans toll bridge program remained vigilant and repeated our Bay Bridge and other Bay Area toll bridge ground motion hazard analyses using the NGA and source models available at the time (EMI, 2009a, 2009b, and 2009c). Our calibration and updated ground motion analyses suggested that for the most parts, the original East Span Bay Bridge Ground Motion criteria is conservative and there may be about a 10% to 15% reserve in the design criteria if the latest and greatest NGA equations are used for design analyses. This is comforting to the design team realizing that the seismology community will continue to propose changes in the future and there is some margin of reserve in the ground motion criteria and hence in the bridge design.

DETERMINISTIC VERSUS PROBABILISTIC

For every project during a 20-year period spanning 1990 to 2010, there were heated debates among the academic community over a deterministic versus a probabilistic design approach. Historically, in California, Caltrans had advocated the use of the deterministic approach for both their ordinary or common bridges (based on a median attenuation) and their other important long-span toll bridges (based on an 84th percentile attenuation). This is consistent with other more critical facilities such as dams. However, after Peer Review introduced the probabilistic approach for comparison during retrofitting of the toll bridges, a formal Ground Motion Committee was set up (chaired by the late Professor Bolt and the late Professor Penzien) for recommending the seismic ground motion criteria for the East Span Bay Bridge project, which resulted in formally adopting the probabilistic approach in California. The committee further recommended a 1,500-year return period for the Safety Evaluation Earthquake (SEE) for the East Span Bay Bridge. Since then, the probabilistic design approach has increasingly been favored as the methodology for developing ground motion design criteria for bridges throughout the United States. The East Span Bay Bridge is locally considered the most important bridge in California, therefore the 1,500-year return period has the effect of setting the upper bound level ground motion criterion for the SEE for bridges. Aside from the East Span Bay Bridge, a 1,000-year return period has often been chosen for other long-span bridges in California [e.g., the Gerald Desmond Cable Stayed Bridge at Port of Long Beach (EMI, 2011)].

Outside California, the probabilistic approach has long been adopted for design, in part because active faults are often poorly mapped in many other states which present implementation problems for the deterministic approach. Major long-span bridges outside California often adopt a 2,500-year return period probabilistic spectrum for SEE. The rationale in adopting a higher

level 2,500-year return period hazard spectrum is because earthquakes, although rare in seismically inactive states, some seismologists have postulated historical earthquakes (e.g., the 1811-1812 New Madrid earthquake and the 1886 Charleston earthquake) had shaking higher than the 1,000-year return period hazard spectrum. Another factor in adopting the 2,500-year return period for important bridges in states outside California may be that the cost involved in designing for a 2,500-year earthquake in eastern United States is less cost-prohibitive than a 2,500-year earthquake in California.

Ordinary or common bridges outside California have traditionally been designed according to AASHTO specifications which has adopted the probabilistic approach for some time. In early years, only the 500-year return hazard maps were available which was the default hazard level for design. Since then a National Center for Earthquake Engineering Research (NCEER)–MCEER project was initiated as long-term multiyear research with the intent to improve the AASHTO specifications. The MCEER seismology team at some points recommended a 2,500-year return period for the SEE for ordinary or common bridges nationally, but this was rejected by the AASHTO committee. With the consensus of bridge engineers from many states, the 1,000-year return period was eventually proposed and approved by AASHTO for ordinary or common bridges. The latest Caltrans Bridge Design Specifications have involved probabilistic 1,000-year return period uniform hazard spectrum but initially still retained some deterministic hazard spectrum criteria to envelope results of both methods. In 2019, Caltrans has abandoned all references of the deterministic criterion and fully adopted a 1,000-year return period probabilistic spectrum for designing ordinary or common bridges, unifying with the AASHTO approach for ordinary or common bridges.

From the designers' perspective, many are indifferent to the ground motion development approach or the philosophies behind the approaches. They are more interested in understanding and correctly applying the actual code requirement, so the resulting design is safe, responsible, and as efficient as possible in terms of the cost of constructing the bridge. The designers must trust that the accepted design level is well vetted and the academic communities to arrive at a consensus, so that the designers can move on with their work, especially for high-profile projects like East Span Bay Bridge. The designers would prefer not to deal with constant changes, especially when the design–construction phase has already commenced. Many major bridge projects take a long time to design and construct. For example the design and construction of the new East Span Bay Bridge occurred over 20 years, encountering several phases of changes in ground motion criteria proposed by the seismologists. These proposed changes caused project delays and higher costs. As several of the postulated changes were proven immature, the authors' opinion is that it seems to be a wiser approach to rely on proven technology for major projects.

From the authors' experience, the probabilistic approach tends to be more stable and robust while a deterministic approach can change significantly (e.g., by changes in the definition of the seismic source, especially in the maximum earthquake magnitude). The probabilistic approach recognizes that large earthquakes are rare and infrequent events make it attractive to many, especially project owners to reasonably quantify design risks. Governmental agencies often need to secure construction funds from a financial world, such as Wall Street, and the interest rates of bonds for bridge construction are tied to risk levels adopted in design. The uniform hazard spectrum (UHS) from the probabilistic analysis provides the basis for defining the risks that are frequently used by financial investors and their insurance companies.

SPECTRUM-COMPATIBLE VERSUS NATURALLY RECORDED INPUT MOTIONS

Another topic that has been hotly debated within the academic community is whether design analyses be conducted using spectrum-compatible or naturally recorded input motions. From our experience, the opinion varies widely depending on the design communities (e.g., bridge versus building engineers, especially the practice is dictated by the makeup of the Peer Review Committee). For highway bridges, the use of spectrum-compatible input motions are widely accepted in all the projects in which we participated. Detailed methodology for developing spectrum-compatible motions, including accounting for the directivity features of near-fault pulse-like motion effects have been presented by Lam and Law (2000).

From experience, the use of spectrum-compatible motions improves the efficiency of the designers tremendously. It requires much fewer input motions for a stable demand solution. Also, the resulting motion has sufficient shaking throughout all periods for excitation of shorter periods (short column bents at approaches), medium periods (taller column bents) and long periods for complex mechanical components (such as cable vibrations for cable supported bridges). Some academicians in building design have argued that actual earthquake ground motions are complicated and there are technical merits to use unmodified input motions to preserve the empirical nature of the earthquake record. However, to justify analyses using a manageable number of input motions, it will be necessary to scale an input motion by a scaling factor. It is common knowledge among seismologists that one will need to apply an identical scaling factor to be applied to all three orthogonal components of the input motion in order to preserve some subtle seismological features (e.g., principal shaking directions). The selection of this single scaling factor becomes a challenge. It will introduce difficulty to achieve a target shaking level in all three component motions to meet the project reference target spectrum criteria. Based on discussions with seismologists (e.g., Abrahamson), at the minimum, naturally recorded (nonspectrum-compatible) motions will involve at least three times the number of spectrum-compatible motions to achieve the equivalent results from spectrum-compatible motions.

During seismic retrofitting of the six California toll bridges listed before, the California Seismic Advisory Seismic Peer Review Panel recommended that Caltrans conduct analyses using a minimum of three sets of spectrum-compatible motions and to design for the envelop of the three sets of input motion demand. The East Span Bay Bridge lies in between two major fault systems: the San Andreas Fault to the west and the Hayward Fault to the ease. Therefore three sets of motions were developed for each of the two events. Figure 5 presents the six sets of the fault normal component displacement time histories generated for the project. As it can be observed in the figure, the time histories are different between the San Andreas and the Hayward event and it is difficult to eliminate certain candidates for design. Eventually, the project team elected to design for all six component motions and to design for the envelope of the six sets of spectrum-compatible motions. If it is to adopt the approach of natural recorded motion, but have the same scaling factor applied to all three component motions, one would expect that it require to envelope the demand of a minimum of nine sets of input motions for seismic retrofitting of the six toll bridges, and may involve enveloping 18 sets of input motions for the East Span Bay Bridge project. Not only does it involve much more design and analysis effort, it may be overly conservative and result in a risk target very far from the intended target.

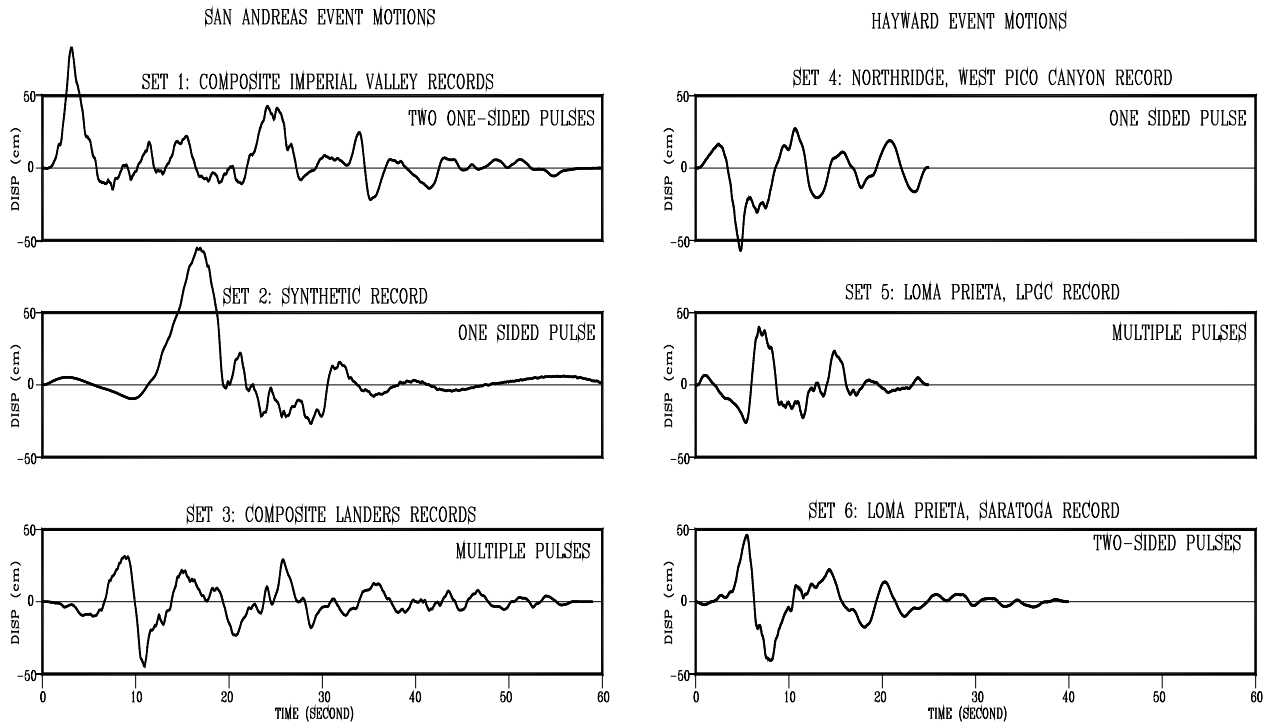

FIGURE 5 Fault normal displacement time history record from the six sets input motions from the East Span Bay Bridge project.

There is a problem in the conservative enveloping multiple input motion concept. Even if one elects to envelop many input motions, there is still a reasonable chance that an additional set of motions can exceed the established envelope. In other projects that we were involved in for designing port facilities, the project team elected to conduct analyses using a larger number of input motions and when the number of input motions is sufficiently large to generate statistically stable solutions, it can be justified to design for a demand other than the enveloping approach (i.e., median or an 84th percentile demand value). Such a statistically based approach will eventually lead to a stable demand criterion if a sufficiently large number of input motions be adopted for design analyses. It will require design analyses using at least seven sets of spectrum-compatible input motion, each reflecting a geologically independent event to justify a statistically based (non-enveloping) ground motion approach. Analyses using spectrum-compatible motions tends to achieve the objective of a statistically stable and yet robust design with fewer number of input motions.

Figure 6 presents time history characteristics of a naturally recorded input motion prior to modification and Figure 7 presents the time history characteristics of the same record after modification for spectrum-compatibility. Figure 8 compares the response spectra for the two records before and after spectrum-compatible modifications. It is hard to distinguish the difference in the time domain representation. The use of the spectrum-compatible time history approach is a convenient way to guarantee that the input motion has provided a minimum but well defined ground shaking level for design and that the approach improved the efficiency for the necessary design analyses.

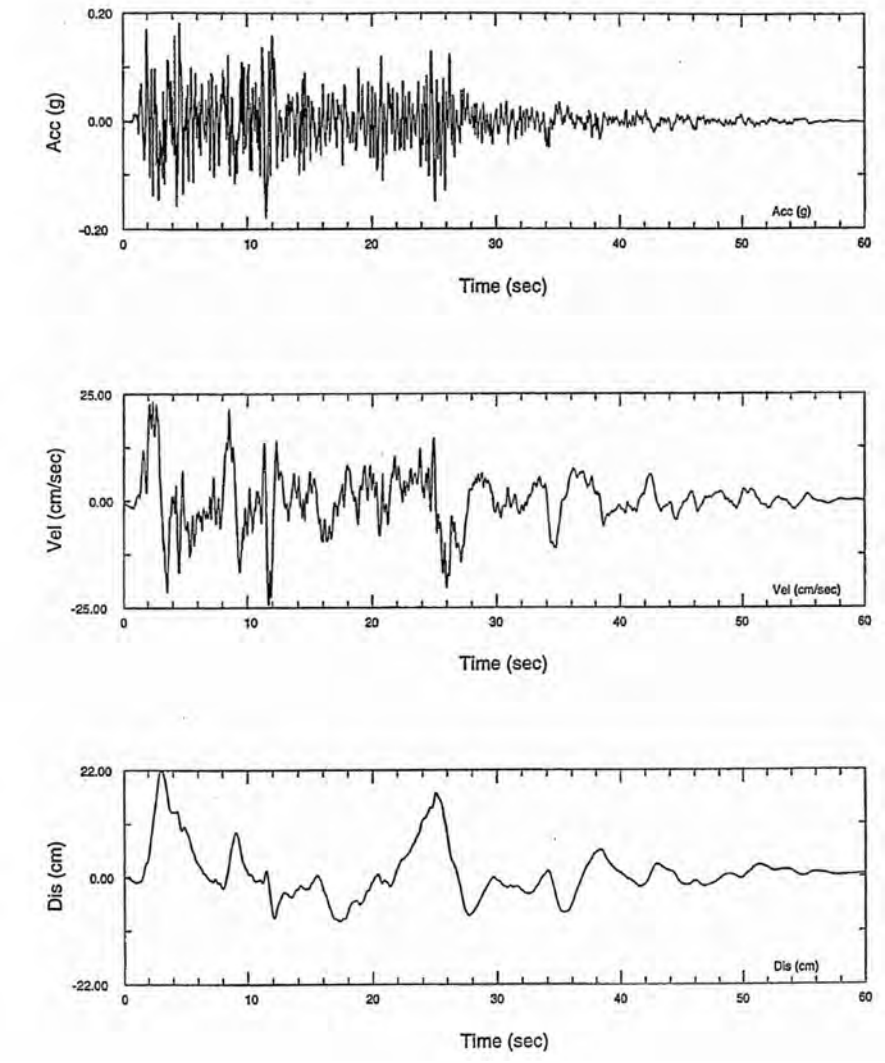

FIGURE 6 Initial time history for fault normal component of El Centro record from 1940 Imperial Valley earthquake.

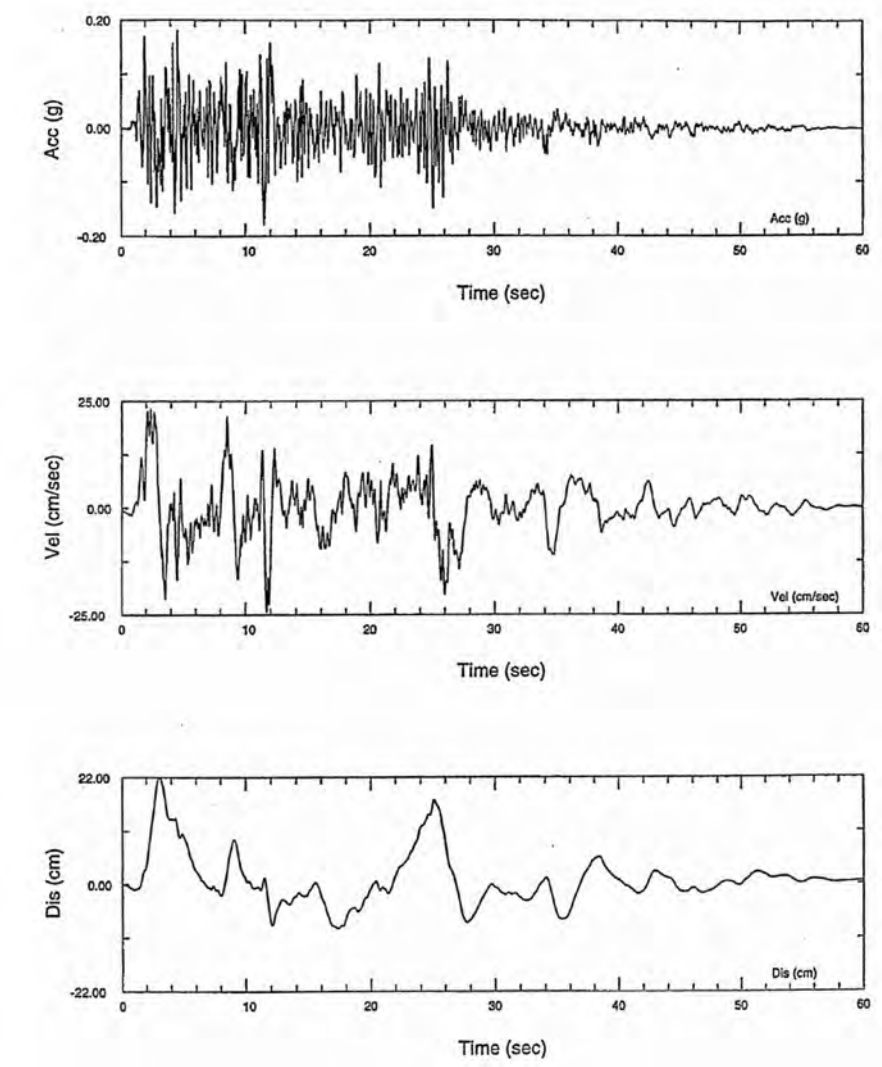

FIGURE 7 Modified motion after spectrum matching.

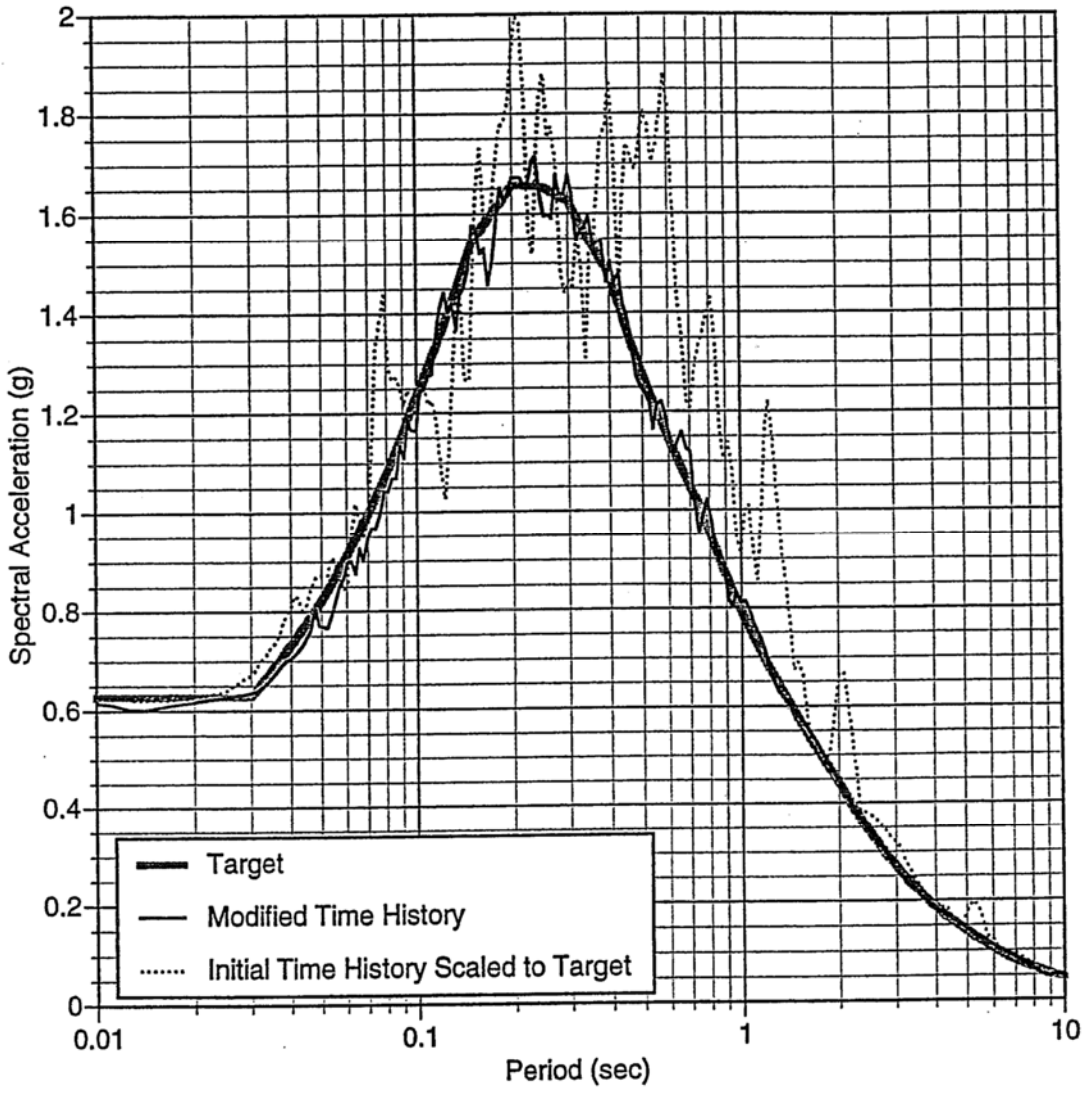

FIGURE 8 Comparison of 5% damped response spectra for the modified fault normal component and initial time history scaled to the target PGA.

CONDITIONAL MEAN SPECTRA VERSUS UHS BASED TIME HISTORY

Design earthquake time histories for California toll bridges were spectrally matched to their target spectra and UHS which were often used as the target in recent bridge projects. There has been a proposal in the academic community to adopt conditional mean spectra (CMS). The UHS is inherently conservative in that it is computed for each spectral period independent of the ground motions at other spectral periods. Observations show a correlation between ground motion amplitudes at multiple spectral periods (Baker and Jayaram, 2008). Given this observation, the selection and associated dynamic analyses using the CMS rather than the UHS can be a more

realistic representation of the expected seismic energy, especially for sites in which the deaggregation results are bi- or even trimodal in their distribution, and the structural response is governed by a narrow range of vibration periods.

The use of CMS had been discussed within the Caltrans toll bridge program along with the Seismic Peer Review Panel. To properly consider the intent of CMS, it would be necessary to anchor the CMS to the UHS at the fundamental period of the structure. However many long span bridges are expected to have a broad range of structural periods owing to the fact that different column heights give rise to different vibration characteristics. Therefore, the use of the CMS spectra as a replacement for the UHS for a bridge structure is problematic since a typical long span bridge structure does not have a narrow range of vibrational periods. Time histories need to be generated to fit multiple CMS curves that are anchored to UHS at several periods. It becomes impractical to implement CMS as many more seismic analyses are needed than when using the traditional UHS approach. Figure 9 shows an example of CMS curves that are anchored to UHS at PGA, 0.2 and 1.0 s. To adequately cover structural periods, it would be necessary to generate time histories that are spectrally matched to all CMS curves on the figure. To the authors' knowledge, no Caltrans bridge project adopted the CMS curve to generate spectrum-compatible time histories. Other than CMS, "risk-targeted" ground motion is also rejected in the bridge design community. The authors feel that predefining risk coefficients applied in the "risk-targeted" ground motion are not appropriate for the development of seismic ground motion as structural performance is usually defined by strain limits in a capacity side, rather than in a demand side.

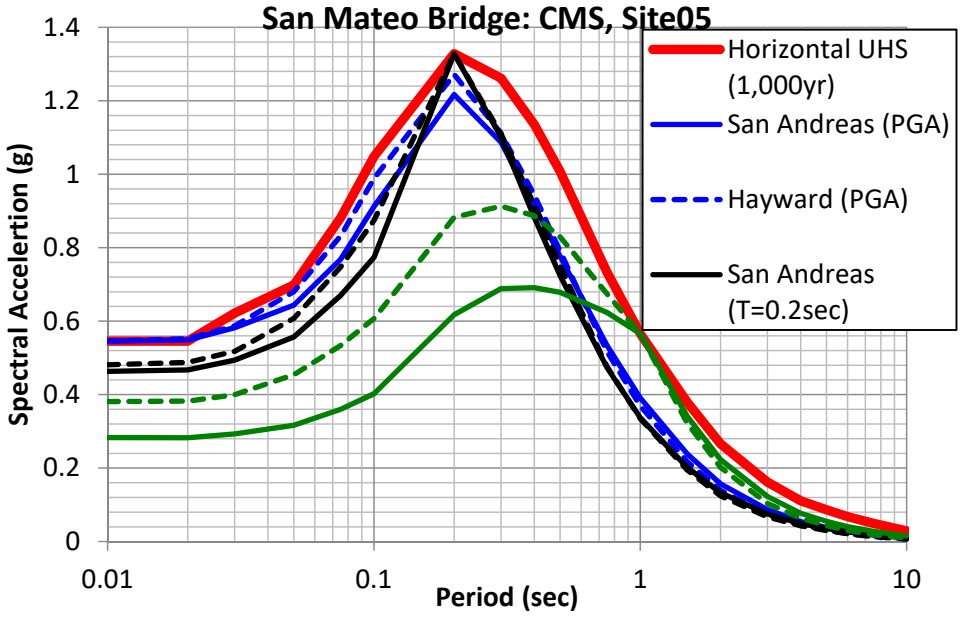

FIGURE 9 1,000-year UHS and CMS spectra for PGA, T = 0.2 and 1.0 s from the San Andreas and Hayward events.

VERTICAL MOTION GROUND MOTION

Vertical input motion criteria is another topic that needs to be addressed. We again will use the East Span Bay Bridge experience to discuss the subject matter in the context of time history analysis design approach and then comment on vertical response spectrum design issues for ordinary or common bridges.

Most of the long span bridges are over water at soft soil sites and horizontal motion site response analyses based on vertically propagating shear wave principles would be the state of practice for design. There had been a lot of debate whether it is appropriate to treat the vertical component motion in the same way by conducting vertically propagating compressional wave analyses to develop vertical input motion for design analyses. Experienced geotechnical engineers have known that vertical site response analyses invariably will yield very high amplitude vertical motions to the degree that cannot be supported by available strong motion recordings. Other consultants who participated in Caltrans toll bridge retrofit contracts also recognized the problem in vertical site response analyses, but still proposed conducting vertical motion site response analyses. But they elected to use a fictitious compressional wave profile, without providing any rationale for their analyses. They proposed to use the same identical fictitiously generated soil column properties for all vertical site response analyses.

The subject matter was discussed with the Peer Review Panel member, I. M. Idriss in the course of the East Span Bay Bridge project. Idriss proposed to evaluate the problem by examining empirical strong motion data, particularly using available downhole array data. He contacted geotechnical researchers around the world, many of them in Japan who have most of the downhole strong motion array data. Our project team then made use of these downhole array data to conduct vertical soil column wave propagation and cross correlation analyses to evaluate how vertical ground motions propagate from depth to ground surface. This enabled the team to identify the apparent wave speed for the propagation of the vertical motions from downhole arrays. Similar studies using downhole array data have been conducted for the horizontal component motion which provided credibility to the horizontal site response analysis procedure (Elgamal et al., 1995).

Our downhole array vertical motion study including the work from the University of California, San Diego (Elgamal et al., 1995), confirmed that vertical motions are complex and vertically propagating compressional wave theory alone cannot account for observed vertical ground motion recordings. This supports our belief that vertical site response analyses will introduce significant errors. In consultation with the Peer Review Panel, all our Caltrans projects used empirical vertical motion recordings directly for design without conducting site response analyses. However, outside California, some geotechnical engineers have continued to conduct vertical site response analyses with the blessings of their Peer Review Panel. We are aware of various modeling issues which make it difficult to capture vertical motion response properly and exaggerates the vertical ground motions from site response analyses. We believe that the damage effects from vertical motions are often over exaggerated in view of the very short duration of the vertical motion response.

For ordinary or common bridges, vertical motion effects theoretically should be taken into account by modal superposition analyses using a vertical response spectrum. However, to our knowledge, such practices were rarely conducted due to difficulty to capture very high frequency modes in vertical response. The Caltrans Seismic Design Criteria (SDC) for ordinary or common bridges most often relies on presumptive methods, such as using a pseudostatic vertical force coefficient to design for vertical shaking effects, except in unusual circumstances, such as when outrigger bents are encountered.

LONGITUDINAL RESPONSE FOR LONG VIADUCT STRUCTURES

Another bridge design problem that we encountered in the course of our retrofit projects was the issue of longitudinal response of long viaducts. Demand analyses for ordinary or common bridges are conducted by the RSA method which implicitly implies that the input motions along the full length of the bridge are identical and in-synchronous over the extended longitudinal length of the viaduct. In conjunction with the assumption of synchronized ground motions, a linear RSA does not consider geometric nonlinearity at expansion joints. Such analysis assumptions led to large longitudinal displacement results which have sometimes led to concerns by the designers about the stability of the viaduct (e.g., collapse from the p-delta effects). These concerns resulted in costly proposals to strengthen the stiffness of some intermediate bents and/or the abutments. Professor Nigel Priestley, who served on the Peer Review Panel for several long viaduct structures, objected to the notion that long viaducts are inherently unstable and considered the large longitudinal displacement response issue to be unrealistic due to over exaggeration of resonance response arising from the afore mentioned over idealization in the input ground motion as well as linearized structural modeling simplifications. He, along with other Peer Review Panel members, commented that most of the evidence of structural collapse in long viaduct structures (including the Cypress viaduct that collapsed in the 1989 Loma Prieta earthquake) relates to the stiffer transverse bridge response direction or other stiff brittle structural components.

LONG-PERIOD RESPONSE SPECTRUM

The characterization of long periods in the response spectrum is an important issue for the design of long-span bridges or other long-period structures. Many of old (nondigital era) strong motion records are unreliable at long periods (>2.5 s). Many geotechnical engineers do not pay adequate attention to the long period range of the response spectrum since they are unfamiliar with displacement-based design approaches used in the structural engineering community. They merely made use of the acceleration response spectra which have a very low acceleration value at long period which tends to obscure the high displacement demands at long period range.

The authors recommend to always present the response spectra depicting both the acceleration and the displacement demands simultaneously (such as shown in Figure 10) to structural designers. From our experience, the displacement spectra are more useful and meaningful to structural engineers than the acceleration spectra preferred by seismologists. Some geotechnical engineers are unaware of the problem that displacements at the long period range can introduce problems for displacement-based structural design, because accelerations in this range are low. Both the structural and geotechnical engineer must understand that spectral displacements are proportional to the acceleration value but also to the squares of the period, T. As the example shown in Figure 11 from well-known site factor charts adopted by most geotechnical analyses, the response spectrum is calculated and anchored at the 1-s period, and then acceleration values are extrapolated to longer periods based on the 1/T equation. Such an equation would imply ever increasing displacement values at increasing periods which contradict available strong motion recordings where the displacement will level off and even decrease with period T at long periods. Such site factor procedures can introduce problems for structural design for long period structures, especially at high seismicity states.

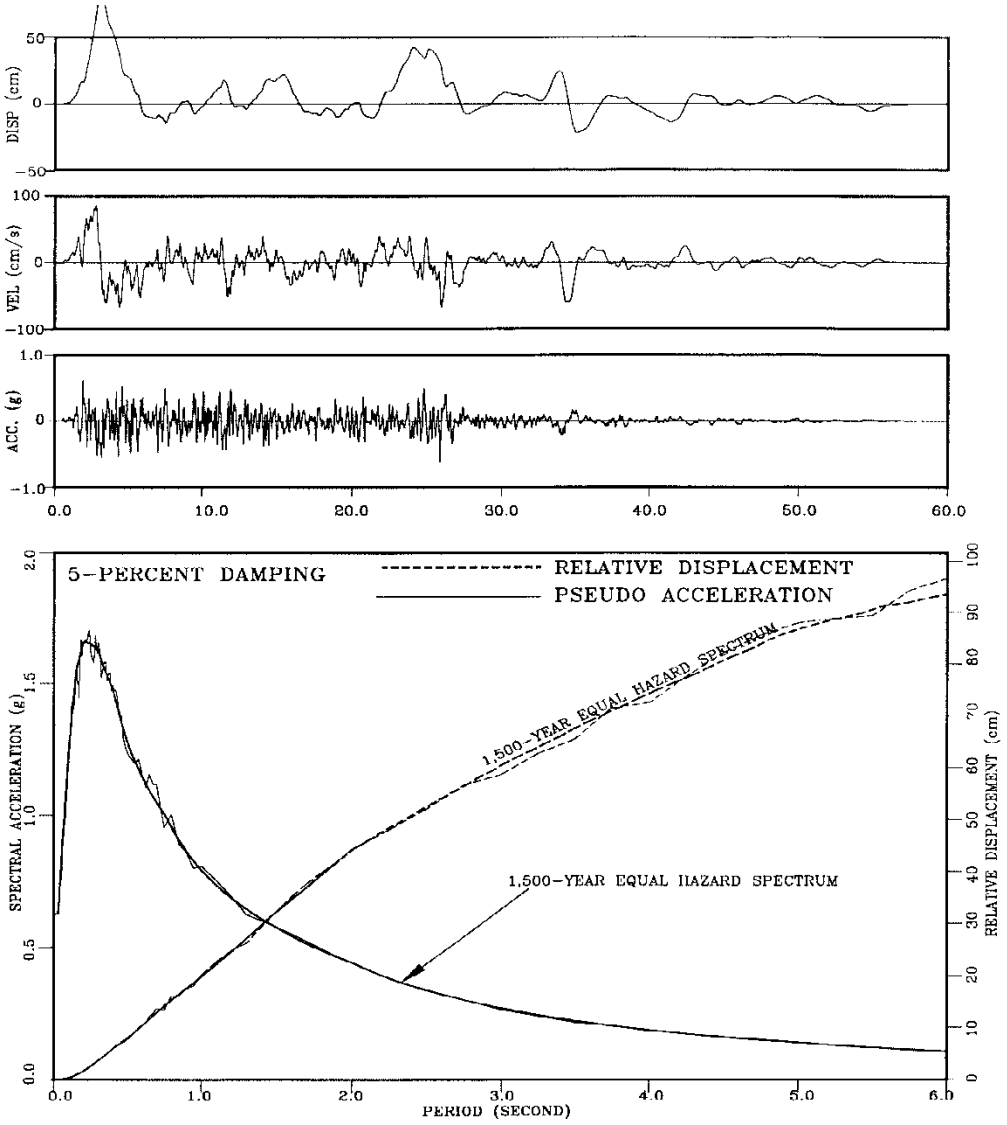

FIGURE 10 Set-1 fault normal component rock motion adopted for East Span Bay Bridge (Fugro–EMI, 2001).

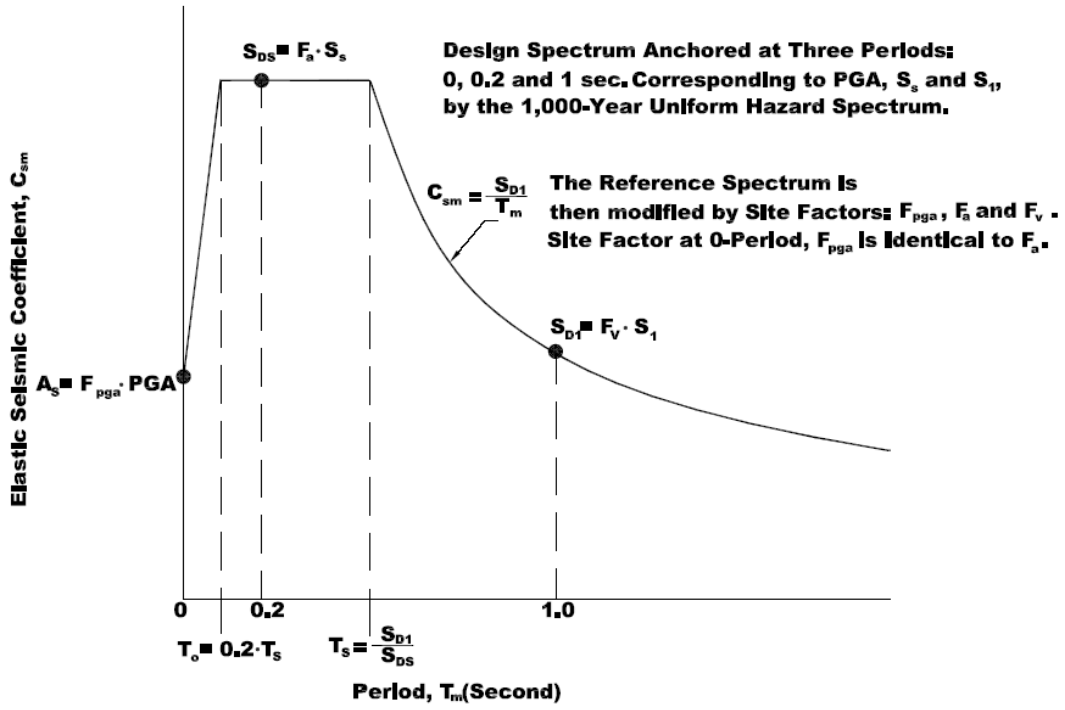

FIGURE 11 Site factor procedures in AASHTO Specifications. (Note that the acceleration spectrum is extrapolated for periods longer than 1 s using the 1/T equation which greatly exaggerated the implication of displacement demand at long periods.)

CONCLUSIONS

The subject of ground motion is a multidiscipline topic which involves all the stake holders in a design project including: administrators and owners, who have to finance and administer the project, as well as geoscientists (seismologists, geologists, and geotechnical engineers) and structural designers. It will take the collaboration and consensus building of the entire team to smoothly navigate the ground motion design issue. It will be necessary for each party to have an appreciation of issues faced by each of the discipline in order to resolve the complex problem. Once a project has been initiated with a defined budget and schedule, continued debates of technical details can be counterproductive. From hindsight, force feeding unproven ground motion subject matter, or trying to conduct seismological research in a fast pace design–construction project schedule can be counterproductive, especially when some of the proposed changes were proven overblown based on our East Span Bay Bridge experience. The bay bridge have seen long period motion at 3-s period increasing by a postulated 80% from the 1995 vintage ground motion criteria, then changed to a 30% increase adopted for the project and eventually found that it still have about a 15% over prediction if we used the latest and the best information as currently compiled by the NGA–West research. There are probably unaccountable over conservatism laden in the design practice. For example, enveloping the demand of six sets of motions with each of them matching a target 1,500-year return period risk level might imply that the

structure has been designed to a return period longer than the assumed 1,500-year return period. In a nutshell, there are many layers of conservatism in a given major project that is difficult to quantify and likely render some of the debates among seismologists relatively minor. Ultimately, the safety of structures might be more dependent on sound structural design strategies (e.g,. designing the structure for toughness and ductile behavior to guard against collapse at over load). The implementation of proper structural detailing might be more important than the exactness of predictions by the geoscientists about the design earthquake. The Bay Bridge included many seismic performance features that are very unique which probably are the real protection for earthquake safety for the bridge. From our experience in working on many bridge projects, there are tremendous benefits to have the seismologists and the structural designers work more closely so that seismologists can appreciate which of the ground motion parameters are of more importance for design.

REFERENCES

Abrahamson, N. A., and W. J. Silva. Empirical Response Spectra Attenuation Relations for Shallow Crustal Earthquakes. *Seismological Research Letters*, Vol. 68, No. 1, 1997. https://doi.org/10.1785/gssrl.68.1.94.

Baker, J. W. Quantitative classification of near-fault ground motions using wavelet analysis. *Bulletin of the Seismological Society of America*, Vol. 97, No. 5, 2007, pp. 1486–1501. https://doi.org/10.1785/0120060255.

Baker, J. W., and N. Jayaram. Correlation of spectral acceleration values from NGA ground motion models. *Earthquake Spectra*, Vol. 24, No. 1, 2008, pp. 299–317. https://doi.org/10.1193/1.2857544.

Earth Mechanics, Inc. Corridor Ground Motion Study Report, San Francisco-Oakland Bay Bridge. Prepared for California Department of Transportation, March 2009a.

Earth Mechanics, Inc. Ground Motion Study Report, Antioch Bridge Seismic Retrofit Project. Prepared for Bay Area Toll Authority and California Department of Transportation, December 2009b.

Earth Mechanics, Inc. Ground Motion Study Report, Dumbarton Bridge Seismic Retrofit Project, Prepared for Bay Area Toll Authority and California Department of Transportation, March 2009c.

Earth Mechanics Inc., 2011. Seismic Ground Motion Report for Gerald Desmond Bridge Replacement Project, Long Beach, California, Prepared for Parsons/HNTB Joint Venture, June.

Elgamal, A. W., M. Zeghal, H. T. Tang, and J. C. Stepp. Lotung Downhole Array. I: Evaluation of Site Dynamic Properties. *Journal of Geotechnical Engineering*, Vol. 121, No. 4, 1995. https://doi.org/10.1061/(ASCE)0733-9410(1995)121:4(350).

Fugro–EMI. *Ground Motion Report.* San Francisco–Oakland Bay Bridge East Span Seismic Safety Project. Prepared for California Department of Transportation, 2001.

Geomatrix. Seismic Response Study for Proposed Carquinez Bridge. Contract No. 59K167. Prepared for California Department of Transportation, Division of Structures, 1993.

Geomatrix (1995). Adjustments to Rock Response Spectra for Caltrans Toll Bridges in Northern California. Report prepared for California Department of Transportation, Division of Structures, 1995.

Housner, G. W. Competing Against Time: Report to Governor George Deukmejian from the Governor's Board of Inquiry on the 1989 Loma Prieta Earthquake, May 1990.

Housner, G. W., and C. C. Thiel, Jr. The Continuing Challenge: Report on the Performance of State Bridges in the Northridge Earthquake. *Earthquake Spectra*, Vol. 11, No. 4, Nov. 1995, pp. 607–636. https://doi.org/10.1193/1.1585829.

Lam, I. P., and H. Law. *Soil-Structure Interaction of Bridges for Seismic Analysis.* Technical Report MCEER-00-0008. University at Buffalo, the State University of New York, 2000.

Mualchin, L., and A. L. Jones. (1992). Peak Acceleration from Maximum Credible Earthquakes in California Rock and Stiff Soil Sites. Open-File Report 92-1. California Department Conservation, Division Mines and Geologist, 1992.

PEER. Final Report of the NGA–West 2 Directivity Working Group (P. Spudich, ed.). USGS, 2013.
Somerville, P. G., N. F. Smith, R. W. Graves, and N. A. Abrahamson. Modification of Empirical strong ground motion attenuation relations to include the amplitude and duration effects of rupture directivity. *Seismological Research Letters*, Vol. 68, No. 1, 1997, pp. 199–222. https://doi.org/10.1785/gssrl.68.1.199.

Development of Deep Foundation Design for Highway Bridges in United States Considering Earthquake-Induced Liquefaction and Lateral Spread

A Synopsis

SHARID K. AMIRI
California Department of Transportation

After World War II, President Eisenhower proposed a national highway network that eventually became the U.S. Interstate Highway System (IHS). This led to considerable construction of highway bridges in the United States that began in the early 1960s. Thirteen states are considered the "seismic states" in the United States and the impact of earthquake events on the performance of our IHS plays a crucial role in the lives of our people and the economy of our country.

Performance of highway bridges relies considerably on its foundation system, which is especially true when the highway bridges are subject to geoseismic hazards. This paper presents a summary of the developments for the deep foundation design and analysis methods for highway bridges considering liquefaction and lateral spread corresponding to the major earthquake events that shaped them, spanning from the 1960's to the present time.

PRE-1964 ALASKA EARTHQUAKE

When analyzing the response of a deep foundation under earthquake conditions, one of the main elements is the assessment of the pile behavior under the lateral load. Matlock and Reese (1960) contributed to the evaluation of pile capacities and generalized solutions for laterally loaded piles using beam on elastic foundation theory to include the nonlinearity for force-deformation characteristics of the soil.

Soil modulus is defined as:

$$E_s = -p/y$$

and

$$p = EI\, d^4y/d^4x$$

where

p = soil resistance expressed as force per unit length of pile;
x = incremental pile length;
y = lateral deflection of the pile;
E = elastic modulus of pile; and
I = moment inertia of pile.

1964: ALASKA (ANCHORAGE) EARTHQUAKE

On March 27, 1964, the “Good Friday” or Great Alaska Earthquake struck with a moment magnitude of 9.2 and was one of the most powerful earthquakes in the 20th century. The epicenter of this northern American continent earthquake was in the Chugach Mountains near the northern end of Prince William Sound about 80 mi east–southeast of Anchorage. In terms of human loss, 114 people lost their lives and private property damage was estimated at $311 million in 1964 value (Amiri, 2008). The earthquake caused extensive damage to highway bridges. Nine bridges suffered complete collapse and 26 suffered severe deformation or partial collapse. The earthquake also caused extensive damage to a wide variety of bridge foundation types located within approximately 80 mi from the epicenter. A review of the bridge foundation performance did indicate that areas of major damage coincided with areas of major liquefaction. Post-earthquake investigation showed liquefaction of the foundation soil, the resulting loss of the foundation soil and major displacement at the abutments and piers, were major contributing factors for the damage. (Martin, 1979). Figure 1 shows the partial collapse of a bridge during the Alaska Earthquake.

The 1964 Alaskan earthquake demonstrated that bridge structures built in liquefiable soils and subject to lateral spread could suffer severely from liquefaction-induced lateral spread.

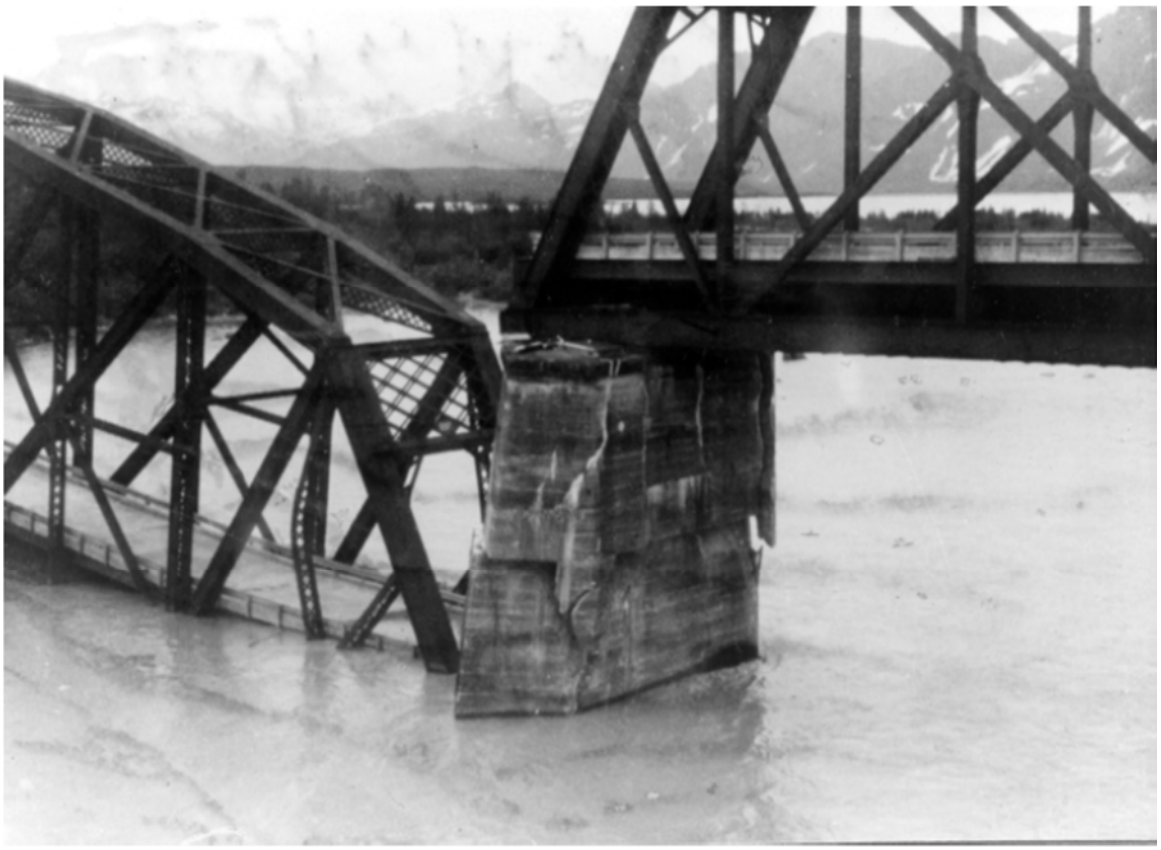

FIGURE 1 Span collapse, Million Dollar Bridge, Copper River Highway (USGS, 1968).

1964: NIIGATA EARTHQUAKE

The June 16, 1964, Niigata earthquake, with the moment magnitude of 7.5, occurred at 1:01 p.m. The epicenter of this Japanese earthquake was located near Awa Island in the Japan Sea, 22 km off the coast with the focus 25 mi (40 km) deep, about 31 mi (50 km) from the Niigata city. In terms of human loss, 26 people lost their lives (Auckland Regional Government, 2008).

The collapse of the 12-span steel girder Showa Bridge (Figure 2) was one of the worst instances of damage to structures during the Niigata earthquake. Five simply supported girders fell into the water. Post-earthquake reconnaissance showed that the retrieved steel pipe piles did undergo damage and were bent due to the liquefaction-induced lateral ground movement. The permanent ground displacement reached several meters substantially deforming the foundation piles and causing the girders to fall (Figure 3).

FIGURE 2 Showa Bridge collapse (Kramer and Elgamal, 2001).

FIGURE 3 Damage to a pile by 6+ ft of ground displacement (Finn and Fujita, 2002).

POST ALASKA AND NIIGATA EARTHQUAKE

The 1964 Alaska and Niigata Earthquakes shed light on the performance of the bridges subject to earthquake and lessons learned from their failure. These two earthquakes helped identify liquefaction as a major problem in earthquake engineering and much was learned from examination of soil behavior in these two events (Caltrans Seismic Advisory Board, 2003). They marked the dawn of an important period in the study of the geoseismic hazards, mainly the liquefaction phenomenon of the saturated granular sand, the role of which played a critical role on the performance of the highway bridges. The catastrophic failures in these earthquakes provided a sobering reminder that liquefaction of sandy soils because of earthquake ground shaking poses a major threat to the safety of civil engineering structures (Seed and Idriss,1971).

1970: LATERAL RESPONSE OF DEEP FOUNDATION IN SOFT CLAY

Matlock (1970) performed lateral load tests with an instrumented steel pipe pile that was 324 mm (12.75 in.) in diameter and 12.8 m (42 ft) long. The test pile was driven into clay near Lake Austin, Texas, that had an average shear strength of about 38 kPa (800 psf). The test pile was exhumed after the first test and taken to Sabine Pass, Texas, and driven into soft clay with a shear strength that averaged about 14.4 kPa (300 psf) in the significant upper zone. Pile bending moments were measured by instrumentation and the soil response was evaluated by differentiation. The *p–y* curves developed for and the lateral response of the pile in soft clay (Figure 4) forms the basis for designing piles in liquefiable soil, modeled as soft clay subject to earthquake.

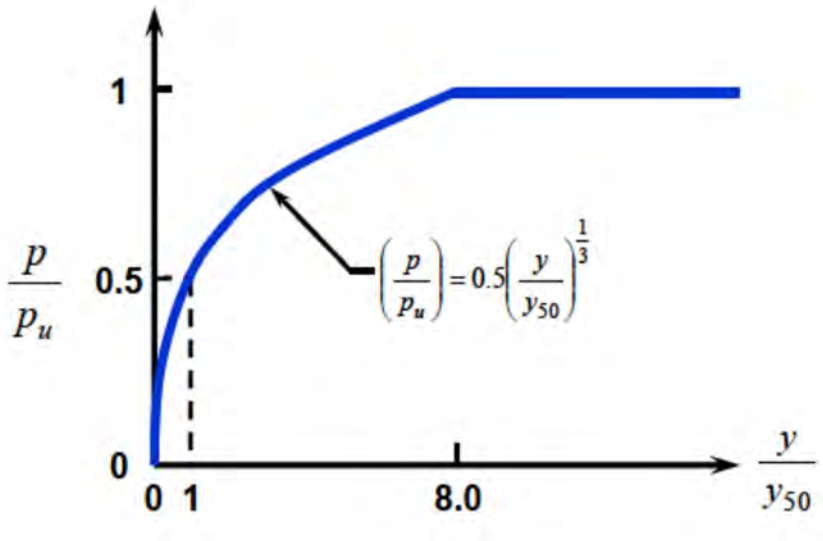

FIGURE 4 *p–y* curves in soft clay.

1971: SAN FERNANDO (SYLMAR) EARTHQUAKE

The February 9, 1971, earthquake rolled across Southern California, leaving 65 dead and considerable damage to the civil structures and highway facilities (Figure 5). The earthquake presented a major turning point in the development of SDC for bridges in the United States. Prior to 1971 the AASHTO specifications for the seismic design of bridges were based in part on the lateral force requirements for buildings developed by the Structural Engineers Association of Ca1ifornia. In 1973 Caltrans introduced new SDC for bridges that included the relationship of the site to active faults, the seismic response of the soils at the site and the dynamic response characteristics of the bridge (Sharpe and Mayes, 1979). In California, the February 1971 San Fernando earthquake caused bridge damage far in excess of any previous California earthquake. From 1933 until 1971, 11 separate earthquakes ranging in magnitude from 5.4 to 7.7 affected approximately 1,100 bridge structures in California. In no case were any of these bridges close to the area of intense shaking. The total damage sustained from these events (not including San Fernando) amounted to about $100 million in today's dollars. Only 33 bridges were damaged during these years and the damage was primarily nonvibrational in nature. In contrast, during the 1971 San Fernando (Sylmar) earthquake, 67 bridges on five major freeways were damaged.

The recurring themes which seem to appear in discussions of numerous failures of bridges in earthquakes are true in the bridge failures of the San Fernando earthquake. Generally, superstructures behaved well with major damage to girders occurring upon impact when they fell to the ground. Except for such impacts on falling, the superstructures generally showed only minor damage to joints and near abutments. Throughout the area extensive damage was incurred at abutments where large foundation movements took place and where consolidation and compaction of loose strata produced large differential movements. Consequent settlement and both transverse and longitudinal movement of abutments and piers literally pulled the supports out from under girders, producing heavy demands on other columns and abutments to attempt to stabilize the structure. Lack of restraining devices at bearings, hinges, and joints permitted the girders to pull free from the supports and fall to the ground.

FIGURE 5 I-5 and Route 14 interchange.

1971: SAN FERNANDO DAM FAILURE

The Upper Van Norman Reservoir with a capacity of 1,800 acre-ft, was damaged by the February 1971 San Fernando earthquake. The Upper San Fernando dam, which was built in 1919–1921, is about 1,200 ft in length along its axis and about 60 ft high. It settled about 3 ft and displaced laterally about 5 ft at the crest. However, the dam did not collapse.

From a geoseismic perspective, liquefaction-induced ground movements and slope failures caused substantial structural damage. Studies of the sliding mechanisms and dynamic instabilities affecting the San Fernando Dams have improved our understanding of soil liquefaction. Seed (1990) proposed a technique for evaluation of in situ undrained residual strength based on Standard Penetration testing. He presented the results of back-analyses of several liquefaction failures from which values of the residual undrained strength could be calculated for soil zones in which SPTs are available. This technique is often used in modeling the lateral response of the highway bridge foundation subject to liquefaction and the evaluation of the liquefaction-induced lateral spread.

1971: LIQUEFACTION TRIGGERING EVALUATION METHODOLOGY

Seed and Idriss (1971) provided a simplified procedure to evaluate liquefaction potential of soil deposits. The procedure consisted of directly using the SPT blow counts in the field to quantify the potential for liquefaction. A different approach was initiated by Castro (Castro, 1975) which consisted of conducting cyclic triaxial tests to evaluate the liquefaction potential. Both methods recognized the importance of developing methods for liquefaction triggering evaluation, given the massive failures of structures due to their foundation performance.

The current approaches for evaluating the potential for triggering liquefaction and for developing defensive measures were instigated by the results of field studies following the occurrence of the 1964 Alaska (Anchorage) and Niigata earthquakes. These were followed by extensive laboratory studies on small and large samples tested on shaking tables to evaluate the factors that influence the onset of liquefaction, the consequences of liquefaction, and how to mitigate these consequences. Field-based procedures for assessing the liquefaction potential were developed to overcome many of the difficulties of obtaining representative samples of cohesionless soils (Caltrans Seismic Advisory Board, 2003).

1974: LATERAL RESPONSE OF DEEP FOUNDATION IN SAND

Reese (1974) performed lateral load tests where data were taken during the lateral loading of two 24-in. diameter test piles installed at a site where the soil consisted of clean fine sand to silty fine sand. Two types of loading were employed, static loading and cyclic loading. The data were analyzed, and families of curves were developed which showed the soil behavior presented in terms of soil resistance p as a function of pile deflection y (Figure 6).

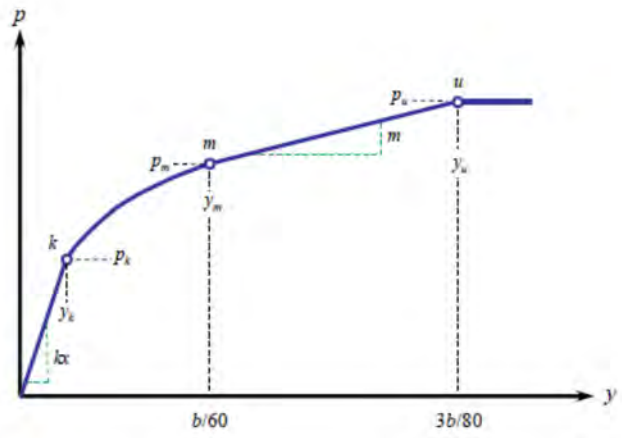

FIGURE 6 Characteristics shape of *p–y* curves for static and cyclic loading in sand.

1975: EFFECTIVE STRESS APPROACH IN LIQUEFACTION ANALYSIS

Martin and Finn (1975) developed computational methods for the mechanism of progressive pore water pressure increases and its buildup during cyclic loading theoretically using effective stress parameters of the sand. The computational methods using effective stress approach were of considerable benefit in improving the evaluation of the liquefaction potential during earthquakes.

1979: SEISMIC DESIGN CONSIDERATIONS FOR BRIDGE FOUNDATIONS AND SITE LIQUEFACTION POTENTIAL

Martin recognized the importance of lateral ground displacement due to liquefaction and its impact on the bridge foundation: “The application of pile stiffness characteristics to determine earthquake-induced pile bending moments using a pseudostatic approach, assumes that moments are induced only by lateral loads arising from inertial effects on the bridge structure. However, it must be remembered that the inertial loads are generated by interaction of the free-field earthquake response with the piles, and that the free-field displacements themselves can influence bending moments” (Martin, 1979).

1979: IMPERIAL VALLEY EARTHQUAKE

On October 15, 1979, a magnitude 6.6 earthquake struck the Imperial Valley near El Centro, California. The earthquake produced a 22-mi-long (35-km-long) surface rupture on the Imperial Fault, the same fault that ruptured during the 1940 El Centro earthquake and generated sand boils, ground cracks, and other surficial liquefaction effects at many localities. Damage caused by liquefaction included differential settlements. Site liquefaction investigation was performed using CPT and SPT.

The cone penetrometer is an efficient and effective tool for determining subsurface stratigraphy. CPT values proved useful for identifying sediment layers, making qualitative estimates

of soil types and relative densities, and determining which layers liquified. Preliminary stratigraphy based on CPT data allowed optimal placement of SPT and other tests and in selection of locations for taking samples. *N*-values estimated from CPT data permitted predictions of liquefaction susceptibility that were consistent with similar estimates from SPT data and generally consistent with field behavior (Youd et al, 1983).

The bridge over the New River west of Brawley, California, was damaged and had to be closed after the earthquake (Figure 7). During the earthquake, ground displacements caused by settling (0.15 m) and slumping (0.1 mr) of the approach fill and streambank caused the superstructures of the bridges to rotate counterclockwise (0.3 degree). This movement cracked and tilted several supporting piles (Caltrans, 1979).

1980: EVALUATION OF CONE PENETROMETER (CPT) FOR LIQUEFACTION HAZARD ASSESSMENT

The applicability of CPT in evaluating the liquefaction hazard potential was addressed by Martin and Douglas in their 1980 published report (Martin and Douglas, 1980) which described the activities and results of the investigations of the correspondence between CPT and SPT performed. The program involved performance of CPTs and SPTs at several sites in California and at one site in Oklahoma. The comparison of the correspondence between those test results had as a primary goal the development of a data base facilitating the use of the CPT for use in liquefaction potential assessments.

FIGURE 7 State Highway 86 bridge over New River.

1984: DESIGN OF PILES AND DRILLED SHAFTS UNDER LATERAL LOAD

The *p–y* method was developed originally from proprietary research sponsored by the petroleum industry in the 1950s and 1960s. During this period, large piles were being designed to support offshore oil production platforms. These structures were to be subjected to remarkably large horizontal forces from storm waves and wind. Rules and recommendations for the use of the *p–y* method for design of such piles are presented by the American Petroleum Institute (API, 2010).

The use of the *p–y* method has been extended to the design of onshore foundations. For example, FHWA has sponsored a reference publication dealing with the design of piles and drilled shafts under lateral load for transportation facilities (Reese, 1984).

1985: NRC WORKSHOP ON LIQUEFACTION OF SOILS DURING EARTHQUAKES

Twenty-one years after the Alaska and Niigata earthquakes, a workshop was organized by the Committee on Earthquake Engineering of the National Academies of Science, Engineering, and Medicine at which liquefaction specialists from United States, Japan, Canada and the United Kingdom came together to discuss the state of knowledge at the time and agree on directions for the future (NRC, 1985). Amongst the recommendations at the conclusion of the workshop, were the need for assessing liquefaction for soils other than clean sands, instrumentation of sites subject to liquefaction, and methods for evaluating magnitude of permanent soil deformation due to liquefaction. The committee recommended the standard procedure for evaluating liquefaction primary based on the studies by Seed and Idriss (1971).

1986: FHWA SEISMIC DESIGN OF HIGHWAY BRIDGE FOUNDATIONS

The first specific guidelines with respect to bridge foundation analysis and design during earthquake loading, where a bridge designer could find specific guidance on the various facets of seismic foundation design was published by Lam and Martin (1986).The new design guidelines presented in this document were intended to supplement the existing seismic design guidelines by FHWA–AASHTO at the time. The procedures for liquefaction potential, dynamic settlement, pile and pile group stiffness, deformation behavior of piles and pile groups, drilled piers stiffness, earth pressure on abutment walls and others were presented. Moreover, the role of battered piles was also discussed and evaluated.

1987: EDGECUMBE, NEW ZEALAND, EARTHQUAKE

Liquefaction also occurred at the Landing Road Bridge during the 1987 earthquake in Edgecumbe, New Zealand. In this case, the approach spans over the riverbank were supported on concrete wall piers founded on battered prestressed concrete piles. Liquefaction-induced lateral spreads in the liquefiable sand layer were of the order of 2 m (6.5 ft). Back-analyses and observations from site excavations indicated that the piles successfully resisted the passive pressures mobilized against the piers, although cracks in the piles suggested that plastic hinges were on the verge of forming, as shown schematically in Figure 8 (Berrill et al., 1997).

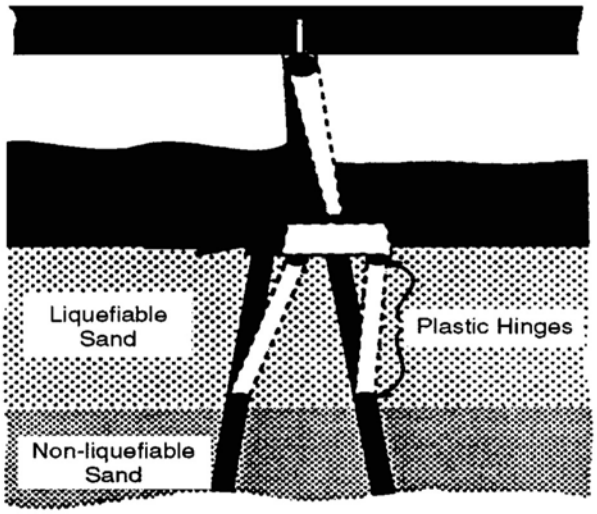

FIGURE 8 Substructure collapse mechanism.

1990: CYCLIC PORE PRESSURE GENERATION AND UNDRAINED RESIDUAL STRENGTH

Seed and Harder (1990) recommended an alternate technique for evaluation of in situ undrained residual strength (S_r) based on Standard Penetration testing. He presented the results of back-analyses of several liquefaction failures from which values of the residual undrained strength could be calculated for soil zones in which SPT data was available, and proposed a correlation between S_r and $(N_1)_{60cs}$. $(N_1)_{60cs}$ is a "corrected" penetration resistance, but with an additional correction for fines content to generate an equivalent "clean sand" blow count as $(N_1)_{60cs} = (N_1)_{60} + N_{corr,}$ where N_{corr} is a function of percent fines (Figure 9).

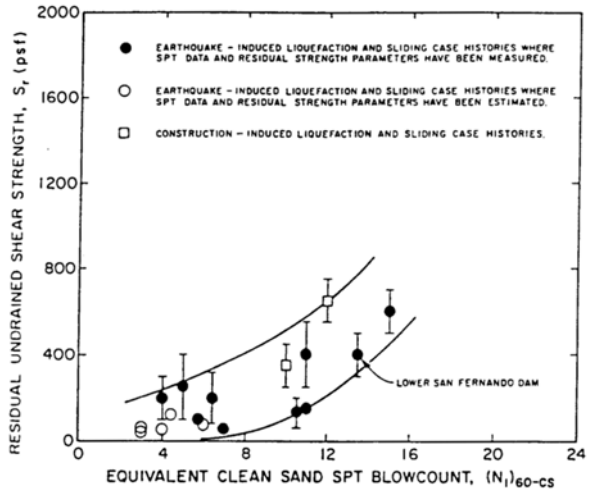

FIGURE 9 Relationship between corrected clean sand blow count $(N_1)_{60cs}$ and undrained residual strength S_r from case studies (Seed and Harder, 1990).

The results of this evaluation are routinely used in practice for design of highway deep foundation practice in liquefiable soil in general and the assessment of the undrained shear strength of the liquefiable soil.

1989: LOMA PRIETA EARTHQUAKE

The moderately large (M_w = 6.9) Loma Prieta earthquake took 63 lives, cost $10 billion, and damaged more than 27,000 structures. The Loma Prieta earthquake occurred on the San Andreas fault in the Santa Cruz Mountains of Northern California. The earthquake caused damage to roads and bridges within about 100 mi of the epicenter including major damage to bridges in the cities of San Francisco and Oakland that resulted in a tragic loss of life. On the Cypress Viaduct in the City of Oakland, 42 people died, and 108 people were injured. One person died and 13 people were injured on the nearby East Bay Crossing of the San Francisco–Oakland Bay Bridge. Approximately 100 bridges suffered some damage from the earthquake. Eleven bridges and several roads were closed, resulting in traffic problems in the weeks and years following the quake (Yashinsky, 1998).

The failure of a bridge across Struve Slough on Highway 1 (Figure 10), demonstrated that piles embedded in soft subsoils can lead to significant damage during earthquake shaking. The bridge was supported on concrete pile columns that were embedded into very soft clay and peat underlying the site. During the earthquakes the piles settled and moved laterally causing plastic deformation and shear failures at top of the piles.

FIGURE 10 Collapse of Struve Bridge–Highway 1, Watsonville, California.

1994: NORTHRIDGE EARTHQUAKE

The 6.8 magnitude Northridge earthquake is the largest event to have occurred in the Los Angeles area in the last century. The epicenter of the earthquake that occurred in the Los Angeles area at 4:31 a.m. local time on January 17, 1994, was located about 19 mi (30 km) west–northwest of Los Angeles in Northridge. In the Northridge earthquake, six major highway bridges collapsed (Figure 11) and 157 other highway bridges were damaged. The estimated cost to replace or repair these bridges was $1.5 billion. Before the Northridge earthquake, the estimated cost of retrofitting the approximately 1,000 bridges remaining on the Caltrans retrofit list was $1.1 billion.

BATTER PILES

Towards the end of the 20th century, poor performance of batter piles in a series of earthquakes cast batter piles in a poor light (Kavazanjian, 2006). The performance of prestressed concrete batter piles supporting container cranes at the Port of Oakland 7th Street Terminal in the 1989 Loma Prieta earthquake was the first of several such incidents. Liquefaction-induced lateral displacement of a rock-fill dike through which the batter piles were driven resulted in shearing of the pile heads. The pier was retrofitted using large diameter vertical drilled piers to replace the batter piles at this location. The earthquake provided insight into the ability of battered pile foundation systems to resist lateral loadings. As discussed earlier, failures of a concrete wharf occurred at the seventh street terminal in Oakland due to the failures of two rows of battered piles installed along the outboard edge of the wharf to resist lateral loads.

Similar damage was observed in prestressed concrete batter piles in the Port of Los Angeles in the 1994 Northridge earthquake.

FIGURE 11 The Antelope Valley Freeway in the aftermath of the 1994 Northridge earthquake.

1995: KOBE EARTHQUAKE

The 1995 Hyogoken–Nambu Earthquake, or Kobe earthquake as it is more commonly known overseas, was an earthquake in Japan that measured 7.3 on the Richter magnitude scale and 6.8 on the moment magnitude scale. It occurred on Tuesday January 17, 1995, at 5:46 a.m. in the southern part of Hyōgo Prefecture and lasted for approximately 20 s. Extensive soil liquefaction and lateral spreading occurred during the Kobe earthquake that led to damage of nonductile piles. Figure 12 shows such damage.

1995: SEISMIC DESIGN OF PILE FOUNDATIONS— STRUCTURAL AND GEOTECHNICAL ISSUES

Martin and Lam (1995) discussed the state of the art on seismic design of pile foundations based on the findings at the time. The 20 years research period prior to 1995 led to a variety of analysis approaches of varying complexity to address a range of dynamic problems. The focus of their discussion was on design concepts and issues more routinely used or encountered by structural engineers during seismic design of new or retrofitted pile foundation systems representative of those used for bridges and buildings. Although the paper focused on simplified design approaches to the soil–pile–structure interaction problem, considering primarily a Winkler spring approach to inertial interaction, it recognized that there is a continued need for developing an improved understanding of the mechanics of nonlinear fully coupled behavior under earthquake loading. The authors suggested carefully planned and designed experiments, involving the combined strengths of nonlinear numerical analyses and centrifuge experiments. A number of design and analysis issues were identified and discussed in the paper, which have significant influence on design analyses and practice. These included:

FIGURE 12 Shearing of pile by ground displacement in Kobe Earthquake (Finn, 2002).

1. Effects of pile installation methods;
2. Effects of pile fixity;
3. Effects of pile stiffness (intact versus cracked);
4. The effects and role of the pile cap;
5. The effects of free-field and localized liquefaction; and
6. Moment-rotation capacity.

1996: NCEER WORKSHOP FOR LIQUEFACTION

In 1996, a workshop sponsored by the NCEER was convened by Professors T. L. Youd and I. M. Idriss with 20 experts to review developments over the previous 10 years. The purpose was to gain consensus on updates and augmentations to the simplified procedure for liquefaction. The report of the proceedings was prepared by the NCEER (1997).

2001: LRFD SEISMIC DESIGN OF BRIDGES

Damaging earthquakes in California, Japan, and around the world demonstrated the earthquake vulnerability of highway bridges that were designed to existing seismic codes. To address this inadequate performance, extensive research programs were carried out. These programs advanced the state of the art to the point where a new specification—LRFD—for seismic design was necessary to take advantage of new insight into ground motion and geotechnical effects, improved performance criteria, and more-advanced analytical and design methodologies. A major study on liquefaction hazard assessment and impacts was conducted to assess the effects of liquefaction and associated hazards, including lateral spreading and ground flow failures. Procedures for quantifying the consequences of liquefaction, such as lateral flow or spreading of approach fills and settlement of liquefied soils, were also given. The provisions also provided specific reference to methods for treating deep foundations extending through soils that are spreading or flowing laterally because of liquefaction (*NCHRP Research Report 472*, 2002).

2006: SEISMIC RETROFITTING MANUAL FOR HIGHWAY STRUCTURES

The seismic retrofitting document (Buckle et al., 2006) improved and updated the 1995 *Seismic Retrofitting Manual for Highway Bridges*. In particular, a performance-based retrofit philosophy was introduced. Performance criteria were given for two earthquake ground motions with different return periods, 100 and 1,000 years. A higher level of performance was required for the event with shorter return period (Lower-level earthquake ground motion) than for the longer return period (upper-level earthquake ground motion). Selection of retrofit strategy based on objectives of retrofitting and acceptable damage were introduced.

2011: LRFD SEISMIC ANALYSIS AND DESIGN OF TRANSPORTATION GEOTECHNICAL FEATURES AND STRUCTURAL FOUNDATIONS

The LRFD seismic document (Kavazanjian et al., 2011) discussed the seismic vulnerability of deep foundations. Perhaps the most recognized case history of pile damage from earthquakes in the United States is the extensive damage to battered piles at the Seventh Street Pier at the Port of Oakland from the 1989 Loma Prieta Earthquake which was discussed earlier in this document. This case history suggests that battered piles are particularly vulnerable to liquefaction-induced lateral spreading but that well-designed pile foundations can perform satisfactorily, even at liquefied sites.

As observed from the case histories of damage to pile foundations in earthquakes, permanent ground displacement is an important load case. The response of a pile foundation to permanent ground deformation is unrelated to the mechanism of inertial loading. Therefore, it is necessary to formulate an additional load case for design of pile foundations subject to earthquake-induced permanent ground displacement. This load case is generally referred as kinematic loading.

2014: LRFD SEISMIC ANALYSIS AND DESIGN OF BRIDGES

The seismic analysis document by Kramer et al. (2014) concluded that essentially there are no data for calibration of reliability-based design procedures using the type of statistical analyses commonly used for calibration of LRFD procedures. Data on the seismic response of full-scale pile foundations subjected to earthquake loading is virtually nonexistent. While a framework for handling uncertainty in pile foundation seismic response can be developed, the appropriate values of that uncertainty are themselves uncertain.

2017: CALTRANS MEMO TO DESIGNERS 20-15: LATERAL SPREADING ANALYSIS FOR NEW AND EXISTING BRIDGES

This memo describes a procedure to estimate the deformation demands (and capacities) of bridge foundations and abutments resulting from liquefaction-induced spreading ground (i.e., horizontal ground displacement).

LOOKING INTO THE FUTURE

The future roadmap for seismic design of the highway pile foundation will be geared toward developing massive data bases that enable the practitioners to calibrate the seismic pile response based on the geoseismic hazards. The consequences of the seismic event and the piles' responses will be monitored and evaluated in real time. There is also ongoing research on the pile response to liquefaction-induced lateral spread considering an effective stress approach that will shed light on a more realistic seismic and kinematic response of the bridge pile foundation. The role of the artificial intelligence (AI) in evaluating the mega data will be important in the future development of the seismic codes for the design of bridge foundation.

REFERENCES

Amiri, S. K. (2008). The Earthquake Response of Bridge Pile Foundations to Liquefaction-Induced Lateral Spread Displacement Demands. PhD dissertation. 2008

American Petroleum Institute. Recommended Practice for Planning, Designing and Constructing Fixed Offshore Platforms, Working Stress Design. 2010.

Auckland Regional Government. 1964 Niigata Earthquake. 2008. Available at http://www.arc.govt.nz/council/civil-defence-emergency-management/natural-hazards/earthquakes.cfm.

Berill, J. B., S. A. Christensen, R. J. Keenan, W. Okada, and J. R. Pettinga. Lateral-Spreading Loads on a Piled Bridge Foundation. In *Seismic Behaviour of Ground and Geotechnical Structures*, 1997.

Buckle, I. G., I. Friedland, J. Mander, G. Martin, R. Nutt, and M. Power. *Technical Report MCEER-06-SP10: Seismic Retrofitting Manual for Highway Structures, Part 1: Bridges*, 2006.

Caltrans Memo to Designers. Lateral Spreading Analysis for New and Existing Bridges, 2017.

Caltrans Seismic Advisory Board. *The Race to Seismic Safety*. 2003.

California Department of Transportation. Supplementary Bridge Report 58-05R (unpublished report), 1979.

Castro. Liquefaction and Cyclic Mobility of Saturated Sands. *Journal of the Geotechnical Engineering Division*, 1975.

Finn, W. D. L., and N. Fujita. Piles in Liquefiable Soils: Seismic Analysis and Design Issues. *Soil Dynamics and Earthquake Engineering*, Vol. 22, 2002, pp. 731–742.

Finn, W. D. L., and N. Fujita. Behavior of Piles in Liquefiable Soils During Earthquakes: Analysis and Design Issues. Fifth International Conference on Case Histories in Geotechnical Engineering, 2004.

Kavazanjian, E. A Driven-Pile Advantage: Batter Piles. *Piledriver*, Vol. Q4, 2006, pp. 21–25.

Kavazanjian, E., J. J. Wang, G. R. Martin, A. Shamsabadi, I. P. Lam, S. E. Dickenson, and C. J. Hung. *LRFD Seismic Analysis and Design of Transportation Geotechnical Features and Structural Foundations*, 2011.

Kramer, S. L., and A. W. Elgamal. *Modeling Soil Liquefaction Hazards for Performance-Based Earthquake Engineering.* Pacific Earthquake Engineering Research Center, University of California, Berkeley, February 2001.

Kramer, S. L., C. Valdez, B. Blanchette, and J. W. Baker. *LRFD Seismic Analysis and Design of Bridges*, 2014.

Lam, I. P., and G. R. Martin. Design Procedures and Guidelines. In *Seismic Design of Highway Bridge Foundations*, Vol. 2, Federal Highway Administration, U.S. Department of Transportation, 1986, p. 18.

Martin; G. R. Seismic Design for Bridge Foundations and Site Liquefaction Potential. *Proceeding of a Workshop on Earthquake Resistance of Highway Bridges*. National Science Foundation, Palo Alto, Calif., 1979.

Martin, G. R., and W. D. L. Finn. Fundamentals of Liquefaction under Cyclic Loading. *Journal of the Geotechnical Engineering Division*, 1975.

Martin, G. R., and B. J. Douglas. *Evaluation of the Cone Penetrometer for Liquefaction Hazard Assessment*. U.S. Geological Survey, OPEN FILE REPORT-OPEN-FILE NO.81-284, 1980.

Martin, G. R., and I. P. Lam. *Seismic Design of Pile Foundations: Structural and Geotechnical Issues*. International Conference on Recent Advances in Geotechnical Earthquake Engineering and Soil Dynamics, 1995.

Matlock, H. *Correlations for Design of Laterally Loaded Piles in Soft Clay*. Second Annual Offshore Technology Conference, Houston, Tex., 1970.

Matlock, H., and L. C. Reese. Generalized Solutions for Laterally Loaded Piles. *Journal of Soil Mechanics and Foundations*, 1960.

Committee on Earthquake Engineering. *Liquefaction of Soils During Earthquakes*. National Research Council, 1985.

NCHRP Research Report 472: Comprehensive Specification for the Seismic Design of Bridges, Transportation Research Board, Washington, D.C., 2002. Available at http://onlinepubs.trb.org/onlinepubs/nchrp/nchrp_rpt_472.pdf.

Reese, L. C., W. R. Cox, and F. D. Koop. Analysis of Laterally Loaded Piles in Sand. Sixth Annual Offshore Technology Conference, Houston, Tex., 1974. https://doi.org/10.4043/2080-MS.

Reese, L. C. *Handbook on Design of Piles and Drilled Shafts Under Lateral Load*. FHWA IP-84-11. Federal Highway Administration, U.S. Department of Transportation, 1984.

Seed, H. B., and I. M. Idriss. Simplified Procedure for Evaluating Soil Liquefaction Potential. *Journal of Soil Mechanics and Foundations*, 1971.

Seed, R. B., and L. F. Harder. SPT-Based Analysis of Cyclic Pore Pressure Generation and Undrained Residual Strength. *Proc., H. Bolton Seed Memorial Symposium*, University of California at Berkeley and Bitech Publishers, 1990, pp. 351–376.

Sharpe, R. L., and R. L. Mayes. Development of the Highway Bridge Seismic Design Criteria for the U.S. *Proc., Earthquake Resistance of Highway Bridges*. ATC, Palo Alto, California, 1979.

United State Geological Survey. *The Alaska Earthquake Effects on Transportation and Utilities*. Paper 545C, 1968.

Yashinsky, M. The Loma Prieta, California, Earthquake of October 17, 1989. *Highway Systems*, Vol. 1552-B, U.S. Geological Survey Professional Paper, 1998. https://doi.org/10.3133/pp1552B.

Youd, T., and M. J. Bennett. Liquefaction Sites, Imperial Valley, California. *Journal of Geotechnical Engineering*, Vol. 109, No. 3, 1983. https://doi.org/10.1061/(ASCE)0733-9410(1983)109:3(440).

Youd, T. L., and I. M. Idriss. *Proc., NCEER Workshop on Evaluation of Liquefaction Resistance of Soils*, 1997.

Structural Implications Related to Foundation Movements in AASHTO LRFD

NARESH C. SAMTANI
NCS GeoResources

JOHN M. KULICKI
Consultant

In the United States, the highway bridge design practice is based on the LRFD method developed by AASHTO. In AASHTO LRFD (*1*), which is based on the concept of limit states, the effect of foundation movements is expressed in terms of a force effect and not in terms of geotechnical resistance. In fact, all design codes worldwide recognize this observation by including a representation of structural effects of foundation movements in terms of force. AASHTO LRFD uses the *SE* load factor, γ_{SE}, for such evaluations. The structural effect of foundation movements is manifested in the form of additional force effects such as induced torques, moments, and shears in a bridge structure that can lead to adverse consequences such as cracking. In AASHTO LRFD, γ_{SE} occurs in four out of the five load combinations for strength limit state and three out of the four load combinations for Service limit state.

In the 8th Edition of AASHTO LRFD ("2017 provisions" in this paper), $\gamma_{SE} = 1.00$ is used regardless of the type of foundation movement and the method used to predict the value of the movement. This is true for all previous editions of AASHTO LRFD. A reliability-based procedure for calibrating γ_{SE} based on consideration of structural limit states was developed during the Second Strategic Highway Research Program (SHRP2) Project R19B (*2*). The Project R19B work examined the uncertainty in predicted settlements from various analytical methods and developed procedures to calibrate γ_{SE} values for different methods used to predict foundation movements. Calibrated γ_{SE} values based on Project R19B procedures are included in the 9th Edition of AASHTO LRFD issued in 2020 ("2020 provisions" in this paper).

Under the 2017 provisions most designers use predicted total foundation movements for final loads. This implies a scenario in which a bridge structure is instantaneously set into place and all the loads are applied at the same time. However, foundation movements occur as the loads are applied sequentially during various construction stages. The foundation movements predicted to occur before placement of the superstructure may not be relevant to the design or performance of the superstructure. For example, depending on the type of superstructure and the construction sequence, the immediate settlement between construction stage at which the stresses in the superstructure elements are affected by differential settlements and the end-of-construction can be between 25% and 75% of the total settlement (*2–4*). Thus, the predicted relevant settlement that may affect a bridge structure can be much less than the predicted total settlement. Consideration of the construction sequence to determine the relevant foundation movements is referenced as the construction-point concept (*2–4*). To ensure more realistic designs, the 2020 provisions recommend use of the construction–point concept.

NEED FOR STUDY

As part of the review and balloting processes for the 2020 provisions by AASHTO T-15 and T-5 technical committees, the following items were noted:

- Bridge designers do not consider foundation settlements in a consistent manner in the bridge design process or in accordance with 2017 provisions. The need to demonstrate correct procedures for consideration of settlements in bridge design process was identified.
- Most of the bridge designers who did consider settlement in bridge design tended to limit settlements to arbitrary and small values of settlement, e.g., less than 0.5 or 1 in. This can result in costlier and inefficient foundation systems and in some cases ground improvement.
- The effect of proposed γ_{SE} values in conjunction with the implementation of the construction-point concept on the bridge design process needed to be assessed.

To address the above items, a need for study with the following goals was identified: (a) demonstration of the correct implementation of foundation movements in bridge design process, and (b) evaluation of the structural implications of the 2020 provisions on the bridge design process.

DATA AND SCOPE FOR STUDY

To achieve the study goals, data from several continuous span steel girder constructed bridges were collected and evaluated for a range of foundation settlements and γ_{SE} values. The following bridge configurations were evaluated (*3*):

- Two-span bridge with equal span lengths, L_S, of 50 ft;
- Four-span bridge with L_S of 168, 293, 335, and 165 ft; and
- Five-span bridge with L_S of 120, 140, 140, 140, and 120 ft.

Thus, several bridge configurations with short, medium, and long spans were evaluated. Structural computations for incorporation of calibrated values of a range of foundation settlements and γ_{SE} values are demonstrated in this paper using the 4-span bridge example. The computations for the other (two-span and five-span) bridges were performed in a similar manner (*3*).

Table 1 and Table 2 provide the unfactored moment and unfactored shear values, respectively, for a typical interior girder based on dead load (DL), live load (LL) and unit (1 in.) settlement at each of the supports for the four-span bridge. The term “unfactored” indicates a nominal value or alternatively that a value of 1.00 is used for the load factor for the considered load type. These values were developed by use of a commercially available bridge analysis program (*3*).

The largest γ_{SE} value that was adopted by AASHTO for the 2020 provisions is 1.40. As part of the study, AASHTO decided to consider γ_{SE} = 1.00, 1.25, and 1.75 to evaluate the structural implications on the bridge design practice based on γ_{SE} = 1.00 in 2017 provisions. The value of γ_{SE} = 1.75 was chosen to explore the effect of a large increase in γ_{SE} in bridge design and to account for any future values of γ_{SE} which may be in the range of 1.75 based on regional (i.e., local) calibrations that are recommended by AASHTO and FHWA (*3*). The value of γ_{SE} = 1.25

which was developed for a regional database from northeast USA (*2–4*) was chosen as an intermediate value. The parametric study further involved evaluation of the following:

- Use of the total settlement, S_t, that is used by most designers based on 2017 provisions. Total settlements ranging from 0.50 in to 4.80 in. were considered
- Use of total relevant settlement, S_{tr}, which is based on the construction-point concept.

The wide range of total settlement values coupled with the wide range of γ_{SE} values explore most of the possibilities that may be encountered in practice. The other bridge configurations (i.e., two-span and five-span) bridges were also evaluated in a similar manner (*3*).

TABLE 1 Unfactored Moment Values (*3*)

Item		Moment (kip-ft)						
		Span 1–0.4 L_S	Pier 1	Span 2–0.5 L_S	Pier 2	Span 3–0.5 L_S	Pier 3	Span 4–0.6 L_S
Unfactored DL moment (no settlement)		3884	–15561	8001	–33891	13513	–25824	1651
Unfactored LL moment (no settlement)	+ve	6401	2807	8639	1166	9741	2662	4379
	–ve	–3171	–10609	–3174	–13208	–2257	–14582	–2270
Unfactored effect of 1 in. settlement at Abutment 1		–329	–822	–273	278	84	–110	–22
Unfactored effect of 1 in. settlement at Pier 1		702	1753	609	–534	–161	212	43
Unfactored effect of 1 in. settlement at Pier 2		–469	–1174	–79	1016	344	–328	–65
Unfactored effect of 1 in. settlement at Pier 3		192	452	–479	–1409	321	2050	411
Unfactored effect of 1 in. settlement at Abutment 2		–82	–208	221	651	–587	–1825	–364

TABLE 2 Unfactored Shear Values (*3*)

Item		Shear (kip)							
		Right of Abut 1	Left of Pier 1	Right of Pier 1	Left of Pier 2	Right of Pier 2	Left of Pier 3	Right of Pier 3	Left of Abut 2
Unfactored DL moment (no settlement)		157.1	–345.5	384.0	–526.5	564.0	–502.5	428.5	–100.7
Unfactored LL moment (no settlement)	+ve	159.5	15.4	213.9	12.9	232.3	26.0	203.7	63.1
	–ve	–43.4	–191.7	–36.3	–224.4	–9.9	–229.9	–14.8	–158.7
Unfactored effect of 1 in. settlement at Abutment 1		–4.9	–4.9	3.8	3.8	–1.2	–1.2	0.7	0.7
Unfactored effect of 1 in. settlement at Pier 1		10.4	10.4	–7.8	–7.8	2.2	2.2	–1.3	–1.3
Unfactored effect of 1 in. settlement at Pier 2		–7.0	–7.0	7.5	7.5	–4.0	–4.0	2.0	2.0
Unfactored effect of 1 in. settlement at Pier 3		2.7	2.7	–6.4	–6.4	10.3	10.3	–12.4	–12.4
Unfactored effect of 1 in. settlement at Abutment 2		–1.2	–1.2	2.9	2.9	–7.4	–7.4	11.1	11.1

SETTLEMENT VALUES FOR FOUR-SPAN BRIDGE

In Table 3, which presents the settlement data for the four-span bridge, the S_t values represent the predicted unfactored total settlement at each of the support elements. The term "unfactored" indicates use of γ_{SE} = 1.00 which is recommended in the 2017 provisions. The S_{tr} values represent the unfactored estimated total relevant settlement at each of the support elements. For this example, these values are assumed to be 50% of S_t. The S_{FR} values represent the factored relevant settlements at each support element using the values of γ_{SE} = 1.25 and γ_{SE} = 1.75. These values are computed by multiplying the S_{tr} values with the applicable γ_{SE} value. For γ_{SE} = 1.00, S_{FR}=S_{tr}.

Two sets of settlement values were evaluated for the four-span bridge. These sets are herein referred to as "large settlement" and "small settlement." Table 3 presents the values of S_t, S_{tr}, and S_{FR}, values for both sets. Figure 1 shows the settlement profiles for the two sets. The values of S_t in the small settlement set are approximately 25% of those in the large settlement set (values have been rounded to 3 significant digits).

TABLE 3 Unfactored and Factored Total and Relevant Settlements (*3*)

Settlement	γ_{SE}	Abutment 1	Pier 1	Pier 2	Pier 3	Abutment 2
Large Settlement Set						
S_t (in.)	1.00	1.90	3.90	4.80	1.90	2.50
S_{tr} (in.)	1.00	0.95	1.95	2.40	0.95	1.25
$S_{FR} = \gamma_{SE}(S_{tr})$	1.25	1.19	2.44	3.00	1.19	1.56
	1.75	1.66	3.41	4.20	1.66	2.19
Small Settlement Set						
S_t (in.)	1.00	0.50	1.00	1.20	0.50	0.60
S_{tr} (in.)	1.00	0.25	0.50	0.60	0.25	0.30
$S_{FR} = \gamma_{SE}(S_{tr})$	1.25	0.31	0.63	0.75	0.31	0.38
	1.75	0.44	0.88	1.05	0.44	0.53

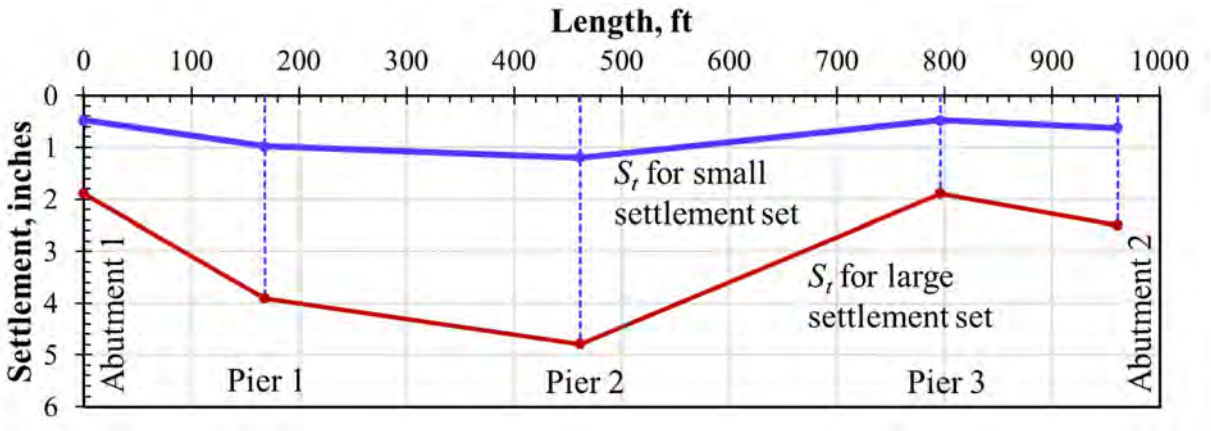

FIGURE 1 Profiles of total settlement (S_t) for small and large settlement sets.

AASHTO PROVISIONS FOR CONSIDERATION OF SETTLEMENTS

AASHTO LRFD Article 3.12.6 states "Force effects due to extreme values of differential settlement among substructures and within individual substructure units shall be considered." The commentary to this article states "Force effects due to settlement may be reduced by considering creep. Analysis for the load combinations in Tables 3.4.1-1 and 3.1.4-2 which include settlement should be repeated for settlement of each possible substructure unit settling individually, as well as combinations of substructure units settling, that could create critical force effects in the structure." The use of words such as "extreme values of differential settlement" and "critical force effects" are reflective of the concern that some of the foundation units may settle less than predicted, or even undergo no settlement. In application of these provisions it must be recognized that γ_{SE} addresses uncertainty in the foundation movement at a given support location and for a certain model for prediction of movement. It does not address the uncertainty in differential settlement between two support locations. Depending on the underlying values of total settlements and the method used to compute them, the uncertainty in calculated differential settlement can vary significantly (*5*). Indeed, the uncertainty of the calculated differential settlement between adjacent support elements is larger than the uncertainty of the predicted total settlement at each of the two support elements used to calculate the differential settlement (*5*).

Further, AASHTO LRFD Article 3.4.1 states "Load combinations which include settlement shall also be applied without settlement." The purpose of this provision is to alert the designer to make sure that the force effect due to settlement must not be used to reduce the permanent force effects.

The effects of these provisions need to be considered in two-fold manner (*4*): geometric and structural. The geometric effect is evaluated through change in grade in terms of angular distortion. The structural effect is evaluated through the values of the additional force effects in the form of induced torque, moment and shear due to settlement. However, in both cases, as noted above, consideration of "extreme values of differential settlement" and evaluation of "critical force effects" is required. To address these aspects, the following criteria to estimate extreme values of differential settlements are recommended (*3*, *4*):

> "1. Assume that the actual (measured) settlement of any support element could be as large as the predicted factored relevant settlement value, S_{FR}, calculated by using a given method.
>
> 2. Assume that the actual (measured) settlement of the adjacent support element could be less, taken as zero in the limit, instead of the predicted factored relevant settlement value, S_{FR}, calculated by using the same given method."

This approach is referred to as the "S_{FR}–0" concept where S_{FR} represents the predicted factored relevant settlement at one support of a span and the value of "0" represents zero settlement at an adjacent support, i.e., the limiting small value. Since one support is assumed to have zero settlement, the resulting differential settlement becomes the extreme value as required by AASHTO. This approach helps eliminate the additional uncertainty associated with differential settlement (*5*). Thus, after use of S_{FR}–0 approach, the only uncertainty left is that associated with the settlement values at each of the support elements used to compute the differential settlement and this uncertainty is addressed by γ_{SE} (*5*). Procedures to estimate the additional uncertainty in differential set-

tlement if S_{FR}–0 approach is not used are provided elsewhere (*5*). In any case, two modes of differential settlement within any span must be evaluated. In Mode 1 the left support is assumed to have zero settlement while in Mode 2 the right support is assumed to have zero settlement. The bridge design process must explore all viable deformed shapes based on evaluation of these two modes for all bridge spans. This approach also helps create the extreme values of differential settlement and evaluate the critical force effects as required by 2017 and 2020 provisions.

GEOMETRIC EFFECTS

Differential settlement leads to a change in grade which can be expressed as angular distortion, A_d. In the longitudinal direction of the bridge $A_d = \Delta_S/L_S$, where Δ_S is the differential settlement between adjacent support elements and L_S is the distance between supports (span length). Table 4 shows the values of the factored angular distortion, $A_{dF} = \Delta_{SFR}/L_S$, using the S_{FR}–0 concept where Δ_{SFR} is the differential settlement based on factored relevant settlements.

The values of A_{dF} and S_{FR} are compared with owner specified criteria for tolerable movements to evaluate the geometric effects. The value of A_{dF} should be evaluated by comparison with acceptable angular distortion criteria based on considerations of drainage, tolerances of appurtenances attached to bridge, etc. For example, permissible angular distortion criteria are provided in Article 10.5.2 of 2017 provisions which permits an angular distortion of 0.004 for multiple-span (continuous span) bridges and 0.008 for simple span bridges. Newer criteria in Article 10.5.2 of 2020 provisions based on Project 12-103 of NCHRP (*6*) can also be used. Similarly, the value of S_{FR} should be evaluated by comparison with tolerable values at abutment interfaces which can lead to creation of the ubiquitous “bump at the end of a bridge,” reduction in vertical clearance under a bridge, and or the detrimental effect on the joints.

The bridge structure is reproportioned and reevaluated if A_{dF} and S_{FR} are found to be unacceptable based on evaluation of geometric effects. The bridge analysis is continued to evaluation of structural effects if A_{dF} and S_{FR} are found to be acceptable. In the case of the 4-span bridge, the values in Table 4 are much smaller than those noted in Article 10.5.2 of 2017 provisions and are deemed acceptable.

TABLE 4 Factored Angular Relevant Distortions to Check for Geometric Effects (*3*)

γ_{SE}	Mode	Factored Angular Relevant Distortion, $A_{dF}=\Delta_{SFR}/L_S$ (rad.)			
		Span 1 [L_S=168 ft]	Span 2 [L_S=293 ft]	Span 3 [L_S=335 ft]	Span 4 [L_S=165 ft]
Large Settlement Set					
1.25	1	0.0006	0.0007	0.0007	0.0006
	2	0.0012	0.0009	0.0003	0.0008
1.75	1	0.0008	0.0010	0.0010	0.0008
	2	0.0017	0.0012	0.0004	0.0011
Small Settlement Set					
1.25	1	0.0002	0.0002	0.0002	0.0002
	2	0.0003	0.0002	0.0001	0.0002
1.75	1	0.0002	0.0002	0.0003	0.0002
	2	0.0004	0.0003	0.0001	0.0003

NOTE: Mode 1: S_{FR} at left end of span divided by L_S; Mode 2: S_{FR} at right end of span divided by L_S.

STRUCTURAL EFFECTS

Most bridges are designed using linear (elastic) approach wherein sets of loads acting simultaneously can be evaluated by superimposing (adding) the loads, force effects, or movements at the point of interest. In this approach, the induced force effects due to foundation movements can be prorated (scaled) and superimposed on force effects from primary loads such as DL and LL. Thus, the unfactored effect of 1 in. (i.e., unit) settlement at each of the support elements noted in Table 1 and Table 2 are prorated for the settlement value of interest and the resulting force effects are added to the primary force effects. Table 5 and Table 6 show the prorated induced moments and shears, respectively, due to settlement.

Computations in the Tables 5 and 6 are demonstrated below with respect to Pier 1 in Table 5 which contains computations for induced moments using the large settlement data from Table 3 (values in Table 5 are rounded to the nearest whole number):

- Effect of unfactored S_{tr} at Abutment 1: (0.95 in./1.00 in.)(–822 kip-ft) = –780.9 kip-ft.
- Effect of unfactored S_{tr} at Pier 1: (1.95 in./1.00 in.)(1753 kip-ft) = 3418.3 kip-ft.
- Effect of unfactored S_{tr} at Pier 2: (2.40 in./1.00 in.)(–1174 kip-ft) = –2817.6 kip-ft.
- Effect of unfactored S_{tr} at Pier 3: (0.95 in./1.00 in.)(452 kip-ft) = 429.4 kip-ft.
- Effect of unfactored S_{tr} at Abutment 2: (1.25 in./1.00 in.)(–208 kip-ft) = –260.0 kip-ft.
- Total unfactored effect of S_{tr} at all supports:
  - +ve value: 3418.3 kip-ft + 429.4 kip-ft = 3847.7 kip-ft and
  - –ve value: –780.9 kip-ft – 2817.6 kip-ft – 260.0 kip-ft = –3858.5 kip-ft.
- Total factored effect of settlement using Δ_{SE} = 1.00 and S_t:
  - +ve value: (3.90 in. /1.00 in.)(1753 kip-ft) (1.00) + (1.90 in./1.00 in.)(452 kip-ft)(1.00) = 7695.5 kip-ft.
  - –ve value: (1.90 in./1.00 in.)(–822 kip-ft)(1.00) + (4.80 in. /1.00 in.)(–1174 kip-ft) (1.00) + (2.50 in. /1.00 in.)(–208 kip-ft) (1.00) = –7717.0 kip-ft.
- Total factored effect of settlement using Δ_{SE} = 1.25 and S_{tr}:
  - +ve value: (1.95 in. /1.00 in.)(1753 kip-ft) (1.25)+ (0.95 in./1.00 in.)(452 kip-ft)(1.25) = 4809.7 kip-ft.
  - –ve value: (0.95 in./1.00 in.)(–822 kip-ft)(1.25) + (2.40 in. /1.00 in.)(–1174 kip-ft) (1.25) + (1.25 in. /1.00 in.)(–208 kip-ft) (1.25) = –4823.1 kip-ft.
- Total factored effect of settlement using Δ_{SE} = 1.75 and S_{tr}:
  - +ve value: (1.95 in. /1.00 in.)(1753 kip-ft) (1.75) + (0.95 in./1.00 in.)(452 kip-ft)(1.75) = 6733.6 kip-ft.
  - –ve value: (0.95 in./1.00 in.)(–822 kip-ft)(1.75) + (2.40 in. /1.00 in.)(–1174 kip-ft) (1.75) + (1.25 in. /1.00 in.)(–208 kip-ft) (1.75) = –6752.4 kip-ft.
- Total factored effect of settlement using Δ_{SE} = 1.00 and S_{tr} (since Δ_{SE} = 1.00, these values are the same as those above for total unfactored effect of S_{tr} at all supports):
  - +ve value: 3418.3 kip-ft + 429.4 kip-ft = 3847.7 kip-ft.
  - –ve value: –780.9 kip-ft – 2817.6 kip-ft – 260.0 kip-ft = –3858.5 kip-ft.

TABLE 5 Prorated Induced Moment Values Due to Settlement (*3*)

Item		Moment (kip–ft)						
		Span 1 –0.4L_S	Pier 1	Span 2 –0.5L_S	Pier 2	Span 3 –0.5L_S	Pier 3	Span 4 –0.6L_S
Effect of unfactored S_{tr} at Abut 1		–313	–781	–259	264	80	–105	–21
Effect of unfactored S_{tr} at Pier 1		1369	3418	1188	–1041	–314	413	84
Effect of unfactored S_{tr} at Pier 2		–1126	–2818	–190	2438	826	–787	–156
Effect of unfactored S_{tr} at Pier 3		182	429	–455	–1339	305	1948	390
Effect of unfactored S_{tr} at Abut 2		–103	–260	276	814	–734	–2281	–455
Total unfactored effect of S_{tr} at all supports	+ve	1551	3848	1464	3516	1210	2361	474
	–ve	–1541	–3859	–904	–2380	–1048	–3173	–632
Total factored effect using γ_{SE} = 1.00 and S_t	+ve	3103	7696	2928	7033	2421	4722	949
	–ve	–3081	–7717	–1808	–4760	–2095	–6346	–1264
Total factored effect using γ_{SE} = 1.25 and S_{tr}	+ve	1939	4810	1830	4395	1513	2951	593
	–ve	–1926	–4823	–1130	–2975	–1310	–3966	–790
Total factored effect using γ_{SE} = 1.75 and S_{tr}	+ve	2715	6734	2562	6153	2118	4132	830
	–ve	–2696	–6752	–1582	–4165	–1833	–5553	–1106
Total factored effect using γ_{SE} = 1.00 and S_{tr}	+ve	1551	3848	1464	3516	1210	2361	474
	–ve	–1541	–3859	–904	–2380	–1048	–3173	–632

TABLE 6 Prorated Induced Shear Values Due to Settlement (*3*)

Item		Shear (kip)							
		Right of Abut 1	Left of Pier 1	Right of Pier 1	Left of Pier 2	Right of Pier 2	Left of Pier 3	Right of Pier 3	Left of Abut 2
Effect of unfactored S_{tr} at Abut 1		–4.7	–4.7	3.6	3.6	–1.1	–1.1	0.6	0.6
Effect of unfactored S_{tr} at Pier 1		20.4	20.4	–15.2	–15.2	4.3	4.3	–2.5	–2.5
Effect of unfactored S_{tr} at Pier 2		–16.8	–16.8	17.9	17.9	–9.6	–9.6	4.8	4.8
Effect of unfactored S_{tr} at Pier 3		2.5	2.5	–6.0	–6.0	9.8	9.8	–11.8	–11.8
Effect of unfactored S_{tr} at Abut 2		–1.6	–1.6	3.7	3.7	–9.2	–9.2	13.8	13.8
Total unfactored effect of S_{tr} at all supports	+ve	23	23	25	25	14	14	19	19
	–ve	–23	–23	–21	–21	–20	–20	–14	–14
Total factored effect using γ_{SE} = 1.00 and S_t	+ve	46	46	50	50	28	28	38	38
	–ve	–46	–46	–43	–43	–40	–40	–29	–29
Total factored effect using γ_{SE} = 1.25 and S_{tr}	+ve	29	29	31	31	18	18	24	24
	–ve	–29	–29	–27	–27	–25	–25	–18	–18
Total factored effect using γ_{SE} = 1.75 and S_{tr}	+ve	40	40	44	44	25	25	34	34
	–ve	–40	–40	–37	–37	–35	–35	–25	–25
Total factored effect using γ_{SE} = 1.00 and S_{tr}	+ve	23	23	25	25	14	14	19	19
	–ve	–23	–23	–21	–21	–20	–20	–14	–14

The numerical computations for induced moments at other supports in Table 5 as well as induced shear forces in Table 6 follow the same approach as demonstrated above for Pier 1. In these computations, the AASHTO provisions for consideration of settlements noted earlier were implemented efficiently by summing all the positive and all the negative moments and shears at each point of interest in the example structure.

For comparison purposes, four cases of Service I and Strength I load combinations were developed as follows in upper half of Tables 7 to 10.

- Case 1: DL + LL with no settlement. This case represents designs performed without consideration of settlement. In this case, DL and LL are factored according to the load factors for Service I and Strength I load combinations.
- Case 2: DL + LL with settlement using γ_{SE}=1.00. This case represents the 2017 provisions. In this case, (a) DL and LL are factored according to the load factors for Service I and Strength I load combinations, and (b) the total settlement, S_t, with γ_{SE} = 1.00 is used.
- Case 3: DL + LL with settlement using construction-point concept and method-specific γ_{SE} value. This case represents the 2020 provisions. In this case, (a) DL and LL are factored according to the load factors for Service I and Strength I load combinations, and (b) the relevant settlement, S_{tr}, is used with γ_{SE} value appropriate to the method used to estimate the settlement. As noted earlier, γ_{SE} = 1.25 and 1.75 have been used to explore a range of γ_{SE} values.
- Case 4: This case is the same as Case 2 except that the total relevant settlement, S_{tr}, with γ_{SE} = 1.00 is used. This case represents the practice in some DOT and by some designers where total relevant settlements are used instead of total settlements.

In Tables 7 to 10, the "Max" and "Min" refer to the maximum and minimum values of the total force effects and are developed using the following two rules:

- Rule 1: Combine the sum of the positive settlement contributions, factored as shown, with the DL and positive LL contributions to determine the maximum value of the force effect under consideration.
- Rule 2: Combine the sum of the negative settlement contributions, factored as shown, with the DL and the negative live contributions to determine the minimum (i.e., maximum negative) value of the force effect under consideration.

This process of calculating positive and negative force effects (settlement and LL) and then adding those values to the DL force effects is a simple and practical way to implement the AASHTO provisions for consideration of settlement discussed previously. The computations for induced shear forces were done in a similar manner (*3*).

The following five ratios (see lower half of Tables 7 to 10) were computed to evaluate the results:

- Ratio 1: Case 3 to Case 1. This ratio compares the 2020 provisions using relevant settlement and $\gamma_{SE} \geq 1.00$ with 2017 provisions without consideration of settlement. This ratio provides information regarding the level of potential under-design when the effect of settlement is not considered in analysis.
- Ratio 2: Case 3 to Case 2. This ratio compares the 2020 provisions using relevant settlement and $\gamma_{SE} \geq 1.00$ with 2017 provisions using total settlement and γ_{SE} = 1.00.

TABLE 7 Comparison of Service I Moments with Case 3 Based on γ_{SE} = 1.25 (*3*)

Load Combination Case and Ratio of Cases	Value	Moment (kip–ft)						
		Span 1 – 0.4L_S	Pier 1	Span 2 – 0.5L_S	Pier 2	Span 3 – 0.5L_S	Pier 3	Span 4 – 0.6L_S
Case 1:1.00DL + 1.00LL without S_E	Max	10285	–12754	16640	–32725	23254	–23162	6030
	Min	713	–26170	4827	–47099	11256	–40406	–619
Case 2:1.00DL + 1.00LL + Δ_{SE}SE (use Δ_{SE} = 1.00 and S_t)	Max	13388	–5059	19568	–25693	25675	–18440	6979
	Min	–2368	–33887	3019	–51859	9161	–46752	–1883
Case 3:1.00DL + 1.00LL + Δ_{SE}SE (use Δ_{SE} = 1.25 and S_{tr})	Max	12224	–7944	18470	–28330	24767	–20211	6623
	Min	–1213	–30993	3697	–50074	9946	–44372	–1409
Case 4:1.00DL + 1.00LL + Δ_{SE}SE (use Δ_{SE} = 1.00 and S_{tr})	Max	11836	–8906	18104	–29209	24464	–20801	6504
	Min	–828	–30029	3923	–49479	10208	–43579	–1251
Ratios								
Ratio 1: Case 3 to Case 1	Max	**1.189**	*0.623*	**1.110**	*0.866*	**1.065**	*0.873*	**1.098**
	Min	*–1.701*	**1.184**	*0.766*	**1.063**	*0.884*	**1.098**	*2.276*
Ratio 2: Case 3 to Case 2	Max	**0.913**	*1.570*	**0.944**	*1.103*	**0.965**	*1.096*	**0.949**
	Min	*0.512*	**0.915**	*1.225*	**0.966**	*1.086*	**0.949**	*0.748*
Ratio 3: Case 2 to Case 1	Max	**1.302**	*0.397*	**1.176**	*0.785*	**1.104**	*0.796*	**1.157**
	Min	*–3.322*	**1.295**	*0.625*	**1.101**	*0.814*	**1.157**	*3.042*
Ratio 4: Case 3 to Case 4	Max	**1.033**	*0.892*	**1.020**	*0.970*	**1.012**	*0.972*	**1.018**
	Min	*1.465*	**1.032**	*0.942*	**1.012**	*0.974*	**1.018**	*1.126*
Ratio 5: Case 4 to Case 2	Max	**0.884**	*1.761*	**0.925**	*1.137*	**0.953**	*1.128*	**0.932**
	Min	*0.349*	**0.886**	*1.299*	**0.954**	*1.114*	**0.932**	*0.664*

TABLE 8 Comparison of Strength I Moments with Case 3 based on γ_{SE}=1.25 (*3*)

Load Combination Case and Ratio of Cases	Value	Moment (kip–ft)						
		Span 1 –0.4L_S	Pier 1	Span 2 –0.5L_S	Pier 2	Span 3 –0.5L_S	Pier 3	Span 4 –0.6L_S
Case 1: 1.25DL + 1.75LL without SE	Max	16057	–14539	25120	–40323	33938	–27622	9727
	Min	–694	–38017	4447	–65478	12942	–57799	–1909
Case 2: 1.25DL + 1.75LL + γ_{SE}SE (use γ_{SE} = 1.00 and S_t)	Max	19159	–6844	28047	–33291	36359	–22900	10676
	Min	–3776	–45734	2639	–70237	10846	–64144	–3173
Case 3: 1.25DL + 1.75LL + γ_{SE}SE (use γ_{SE} = 1.25 and S_{tr})	Max	17996	–9729	26949	–35928	35451	–24670	10320
	Min	–2620	–42840	3317	–68453	11632	–61765	–2699
Case 4: 1.25DL + 1.75LL + γ_{SE}SE (use γ_{SE} = 1.00 and S_{tr})	Max	17608	–10691	26583	–36807	35148	–25261	10201
	Min	–2235	–41876	3543	–67858	11894	–60971	–2541
Ratios								
Ratio 1: Case 3 to Case 1	Max	**1.121**	*0.669*	**1.073**	*0.891*	**1.045**	*0.893*	**1.061**
	Min	*3.774*	**1.127**	*0.746*	**1.045**	*0.899*	**1.069**	*1.414*
Ratio 2: Case 3 to Case 2	Max	**0.939**	*1.422*	**0.961**	*1.079*	**0.975**	*1.077*	**0.967**
	Min	*0.694*	**0.937**	*1.257*	**0.975**	*1.072*	**0.963**	*0.851*
Ratio 3: Case 2 to Case 1	Max	**1.193**	*0.471*	**1.117**	*0.826*	**1.071**	*0.829*	**1.098**
	Min	*5.438*	**1.203**	*0.593*	**1.073**	*0.838*	**1.110**	*1.662*
Ratio 4: Case 3 to Case 4	Max	**1.022**	*0.910*	**1.014**	*0.976*	**1.009**	*0.977*	**1.012**
	Min	*1.172*	**1.023**	*0.936*	**1.009**	*0.978*	**1.013**	*1.062*
Ratio 5: Case 4 to Case 2	Max	**0.919**	*1.562*	**0.948**	*1.106*	**0.967**	*1.103*	**0.956**
	Min	*0.592*	**0.916**	*1.343*	**0.966**	*1.097*	**0.951**	*0.801*

TABLE 9 Comparison of Service I Moments with Case 3 based on γ_{SE}=1.75 (*3*)

Load Combination Case and Ratio of Cases	Value	Moment (kip–ft) Span 1 –0.4L_S	Pier 1	Span 2 –0.5L_S	Pier 2	Span 3 –0.5L_S	Pier 3	Span 4 –0.6L_S
Case 1: 1.00DL + 1.00LL without SE	Max	10285	–12754	16640	–32725	23254	–23162	6030
	Min	713	–26170	4827	–47099	11256	–40406	–619
Case 2: 1.00DL + 1.00LL + γ_{SE}SE (use γ_{SE} = 1.00 and S_t)	Max	13388	–5059	19568	–25693	25675	–18440	6979
	Min	–2368	–33887	3019	–51859	9161	–46752	–1883
Case 3: 1.00DL + 1.00LL + γ_{SE}SE (use γ_{SE} = 1.75 and S_{tr})	Max	13000	–6020	19202	–26572	25372	–19030	6860
	Min	–1983	–32922	3245	–51264	9423	–45959	–1725
Case 4: 1.00DL + 1.00LL + γ_{SE}SE (use γ_{SE} = 1.00 and S_{tr})	Max	11836	–8906	18104	–29209	24464	–20801	6504
	Min	–828	–30029	3923	–49479	10208	–43579	–1251
Ratios								
Ratio 1: Case 3 to Case 1	Max	**1.264**	*0.472*	**1.154**	*0.812*	**1.091**	*0.822*	**1.138**
	Min	*–2.781*	**1.258**	*0.672*	**1.088**	*0.837*	**1.137**	*2.786*
Ratio 2: Case 3 to Case 2	Max	**0.971**	*1.190*	**0.981**	*1.034*	**0.988**	*1.032*	**0.983**
	Min	*0.837*	**0.972**	*1.075*	**0.989**	*1.029*	**0.983**	*0.916*
Ratio 3: Case 2 to Case 1	Max	**1.302**	*0.397*	**1.176**	*0.785*	**1.104**	*0.796*	**1.157**
	Min	*–3.322*	**1.295**	*0.625*	**1.101**	*0.814*	**1.157**	*3.042*
Ratio 4: Case 3 to Case 4	Max	**1.098**	*0.676*	**1.061**	*0.910*	**1.037**	*0.915*	**1.055**
	Min	*2.396*	**1.096**	*0.827*	**1.036**	*0.923*	**1.055**	*1.379*
Ratio 5: Case 4 to Case 2	Max	**0.884**	*1.761*	**0.925**	*1.137*	**0.953**	*1.128*	**0.932**
	Min	*0.349*	**0.886**	*1.299*	**0.954**	*1.114*	**0.932**	*0.664*

TABLE 10 Comparison of Strength I Moments with Case 3 based on γ_{SE}=1.75 (*3*)

Load Combination Case and Ratio of Cases	Value	Moment (kip–ft) Span 1 – 0.4L_S	Pier 1	Span 2 – 0.5L_S	Pier 2	Span 3 – 0.5L_S	Pier 3	Span 4 – 0.6L_S
Case 1: 1.25DL + 1.75LL without SE	Max	16057	–14539	25120	–40323	33938	–27622	9727
	Min	–694	–38017	4447	–65478	12942	–57799	–1909
Case 2: 1.25DL + 1.75LL + γ_{SE}SE (use γ_{SE} = 1.00 and S_t)	Max	19159	–6844	28047	–33291	36359	–22900	10676
	Min	–3776	–45734	2639	–70237	10846	–64144	–3173
Case 3: 1.25DL + 1.75LL + γ_{SE}SE (use γ_{SE} = 1.75 and S_{tr})	Max	18772	–7805	27681	–34170	36056	–23490	10557
	Min	–3390	–44769	2865	–69642	11108	–63351	–3015
Case 4: 1.25DL + 1.75LL + γ_{SE}SE (use γ_{SE} = 1.00 and S_{tr})	Max	17608	–10691	26583	–36807	35148	–25261	10201
	Min	–2235	–41876	3543	–67858	11894	–60971	–2541
Ratios								
Ratio 1: Case 3 to Case 1	Max	**1.169**	*0.537*	**1.102**	*0.847*	**1.062**	*0.850*	**1.085**
	Min	*4.884*	**1.178**	*0.644*	**1.064**	*0.858*	**1.096**	*1.579*
Ratio 2: Case 3 to Case 2	Max	**0.980**	*1.141*	**0.987**	*1.026*	**0.992**	*1.026*	**0.989**
	Min	*0.898*	**0.979**	*1.086*	**0.992**	*1.024*	**0.988**	*0.950*
Ratio 3: Case 2 to Case 1	Max	**1.193**	*0.471*	**1.117**	*0.826*	**1.071**	*0.829*	**1.098**
	Min	*5.438*	**1.203**	*0.593*	**1.073**	*0.838*	**1.110**	*1.662*
Ratio 4: Case 3 to Case 4	Max	**1.066**	*0.730*	**1.041**	*0.928*	**1.026**	*0.930*	**1.035**
	Min	*1.517*	**1.069**	*0.809*	**1.026**	*0.934*	**1.039**	*1.187*
Ratio 5: Case 4 to Case 2	Max	**0.919**	*1.562*	**0.948**	*1.106*	**0.967**	*1.103*	**0.956**
	Min	*0.592*	**0.916**	*1.343*	**0.966**	*1.097*	**0.951**	*0.801*

- Ratio 3: Case 2 to Case 1. This ratio compares the 2017 provisions using total settlement and γ_{SE} = 1.00 with 2017 provisions without consideration of settlement. Like Ratio 1, this ratio provides information regarding the level of potential under-design when the effect of settlement is not considered in analysis using 2017 provisions.
- Ratio 4: Case 3 to Case 4. This ratio compares the 2020 provisions using relevant settlement and $\gamma_{SE} \geq 1.00$ with 2017 provisions using relevant settlement and γ_{SE} = 1.00.
- Ratio 5: Case 4 to Case 2. This ratio compares the 2017 provisions using relevant settlement and γ_{SE} = 1.00 with 2017 provisions using total settlement and γ_{SE} = 1.00.

Because all results are compared for both the maximum and minimum values of the force effects, the ratios representing the controlling force effects are shown in bold large font typeface in the Tables 7 to 10. Conversely, all noncontrolling force effects are italicized. Only the controlling values are carried forward in the design process.

EVALUATION OF RESULTS

The results were evaluated based on comparisons between the four cases through ratios for both moment and shear values. The following general observations are made based on four-span bridge example presented in this paper and others studied by the authors (*3*):

1. Ratio 1 (Case 3 to Case 1) and Ratio 3 (Case 2 to Case 1), in terms of controlling value, are always greater than 1. This is expected because Case 1 does not consider settlement and the induced force effects due to settlement always add to the primary force effects due to DL and LL. These ratios indicate the level of under-design that increases the possibility of occurrence of undesirable consequences such as cracking.
2. Ratio 2 (Case 3 to Case 2) provides a direct comparison of the 2020 provisions with 2017 provisions. In all instances in Tables 7 to 10, Ratio 2 for controlling force effects is less than 1. This indicates that even for γ_{SE} ranging up to 1.75, the current bridge practice will not be affected in terms of change in member sizes for superstructure. This is because the relevant settlements are considered for Case 3. Ratios less than 1 indicate the structure has reserve capacity and an opportunity for further optimization of structure exists. While the whole structural system should be evaluated for improved economy, the focus of this paper is on foundation aspects. It may be possible to tolerate more foundation movement which provides an opportunity to optimize the foundation configuration to realize cost savings. For example, a shallow foundation may be found viable instead of a deep foundation, or the size of a deep foundation may be reduced (*4*).
3. In exploring Ratio 2 further, it is found that the increase in total force effects for Case 3 (γ_{SE} >1.00) based on 2020 provisions as compared to Case 2 (γ_{SE} = 1.00) based on 2017 provisions are not in direct proportion to the value of the load factor, i.e., γ_{SE} = 1.25 or 1.75. For example, if γ_{SE} = 1.25 is used then the total force effects do not increase by 25%. This is to be expected because the effect of the settlement is one of several components combined to determine the design load effect for a load combination. The exact value of the change in total force effects would be a function of many factors such as bridge superstructure type and configuration, substructure type, foundation type, and use of construction-point concept. In general, the use of the construction-point concept reduces the effect of the settlement on the total force effects. In the example problems, the changes in total force effects did not significantly alter the controlling

values for design. In such cases, consideration could be given to use of more efficient and cost-effective foundation types as well as other appropriate members of the bridge structure.

4. Depending on the magnitude of the differential settlement and the direction of the angular rotation in different spans, the values from Case 3 may be larger or smaller than the results from Case 1 or Case 2

5. The four-span bridge example considered herein indicates the difference in the controlling moments and shears is not significant regardless of whether Case 3 is compared to Case 1 or Case 2. Based on results from the two-span bridge with short spans (*3*) it was found that for shorter span bridges, depending on the stiffness and settlement values, the difference may be more significant.

6. For the four-span bridge, Figure 2 shows a summary of the results for the large settlement data set from Table 3 for both $\gamma\gamma_{SE}$ = 1.25 and $\gamma\gamma_{SE}$ = 1.75. Hence, the effect of an increase in load factor of 40% (1.25 to 1.75) can be directly compared. In Figure 2, the results are tabulated in terms of Ratio 2 (Case 3 to Case 2) and Ratio 4 (Case 3 to Case 4) for Service I moments, Strength I moments, Service I shears, and Strength I shears.

For a 40% increase in γ_{SE} (i.e., 1.25 to 1.75), the evaluation of Ratio 2 and Ratio 4 indicates a maximum increase in induced force effects of 6.4% and 6.3%, respectively. Thus, for the specific four-span bridge example herein, the controlling force effects for moments and shears did not change appreciably when the 2020 provisions were implemented. Comparable effects were noted in the other two examples (two-span and five-span bridges) studied by the authors (*3*).

7. For the four-span bridge, Figure 3 shows a summary of the results for the small settlement data set from Table 3 for both $\gamma\gamma_{SE}$ = 1.25 and $\gamma\gamma_{SE}$ = 1.75. Hence, the effect of an increase in load factor is 40% (1.25 to 1.75) can be evaluated for the small settlement data set and can be directly compared with those discussed above for the large settlement data set. In Figure 3, the results are tabulated in terms of Ratio 2 and Ratio 4 for Service I moments, Strength I moments, Service I shears, and Strength I shears.

For a 40% increase in γ_{SE} (i.e., 1.25 to 1.75), the evaluation of Ratio 2 and Ratio 4 indicates a maximum increase in induced force effects of 1.7% and 1.8%, respectively. As expected, in comparison with the large settlement data in Figure 2, the effect of smaller settlements is reflected in the smaller values of the maximum increases. Similar trends should be expected in practice. For the specific four-span bridge example herein, the controlling force effects for moments and shears did not change appreciably when the 2020 provisions were implemented. Comparable effects were noted in the other two examples (two-span and five-span bridges) studied by the authors (*3*).

8. For controlling forces effects, Ratio 5 in all instances in Tables 7 to 10 is less than 1. This is to be expected because Case 4 considers the relevant settlement that is less than the total settlement that is considered in Case 2.

Governing Force Effects for Ratio 2: Case 3 to Case 2			
Service I - Moments			
Location	Load Factor, γ_{SE}		Difference
	1.25	1.75	
Span 1-0.4L_S	0.913	0.971	6.4%
Pier 1	0.915	0.972	6.2%
Span 2-0.5L_S	0.944	0.981	3.9%
Pier 2	0.966	0.989	2.4%
Span 3-0.5L_S	0.965	0.988	2.4%
Pier 3	0.949	0.983	3.6%
Span 4-0.6L_S	0.949	0.983	3.6%

Governing Force Effects for Ratio 4: Case 3 to Case 4			
Service I - Moments			
Location	Load Factor, γ_{SE}		Difference
	1.25	1.75	
Span 1-0.4L_S	1.033	1.098	6.3%
Pier 1	1.032	1.096	6.2%
Span 2-0.5L_S	1.020	1.061	4.0%
Pier 2	1.012	1.036	2.4%
Span 3-0.5L_S	1.012	1.037	2.5%
Pier 3	1.018	1.055	3.6%
Span 4-0.6L_S	1.018	1.055	3.6%

Governing Force Effects for Ratio 2: Case 3 to Case 2			
Strength I - Moments			
Location	Load Factor, γ_{SE}		Difference
	1.25	1.75	
Span 1-0.4L_S	0.939	0.980	4.4%
Pier 1	0.937	0.979	4.5%
Span 2-0.5L_S	0.961	0.987	2.7%
Pier 2	0.975	0.992	1.7%
Span 3-0.5L_S	0.975	0.992	1.7%
Pier 3	0.963	0.988	2.6%
Span 4-0.6L_S	0.967	0.989	2.3%

Governing Force Effects for Ratio 4: Case 3 to Case 4			
Strength I - Moments			
Location	Load Factor, γ_{SE}		Difference
	1.25	1.75	
Span 1-0.4L_S	1.022	1.066	4.3%
Pier 1	1.023	1.069	4.5%
Span 2-0.5L_S	1.014	1.041	2.7%
Pier 2	1.009	1.026	1.7%
Span 3-0.5L_S	1.009	1.026	1.7%
Pier 3	1.013	1.039	2.6%
Span 4-0.6L_S	1.012	1.035	2.3%

Governing Force Effects for Ratio 2: Case 3 to Case 2			
Service I - Shears			
Location	Load Factor, γ_{SE}		Difference
	1.25	1.75	
Right of Abut 1	0.953	0.984	3.3%
Left of Pier 1	0.970	0.990	2.1%
Right of Pier 1	0.971	0.990	2.0%
Left of Pier 2	0.980	0.993	1.3%
Right of Pier 2	0.987	0.996	0.9%
Left of Pier 3	0.981	0.994	1.3%
Right of Pier 3	0.979	0.993	1.4%
Left of Abut 2	0.963	0.988	2.6%

Governing Force Effects for Ratio 4: Case 3 to Case 4			
Service I - Shears			
Location	Load Factor, γ_{SE}		Difference
	1.25	1.75	
Right of Abut 1	1.017	1.051	3.3%
Left of Pier 1	1.010	1.031	2.1%
Right of Pier 1	1.010	1.030	2.0%
Left of Pier 2	1.007	1.021	1.4%
Right of Pier 2	1.004	1.013	0.9%
Left of Pier 3	1.007	1.020	1.3%
Right of Pier 3	1.007	1.022	1.5%
Left of Abut 2	1.013	1.039	2.6%

Governing Force Effects for Ratio 2: Case 3 to Case 2			
Strength I - Shears			
Location	Load Factor, γ_{SE}		Difference
	1.25	1.75	
Right of Abut 1	0.967	0.989	2.3%
Left of Pier 1	0.979	0.993	1.4%
Right of Pier 1	0.979	0.993	1.4%
Left of Pier 2	0.985	0.995	1.0%
Right of Pier 2	0.991	0.997	0.6%
Left of Pier 3	0.986	0.995	0.9%
Right of Pier 3	0.985	0.995	1.0%
Left of Abut 2	0.975	0.992	1.7%

Governing Force Effects for Ratio 4: Case 3 to Case 4			
Strength I - Shears			
Location	Load Factor, γ_{SE}		Difference
	1.25	1.75	
Right of Abut 1	1.011	1.034	2.3%
Left of Pier 1	1.007	1.022	1.5%
Right of Pier 1	1.007	1.021	1.4%
Left of Pier 2	1.005	1.015	1.0%
Right of Pier 2	1.003	1.009	0.6%
Left of Pier 3	1.005	1.014	0.9%
Right of Pier 3	1.005	1.016	1.1%
Left of Abut 2	1.009	1.026	1.7%

FIGURE 2 Summary of ratios based on large settlement data in Table 3 (*3*).

Governing Force Effects for Ratio 2: Case 3 to Case 2			
Service I - Moments			
Location	**Load Factor, γ_{SE}**		**Difference**
	1.25	**1.75**	
Span 1-0.4L_S	0.974	0.991	1.7%
Pier 1	0.974	0.991	1.7%
Span 2-0.5L_S	0.984	0.995	1.1%
Pier 2	0.991	0.997	0.6%
Span 3-0.5L_S	0.990	0.997	0.7%
Pier 3	0.986	0.995	0.9%
Span 4-0.6L_S	0.986	0.995	0.9%

Governing Force Effects for Ratio 4: Case 3 to Case 4			
Service I - Moments			
Location	**Load Factor, γ_{SE}**		**Difference**
	1.25	**1.75**	
Span 1-0.4L_S	1.009	1.027	1.8%
Pier 1	1.009	1.027	1.8%
Span 2-0.5L_S	1.005	1.016	1.1%
Pier 2	1.003	1.009	0.6%
Span 3-0.5L_S	1.003	1.010	0.7%
Pier 3	1.005	1.014	0.9%
Span 4-0.6L_S	1.005	1.014	0.9%

Governing Force Effects for Ratio 2: Case 3 to Case 2			
Strength I - Moments			
Location	**Load Factor, γ_{SE}**		**Difference**
	1.25	**1.75**	
Span 1-0.4L_S	0.983	0.994	1.1%
Pier 1	0.982	0.994	1.2%
Span 2-0.5L_S	0.989	0.996	0.7%
Pier 2	0.993	0.998	0.5%
Span 3-0.5L_S	0.993	0.998	0.5%
Pier 3	0.990	0.997	0.7%
Span 4-0.6L_S	0.991	0.997	0.6%

Governing Force Effects for Ratio 4: Case 3 to Case 4			
Strength I - Moments			
Location	**Load Factor, γ_{SE}**		**Difference**
	1.25	**1.75**	
Span 1-0.4L_S	1.006	1.018	1.2%
Pier 1	1.006	1.019	1.3%
Span 2-0.5L_S	1.004	1.011	0.7%
Pier 2	1.002	1.007	0.5%
Span 3-0.5L_S	1.002	1.007	0.5%
Pier 3	1.003	1.010	0.7%
Span 4-0.6L_S	1.003	1.009	0.6%

Governing Force Effects for Ratio 2: Case 3 to Case 2			
Service I - Shears			
Location	**Load Factor, γ_{SE}**		**Difference**
	1.25	**1.75**	
Right of Abut 1	0.987	0.996	0.9%
Left of Pier 1	0.992	0.997	0.5%
Right of Pier 1	0.992	0.997	0.5%
Left of Pier 2	0.995	0.998	0.3%
Right of Pier 2	0.997	0.999	0.2%
Left of Pier 3	0.995	0.998	0.3%
Right of Pier 3	0.994	0.998	0.4%
Left of Abut 2	0.990	0.997	0.7%

Governing Force Effects for Ratio 4: Case 3 to Case 4			
Service I - Shears			
Location	**Load Factor, γ_{SE}**		**Difference**
	1.25	**1.75**	
Right of Abut 1	1.004	1.013	0.9%
Left of Pier 1	1.003	1.008	0.5%
Right of Pier 1	1.003	1.008	0.5%
Left of Pier 2	1.002	1.005	0.3%
Right of Pier 2	1.001	1.003	0.2%
Left of Pier 3	1.002	1.005	0.3%
Right of Pier 3	1.002	1.006	0.4%
Left of Abut 2	1.003	1.010	0.7%

Governing Force Effects for Ratio 2: Case 3 to Case 2			
Strength I - Shears			
Location	**Load Factor, γ_{SE}**		**Difference**
	1.25	**1.75**	
Right of Abut 1	0.991	0.997	0.6%
Left of Pier 1	0.994	0.998	0.4%
Right of Pier 1	0.995	0.998	0.3%
Left of Pier 2	0.996	0.999	0.3%
Right of Pier 2	0.998	0.999	0.1%
Left of Pier 3	0.996	0.999	0.3%
Right of Pier 3	0.996	0.999	0.3%
Left of Abut 2	0.993	0.998	0.5%

Governing Force Effects for Ratio 4: Case 3 to Case 4			
Strength I - Shears			
Location	**Load Factor, γ_{SE}**		**Difference**
	1.25	**1.75**	
Right of Abut 1	1.003	1.009	0.6%
Left of Pier 1	1.002	1.006	0.4%
Right of Pier 1	1.002	1.005	0.3%
Left of Pier 2	1.001	1.004	0.3%
Right of Pier 2	1.001	1.002	0.1%
Left of Pier 3	1.001	1.004	0.3%
Right of Pier 3	1.001	1.004	0.3%
Left of Abut 2	1.002	1.007	0.5%

FIGURE 3 Summary of ratios based on small settlement data in Table 3 (*3*).

SUMMARY AND FINAL REMARKS

This paper has presented results of a study performed to evaluate the structural implications related to the use of calibrated and relevant foundation movements in the AASHTO LRFD bridge design process. Following are key observations:

- Use of the construction-point concept with Δ_{SE} results in much less effects on controlling total moments and shears than would be indicated by the value of Δ_{SE}.
- Even with a 40% increase in the value of Δ_{SE} (i.e., change from 1.25 to 1.75), the difference in the controlling force effects is small.
- The changes in the controlling force effects increase as the settlements increase and vice versa.

These key observations are as expected because (a) within the overall AASHTO LRFD framework Δ_{SE} is just one of the many load factors in the service and strength limit state load combinations, (b) compared to the primary force effects due to DL and LL, the induced force effects due to settlement are much smaller, and (c) the differential settlements have a direct and proportionate (scalable) influence on the induced force effects. Because of all these considerations, the effect of settlements on a bridge structure must always be evaluated for all projects and on a project-specific basis. While evaluating the structural implications of foundation movements on a project-specific basis, it should be realized that the notion of a universal "tolerable" movement (settlement, lateral, etc.) value that is applicable to an entire structure is unrealistic because various elements of a structure will have different abilities to absorb the induced force effects due to movement.

Use of calibrated foundation movements in conjunction with the construction-point concept can lead to the use of cost-effective structures with more efficient foundation systems (*3*, *4*). With the implementation of the construction-point concept, larger total settlements under final loads can be found to be acceptable. It is well recognized that the cost of the foundation system increases rapidly if the foundation movements are limited to small values. For example, a deep foundation system may be required if the limiting settlement at a support is small while a shallow foundation system may be acceptable if larger settlements can be considered. Thus, the most important lesson from this study is that significant savings in bridge foundation costs can be realized using the approach described in the paper. Additional examples of optimization of bridge foundation sizes based on consideration of uncertainty in differential settlement are included in (*5*).

AUTHOR CONTRIBUTION STATEMENT

The authors confirm contribution to the paper as follows: study conception and design: 1. Naresh C. Samtani, 2. John M. Kulicki; analysis and interpretation of results: 1. Naresh C. Samtani, 2. John M. Kulicki; draft manuscript preparation: 1. Naresh C. Samtani, 2. John M. Kulicki. All authors reviewed the results and approved the final version of the manuscript.

ACKNOWLEDGMENTS

The permission of FHWA and AASHTO to develop this paper is acknowledged. The reviews and evaluations provided by the AASHTO T-15 committee and FHWA are also acknowledged. The authors gratefully acknowledge the effort of Dr. Wagdy Wassef who provided the moment and shear data for the bridges considered in the study. The authors would also like to acknowledge Silas Nichols, Principal Geotechnical Engineer, FHWA, for reviewing the draft versions of this paper and providing useful comments.

FUNDING

This work was supported by the FHWA in Cooperation with AASHTO. It was conducted in the Second Strategic Highway Research Program (SHRP 2) [contracts: SHRP R-19(b) DOT 7555-002, FHWA DTFH61-14-h-00015, and FHWA DTFH61-14-H-00015/0009], which is administered by the TRB of The National Academies of Science, Engineering, and Medicine.

REFERENCES

1. AASHTO. *AASHTO LRFD Bridge Design Specifications.* 8th (2017) and 9th (2020) Edition, American Association of State Highway and Transportation Officials, Washington, D.C.
2. Kulicki, J., W. Wassef, D. Mertz, A. Nowak, N. Samtani, and H. Nassif. SHRP2 Project R19B, Bridges for Service Life Beyond 100 Years: Service Limit State Design. *SHRP2 Report, Issue S2-R19B-RW-1*. Transportation Research Board, Washington, D.C., 2015. https://trid.trb.org/view/1305296.
3. Samtani, N. C., and J. M. Kulicki. *Incorporation of Foundation Movements in AASHTO LRFD Bridge Design Process*, 2nd ed. Federal Highway Administration, U.S. Department of Transportation, 2018.
4. Samtani, N. C., and J. M. Kulicki. Calibration of Foundation Movements for AASHTO LRFD Bridge Design Specifications. *Georisk: Assessment & Management of Risk for Systems*, Vol. 13, No. 3,Taylor & Francis, U.K., 2019. https://doi.org/10.1080/17499518.2018.1554818.
5. Samtani, N. C., and J. M. Kulicki. Uncertainty in Differential Settlements of Bridge Foundations and Retaining Walls. *Georisk: Assessment & Management of Risk for Systems*, Vol. 14, No. 3, Taylor & Francis, U.K., 2019. https://doi.org/10.1080/17499518.2020.1711526.
6. Moon, F., N. Romano, D. Masceri, J. Braley, D. R. Mertz, N. Samtani, T. Murphy, and M. Lopez. NCHRP Project 12-103, Bridge Superstructure Tolerance to Total and Differential Foundation Movements. Transportation Research Board, Washington, D.C., 2017.

Compendium of Service Limit State Development for Geotechnical Elements Designed by AASHTO LRFD

NARESH C. SAMTANI
NCS GeoResources, LLC

JOHN M. KULICKI
Consultant

The purpose of this paper is to provide a compendium of the development of service limit state design process for geotechnical elements that are designed using the reliability-based LRFD approach in the Bridge Design Specifications of the AASHTO hereinafter referred to as AASHTO LRFD (*1*). This compendium will help future researchers to better understand the basis of decisions made by AASHTO, with input from the FHWA, and thus will serve as an important benchmark for future work.

In 2007–2008 two projects, R19A and R19B, were initiated through the second Strategic Highway Research Program (SHRP2) of the TRB. Project R19A, titled "Bridges for Service Life Beyond 100 Years: Innovative Systems, Subsystems, and Components," (*2, 3*) produced the "Design Guide for Bridges for Service Life," which aimed to "define procedures to systematically design for service life and durability for both new and existing bridges." Project R19B was titled "Bridges for Service Life Beyond 100 Years: Service Limit State Design" (*4*). The goal of Project R19B was to "develop design and detailing guidance and calibrated service limit states (SLSs) to provide 100-year bridge life, and to develop a framework for further development of calibrated SLSs." The reports for these projects were issued in 2014–2015 (*2–4*). Development of Service limit state design guidance continued with the initiation of Project 12-108 (*5*) in 2016 through TRB's NCHRP. The goal of Project 12-108 work was to develop guide specification for extended service life for highway bridges that are designed using AASHTO LRFD (*1*). In 2019, the report for Project 12-108 (*5*) was released based on which AASHTO, in 2020, issued its new Guide Specification for Service Life Design of Highway Bridges (*6*). Thus, between 2007 and 2020 significant work was supported in part by TRB that led to the development of guidance for service life considerations. This work spawned other research and activities (*7–14*) that included development of specific design recommendations for calibration of several structural limit states, e.g., cracking, fatigue, foundation movements, etc., and re-evaluation of the criteria related to differential movements of foundations.

The formal consideration of SLSs in geotechnical engineering dates back decades to the pioneering efforts by researchers such as Brinch Hansen (*15*) and others. The underlying considerations in terms of the effect on functionality of the structure supported by geotechnical elements remain the same since these original efforts. With due acknowledgment of the past efforts, the focus of this paper is on the latest research projects that were specifically indexed to the format of modern AASHTO LRFD and FHWA documents.

REVIEW PROCESSES

The research projects summarized in this paper underwent extensive reviews. This section provides an overview of the review processes so that the reader can develop an appreciation for the level of vetting done prior to the research being published and accepted for incorporation into AASHTO and other guidance documents such as FHWA Geotechnical Engineering Circulars (GECs). The process often starts with the evaluation of research needs statements from which some are selected for potential funding. A research project may be initiated with the selection of a panel to guide the work. That group may develop a scope, often by refining the needs statement. While a research team (RT) is sometimes sole sourced, more typically competitive proposals are openly solicited and a RT selected based on the panel's evaluation of the merits of the submissions. The panel has several opportunities to evaluate and guide the work as interim and final reports are reviewed. If revisions to existing documents or new documents are a product of the research the proposed change is forwarded to the appropriate Technical Committee (TC) of the AASHTO Committee on Bridges and Structures (COBS) which then further evaluates it for possible inclusion in the agenda for an annual meeting of COBS. COBS is comprised of a senior bridge engineer from the 50 states and several other jurisdictions and agencies, 53 of whom are the "Voting Members." During this part of the process the members of the TC, or their staff, review the work and may propose revisions. FHWA representatives are often part of TCs as non-voting members and provide input to ensure the review processes consider the information available through their guidance documents such as the GECs. The TC may reject the revisions or approve them, possibly with further revisions, for inclusion in the agenda for the full COBS annual meeting. Drafts of all agenda items are provided for the members of COBS in advance of the meeting to provide an opportunity for all the members to review and comment. The TC receives the comments and responds as it deems appropriate which may include further revisions. The agenda items are presented to the full membership in an open meeting which provides yet another opportunity for comments from the members and from the floor before a vote for or against acceptance is taken. In summary, the review processes are comprehensive.

Many of the recommendations from all the research projects noted in this paper were adopted, with some modifications, for incorporation in AASHTO LRFD (*1*). Since these recommendations addressed both structural and geotechnical aspects, the reviews and approvals were done by several TCs of the COBS with the T-15 TC for "Substructures and Retaining Walls" leading the effort in association with the T-5 TC for "Loads and Load Distribution." The geotechnical elements of these research projects are also in various stages of incorporation into geotechnical guidance documents by the FHWA GECs.

AASHTO LRFD and Limit States

AASHTO LRFD (*1*) considers four primary limit states: strength, extreme event, service, and fatigue. Strength (or ultimate) limit states pertain to structural safety and evaluation of the loss of load-carrying capacity (i.e., ultimate resistance). Early work in 1990s by AASHTO for development of LRFD methodology concentrated on development of specific load and resistance factors for different load combinations in strength limit state based on use of reliability principles, backfitting with past practice based on ASD, LFD, or judgment based on expert elicitation (an element of the Delphi process). Extreme Event limit states, like strength limit states, also deal with

ultimate resistance (capacity), and, based on their low frequency of occurrence, are generally assigned load factors of 1.0 and resistance factors of 1.0 or close to 1.0.

Project R19B was tasked with calibration of service and fatigue limit states. Fatigue limit state, which involves considerations of a large number of load cycles, is generally not applicable to geotechnical elements. In contrast, serviceability limit states are the limiting conditions affecting the function of the structure under expected service conditions. Serviceability limit states occur before collapse, i.e., attainment of strength limit states. These include conditions that may restrict the intended use of the structure. In general, from a geotechnical viewpoint, evaluation of SLSs involves the following two considerations:

1. Evaluation of the reliability (uncertainty) of predicted total and differential foundation movements which can lead to: (a) structural limit states such as cracking, shearing at a joint, distress to bearing elements, etc., and/or (b) undesirable geometric effects such as change in grades (which can lead to drainage issues), rough rideability, e.g., bump-at-end-of-a-bridge, etc.
2. Evaluation of material deterioration which over time can lead to reduction in load-carrying capacity and manifestation of deformations that can lead to undesirable consequences noted in the Consideration 1 above.

The long-term performance of the foundation and retaining walls can be affected by the environment provided by the geomaterials. Evaluation of the effect of deterioration of structural elements through degradation or corrosion on serviceability is a significant aspect in the design process that must be indexed to long-term risk of adverse performance. The term *degradation* applies to nonmetallic components such as polymeric soil reinforcements in mechanically stabilized earth (MSE) walls, and *corrosion* applies to metal components.

This paper provides information on (a) overarching contributions of various research projects (*7–14*) in the context of the two considerations noted above, (b) how the research projects were evaluated by AASHTO and FHWA, (c) how all the research projects fit together, and (d) opportunities for future work. A common theme in all the research projects is that the geotechnical aspects were developed in the context of structural limit states since the geotechnical performance directly affects the structural aspects. Furthermore, the framework for geotechnical work was developed in a general manner that would easily allow incorporation of future research. Thus, future researchers should carefully examine each cited work in detail to ensure that their work fits properly in the overall framework described herein.

Consideration 1: Reliability of Predicted Foundation Movements

Work reported in (*4*) and (*7–14*) is related to this consideration. The main features of these research projects are discussed below.

Project R19B

Project R19B developed reliability-based calibrated load factors or resistance factors, or both, for (a) foundation movements, (b) cracking of reinforced concrete components, (c) LL deflections, (d) permanent deformations, (e) cracking of prestressed concrete components, and (f) fatigue of steel and reinforced concrete components. This paper concentrates on the foundation movements.

Foundation movements induce additional force effects such as moments and shears in a bridge structure which can lead to adverse consequences such as cracking. The basic AASHTO LRFD framework in terms of distributions of loads and resistances is shown in the *f(Q,R)* – *Q,R* space (upper quadrant) in Figure 1. For the evaluation of movements, this framework needs to be modified to include the load-movement (*Q*–δ) curve. The *Q*–δ curve, which also represents mobilized resistance due to movement (i.e., *R*–δ), can be considered as another dimension (lower quadrant) as shown in Figure 1.

Although *Q*–δ curves can have many different shapes, for illustration purposes, a simple strain hardening curve at initiation of service life is shown in Figure 1. Furthermore, the mean *Q*–δ curve is shown, and the spread of the *Q*–δ data about the mean curve is represented by a probability distribution function (PDF). The force effects at Point *S* corresponding to nominal load (i.e., service limit state) are of primary interest for calibration of movement. Point *F* corresponds to factored load and resistance, i.e., strength limit state. Point *N* corresponds to nominal resistance which is a consideration for evaluation of the Extreme Event limit state. Now that a link between the limit states and movement has been made, the effect of material brittleness (or ductility) and deterioration aspects can be introduced in the AASHTO LRFD framework through an appropriate *Q*–δ curve. Examples of *Q*–δ curves include vertical load-settlement curves for foundations, lateral load-lateral displacement curves for deep foundations, shear force-shear strain curves, and moment-curvature curves. The effect of deterioration can be thought of in terms of moving from resistance corresponding to Point *F* (strength limit state) to Point *S* (service limit state) and below towards Point *O*. Since deterioration occurs over time, the *Q*–δ curve can also be expressed in terms of time. The proposed formulation can incorporate any *Q*–δ curve and is, therefore, a general formulation that can be used for geotechnical or structural calibrations and can also include consideration of deterioration.

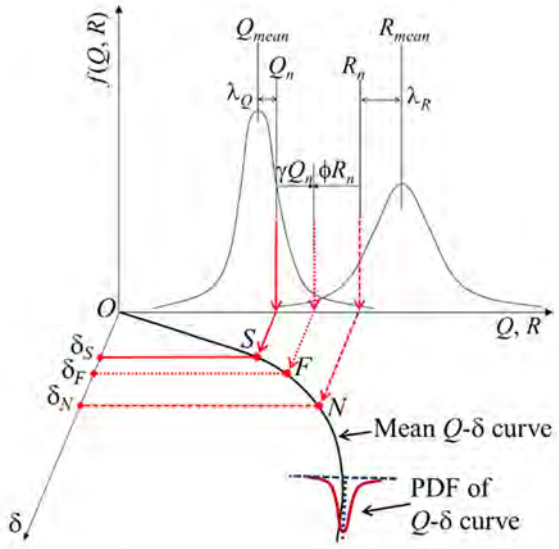

FIGURE 1 Incorporation of *Q*–δ curve into the AASHTO LRFD framework (adapted from *4*, *7*). NOTES: *Q*: load, Q_{mean}: mean load, Q_n: nomimal load, λ_Q: bias factor for load, γ: load factor, *R*: resistance, R_{mean}: mean resistance, R_n: nominal resistance, λ_R: bias factor for resistance, *f*: frequency, *O*: origin of *Q*-δ curve, δ: movement, δ_S: movement at Q_n, δ_F: movement at factored load $Q_F=\gamma(Q_n)$, and δ_N=movement at load corresponding to R_n.

The framework in Figure 1 recognizes that there is uncertainty in the mean *Q*–δ curve which is schematically represented by the PDF shown on the mean *Q*–δ curve. Quantification of this uncertainty is necessary to evaluate the reliability of predicted movement. At this stage, it is important to realize that the structural effects due to superimposed movement caused by any reason (e.g., temperature change, foundation movements) are in the form of induced force effects such as moments and shears. Thus, the manifestation of any type of superimposed movement must be considered in terms of additional loads and not in terms of resistances. This necessitates a paradigm shift in thinking that the effect of foundation movements must be thought in terms of a load effect and not in terms of geotechnical resistance. In fact, all design codes worldwide recognize this observation by including a representation of structural effects of foundation movements in terms of load. AASHTO LRFD (*1*) uses the *SE* load factor, γ_{SE}, for such evaluations. The *SE* load factor occurs in four out of the five load combinations for strength limit state and three out of the four load combinations for service limit state. Clearly, AASHTO LRFD recognizes that foundation movements can have both strength and serviceability implications. This recognition has been there ever since the first edition of AASHTO LRFD in 1994 and can also be traced back to similar stipulations in the Standard Specifications of AASHTO that were based on ASD and LFD.

After the framework was established, the task was to express the uncertainty in foundation movements represented by the PDF around the mean *Q*–δ curve in terms of the *SE* load factor. Foundation movements may be predicted using various methods. This is a distinction compared to structural design for which there is more consensus on specified calculation methods. This means that the *SE* load factor needs to be calibrated for different prediction methods and different types of foundation movement such as vertical (settlement), horizontal (lateral), and rotation.

Another challenge was to evaluate the movements in the context of structural limit states and reliability index, β. This challenge first required an evaluation of the structural limit states such as cracking to establish acceptable target values of reliability index, β_T. This evaluation led to the identification of three variations of SLSs: (a) reversible, (b) irreversible, and (c) reversible-irreversible. Reversible limit states are those for which no consequences remain once the load is removed; e.g., a bridge span returning to its original state once a truck has crossed it. Irreversible limit states are those for which consequences are realized; e.g., permanent deformations induced from transient loads such as LL, temperature changes, or foundation movements. Reversible-irreversible limit states are those where the effects of consequences are reversed by active interventions; e.g., while foundation movements are clearly irreversible with respect to the bridge substructure, the effects of such movements on the bridge superstructure can be reversed by shimming or jacking. Based on these evaluations, the Project R19B team established the following criteria: $\beta_T = 0.50$ for reversible or reversible-irreversible limit states, and $\beta_T = 1.00$ for irreversible limit states. These values correspond to a target probability of exceedance, P_{ET}, of approximately 30% (for $\beta_T = 0.50$) and 15% (for $\beta_T = 1.00$).

Now that the target values of β_T (or P_{ET}) for an acceptable performance were established, the *SE* load factor needed to be expressed in terms of the tolerable values of movement, δ_T. for any given predicted value of movement, δ_P, that is computed based on a chosen analytical method. The values of δ_T are a function of the bridge type and its components such as girders, bearings, and foundations. In reality, a deterministic value for δ_T is often chosen by the bridge designer based on intangibles such as the use of arbitrary criteria (e.g., the settlement shall not exceed 1-in.) established by an owner, the judgment of the designer based on past experience, and/or simply some sort of comfort level based on basic human instinct for conservativeness. For

the case of a deterministic δ_T, the conventional Monte Carlo method that is used for calibration of strength limit state was found not to be feasible for various reasons noted in (*7*, *8*). A new reliability-based procedure was developed for calibration of the *SE* load factor and details of this procedure can be found in (*4*, *7*, *8*). This procedure was demonstrated through use of an FHWA database for immediate settlements based on measurements of 20 spread footings from 10 bridges in northeast United States and five analytical methods for predictions. The recommended γ_{SE} values for different prediction methods and types of movement (e.g., immediate settlement, consolidation settlement, and lateral movement of deep foundations) were developed. Due to unavailability of some databases coupled with budgetary and schedule constraints, extensive evaluation of other datasets reported was not possible. However, it was recognized that regional geology and local subsurface investigation, design, construction, and maintenance practices can have a strong influence. Thus, it was recommended (*4*, *7*, *8*) that owners should be encouraged to calibrate a "local" method where local conditions are not consistent with conditions identified in cited reports.

Finally, as part of the calibration process, it was recognized that most designers analyze foundation movements as if all the loads applied at the same time, i.e., a bridge structure was instantaneously set into place. However, loads and movements occur gradually as construction proceeds. The movements predicted to occur before placement of the superstructure may not be relevant to the design or performance of the superstructure. Depending on the type of superstructure and the construction sequence, the immediate settlement between the construction stage at which the stresses in the superstructure elements are affected by differential settlements and end-of-construction can be between 25% and 75% of the total settlement. Thus, the predicted relevant settlement that may affect a bridge structure can be much less than the predicted total settlement. Therefore, to ensure realistic bridge designs, the Project R19B work recommended that predicted relevant settlements should be used with the calibrated γ_{SE} values. This is referred to as the construction-point concept.

Use of calibrated foundation movements in conjunction with the construction-point concept can lead to the use of cost-effective structures with more efficient foundation systems (*4*, *7*, *8*). With the implementation of the construction-point concept, larger total settlements under final loads can be found to be acceptable. It is well recognized that the cost of the foundation system increases rapidly if the foundation movements are limited to small values. For example, a deep foundation system may be required if the limiting settlement at a support is small while a shallow foundation system may be acceptable if larger settlements can be considered. Thus, an important geotechnical contribution from the Project R19B study is that significant savings in bridge foundation costs can be realized while ensuring uniform levels of reliability in different bridge components.

The "White Paper"

All SHRP2 work done through TRB was intended for incorporation into practice which, for the case of bridge design, is implemented through AASHTO LRFD and FHWA guidance documents such as GECs. This is facilitated through an Implementation Assistance Program (IAP) sponsored by the FHWA and AASHTO. The IAP includes collaboration with AASHTO COBS as well as providing live (i.e., in person classes) training, distance (i.e., webinar style) training, and as-needed assistance requested by any of the 50 member states of AASHTO. Many presentations were made by the authors in different forums including mid-year and annual meetings of

AASHTO COBS. As noted earlier, since Project R19B included aspects related to load factors and geotechnical prediction methods, the T-5 and T-15 TCs were involved in the review and consideration processes with T-15 taking the lead. An historic first joint mid-year meeting of T-5 and T-15 TCs was held in October 2015 in Chicago, Illinois, where the work related to foundation movements was presented by the authors and discussed. These discussions led to the following observations:

1. Because Project R19B addressed many topics resulting in a large final report, it was requested that, for convenience, the work for foundation movements be extracted and presented in the form of a stand-alone "White Paper."
2. The White Paper should include: (a) a detailed flow chart that provides a step-by-step process for implementation of the proposed changes based on calibration of the *SE* load factor, (b) detailed bridge design example problems using actual bridges to demonstrate the application of the process in the flow chart, (c) expanded discussions to provide clarifications that would capture the discussions at the T-5 and T-15 joint meeting, and (d) updated draft agenda items for changes in AASHTO LRFD format for consideration of the committees.

Thus, a White Paper (first edition) was developed in 2016. The FHWA then required that this White Paper be used as a reference manual for live training at the Federal Lands Highway Division (FLHD) offices in Denver, Colorado (Central FLHD); Sterling, Virginia (Eastern FLHD); and Portland, Oregon (Western FLD). Both agency and consultant designers from structural and geotechnical disciplines attended these trainings. This provided FHWA an opportunity to solicit comments from a wide and representative audience of end-users. Additional presentations were made at regional conferences, e.g., the 2017 Southwest Geotechnical Engineering conference in Phoenix, Arizona. The process of soliciting and collecting comments from these training sessions and presentations coupled with the comments provided by the T-15 and T-5 committee members served as a comprehensive vetting process for the proposed changes to AASHTO LRFD. The original version (i.e., first edition) of the White Paper was revised to incorporate the comments and an updated (second edition) of the White Paper (*7*) was issued in 2018. The updated document includes additional bridge design example problems to evaluate a range of γ_{SE} values. Since this document is a stand-alone report it was accorded the status of a formal FHWA geotechnical resource document and published by the FHWA for public domain. A succinct discussion of the calibration in Samtani et al. (*7*) can be found in Samtani et al. (*8*).

The Implementation Report

As part of its deliberations, the T-15 TC noted that the calibrations for foundation movements and the recommended γ_{SE} values in Kulickiet al. (*4*) and Samtani et al. (*7*) were based on a database of 20 data points that concentrated on bridges in the northeastern United States. All the data points showed measured immediate settlement values smaller than 1.0 in. The minimum value was 0.23 in. and the maximum value was 0.94 in. Therefore, T-15 TC desired to test and validate the proposed calibration framework and the γ_{SE} values in Kulickiet al. (*4*) and Samtani et al. (*7*) by expanding the database to include case histories from different geographical areas of the United States as well as projects where settlements larger than 1.0 in. were predicted and/or measured.

Data for settlements ranging up to 40 in. for bridge footings, fills, and walls was collected from various sources in the United States (including DOTs of Washington State, Ohio, and South

Carolina) and Europe. A total of 80 and 61 data points that were based on SPTs and CPTs, respectively, were obtained. Prediction methods by Schmertmann, et al. (*16*) and Hough (*17*) were used since these are the two methods that are recommended by FHWA and AASHTO LRFD and are commonly used by state DOTs. All the datasets and accompanying calibrations were included in Samtani and Allen (*9*). Data correlation issues were evaluated using Pearson correlation coefficients. The calibrations were performed using β_T =1.00. Recommendations for compiling a quality database for future calibrations were provided.

As expected, the values of γ_{SE} varied depending on the geographical location. However, for a national document such as AASHTO LRFD a single γ_{SE} value for a given target reliability index and prediction analytical method is needed. Thus, for developing γ_{SE} values, the aggregated dataset from all sources was used. It was found that predicted settlement values less than 0.5-in. exhibit considerable data scatter and therefore a minimum differential settlement value of 0.5-in. was recommended in such cases. Once the data points corresponding to less than 0.5-in. predicted settlement were removed from the dataset, the data scatter reduced and resulting γ_{SE} values were somewhat smaller than those recommended in Kulickiet al. (*4*) and Samtani et al. (*7*). However, given the range of γ_{SE} values based on the subset datasets, it was clear that the original recommendation in Kulickiet al. (*4*) of calibrating γ_{SE} based on local conditions was valid. Thus, the recommendation for calibrating a local method was retained and included in the agenda items for balloting. Furthermore, the recommendation to use the construction-point concept with γ_{SE} values was also retained. Finally, the method for predicting immediate settlements using the version of Schmertmann et al. (*16*) in Samtani and Nowatzki (*18*) was included in the agenda items supplementing the existing Hough method. The version of Schmertmann et al. in (*18*) was selected because it is consistent with the criteria for determination of elastic modulus in AASHTO LRFD (*1*).

The findings by Samtani and Allen (*9*) were incorporated into the agenda items for Section 3 (Loads and Load Factors) and Section 10 (Foundations) for consideration at the annual AASHTO conference in 2018 held in Burlington, Vermont. Among the proposed changes in Section 3 was a new table that is dedicated to *SE* load factors. Having this dedicated table allows future geotechnical modifications in a modular manner. For example, at the current time, γ_{SE} = 1.00 has been assigned to lateral movements for deep foundations based on the *p–y* and strain wedge method. These are placeholder values until calibrations have been performed using high-quality databases. Similarly, the table can be expanded in the future to address other types of movements, e.g., rotation at top of deep foundations under lateral forces and moments. The agenda item was approved at the 2018 annual AASHTO meeting in Burlington for inclusion in the 9th edition of AASHTO LRFD that was issued in 2020.

NCHRP Project 12-103

As the Project R19B was being completed, TRB's NCHRP Project 12-103, Bridge Superstructure Tolerance to Total and Differential Foundation Movements (*10*) was initiated in December 2013. The objectives of this research were to "(*a*) develop procedures to determine the acceptable levels of bridge foundation movements based upon superstructure tolerance to total and differential movements considering Service and Strength limit states, and (*b*) propose revisions to the AASHTO LRFD Bridge Design Specifications." Thus, in contrast to the foundation movement work in Project R19B which concentrated on quantifying the uncertainty in foundation movement

at a given support element, Project 12-103 concentrated on differential movement aspect of foundation movements and quantifying threshold values at which Service and Strength limit states may be affected. Thus, the two projects (R19B and 12-103) complemented each other.

With respect to revisions for AASHTO LRFD the focus of Project 12-103 was an evaluation of Article 10.5.2.2 in the 8th Edition of AASHTO LRFD which provides guidance for tolerable movements and movement criteria for highway bridges. The guidance for tolerable angular distortions in the commentary, Article C10.5.2.2 in the 8th Edition of AASHTO LRFD, states that "…studies indicate that angular distortions between adjacent foundations greater than 0.008 rad. in simple spans and 0.004 rad. in continuous spans should not be permitted in settlement criteria (Moulton et al. 1985; DiMillio 1982; Barker et al. 1991)." These criteria can be traced back to AASHTO Standard Specifications since the mid-1980s that were grandfathered into the AASHTO LRFD. The White Paper (*7*) provides more information on the background and basis of the criteria in AASHTO LRFD.

The criteria in Article 10.5.2.2 in 8th Edition of AASHTO LRFD were the only quantifiable "deemed-to-satisfy" values related to the effect of foundation movements on bridge structures. As per these criteria, a longitudinal differential support movement, Δ, of 9.6 and 4.8 in. for simple span and continuous span, respectively, would be tolerable for a span, L = 100 ft. These values are in addition to any uniform settlement over the span. It is difficult for most designers to consider such large values as tolerable. Therefore, often bridge designers use arbitrarily small values of angular distortions (Δ/L). Such arbitrary conservatism can lead to a significant increase in foundation costs because deep foundations are often used where more cost-effective shallow foundations would have been feasible.

Using the bridge design requirements as per the 8th Edition of AASHTO LRFD, Project 12-103 concentrated on refinement of the "deemed-to-satisfy" angular distortion criteria. A multivariate parametric study was performed to examine a large number of steel and prestressed concrete multi-girder bridge configurations and parameters. A large sample population of bridges was evaluated using an automated process that included a member sizing algorithm, three-dimensional (3D) finite element model construction, simulation, and results extraction. For each sample, tolerable support movements were calculated and compared to the AASHTO LRFD guidance when applicable. This evaluation led to more refined criteria that, in addition to the angular distortion, are a function of the bridge superstructure type (steel or concrete), skew angle, girder spacing, and method of structural analysis. Refer to (*10*) for more information on the refined criteria. These refined criteria were considered by AASHTO COBS and were approved at the 2018 annual AASHTO meeting in Burlington, VT, for inclusion in the 9th edition of AASHTO LRFD that was issued in 2020.

Uncertainty in Predicted Differential Settlement

Between Project R19B and Project 12-103 two significant milestones were attained in that (*a*) the uncertainty in predicted foundation movements at a given support could be quantified through the *SE* load factor and (*b*) refined differential settlement criteria conforming to AASHTO LRFD were developed. However, a significant question about the uncertainty in computed (predicted) differential foundation movement remained. γ_{SE} only addresses uncertainty in the foundation movement at a given support location for a certain model for prediction of movement. It does not address the uncertainty in differential movement between two support locations. Differential movement involves an evaluation of the joint uncertainty in total movement

between two support locations. Research conducted by the authors indicates two important aspects in this regard: (i) depending on the underlying values of total settlements and the method used to compute them, the uncertainty in calculated differential settlement can vary significantly, and (ii) the uncertainty of the calculated differential settlement between adjacent support elements is larger than the uncertainty of the predicted total settlement at each of the two support elements used to calculate the differential settlement. To address these aspects, the following criteria to estimate differential settlements were recommended (*7*, *8*):

"1. Assume that the actual (measured) settlement of any support element could be as large as the predicted factored relevant settlement value, S_{FR}, calculated by using a given method.

2. Assume that the actual (measured) settlement of the adjacent support element could be less, taken as zero in the limit, instead of the predicted factored relevant settlement value, S_{FR}, calculated by using the same given method."

This approach is referred to as the $S_{FR} – 0$ concept where S_{FR} represents the predicted factored relevant settlement at one support of a span and the value of "0" represents zero settlement at an adjacent support, i.e., the limiting small value. Since one support is assumed to have zero settlement, the resulting differential settlement becomes the extreme value as required by Article 3.4.1 AASHTO LRFD that stipulates, "Force effects due to extreme values of differential settlement among substructures and within individual substructure units shall be considered." The use of words such as "extreme values of differential settlement" acknowledge the concern that some of the foundation units may settle less than predicted, or even undergo no settlement. The $S_{FR} – 0$ approach helps address this stipulation and eliminate the additional uncertainty associated with differential settlement. Thus, after use of $S_{FR} – 0$ approach, the only uncertainty left is that associated with the settlement values at each of the support elements used to compute the differential settlement, and this uncertainty is addressed by γ_{SE}. In any case, two modes of differential settlement within any span must be evaluated. In Mode 1 the left support is assumed to have zero settlement while in Mode 2 the right support is assumed to have zero settlement. The bridge design process must explore all viable deformed shapes based on evaluation of these two modes for all bridge spans. This approach also helps create the extreme values of differential settlement and evaluate the critical force effects as required by AASHTO LRFD.

The $S_{FR} – 0$ approach was considered by AASHTO T-15 COBS at their 2018 annual meeting in Burlington, VT. It was decided to include $S_{FR} – 0$ approach but express it in terms of the quality of the subsurface information available based on judgment of the designer. Accordingly, it was recommended that if the variability in the subsurface conditions between foundation elements is high, the $S_{FR} – 0$ approach as described in (*7*, *11*) should be considered to determine the maximum differential movement between adjacent foundation elements. Otherwise, the actual total settlements may be used to compute the differential settlements rather than assuming that the settlement at one support is zero.

When left to judgment whether to use $S_{FR} – 0$ approach or not, a designer may resort to use of arbitrary intermediate differential settlement criteria found in geotechnical literature that express limiting differential settlement as a fraction of total settlement, e.g., ½ to ¾ of total settlement. Using probabilistic analysis with datasets included in Samtani and Allen (*9*), a normalized probability exceedance chart (NPEC) approach was developed by Samtani and Kulicki (*12*) that permits a designer to select an appropriate value of differential settlement based on the target

probability of exceedance of tolerable differential settlement. The NPEC approach has been accepted for inclusion in FHWA's GEC 1 titled "Geotechnical Fundamentals for Transportation Projects" that will be released in fall 2021.

National Highway Institute 5-Module Web-based Training (13)

Once the AASHTO COBS approved the various research elements related to geotechnical elements as discussed above, FHWA initiated an effort to develop a self-paced web-based training course that can be used to develop local *SE* load factors in fall 2018. This training represents a condensed version of the live training that was mentioned earlier. The goal of the course is "To understand, learn, and demonstrate the calibrations for foundation movements so that the undesirable consequences of foundation movements can be mitigated when designing structures." The course is approximately 4-h in duration and includes five modules. All discussion is indexed to the White Paper (*7*) which is treated as the reference manual. Further, FHWA resources are also identified in the course. The overarching learning outcomes for the course are for the participants to be able to (a) recognize the undesirable consequences due to foundation movements, and (b) calibrate foundation movements using principles of limit state design. Finally, the course is framed in the context of general principles of limit state design and therefore the course can be useful to researchers using other design regulations such as the Canadian Highway Bridge Design Code or the Eurocode which are also based on concept of limit states.

Consideration 2: Material Deterioration

Work reported in Project R19A (*2, 3*) and NCHRP Document 269 (*5*) is related to this consideration. From a geotechnical perspective, Project R19A (*2-3*) did not include tangible information. Thus, the discussion below concentrates on the work in (*5*).

NCHRP Project 12-108 (5)

While the Project R19A provided a general framework for establishing recommendations for extending service life of structural elements it was felt by bridge owners that there was not enough specific guidance for service life design of highway bridges. Therefore, bridge owners were forced to make subjective evaluation of practices for the identification and assessment of design alternatives to improve the service life of highway bridges. Hence Project 12-108 was commissioned by AASHTO and directed by NCHRP for which the objectives were to develop "(1) proposed AASHTO guide specification for service life design of highway bridges and (2) case studies to demonstrate the application of the proposed guide specification." Specifically, the goals and purpose of the guide specification were to (*5*):

- Provide practical guidance to designers of highway bridges on how to implement service life design during the design phase, including how to define a target service life and how to provide adequate implementation methods;
- Utilize currently available data as well as bridge owner experience to tie various design practices to service life; and
- Allow for the future incorporation of improved deterioration and service life models as they become available that will eventually evolve into calibrated partial factor semi-probabilistic limit states.

Definitions and Three-Tier Approach

A key task for the guide specification was to develop guidance for extended service life up to 150 years which is considerably more than the typical 50 to 75 years that is currently used. One of the early items in the development of the guide specification was to evaluate the various definitions pertaining to life of a bridge structure. In this regard, AASHTO LRFD was developed to address bridges with a "design" life of 75 years which is "the period of time on which the statistical derivation of transient loads is based" (*1*). The "design" life is used to define the design values for variable and time-dependent loads in order to meet target structural reliability indices. In contrast, AASHTO LRFD indicates that "service" life is "the period of time that the bridge is expected to be in operation" (*1*). Neither of these definitions includes a reference to maintenance. Based on a review of definitions worldwide and internal discussions between the RT and NCHRP review panel, the guide specification (*6*) defines "service" life as "the period of time a bridge remains in operation, without rehabilitation or significant repair, and with only routine maintenance. This includes replacement of renewable elements." The words "actual," "intended," or "target" are used as interchangeable prefixes with this definition, e.g., "target service life."

Once the definition of service life was established, the guide specification used a three-tiered approach to delineate different levels of service life. The first level was identified as "normal" service life which was indexed to 75 years. The service life of 150 years was called "maximum" service life. An intermediate category called "enhanced" was defined as having a service life of 100 years. To ensure consistency with the superstructure and substructure elements of bridges, the practices in the geotechnical industry now needed to be evaluated in a similar three-tier approach.

Content

The guide specification was organized in a two-column format like AASHTO LRFD with the left column providing specification and the right column providing commentary. The first few sections contain introductory and general guidance information. A section is dedicated to defining the environmental "loads" on a bridge structure, followed by several sections for the main types of materials and common bridge elements, and ending with a section on life-cycle cost analysis. An appendix is included that provides a framework for expanding the guide specification to include probabilistic service life limit states once they have been sufficiently developed through research. A second appendix includes two case studies demonstrating the application of the guide specification. From a geotechnical perspective, there is a Section 6 titled "foundations and retaining walls" which is intended to provide a counterpart to Sections 10 ("Foundations") and Section 11 ("Walls, Abutments, and Piers") in AASHTO LRFD.

Exposure Classes

From a service life and deterioration standpoint, the environment surrounding a bridge and its components represents the load on the structure. These environmental loads are typically represented using exposure classes. Within the guide specification, definitions of exposure classes are presented for the most prevalent deterioration mechanisms of the most common bridge materials (i.e., concrete and steel). The exposure classes are grouped by deterioration mechanism and vary by the severity of the environment. For concrete, the following four exposure "categories" were

identified: Corrosion (C), Freezing and Thawing (FT), Sulfate (S), and In Contact with Water (W). For steel, two exposure classes were identified: Corrosion (C) and fatigue (F).

Each exposure category was subdivided into classes. For example, exposure class C-M2 for concrete entailed consideration of submerged structures in marine environment. All the exposure categories and classes are described in a tabular matrix in the guide specification.

From a geotechnical perspective, an exposure class C-B was introduced that was described as being applicable to "buried elements (deep and shallow foundations, retaining structures, etc.) below finished grade (mudline in case of submergence)." This assignment of a specific C-B exposure class was found to be necessary because a buried environment is distinctly different than atmospheric or submerged environment in that the deterioration mechanisms and rates are different. For example, if the concrete cover for buried structures is determined using the deterioration model for chloride-induced corrosion of steel in reinforced concrete in atmospheric or marine environment then concrete covers in excess of 8 in. were found to be necessary. Clearly, concrete covers in the realm of 1.5 to 3 in. have been successfully used of many decades and are included in design regulations; for example, Table 5.10.1-1 of AASHTO LRFD (*1*) stipulates a concrete cover of 3.0 in. for concrete structures cast against earth. Back analysis of concrete cover for buried structures using a fully probabilistic chloride-induced corrosion model in Appendix A of the Guide Specification indicated the need to have a separate exposure class for buried concrete structures and hence the C-B exposure class was introduced. A detailed background of processes that formed the basis for the recommendations for buried structures in (*5*, *6*) is provided by Samtani and Kulicki (*14*).

A step-by-step procedure for evaluating the concrete cover for buried structures in included in (*5, 14*). The single exposure class of C-B serves as a catch-all class for all types of geotechnical elements that use cementitious materials to protect against deterioration, e.g., steel in reinforced concrete, grout cover for ground anchors, etc. Based on future research, this category can be broadened to include subsets such as C-B1, C-B2, etc. to address specific needs for a given application, e.g., bare steel in geomaterial, spread footing, drilled shaft, precast concrete piles, etc. Thus, the framework was made general for future use.

Protection Index Approach

Another important geotechnical challenge was the consideration of many disparate guidance documents for consideration of durability that are in use for different types of foundation and retaining wall components. For example, ground anchors typically rely on grout cover and encapsulation, drilled shafts usually rely on concrete cover with field verification of the concrete cover, while metallic reinforcements in MSE walls use zinc coatings and sacrificial steel. These methods have been developed on a component basis, often by the industries that produce or promote those components. A general underlying theme is the consideration of risk of failure. For example, if the soils are considered aggressive in terms of corrosion potential, then elements such as ground anchors and soil nails are required to have a double corrosion protection such as encapsulation in grout-filled plastic sheath.

However, the established practice is not consistent across all components, e.g., consideration of corrosion in drilled shafts is not consistent with those in ground anchors, and so on. In fact, while all geotechnical elements generally establish aggressiveness of ground in terms of deterioration (corrosion or degradation) based on a suite of electrochemical properties that include pH, resistivity, sulfates and chlorides, different threshold values of these properties are used for

establishing protection measures. This is because different geotechnical elements have been researched by specific industry groups and great importance has been placed on "deemed-to-satisfy" type of criteria that are based on apparent historical success of a given protection measure often using anecdotal evidence.

With the understanding that these historical approaches have resulted in generally successful practices, in the development of the foundations and retaining walls section of the guide specification, importance was placed on incorporating past efforts and practices to the greatest extent possible. However, for the sake of being consistent with a consolidated approach taken for structural elements in the guide specification, i.e., the three-tier approach, it was desired that guidance for geotechnical elements be also consolidated in a similar manner. As part of this consolidation effort, a three-tier approach that combines ascertainment of risk and selection of protection strategy for different geotechnical elements was desired. This led to the development of a system based on a protection index, P_I. In this system a P_I-value is first established based on the environment, consequences of adverse performance, location, and the type of facility carried or protected, as indicated in Table 1.

Thus, the main features of the protection index approach are (*a*) division of design into three categories based on a number of "risk" factors, and (*b*) scaling of the risk mitigation through appropriate protection strategies. This is broadly analogous to the three-level approach of the proposed guide specification and helps to bring together various product-specific requirements thereby integrating existing practice with minimal disruption. The option of $P_I = 1$ was introduced to allow flexibility for the owners in implementing this new concept. An example of protection strategy based on P_I is shown in Table 2 for ground anchors, where (a) Class I protection is the so-called double protection in which the prestressing steel is encased inside a plastic encapsulation filled with either grout or corrosion inhibiting compound, and (b) Class II protection is the so-called simple protection that encases the prestressing steel over the free length and relies on the cement grout to protect the prestressing steel along the bond length.

TABLE 1 Conditions for P_I-value (*5, 6*)

P_I	Conditions
0	Structures in nonaggressive environments, where the consequences of loss of serviceability are not serious, or for structures with low traffic volumes such as local and rural routes.
1	Structures in an aggressive environment, where consequences of loss of serviceability are serious, or for routes with high traffic volumes such as interstates and freeways.
2	Cases between $P_I = 0$ and $P_I = 2$ as determined by the owner in terms of the aggressiveness of the environment, the consequences of loss of serviceability, or routes with intermediate traffic volumes such as arterials, service roads, and state-owned routes.

TABLE 2 Choice of Protection Strategy for Ground Anchors Based on P_I - value (*5, 6*)

P_I	Protection Strategy
0	Class II protection
1	Class II protection or Class I protection as determined by owner
2	Class I protection.

Design provisions for different types of foundation and retaining wall elements are presented in the Guide Specifications using the three-tier protection index and protection strategy approach. For each element, considerations for the deterioration environment are given followed by design provisions to prevent said deterioration. The designer is directed to other sections of the guide specification for additional guidance where appropriate, such as the provisions of concrete when designing a concrete foundation element. Guidance for the following geotechnical elements are included: spread footings, driven piles, micropiles, drilled shafts, non-gravity cantilever walls, anchored walls, soil nails and MSE walls. A brief discussion on durability considerations for approach embankments is also included in the guide specification. The guide specification was considered and approved by AASHTO COBS at the 2019 annual AASHTO meeting in Montgomery, Alabama, and published in 2020 (*6*).

Summary and Opportunities for Future Work

This paper has presented a brief chronological history of the development of service limit state guidelines for geotechnical elements that have been incorporated into AASHTO LRFD. These guidelines are also in various stages of incorporation into FHWA GECs. The overarching considerations in the associated research and development are as follows:

1. The guidelines for geotechnical elements must be in sync with the overall approach for structural elements.
2. The level of reliability between structural and geotechnical elements must be consistent.
3. Selection of the most cost-effective foundation system rather than indiscriminate use of costly deep foundations should be encouraged.
4. The guidelines should be based on AASHTO LRFD framework that is modular and expandable, i.e., results of future research should fit with other previous research.

The calibration process for the *SE* load factor is clearly documented. Placeholder values of $\gamma_{SE} = 1.00$ have been used for lateral movements of deep foundations. Flexibility to calibrate γ_{SE} values for any local method has been provided. Furthermore, γ_{SE} values can also be developed for other actions such as creep movements. It is possible to extend the calibration framework shown in Figure 1 to strength limit states using data at Point F along the $Q - \delta$ curve shown in lower quadrant. These features provide many avenues to encourage future research in this area.

Regarding the geotechnical elements in guide specification, considerable opportunities for future research are available. For example, a useful research topic would be to split the current singular exposure class for buried elements (C-B) into multiple classes using a set of micro exposure zones that are defined by the condition of the surrounding environment. Environmental conditions that could be considered include chloride concentration, sulfate concentration, and pH level, among others. Thus, research is needed to (*a*) define the set of exposure zones that accommodates all geotechnical elements in a consistent manner in terms of deterioration mechanisms, and (*b*) set the appropriate limits on the relevant environmental conditions for each zone. In addition, a critical evaluation of the current AASHTO and ASTM (American Society of Testing and Materials currently known as ASTM International) testing standards should be performed with respect to the procedures to estimate the environment load which leads to material deterioration,

e.g., are the dilution ratios for determination of salt content and resistivity in AASHTO or ASTM standards consistent with the field conditions?

Finally, the development of load factors and consideration of material deterioration have been framed as individual issues, i.e., decoupled issues. The reality is that both issues are coupled in that material deterioration can lead to reduction of load-carrying capacity and associated serviceability concerns. The framework in Figure 1, offers an opportunity to couple both calibration of load effects and deterioration modeling through use of an appropriate Q-δ curve that also considers time. Evaluation of a coupled approach can provide many research opportunities for future researchers.

AUTHOR CONTRIBUTION STATEMENT

The authors confirm contribution to the paper as follows: study conception and design: 1. Naresh C. Samtani, 2. John M. Kulicki; analysis and interpretation of results: 1. Naresh C. Samtani, 2. John M. Kulicki; draft manuscript preparation: 1. Naresh C. Samtani, 2. John M. Kulicki. All authors reviewed the results and approved the final version of the manuscript.

ACKNOWLEDGMENTS

The work represented in this paper was conducted by many individuals in different teams for various projects. The names of these individuals can be gleaned from the references section of this paper. Additionally, AASHTO (particularly T-15 COBS) and FHWA committees performed diligent work for vetting the geotechnical work and fine-tuning it for AASHTO LRFD and FHWA implementation. The authors duly acknowledge everybody's work and the reader is referred to specific references for more details. The authors would also like to acknowledge Silas Nichols, Principal Geotechnical Engineer, FHWA, for reviewing the draft versions of this paper and providing useful comments.

REFERENCES

1. AASHTO. *AASHTO LRFD Bridge Design Specifications*. 8th (2017) and 9th (2020) Edition, American Association of State Highway and Transportation Officials, Washington, D.C.
2. Azizinamini, A., E. H. Power, G. F. Myers, and H. C. Ozyildirim. Bridges for Service Life Beyond 100 Years: Innovative Systems, Subsystems, and Components. *SHRP 2 Report, Issue S2-R19A-RW-1*. Transportation Research Board, Washington, D.C. 2014. https://doi.org/10.17226/22479.
3. Azizinamini, A., E. H. Power, G. F. Myers, H. C. Ozyildirim, E S. Kline, D. W. Whitmore, and D. R. Mertz. Design Guide for Bridges for Service Life. *SHRP 2 Report, Issue S2-R19A-RW-2*. Transportation Research Board, Washington, D.C. 2014.
4. Kulicki, J., W. Wassef, D. Mertz, A. Nowak, N. Samtani, and H. Nassif. Bridges for Service Life Beyond 100 Years: Service Limit State Design. *SHRP2 Report, Issue S2-R19B-RW-1*. Transportation Research Board, Washington, D.C., 2015. https://trid.trb.org/view/1305296.
5. Murphy, T., M. Lopez, T. Hopper, E. Wasserman, J. Kulicki, F. Moon, A.-M. Langlois, and N. Samtani. *NCHRP Web-Only Document 269: Guide Specification for Service Life Design of Highway Bridges.* Transportation Research The National Academies, Washington, D.C., 2019. https://trid.trb.org/view/1681463.

6. AASHTO. *Guide Specification for Service Life Design of Highway Bridges*, 1st edition. American Association of State Highway and Transportation Officials, Washington, D.C., 2020.
7. Samtani, N. C., and J. M. Kulicki. Incorporation of Foundation Movements in AASHTO LRFD Bridge Design Process. The "White Paper", Second Edition. Report No. FHWA-HIF-18-007, Washington, D.C., 2018.
8. Samtani, N. C., and J. M. Kulicki. Calibration of Foundation Movements for AASHTO LRFD Bridge Design Specifications. *Georisk: Assessment & Management of Risk for Systems*, Vol. 13, No. 3, Taylor & Francis, U.K., 2019. https://doi.org/10.1080/17499518.2018.1554818.
9. Samtani, N., and T. Allen. *Implementation Report: Expanded Database for Service Limit State Calibration of Immediate Settlement of Bridge Foundations on Soil*. Report No. FHWA-HIF-18-008. Federal Highway Administration, U.S. Department of Transportation, 2018.
10. Moon, F., N. Romano, D. Masceri, J. Braley, D. R. Mertz, N. Samtani, T. Murphy, and M. Lopez. *NCHRP Web-Only Document 24: Bridge Superstructure Tolerance to Total and Differential Foundation Movements*. Transportation Research Board, Washington, D.C., 2017. https://trid.trb.org/view/1508297.
11. Samtani, N. C., E. A. Nowatzki, and D. R. Mertz. *Selection of Spread Footings on Soils to Support Highway Bridge Structures*, (revised 2017). FHWA-RC/TD-10-001. Federal Highway Administration, Resource Center, Matteson, Ill., 2010.
12. Samtani, N. C., and J. M. Kulicki. Uncertainty in Differential Settlements of Bridge Foundations and Retaining Walls. *Georisk: Assessment & Management of Risk for Systems*, Vol. 14, No. 3, Taylor & Francis, U.K., 2019. https://doi.org/10.1080/17499518.2020.1711526.
13. NHI WBT. Calibration at the Service Limit State—Incorporation of Foundation Movements in Structure Design. 5-Module Web-Based Training, FHWA Course FHWA-NHI-132100. Federal Highway Administration, U.S. Department of Transportation, 2019.
14. Samtani, N. C., and J. M. Kulicki. Reliability Evaluation of Concrete Cover for Buried Structures from Chloride Induced Corrosion Perspective. *Journal of Bridge Engineering*, Vol. 25, No. 8, 2020, p. 04020049. https://doi.org/10.1061/(ASCE)BE.1943-5592.0001572.
15. Brinch, H. J. Limit Design and Safety Factors in Soil Mechanics. *Bulletin 1*, The Danish Geotechnical Institute, Academy for the Technical Sciences, 1956.
16. Schmertmann, J. H., P. R. Brown, and J. P. Hartman. Improved Strain Influence Factor Diagrams. *Journal of the Geotechnical Engineering Division*, Vol. 104, No. 8, 1978, pp. 1131–1135. https://doi.org/10.1061/AJGEB6.0000683.
17. Hough, B. Compressibility as the Basis for Soil Bearing Value. *Journal of the Soil Mechanics and Foundations Division*, Vol. 85, No. 4, 1959, pp. 11–40. https://doi.org/10.1061/JSFEAQ.0000207.

Performance of Rocking Shallow Foundations and the Evolution of Beam-on-Nonlinear-Winkler Foundation Modeling

CHAD WILLIAM HARDEN
ANDRES LOZANO
Michael Baker International

The nonlinear behavior of shallow bridge and building foundations under large-amplitude loading is an important aspect of performance-based earthquake engineering (PBEE). Soil yielding beneath foundations can be an effective energy dissipation mechanism; however, this yielding may lead to excessive permanent deformations. The research and engineering community have established decades of model testing and analytical modeling to understand foundation nonlinearity and uplift. Physical model testing provides insight into the mechanisms at work in rocking, shallow foundations, while analytical modeling and simulation are validated against these experiment results such that modeling recommendations can be applied in practice. This body of work lead to the current design procedures in industry, such that the benefits and consequences of foundations allowed to rock under seismic events can be understood and implemented in practice generally for retrofit of existing structures. While there are various established analytical modeling approaches, this paper focuses specifically on both the elastic and nonlinear Winkler analytical modeling approaches used to better understand, mimic or approximate observations from experiment, current codified design procedures, and includes speculation on the future of research and design in this field.

BACKGROUND AND MOTIVATION

The nonlinear load-displacement behavior of soil provides an opportunity for energy to dissipate from a structural system at the soil-structure interface. This has been recognized for some time; for example, Housner (1963) assumed that a structure (block) allowed to rock would be an effective means of dissipating energy, and presented fundamental equations describing the loss of kinetic energy per impact as the system radiates energy. A scale effect was found which described why squat structures are more prone to toppling compared to taller structures. This study is applicable to the case of stiff structures such as shear walls, which are commonly used in earthquake-prone regions.

The consequences of allowing a shallow foundation to rock (or in some cases accurately representing an existing structure which may rock) and of permanent settlement and rotation must be reasonably estimated and accounted for. This balance of benefit and consequence is the basis for PBEE, such that the desired structure (e.g., building or bridge) has a specific performance for a defined hazard level.

However, the industry has moved from viewing the foundation performance of rocking foundation to a consequence, to potentially superior. Both experiment and simulations of foundations allowed (or considered) to rock have been shown to exhibit superior re-centering compared to conventionally designed ductile columns, (Deng, Kutter and Kenneth, 2012; Gelagoti et al., 2013; Antonellis et al., 2015a). Further, structure hinging and rocking systems with equal hinge yielding and foundation rotation yielding, respectively, will exhibit identical load-displacement

and moment-rotation pushover curves—such that the design approach of these systems could also be similar. (Deng, Kutter and Kenneth, 2012)

The benefits of a rocking shallow foundation (energy dissipation) are well documented, though there is much uncertainty in modeling these systems. Generally, one may anticipate that a more rigorous model representing any real system with a detailed representation of all observed physical mechanisms would lead to better results of the system response. However, the uncertainty in determining the input parameters of the more rigorous model is often contrary to such anticipation. Therefore, the intent of using subgrade type models (springs, gap elements, and dashpots) has always been to strike a balance between theoretically more rigorous solutions and practicality and ease of use in routine geotechnical engineering practice.

Perhaps the most popular method used in design practice when modeling soil-foundation-interaction (SFSI), is the Winkler approach, which originates from Winkler's (1867) early representation of the physical soil medium and assumes a system of discrete, closely spaced independent linear elastic springs. Such an approach assumes that a vertical reaction in the soil per unit length at a given distance along the foundation is related only to the foundation deflection at that distance. Displacements of the foundation are due to contributions of soil (spring) flexibility, foundation flexibility. However, as observed in physical testing and described following, linear elastic springs are too simple an assumption to model actual foundation behavior. A Beam-on-Nonlinear-Winkler Foundation (BNWF) model may better approximate observed behavior from physical testing compared to elastic Winkler models, through a collection of refinements such as allowing the footing to uplift (gapping elements), incorporate local, near field damping elements, and allowing the soil (springs) to permanently settle or displace through load-displacement constitutive laws, among other refinements. Together this group of modeling recommendations and variables is the BNWF approach.

This paper endeavors to summarize the evolution in research and industry from elastic Winkler models to BNWF models as shown in Figure 1, to reasonably predict the benefits and consequences of PBEE for shallow foundations.

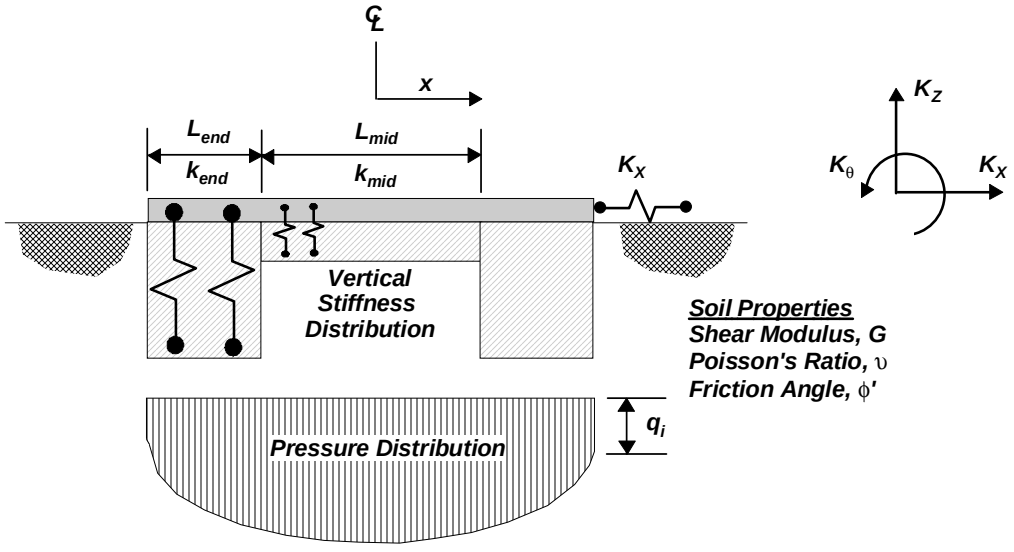

FIGURE 1 Sample BNWF model with horizontal stiffness, and variation in spring stiffness and bearing capacity (Harden, 2003).

PBEE measures are important to quantifying the performance or suitability of a design specific to shallow foundations as well as the moment absorbed into the soil-structure interface versus rotation of the foundation, the settlement of the foundation, and (if allowed) the horizontal sliding of the foundation. Any of the degrees of freedom of the foundation (rotation, settlement, or horizontal sliding) are generally represented as a function of stiffness. Therefore, these degrees of freedom if accurately represented are all possible modes of energy dissipation (benefit), but are subsequently susceptible to permanent displacements (consequence).

PHYSICAL MODEL TESTING

Analytical models are tools which help engineers and researchers estimate how a structure will perform when subjected to a loading criteria. However, paramount to the analytical model is the physical testing (or "model testing") which provides data for comparison, and "real-world" insights and observations. While this paper focuses primarily on the evolution of BNWF modeling, this evolution has developed in parallel with physical testing. The following model test programs, and others not listed, are relevant and important to this topic. They have been classified into either model centrifuge experiments or one-gravity ("one-g") experiments.

Perhaps the earliest model footing experiments were conducted at the University of New Zealand [described in Taylor et al. (1981), Wiessing (1979), and Bartlett (1976)]. The focus of these experiments was to investigate the nonlinearity developed in the soil and the uplift at the interface of the soil and footing upon large-amplitude moment loading. Studies by Wiessing (1979) considered the rocking response of foundations resting on dry sand, while studies by Bartlett (1976) considered foundations resting on clay. In these experiments, horizontal movement of the footing was restrained through the use of a steel tie-rod system.

For Wiessing's experiments, four out of five tests considered the strong direction of loading, with vertical factors of safety ranging from two to ten. A small plate footing was used, 0.5 m by 0.25 m, resting on dry clean quartz sand. Bartlett's experiments consisted of weak direction loading in three out of four tests. A similar sized footing was used.

Model testing of shallow foundations followed at the UC Davis Center for Geotechnical Modeling centrifuge with studies by Rosebrook and Kutter (2001a, b, c), and further model tests by Gajan et al. (2003a, b) (also described in Phalen, 2003).

Centrifuge experiments by Rosebrook and Kutter (2001a, b, c) (also summarized in Rosebrook, 2001) incorporate a range of footing sizes, static vertical factors of safety (from FS_v = 1.6–8), and both clay and sand soil types. In these experiments, series KRR01 consider sandy soils of relative density 60% and 80%, while KRR02 considers sandy (dry) soils of relative density 60%. Series KRR03 considers systems resting on stiff saturated clay.

Centrifuge experiments by Rosebrook and Kutter (2001a, b, c) (also summarized in Rosebrook, 2001) incorporate a range of footing sizes, static vertical factors of safety from 1.6 to 8, and sandy soils with relative density 60% and 80%, or stiff saturated clay.

Centrifuge experiments by Gajan et al. (2003 a, b) (also summarized in Phalen, 2003), performed at UC Davis, also incorporate a range of footing sizes, and design vertical factors of safety from 1.3 to 11.5). The primary difference in the SSG series were the inclusion of more tests with embedment and a lower horizontal push height to allow study of the horizontal displacement–shear relationship. Embedments of one B were considered (where B = footing width). Tests were performed on only 80% relative density (dry) sand.

The KRR and SSG test series include both “slow static” displacement histories of symmetric reversed cycles of varying amplitude, as well as dynamic base excitation (shaking) applied at the bottom of the soil box and involved tapered cosine waves of increasing amplitudes.

One-g experiments completed at the European Laboratory for Structural Assessment in Italy are reported in Negro et al. (1998) and Faccioli et al. (2001). The system considered consisted of a one meter square foundation, placed on a saturated sand base of either 85% or 45% relative density, and subjected to static vertical, slow-cyclic, and dynamic cyclic events.

The test data demonstrates that for the lower factors of safety (< 3.0) a relatively larger amount of damping is mobilized, and in general a greater amount for larger rotations (Harden, et al. 2005)

Liu et al. (2013a, b) investigates systems where the strength of the structural hinge is balanced with the yield strength of the foundation allowed to rotate. Base shear demand is reduced in both Balanced Design (BD) systems and Foundation Rocking-Dominated (FRD) footings compared to Structural Hinging Dominated (SHD) systems with similar load-displacement performance; however, the SHD systems accumulate permanent lateral displacements whereas the BD and FRD systems show superior re-centering with the consequence of accrued settlement.

In Part I of a two-part research program, Antonellis et al. (2015a, c) conducted scaled experiments of rocking bridge footings to provide analytical data for establishing design criteria. Setup included two individual shallow rocking foundations supporting an 18-in column with a mass block fixed at the top. Each foundation had a different skew, 0° and 30°, relative to direction of shaking. Shallow rocking foundations where observed to reliably accommodate earthquake-induced deformations, with minimal 0.5% residual drift for a peak 5.9% drift ratio demand under the MCE. Casting of weak concrete around footings was also observed as a simple construction detail to limit sloughing of soils and limit residual drift. From the experimental results, Antonellis et al. (2015b) developed displacement-based analysis (DBA) guidelines for typical bridges utilizing rocking shallow foundations.

In two recent complimentary studies, Hakhamaneshi et al. (2020) and Gavras et al. (2020) have established a public database of rocking shallow foundation performance for slow-cyclic and monotonic loading, and dynamic shaking, respectively.

ANALYTICAL MODELING

Before discussing the development and evolution of current Winkler-based approaches, it will be beneficial to briefly describe the alternative modeling approaches specific to shallow foundations soil-structure interaction.

Analytical Modeling: Alternative Approaches

Elastic half-space approaches may be the most well-known approach to foundation and general geotechnical models. In this method, the engineer develops a finite element model (FEM) consisting of 2D quadrilateral elements, or more complicated 3D brick elements. The FEM may capture both elastic and nonlinear constitutive models, soil layering specific to a site, and other material, boundary, and geometric constraints, such as ground water table, buried elements such as foundations, tunnels, etc., and quadrilateral elements. Yan and Martin (1999) simulated the tests

by Bartlett (1976) using a hypoplasticity model in the framework of a half-space continuum on the FLAC platform. Settlement is well estimated by approximately one-half to three times.

Nova and Montrasio (1991), Houlsby and Cassidy (2002), and Cremer et al. (2001) have provided theoretical work and numerical simulations to capture shallow foundation soil-structure interaction using a macro-element through empirical, yield surface, hardening law, and plastic potential models. The envisioned macro-element would be implemented into a model through a single element at the base of a structural system. Gajan and Kutter (2008) have implemented a similar but expanded approach in OpenSees.

Analytical Modeling: (Elastic) Winkler-Based Approach

The general Winkler (1867) approach as described earlier in the paper assumes a vertical reaction in the soil per unit length at a given distance along the foundation is related only to the foundation deflection at that distance. Hetényi (1946) provided an important extension to this by considering the deformation of the beam element by accounting for its flexibility. This general approach has become popular in the analysis of pile and pile group systems, whereby individual spring elements are simply placed horizontally (rather than vertically) and used to represent the lateral resistance of the soil and the soil-pile interaction forces. In each case (the shallow or deep foundation), the discretely placed springs result in a lack of coupling between individually placed spring elements; however, the continuum effect provided by the soil may be implicitly included if the resistance curves are back-calculated from monotonic or cyclic loading experiments.

Several publications in the literature describe various Winkler-based approaches used for modeling the rocking response of shallow foundations resting on both an elastic or inelastic soil medium and which consider the inelastic actions through the effect of uplifting of the foundation. Upon uplifting, however, the equations of motion describing the system response become highly nonlinear; therefore, various researchers have also considered simple symmetric two-spring models to allow for linearization of the system of equations. Such an approach is generally more applicable for rigid structural systems. Descriptions of some of these previous works are provided in this section.

Wiessing (1979) used elastic-plastic springs coupled with Coulomb slider elements and subdivided the foundation into finite strips. This work considered two dimensions of loading (moment and vertical loading with horizontal movement restrained), modeled after his experimental studies. Elastic-plastic springs were considered to only have compression capacity, while Coulomb slider elements captured the uplifting of the foundation. Results from this numerical study provided good comparison with experimental studies for the range of soil foundations considered [also conducted by Wiessing (1979)]. Four out of five tests considered the strong direction of loading, with vertical factors of safety, FS_V, ranging from 2 to 10. A small plate footing was used, 0.5 by 0.25 m, and the loading protocol was generally five cycles each for three sets 0.001, 0.005, and 0.02 radians.

Prior to Wiessing's work, Bartlett (1976) completed similar tests on a clay soil, with the same size footings and range of factors of safety. Analytical work was also performed, using a Winkler-based model with elastic perfectly-plastic springs allowed to uplift. Three out of four tests considered the weak direction of loading, and FS_v ranged from 1.5 to 8. A small plate footing was used, 0.5 by 0.25 m, and the loading protocol was generally five cycles each for three sets 0.005, 0.01, and 0.02 radians. Qualitative comparisons were made between the analytical and experimental results, with the following key observations: (1) general degradation of the soil

modulus occurs with increasing loading amplitude, (2) the majority of the permanent deformation occurs in the first large cycle of a set of similar amplitude cycles, and (3) increasing energy dissipation occurs with increasing rotation.

Psycharis (1981) considered two types of soil modeling using base springs: (1) the two-spring model and (2) the distributed Winkler (system) of springs. Nonlinearity at the foundation interface was considered through three mechanisms: (1) viscous dampers, (2) elastic perfectly-plastic nonlinear springs, and (3) an impact mechanism allowing dissipation of energy at impact. Comparison of the solutions from theoretical equations developed on the basis of the two-spring and distributed spring system were provided using response results from the Milliken Library building and a ground motion recording from the 1971 San Fernando earthquake. The primary conclusion from this numerical study was that a two-spring model was much simpler and provided reasonable enough response results for practical design. In a later publication by Psycharis (1983), a simplified two-spring system is used for studying the response of a multi-story building system.

Two separate but similar studies by Chopra and Yim (1985) evaluated the rocking response of single-degree-of-freedom (SDOF) and multi-degree-of-freedom (MDOF) systems. In follow-up work (Yim and Chopra, 1985), the model was extended to an MDOF system supported on a two-spring dashpot system. In each of these studies, the individual spring elements were considered linear elastic. A primary conclusion from this work was that foundation flexibility and uplift has little effect on higher modes of vibration and for a multistory building structure, these effects can be incorporated only by inclusion in the fundamental mode of response. In the SDOF study, the authors develop simplified expressions for determining the base shear resistance of flexible structures allowed to uplift.

In an application specific to the system considered in this report, Nakaki and Hart (1987) used discretely placed vertical elastic springs with viscous dampers at the base of a shear wall structure to illustrate the benefits of uplifting of the foundation supporting shear wall systems during earthquake loading. The Winkler springs had zero tension capacity and provided only elastic compressive resistance. The inelastic shear wall structure was modeled using a nonlinear stiffness-degrading hysteretic model. Nonlinear time history analyses were performed on this system considering two different ground motions: (1) a long duration motion from the 1940 El Centro earthquake and (2) a short, impulsive type motion measured at Pacoima Dam. Important findings from this study included the illustration, through the numerical results, that uplifting of the foundation results in a significant reduction in structural ductility demands. This is primarily because the rocking system has a longer period than that of the fixed-base system. It was also observed that the frequency content of the ground motion has a significant effect on the system ductility demand. In select cases, allowing uplift of the foundation caused greater ductility demands on the structure.

Analytical Modeling: Nonlinear Winkler-Based Approaches

A nonlinear Winkler-based model can be used to study PBEE implications for shallow foundations, as both the benefits and consequences of allowing the structure to rock can be reasonably represented. The current state of the art in shallow foundation research predicts well the expected performance of a foundation, such as the relative magnitude of settlement or displacement, as well as the expected yield capacity at which displacements are achieved. The consequences of allowing a foundation to rock, displace, and settle (or in some cases accurately representing a structure which will displace) come with the advantages of energy dissipation and recentering on

par or exceeding more conventional structure fuses such as bridge column hinges, with respect to performance and reduced cost.

Fenves (1998) models uplift of pile caps using a composite element of multiple-elastic perfectly plastic elements (bilinear) in the computer code DRAIN-3DX. The compression and tension sides of the load-displacement curves are nonsymmetric to model the reduced capacity under uplift, and gapping elements are used that have the ability to capture permanent settlement. The vertical FS was found to significantly influence the moment capacity and the vertical settlement. Accordingly, the vertical FS influences the amount of moment-rotation energy which may be dissipated, as a larger FS will have a moment capacity which may not be reached and therefore exhibit more pinched hysteresis.

The associated accrued settlement through the cumulative strain development within the soil near to the foundation is an important part of the overall performance-based design of the structure with consideration of the soil-structure system.

Harden (2003), Harden et al. (2005), and Harden and Hutchinson (2009) present a simplified BNWF approach to model shallow foundation response, capturing both the dissipation of energy and the associated ramifications such as permanent settlement and translation. A mesh generator was developed in OpenSees, composed of lateral and vertical inelastic, nonlinear springs with gapping and damping capability. Generally, global elastic stiffness was established using equations by Gazetas (1991) with soil properties estimated using the EPRI manual (1990). Modeling recommendations are provided including bearing capacity and stiffness distribution ($Q - z$), horizontal friction ($t - z$) capacity and stiffness, and passive earth pressure ($p - y$) capacity and stiffness; for material descriptions see also Boulanger, (2000a, b, c). Numerical simulations are performed with good comparison to physical testing, including one-g experiments by Wiessing (1979), Bartlett (1976), Negro et al. (1998), and Faccioli et al. (1998), and centrifuge experiments by Rosebrook and Kutter (2001a, b, c), and Gajan et al. (2003 a, b) [see also Phalen (2003)]. Results indicate a factor of two is appropriate to envelope uncertainties in soil properties, while still capturing maximum moment, total settlement, and maximum sliding demand, roughly within a bound of ± two.

Studies performed by Antonellis and Panagiotou (2014) have investigated rocking foundation design methods, shallow and deep, to determine bent behavior relative to conventional design methods. Modeled bents, with varying geometrical proportions of columns and bearings, were subjected to various types of ground motions. Response of conventionally design bents resulted in greater damage post-earthquake due to inelastic deformation of columns; residual drift is minimized for rocking foundations.

Based on the experimental results of the work by Antonellis et al. (2015a), a separate but continued phase of work Antonellis et al. (2015b), developed DBA guidelines for typical bridges utilizing rocking shallow foundations. Reliability of the approach was validated against a three-dimensional nonlinear response history analysis, with excellent comparison. The DBA approach was further refined for multiple-bent bridges through the application of modification factors to account for abutment articulation. The DBA approach is conservative relative to NHRA, demonstrating a 20% overestimate in drift ratio demands.

Kutter et al. (2016) present a rationale as part of ASCE 41-13 to model uncoupled, bilinear springs below the foundation. Recommendations for initial stiffness are based on Gazetas (1991) and nonlinear modeling parameters are derived from a suite of centrifuge model and shake table test results. Various studies contribute to the updated recommendation, including those by Gajan and Kutter (2009) and Johnson (2012) which investigate input parameters related to normalized

moment and shear ratio, elastic strength ratio, and others. Gajan, et al. (2010) provide general input parameters for both BNWF similar to the approach in ASCE 41-13, and a contact interface model. The models are generally consistent with regard to moment-rotation behavior.

In summary, research over the last decade has demonstrated rocking foundations are reliable and "designable," resulting in the following conclusions of the research community:

- Moment capacity of rocking-dominated footings is reliable under known aspect ratios;
- Seismic settlement is tolerable for wider footings;
- Rocking systems are more stable than hinging systems of comparable ductility, due to superior re-centering capability;
- Rocking can also be incorporated on sites with poor soils if ground improvement or piles are incorporated; and
- Direct displacement-based design (DDBD) (Paolucci et al., 2013; Deng et al., 2014) and ASCE 41 design procedures are available. Additional recommendations are provided in FHWA-NHI-11-032 (GEC No. 3).

CODE-BASED DESIGN REQUIREMENTS

In perhaps one of the best examples of timely and practice-ready research, Gazetas (1991) provides elastic stiffness recommendations in a format that is easily implemented by practicing engineers and has provided excellent comparison in research. As a testament to the relevance and robustness of this work, Gazetas (1991) recommendations were incorporated into the earliest design codes which provided recommendations for Winkler-based modeling, including ATC-40 (1996) and FEMA 356 (2000), and have endured as an integral part of current codes such as "LRFD Seismic Analysis and Design of Transportation Geotechnical Features and Structural Foundations." (GEC No. 3) (FHWA-NHI-11-032, Kavazanjian, et al., 2011), and ASCE 41-13 (2014). ATC-40 (1996) and FEMA 356 (2000) recommended using a Winkler-based model to represent the stiffness of the soil-structure interface and the nonlinearity associated with foundation uplift, in conjunction with a range of soil stiffness and capacity to capture the uncertainty of the soil properties and to provide a best estimate of the most sensitive structural elements.

With the popularity in design of the Winkler-based model, regularly used to model the capacity and stiffness of the soil-structure interface, further research continued to provide recommendations for estimating settlement and rotation of the rocking shallow foundation, as described previously.

There are now two current, codified approaches in industry for considering and allowing foundation to rock in design, and by extension use of BNWF in design.

Appendix A to AASHTO Guide Specifications for LRFD Seismic Bridge Design (2011) recognizes the benefit of foundation rocking through increased damping and a 20% reduced spectrum. In turn, an iterative procedure is used to estimate increased horizontal displacements and footing size, while also satisfying ductility limits and a force-based overturning forces. In the companion "LRFD Seismic Analysis and Design of Transportation Geotechnical Features and Structural Foundations." (GEC No. 3) (FHWA-NHI-11-032, 2011), guidance is provided for a general lumped stiffness of the foundation and modifications for foundation stiffness, modulus softening, foundation capacity protection, general FS selection, and other factors.

The recommendations for rocking foundations provided in ASCE 41-13 (2014), "Seismic Evaluation and Retrofit of Existing Buildings," is based on research intended for both rocking building foundations and rocking bridge foundations. Generalized nonlinear recommendations are provided for foundation stiffness and modeling parameters. These procedures also allow for various seismic analysis procedures currently outlined in AASHTO Guide Specifications for LRFD Seismic Bridge Design, including Nonlinear Dynamic Procedures, Nonlinear Static Procedures, Linear Dynamic Procedures, and Linear static procedures.

THE FUTURE OF DESIGN FOR SEISMIC DESIGN OF ROCKING FOUNDATIONS

Both the methods of ASCE 41-13 and AASHTO LRFD Guide Specifications for LRFD Seismic Bridge Design (2011) were recently presented as part of a workshop at the 98th Annual Meeting of Transportation Research Board (Harden and Panagiotou, 2019, Mulla et al., 2019). The primary goal of the workshop was to increase consideration and use of spread footings for highway bridges when appropriate; the presenters addressed obstacles facing highway agencies in consideration and use of these foundations, based on and "Implementation Guidance for Using Spread Footings on Soils to Support Highway Bridges" (FHWA-RC-14-001, Abu-Hejleh, et al. 2014), "LRFD Seismic Analysis and Design of Transportation Geotechnical Features and Structural Foundations." (GEC No. 3) (FHWA-NHI-11-032, 2011), and AASHTO LRFD Guide Specifications for LRFD Seismic Bridge Design (AASHTO, 2011)

Two design examples were presented for sizing a spread foundation following AASHTO LRFD Seismic Bridge Design Guide Specifications, Appendix A (2011). Details from two existing bridges in California were used, one having a relatively short period and the other a long period. As-built footing dimensions were compared to resulting design dimensions considering transverse analysis of a single bent and controlling drift ratio to less than 6% at MCE. Resulting footing sizes were then compared to more detailed models including a simplified RSA, a detailed RSA, a nonlinear time history analysis (NTHA), and a DDBD. The comparisons from the detailed RSA, NTHA, and DDBD shown are results from Antonellis et al. (2015b) and Antonellis and Panagiotou (2014); the DDBD incorporated modifications for additional damping at larger drift ratios, mass participation, abutment strength correction factor, and damping at abutment. Observations from the comparisons generally indicated a single column analysis in combination with the AASHTO Guide Specifications, Appendix A, compare conservatively with more advanced analysis, and this approach would be suitable for feasibility-level study. The engineer should consider the entire bridge in RSA, pushover, or time history for final design and to increase accuracy of expected performance and economy.

It would be helpful to update the AASHTO Guide Specifications for LRFD Seismic Bridge Design (and Appendix A) with the latest research, and possibly reference or mirror the recommendations of ASCE 41-13. With a consistent bridge design framework, engineers within the bridge and transportation community may harness these tools to fully consider and provide appropriate, efficient, and safe bridge solutions.

This is especially true in the case of bridge retrofit, where rocking foundations provide a safe and cost-effective solution compared to other alternatives. In the future of increased use of automated vehicles it is anticipated lanes may reduce and roadway capacity will increase, resulting in a higher demand on existing highway (and bridge) infrastructure, and reduced spending on new

highway (and bridge) construction (Bowman, 2016). Compounding an increase demand on transportation infrastructure, a change in bridge use with "platooning" of truck loads is clear (Grant, 2018 and Dunne, 2018). Will existing bridges be prepared for increased vehicle loading? State transportation departments (DOT) will need to prepare for a shift in spending from new bridge or widening construction to higher spending on maintenance and inspection, load rating, repair, retrofit, or replacement to extend the life of existing infrastructure. Allowing rocking of existing bridge foundations in seismic regions will be a significant tool in the DOT "pocket," to shift funds from expensive foundation retrofits to other areas such as superstructure upgrades or repairs.

In summary, the future of rocking foundation design and guidance in transportation and bridge engineering industry demands critical updates for BNWF modeling (and rocking foundation guidance in general) within the AASHTO Guide Specifications for LRFD Seismic Bridge Design. Coupled with automated advances to premier bridge software to embolden engineers with these tools, DOT owners can fully consider and provide appropriate and safe bridge solutions as bridge use, programming and funding, and maintenance evolve in the next century.

REFERENCES

Allotey, N., and H. El Naggar. Analytical Moment-Rotation Curves for Rigid Foundations Based on a Winkler Model. *Soil Dynamics and Earthquake Engineering*, Vol. 23, No. 5, 2003, pp. 367–381. https://doi.org/10.1016/S0267-7261(03)00034-4.

AASHTO. *AASHTO LRFD: Guide Specifications for LRFD Seismic Bridge Design*. American Association of State Highway and Transportation Officials, Washington, D.C., 2011.

AASHTO. *AASHTO LRFD Bridge Design Specifications*, 7th ed. American Association of State Highway and Transportation Officials, Washington, D.C., 2014.

ASCE. *ASCE/SEI 41-13: Seismic Evaluation and Retrofit of Existing Buildings*. American Society of Civil Engineers, Reston, Va., 2014.

Anastasopoulos, I., F. Gelagoti, R. Kourkoulis, and G. Gazetas. Simplified Constitutive Model for Simulation of Cyclic Response of Shallow Foundations: Validation Against Laboratory Tests. *Journal of Geotechnical and Geoenvironmental Engineering*, Vol. 137, No. 12, 2011, pp. 1154–1168. https://ascelibrary.org/doi/abs/10.1061/(ASCE)GT.1943-5606.0000534. https://doi.org/10.1061/(ASCE)GT.1943-5606.0000534.

Anastasopoulos, I., L. Marianna, F. Gelagoti, R. Kourkoulis, and G. Gazetas. Nonlinear Soil-Foundation Interaction: Numerical Analysis. Presented at 2nd International Conference on Performance-Based Design In Earthquake Geotechnical Engineering, Taormina, Italy, May 28, 2012, pp. 28–30.

Antonellis, G., and M. Panagiotou. *Seismic Design and Performance of Bridges with Columns on Rocking Foundations*. Pacific Earthquake Engineering Research Center, Berkeley, CA, 2013.

Antonellis, G., and M. Panagiotou. Seismic Response of Bridges With Rocking Foundations Compared to That of Fixed-Base Bridges At a Near-Fault Site. *Journal of Bridge Engineering*, Vol. 19, No. 5, 2014, p. 04014007. https://doi.org/10.1061/(ASCE)BE.1943-5592.0000570.

Antonellis, G., A. G. Gavras, M. Panagiotou, B. L. Kutter, G. Guerrini, A. Sander, P. J. Fox, J. I. Restrepo, and S. A. Mahn. *Analytical and Experimental Development of Bridges with Foundations Allowed to Uplift: Part I: Experimental Studies.* California Department of Transportation, Sacramento, 2015a.

Antonellis, G., A. G. Gavras, M. Panagiotou, and B. L. Kutter. *Analytical and Experimental Development of Bridges with Foundations Allowed to Uplift. Part II: Analytical Studies.* California Department of Transportation, Sacramento, 2015b.

Antonellis, G., A. G. Gavras, M. Panagiotou, B. L. Kutter, G. Guerrini, A. C. Sander, and P. J. Fox. Shake Table Test of Large-Scale Bridge Columns Supported on Rocking Shallow Foundations. *Journal of Bridge Engineering*, Vol. 0001284, 2015c.

Applied Technology Council. *Seismic Evaluation and Retrofit of Concrete Buildings ATC-40, Vol. 1 and Vol. 2*, 1996.

ASCE. *ASCE/SEI 41-13: Seismic Evaluation and Retrofit of Existing Buildings*. American Society of Civil Engineers, Reston, Va., 2014.

Bartlett, P. E. *Foundation Rocking on a Clay Soil*. M. E. thesis, University of Auckland, New Zealand. 1976.

Bolton, M. D. The Strength and Dilatency of Sands. *Geotechnique*, Vol. 36, No. 1, 1986, pp. 65–78. https://doi.org/10.1680/geot.1986.36.1.65.

Boulanger, R. W. The PySimple1 Material. Document for the OpenSees platform, 2000a.

Boulanger, R. W. The QzSimple1 Material. Document for the OpenSees platform, 2000b.

Boulanger, R. W. The TzSimple1 Material. Document for the OpenSees platform, 2000c.

Boulanger, R. W., C. J. Curras, B. L. Kutter, D. W. Wilson, and A. Abghari. Seismic Soil-Pile Structure Interaction Experiments and Analyses. *Journal of Geotechnical and Geoenvironmental Engineering*, Vol. 125, No. 9, 1999. https://doi.org/10.1061/(ASCE)1090-0241(1999)125:9(750).

Bowman, J. How Autonomous Vehicles Will Change the Future of Road Design and Construction. *FMI Quarterly*, 2016. https://www.fminet.com/fmi-quarterly/article/2016/09/how-autonomous-vehicles-will-change-the-future-of-road-design-and-construction/.

Broms, B. B. Foundation Engineering. 2003. http://www.geoforum.com/knowledge/texts/broms/index.asp.

Chopra, A. K., and C.-Y. Yim. Earthquake Response of Structures with Partial Uplift on Winkler Foundation. *Earthquake Engineering & Structural Dynamics*, Vol. 12, No. 2, 1984, pp. 263–281. https://doi.org/10.1002/eqe.4290120209.

Chopra, A., and R. Goel. *Capacity-Demand-Diagram Methods for Estimating Seismic Deformation of Inelastic Structures: SDF Systems*. Report No. PEER-1999/02. University of California, Berkeley, 1999.

Chopra, A. K., and S.-C. Yim. Simplified Earthquake Analysis of Structures with Foundation Uplift. *Journal of Structural Engineering*, Vol. 111, No. 4, 1985, pp. 906–930. https://doi.org/10.1061/(ASCE)0733-9445(1985)111:4(906).

Cremer, C., A. Pecker, and L. Davenne. Cyclic Macro-Element for Soil–Structure Interaction: Material and Geometrical Non-Linearities. *International Journal for Numerical and Analytical Methods in Geomechanics*, Vol. 25, No. 13, 2001, pp. 1257–1284. https://doi.org/10.1002/nag.175.

Deng, L., B. Kutter, and S. Kunnath. Seismic Design of Rocking Shallow Foundations: Displacement-Based Methodology. *Journal of Bridge Engineering*, Vol. 19, No. 11, 2014, p. 04014043. https://doi.org/10.1061/(ASCE)BE.1943-5592.0000616.

Deng, L., B. L. Kutter, and S. K. Kunnath. Probabilistic Seismic Performance of Rocking-Foundation and Hinging-Column Bridges. *Earthquake Spectra*, Vol. 28, No. 4, 2012, pp. 1423–1446. https://doi.org/10.1193/1.4000093.

Dunne, R. *Truck Size and Weight: What You Need to Know*. Presented at 97th Annual Meeting of Transportation Research Board, Washington, D.C., 2018. Available at amonline.trb.org; https://annualmeeting.mytrb.org/Workshop/Details/7682.

EPRI. *Manual on Estimating Soil Properties for Foundation Design*. Electric Power Research Institute, Palo Alto, Calif., 1990.

Espinoza, A. O., and S. A. Mahin. Seismic Performance of Reinforced Concrete Bridges Allowed to Uplift during Multi-Directional Excitation. *PEER Report 2012/02*, Pacific Earthquake Engineering Research Center, 2012.

Faccioli, E., R. Paolucci, and G. Vivero. *Investigation of Seismic Soil-Footing Interaction by Large Scale Tests and Analytical Models.* International Conferences on Recent Advances in Geotechnical Earthquake Engineering and Soil Dynamics, 2001. https://scholarsmine.mst.edu/icrageesd/04icrageesd/session14/5

Faccioli, E., R. Paolucci, and M. Vanini. *3D Site Effects and Soil–Foundation Interaction in Earthquake and Vibration Risk Evaluation*. TRISEE, 1998.

Fang, H.-Y. (ed.). *Foundation Engineering Handbook.* Van Nostrand Reinhold, N.Y., 1991.

FEMA 356. *Prestandard and Commentary for the Seismic Rehabilitation of Buildings.* American Society of Engineers, 2000.

Lee, J., and G. L. Fenves. Plastic-Damage Model for Cyclic Loading of Concrete Structures. *Journal of Engineering Mechanics*, Vol. 124, No. 8, 1998, pp. 892–900. https://doi.org/10.1061/(ASCE)0733-9399(1998)124:8(892).

Abu-Hejleh, N., D. Alzamora, K. Mohamed, T. Saad, and S. Anderson. *Implementation Guidance for Using Spread Footings on Soils to Support Highway Bridges*. FHWA-RC-14-001. Federal Highway Administration Resource Center. Matteson, Ill., 2014.

Gadre, A., and R. Dobry. Lateral Cyclic Loading Centrifuge Tests on Square Embedded Footing. *Journal of Geotechnical and Geoenvironmental Engineering*, Vol. 124, No. 11, 1998, pp. 1128–1138. https://doi.org/10.1061/(ASCE)1090-0241(1998)124:11(1128).

Gajan, S., T. C. Hutchinson, B. L. Kutter, P. Raychowdhury, J. A. Ugalde, and J. P. Stewart. *PEER Report 2007/04: Numerical Models for Analysis and Performance-Based Design of Shallow Foundations Subjected to Seismic Loading.* PEER Center, 2008.

Gajan, S., J. D. Phalen, and B. L. Kutter. *Soil-Foundation Structure Interaction: Shallow Foundations. Centrifuge Data Report for the SSG02 Test Series*. UCD/CGMDR-03/01. Center for Geotechnical Modeling, 2003a.

Gajan, S., J. D. Phalen, and B. L. Kutter. *Soil-Foundation Structure Interaction: Shallow Foundations*. Centrifuge Data Report for the SSG03 Test Series UCD/CGMDR-03/02. Center for Geotechnical Modeling, 2003b.

Gajan, S., and B. L. Kutter. Numerical Simulations of Rocking Behavior of Shallow Footings and Comparisons with Experiments. *Proceedings of the BGA International Conference on Foundations, Dundee, Scotland*, IHS BRE Press, 2008.

Gajan, S., and B. L. Kutter. Effect of Moment-to-Shear Ratio on Combined Cyclic Load Displacement Behavior of Shallow Foundations From Centrifuge Experiments. *Journal of Geotechnical and Geoenvironmental Engineering*, Vol. 135, No. 8, 2009, pp. 1044–1055. https://doi.org/10.1061/(ASCE)GT.1943-5606.0000034.

Gajan, S., P. Raychowdhury, T. C. Hutchinson, B. L. Kutter, and J. P. Stewart. Application and Validation of Practical Tools for Nonlinear Soil-Foundation Interaction Analysis. *Earthquake Spectra*, Vol. 26, No. 1, 2010, pp. 111–129. https://doi.org/10.1193/1.3263242.

Gajan, S., P. Raychowdhury, T. Hutchinson, B. Kutter, and J. Stewart. Application and Validation of Practical Tools for Nonlinear Soil-Foundation Interaction Analysis. *Earthquake Spectra*, Vol. 26, No. 1, 2011, pp. 111–129. https://doi.org/10.1193/1.3263242.

Gavras, A. G., G. Antonellis, M. Panagiotou, and B. L. Kutter. *Analytical and Experimental Development of Bridges with Foundations Allowed to Uplift: Part II: Analytical Studies.* California Department of Transportation, Sacramento, 2015.

Gavras, A. G., B. L. Kutter, M. Hakhamaneshi, S. Gajan, A. Tsatsis, K. Sharma, K. Tetsuya, L. Deng, I. Anastasopoulos, and G. Gazetas. Database of rocking Shallow Foundation Performance: Dynamic Shaking. *Earthquake Spectra*, Vol. 36, No. 2, 2020, pp. 960–982. https://doi.org/10.1177/8755293019891727.

Gazetas, G. *Foundation Engineering handbook* (H. Y. Fang, ed.). Van Nostrand Rienhold, 1991.

Gazetas, G. Displacement and Soil-Structure Interaction Under Dynamic and Cyclic Loading. *Proc., Tenth European Conference on Soil Mechanics and Foundation Engineering*, 1991.

Gazetas, G., and J. L. Tassoulas. Horizontal Stiffness of Arbitrary Shaped Embedded Foundations. *Journal of Geotechnical Engineering*, Vol. 113, No. 5, 1987, pp. 440–457. https://doi.org/10.1061/(ASCE)0733-9410(1987)113:5(440).

Gazetas, G., P. Psarropoulos, and A. N. Gerolymos. Seismic Behaviour of Flexible Retaining Systems Subjected to Short-Duration Moderately Strong Excitation. *Soil Dynamics and Earthquake Engineering*, Vol. 24, No. 7, 2004, pp. 537–550. https://doi.org/10.1016/j.soildyn.2004.02.005.

Gelagoti, F., R. Kourkoulis, I. Anastasopoulos, and G. Gazetas. Rocking Isolation of Low-Rise Frame Structures Founded on Isolated Footings. *Earthquake Engineering & Structural Dynamics*, Vol. 41, No. 7, 2013, pp. 1177–1197. https://doi.org/10.1002/eqe.1182.

Grant, L. Can Bridges Handle Weight of Platooning Trucks? Engineering Firm Wants to Know. *Transport Topics*, 2018. https://www.ttnews.com/articles/can-bridges-handle-weight-platooning-trucks-engineering-firm-wants-know.

Hakhamaneshi, M., B. L. Kutter, A. G. Gavras, S. Gajan, A. Tsatsis, W. Liu, K. Sharma, T. K. Pianese, L. Deng, R. Paolucci, I. Anastasopoulos, and G. Gazetas. Database of Rocking Shallow Foundation Performance: Slow-Cyclic and Monotonic Loading. *Earthquake Spectra*, Vol. 36, No. 3, 2020, p. 8755293020906564. https://doi.org/10.1177/8755293020906564.

Harden, C. *Numerical Modeling of the Nonlinear Cyclic Response of Shallow Foundations.* M.S. thesis, University of California, Irvine, 2003.

Harden, C., T. Hutchinson, B. Kutter, and G. Martin. *PEER Report 2005/04: Numerical Modeling of the Nonlinear Cyclic Response of Shallow Foundations.* PEER Center, 2005.

Harden, C., and M. Panagiotou. *Recent Seismic Design Guide Implementation for Spread Footings*. Presented at 98th Annual Meeting of Transportation Research Board, Washington, D.C., 2019. amonline.trb.org.

Harden, C., and T. Hutchinson. Beam-on-Nonlinear-Winkler-Foundation Modeling of Shallow, Rocking-Dominated Footings. *Earthquake Spectra*, Vol. 25, No. 2, May 2009, pp. 277–300. https://doi.org/10.1193/1.3110482.

Harden, C., T. Hutchinson, and M. Moore. Investigation into the Effects of Foundation Uplift on Simplified Seismic Design Procedures. *Earthquake Spectra*, Vol. 22, No. 3, Aug. 2006, pp. 663–692. https://doi.org/10.1193/1.2217757.

Harden, C., T. Hutchinson, B. Kutter, and G. Martin. *Peer Report 2005/14: Numerical Modeling of the Nonlinear Cyclic Response of Shallow Foundations.* PEER Center, 2005. http://peer.berkeley.edu/publications/peer_reports/reports_2005/PEER_504_HARDENetal.pdf

Hetényi, M. *Beams on Elastic Foundations*. University of Michigan Press, Ann Arbor, Mich., 1946.

Houlsby, G., and M. Cassidy. A Plasticity Model for the Behavior of Footings on Sand under Combined Loading. *Geotechnique*, Vol. 52, No. 2, 2002, pp. 117–129. https://doi.org/10.1680/geot.2002.52.2.117.

Housner (1963) "The Behavior of Inverted Pendulum Structures During Earthquakes. *Bulletin of the Seismic Society of America*, Vol. 53, No. 2, 1963, pp. 403–417.

Johnson, K. E. *Characterization of Test Results of Rocking Shallow Foundations Using a Multi-Linear Hysteretic Model.* M.S. thesis. University of California, Davis, 2012.

Kavazanjian, E., J.-N. J. Wang, G. R. Martin, A. Shamsabadi, I. Lam, S. Disckenson, and J. C. Hung. *LRFD Seismic Analysis and Design of Transportation Geotechnical Features and Structural Foundations*.

FHWA-NHI-11-032, GEC No. 3. National Highway Institute and Federal Highway Administration, 2011.

Kutter, B. L., M. Moore, M. Hakhamaneshi, and C. Champion. Rationale for Shallow Foundation Rocking Provisions in ASCE 41-13. *Earthquake Spectra*, Vol. 32, No. 2, 2016, pp. 1097–1119. https://doi.org/10.1193/121914eqs215m.

Kutter, B., G.Martin, T. Hutchinson, C. Harden, G. Sivapalan, and J. Phalen. *Status Report on Study of Modeling of Nonlinear Cyclic Load-Deformation Behavior of Shallow Foundations.* PEER Workshop, March 5, 2003.

Kutter, B. L. *Dynamic Centrifuge Modeling of Geotechnical Structures*. University of California, Davis, 1997.

Liu, W., T. Hutchinson, B. Kutter, M. Hakhamaneshi, M. Aschheim, and S. Kunnath. Demonstration of Compatible Yielding between Soil-Foundation and Superstructure Components. *ASCE Journal of Structural Engineering*, 2013a.

Liu, W., T. Hutchinson, B. Kutter, M. Hakhamaneshi, and A. Gavras. Balancing the Beneficial Contributions of Foundation Rocking and Structural Yielding to Improve Structural Seismic Resilience. *COMPDYN 2013*, Greece, 2013b.

Martin, G., and L. Yan. Simulation of Moment Rotation Behavior of a Model Footing. FLAC and Numerical Modeling in Geomechanics (Detournay and Hart, eds.), Balkema, Rotterdam, 1999.

Martin, G., L. Yan, and I. Lam. *Development and Implementation of Improved Seismic Design and Retrofit Procedures for Bridge Abutments*. University of Southern California, 1997.

Mazzoni, S., F.McKenna, M. H. Scott, G. L. Fenves, and B. Jeremic. 2003. OpenSees Users Manual, version 2.0. 2003. http://peer.berkeley.edu/~silvia/OpenSees/manual/html/.

Mulla, M., A.-H. Naser, D. Dasenbrock, and C. Harden. *Increased Use of Spread Footings on Soils to Support Highway Bridge Projects*. Presented at 98th Annual Meeting of Transportation Research Board, Washington, D.C., 2019. amonline.trb.org.

Nakaki, D. K., and G. C. Hart. Uplifiting Response of Structures Subjected to Earthquake Motions. U.S.–Report No. 2.1-3. *Japan Coordinated Program for Masonry Building Research*. Ewing, Kariotis, Englekirk and Hart, 1987.

Nova, R., and L. Montrasio. Settlements of Shallow Foundations on Sand. *Geotechnique*, Vol. 41, No. 2, 1991, pp. 23–256. https://doi.org/10.1680/geot.1991.41.2.243.

NASA. *New Space Policy Directive Calls for Human Expansion Across Solar System*. National Aeronautics and Space Administration, 2017. https://www.nasa.gov/press-release/new-space-policy-directive-calls-for-human-expansion-across-solar-system.

NASA. *What is Artemis?* National Aeronautics and Space Administration, 2019. https://www.nasa.gov/what-is-artemis

NASA. *SpaceX to Launch First Astronauts to Space Station from U.S. Since 2011*.National Aeronautics and Space Administration, 2020. https://www.nasa.gov/specials/dm2/.

Negro, P., G. Verzeletti, J. Molina, S. Pedretti, D. Lo Presti, and S. Pedroni. *Large-Scale Geotechnical Experiments on Soil-Foundation Interaction: (TRISEE Task 3)*. Special Publication No. I.98.73. European Commission, Joint Research Center, OpenSEES, 1998. http://opensees.berkeley.edu/.

Paolucci, R., R. Figini, and L. Petrini. Introducing Dynamic Non-Linear Soil-Foundation-Structure Interaction Effects In Displacement-Based Seismic Design. *Earthquake Spectra*, 2013, p. 29.

Paolucci, R. Simplified Evaluation of Earthquake-Induced Permanent Displacements of Shallow Foundations. *Journal of Earthquake Engineering*, Vol. 1, No. 3, 1997, pp. 563–579. https://doi.org/10.1080/13632469708962378.

Phalen, J. D. *Physical Modeling of the Soil-Foundation Interaction of Spread Footings Subjected to Lateral Cyclic Loading*. M.S. thesis, University of California, Davis, 2003.

Psycharis, I. Dynamics of Flexible Systems with Partial Lift-Off. *Earthquake Engineering & Structural Dynamics*, Vol. 11, No. 4, 1983, pp. 501–521. https://doi.org/10.1002/eqe.4290110405.

Psycharis, I. N. *Dynamic Behavior of Rocking Structures Allowed to Uplift*. PhD thesis. California Institute of Technology, 1981.

Richards, R., Jr., D. Elms, and M. Budhu. Seismic Bearing Capacity and Settlements of Foundations. *Journal of Geotechnical Engineering*, Vol. 119, No. 4, Apr. 1993, p. •••. https://doi.org/10.1061/(ASCE)0733-9410(1993)119:4(662).

Rosebrook, K. R., and B. L. Kutter. *Soil–Foundation Structure Interaction: Shallow Foundations*. Centrifuge Data Report for the KRR01 Test Series, Center for Geotechnical Modeling Data Report UCD/CGMDR-01/01, 2001a.

Rosebrook, K. R., and B. L. Kutter. *Soil–Foundation Structure Interaction: Shallow Foundations. Centrifuge Data Report for the KRR02 Test Serie*s. Center for Geotechnical Modeling Data Report UCD/CGMDR-01/01, 2001b.

Rosebrook, K. R., and B. L. Kutter. *Soil-Foundation Structure Interaction: Shallow Foundations*. Centrifuge Data Report for the KRR03 Test Series, Center for Geotechnical Modeling Data Report UCD/CGMDR-01/01, 2001c.

Rosebrook, K. R. *Moment Loading on Shallow Foundations: Centrifuge Test Data Archives*. M.S. thesis. University of California, Davis, 2001.

Taylor, P. W., P. E. Bartlett, and P. R. Wiessing. Foundation Rocking Under Earthquake Loading. *Proc., 10th International Conference on Soil Mechanics and Foundation Engineering*. Vol. 3, 1981, pp. 313–322.

The Regents of the University of California. *The Open System for Earthquake Engineering Simulation.* 2016. http://opensees.berkeley.edu/

Wiessing, P. R. Foundation Rocking on Sand. *School of Engineering Report No. 203*, University of Auckland, New Zealand, 1979.

Winkler, E. *Die Lehre von der Elasticitaet und Festigkeit*. Prag, Dominicus, 1867.

Yan, L. *Nonlinear Load-Deformation Characteristics of Bridge Abutments and Footings under Cyclic Loading.* Ph.D. dissertation. University of Southern California, 1998.

Yim, S. C., and A. K. Chopra. Simplified earthquake Analysis of Multistory Structures With Foundation Uplift. *Journal of Structural Engineering*, Vol. 111, No. 12, 1985, pp. 2708–2731. https://doi.org/10.1061/(ASCE)0733-9445(1985)111:12(2708).

Machine Learning in Foundation Design and More

VICTOR AGUILAR
Universidad San Sebastián, Chile

HONGYANG WU
JACK MONTGOMERY
Auburn University

The objective of this article is to summarize relevant applications of machine learning to transportation-related matters with a focus on geotechnical engineering. Furthermore, this paper is intended to serve as an introduction to AI and machine learning for readers who may not have experience in these subjects. A review of the most significant machine learning techniques that could be of interest to the geotechnical community is presented. Relevant available databases are addressed, and applications of machine learning to transportation engineering within the scope of the TRB are highlighted. Applications to geotechnical issues were not found within the Transportation Research Records, nor NCHRP libraries. Nevertheless, the 2019 TRB annual meeting included a session on the topic showing the growing interest in this area. This paper emphasizes the potential of machine learning for solving problems in geotechnical engineering, foundation design, and other related fields. Successful applications from several sources are discussed.

This document aims to contribute to the understanding of machine learning techniques and its use for geotechnical engineering. With the same purpose, collaboration between the Standing Committees on Foundations of Bridges and Other Structures and on Artificial Intelligence and Advanced Computing is strongly recommended.

INTRODUCTION

When solving engineering problems, it is generally desirable to have a mathematical model based on the mechanics and physics of the phenomenon under study. For many problems in geotechnical engineering, this approach is impractical due to the complex nature of the interactions between the soil and the built environment. For instance, when mathematical models can be developed, validation of these models is complicated due to the many sources of uncertainty when comparing small-scale experiments with actual field behavior. Thus, empirical approaches have largely been used to develop many of the design methodologies used in geotechnical engineering. Many methods are available to develop these empirical approaches, but all rely on high-quality data. In the past several decades, geotechnical data generation has increased dramatically due to the development of technology of measuring, recording, and data storage. The growing volume of these databases presents an opportunity for engineers and scientists to develop new empirical approaches to predict the behavior of geotechnical systems, including bridge foundations and other related issues.

Machine learning (ML) is one approach for developing empirical relationships that allows computer systems to learn relevant features from data without the need to know the rules that govern the phenomenon from which the data were collected. Several applications of ML to classical geotechnical problems such as bearing capacity prediction, settlement estimation, load-

settlement response of pile foundations, liquefaction susceptibility, and landslide susceptibility can be found in the literature (*1*–*5*). ML is a subcategory within the broader area of AI. AI is the simulation of human intelligence processes by machines, especially computer systems. The research of AI began in 1956, when the term "artificial intelligence" was first used at the meeting held in Dartmouth College (*6*). AI and ML techniques have been used in a number of disciplines within science, engineering, economics, and in many topics of public interest, such as healthcare, transportation, and finance.

Three factors have helped lead to the growing popularity of AI and ML: (1) availability of data, (2) increases in computer power, and (3) maturity of the algorithms used to process the data. ML toolboxes and user-friendly software are now available to engineers to train their own models and make predictions from their collected data.

The importance of AI and ML is manifested in the recent forum on the Frontiers of Machine Learning (*7*) that took place at the National Academy of Sciences in Washington, D.C. This forum identified many exciting areas where progress in ML is being made and the significant societal and economic opportunities that will follow these advances, but nations also must grapple with how AI might affect society. Within the transportation sector, the U.S. DOT recently published a report highlighting the effects of ML and data analytics on transportation areas as self-driving technology, forecasting of traffic demand, and safety (*8*). The growth of ML and AI within the transportation community is also highlighted by the creation of the Standing Committee on Artificial Intelligence and Advanced Computing within TRB and the increasing number of publications in the *Transportation Research Record* (TRR) on this field. Figure 1 shows the number of papers published in TRR featuring the terms ML, artificial neural networks (ANN), support vector machines (SVMs), and random forest (RF) in the last three decades. ANN, SVMs, and RF are ML approaches that are described in this document.

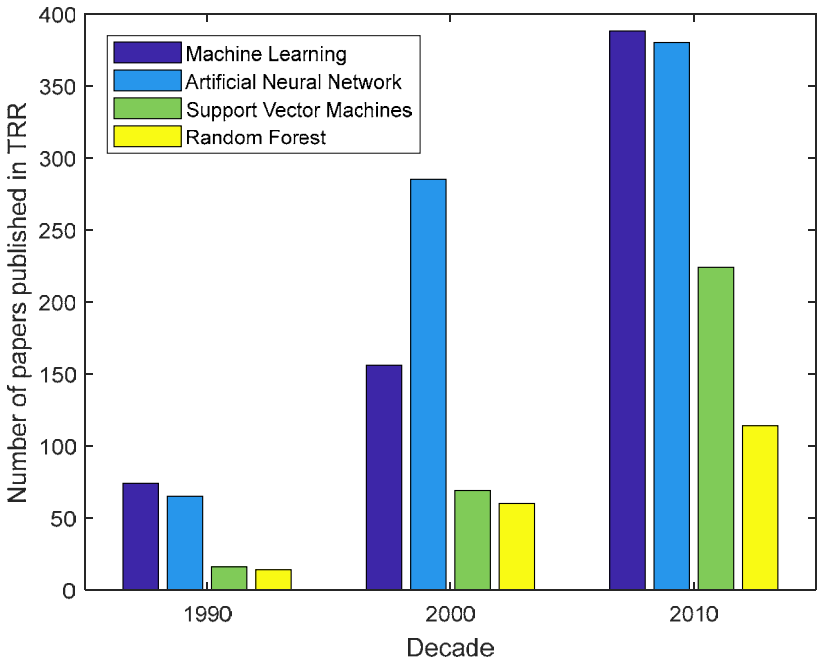

FIGURE 1 Paper published in TRR per decade featuring ML, ANN, SVMs, and RF.

The objective of this manuscript is to summarize relevant applications of ML in transportation engineering matters with a focus on geotechnical engineering. A brief introduction to AI and ML is included. Previous work in applications of ML to transportation engineering and geotechnical engineering are summarized. Several databases are reviewed that contain information that may be useful to future ML studies in the area of foundation engineering. This work also highlights the potential of machine learning-based methods for applications in geotechnical engineering, foundation design, and other related fields. It is hoped that this paper will contribute a better understanding of ML as it relates to geotechnical engineering problems.

MACHINE LEARNING METHODS FOR GEOTECHNICAL ENGINEERING

There are several ways to achieve AI and ML is one of the most popular approaches. Figure 2 illustrates the relationship between AI, ML, and three ML techniques. As shown in Figure 2, AI is a broad category, which includes ML. Besides ML, AI also encompasses the areas where the goal is creating computer systems that simulate human intelligence to perform advanced tasks, e.g., image and speech recognition, real-time language translation, decision-making, planning, and robotics. The tree-based methods, ANN, and SVMs are three different techniques for implementing ML. Each of these methods can be used to obtain outcomes that can be in the form of classification or regression.

Practical applications of ML are different from the traditional approaches to developing empirical models that have been commonly used in geotechnical engineering in the past. In both the traditional and ML approaches, data are collected from various sources, such as laboratory tests, field tests, numerical analyses, and case histories. For traditional approach methods, the "rules" or relationship among the inputs (e.g., loading, soil strength) and outputs (e.g., displacement) in the data are known and derived from fundamental principles, physical tests, computer analysis, and statistics. In a ML approach, the "rules" or relationships among inputs and outputs are created by ML algorithms in the training phase, where a subset of the available data is used for feature extraction. The theory behind the learning algorithm needs to be well understood, but it does not rely on fundamental principles from the phenomenon being studied. The ML-derived relationships generally cannot be written in equation format and they may be difficult for humans to interpret. The main goal of ML approaches is to provide an answer or prediction that is as accurate as possible in the inference phase, where a different subset of data is used for validation or testing purposes. Figure 3 outlines the differences in analysis procedures between the traditional approach and ML approach.

The workflow for ML approach can be divided into four major steps:

1. Data acquisition. Data must be collected from the phenomenon that is under study. In disciplines like geotechnical engineering where experimental data is usually costly, this stage might require obtaining data from literature, existing databases, experimentation, and using judgment to combine data from different sources.
2. Data pre-processing. The collected data need to be organized. If inputs are orders of magnitude apart, or the distribution is far from normal, scaling and normalization might be needed. The data must be divided into two datasets; one dataset will be used for training and the other for testing and validation. Usually, 70% to 80% of the data is used for training and 20%

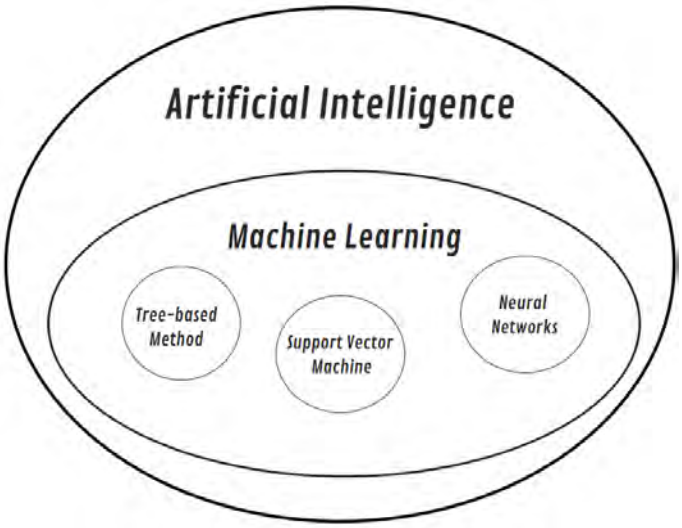

FIGURE 2 Relationship between AI, ML, and ML techniques.

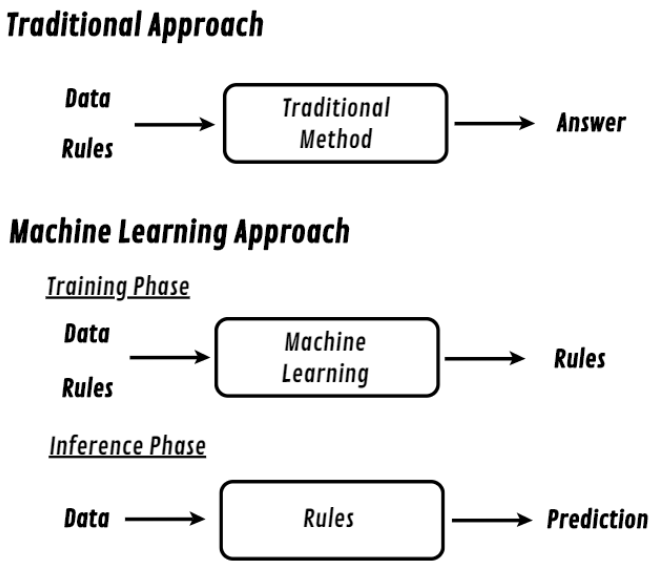

FIGURE 3 Difference between traditional method and ML method.

.

to 30% for testing and validation (e.g., *1*, *9*). This division can be done randomly, but it is beneficial that the testing data is as broad as possible in the range of the inputs and outputs.

3. Feature extraction. Appropriate ML technique, architecture, and training parameters must be selected in order to train a ML model and learn the features of the data.

4. Evaluation. The accuracy of the trained ML model is evaluated using the testing dataset. If the accuracy is not enough, it can be enhanced by improving or enlarging the training dataset and/or adjusting the training parameters. Different architectures and a different ML algorithm may be needed to improve the results.

Numerous ML techniques have been developed in the past several decades, theoretically and practically. Among all these techniques, tree-based methods, ANN, and SVMs have been used for studying geotechnical engineering problems (*9–11*).

Tree-Based Method

Tree-based methods partition the feature space into a set of rectangles and then fit a simple model (i.e., a constant) in each one. They are conceptually simple yet powerful (*12*) . There are two major types of decision trees in tree-based ML approaches. One is classification tree analysis, which means the predicted results are the class to which the data belongs (liquefiable or non-liquefiable; safe or unsafe; shallow or deep; sand, silt, clay, or rock). The other one is regression tree analysis, which means the predicted results are numbers that represent a value of a relevant variable (e.g., pile bearing capacity, settlement, or deflection). Figure 4 illustrates a simple decision tree model that includes a single binary target variable Y (values of 0 or 1), and two continuous variables, x_1 and x_2, that range from 0 to 1. The main components of a decision tree model are nodes, branches, and leaves. A node is where two new branches appear, and a terminal node is called leaf. The depth of a tree is the length of the longest path from the root to a leaf, and the size is the total number of nodes in the tree. Thus, the length of the tree shown in Figure 4 is four, from root to R_5: root, two internal nodes, and one terminal node (leaf). Its size is nine: the root, three internal nodes, and five terminal nodes (leaves). The most important steps in building a model are splitting, stopping, and pruning each of the branches (*13*).

One method of building the tree model is Classification and Regression Tree (CART) analysis, which covers both classification trees and regression trees (*14*). The method will produce either a regression or a classification tree depending on whether the dependent variable is either numerical or categorical, respectively. The CART method addresses the classification and regression problem by building a binary decision tree according to splitting rules based on the predictor variables. In this way, the space of predictor variables is partitioned recursively in a binary fashion. The partitioning is repeated until a node is reached for which no split improves the homogeneity of the response variable, whereupon the splitting is stopped, and this node becomes a terminal node. To understand homogeneity of a classification, consider Figure 5, which contains six polygons. The homogeneity of the response can be improved by subdividing into two groups: triangles and squares. The homogeneity can be again increased with one more split: scalene triangles and right triangles. There are no more differences based on the shape of the polygons, so the split process stops here because the homogeneity cannot be increased with further splitting.

The prediction is determined by terminal nodes and takes the form of either a class level in classification problems or the average of the response variable in a least squares regression problems (*14*). One limitation of the CART method is that it only constructs one decision tree, which may or may not lead to good predictions. Other, more complicated, decision tree methods are available that can construct multiple decision trees to make predictions that may be more accurate and reliable, such as RF (*15*) and boosting approaches (*16*).

RF is an ensemble learning method of classification and regression, which constructs multiple decision trees during the training process and uses them to predict the class or the value as an output (*15*). This method grows many deep trees using randomized subsets of the training data and averages the output of each tree. The approach to select the randomized samples can take

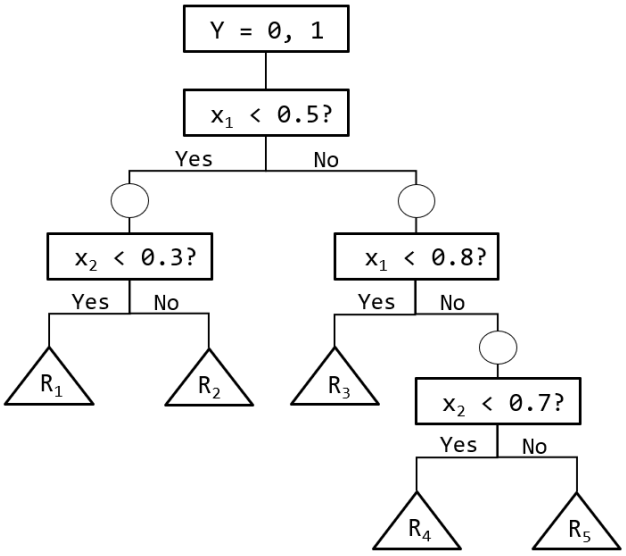

FIGURE 4 Sample decision tree-based on binary target variable Y (adapted from (*13*)).

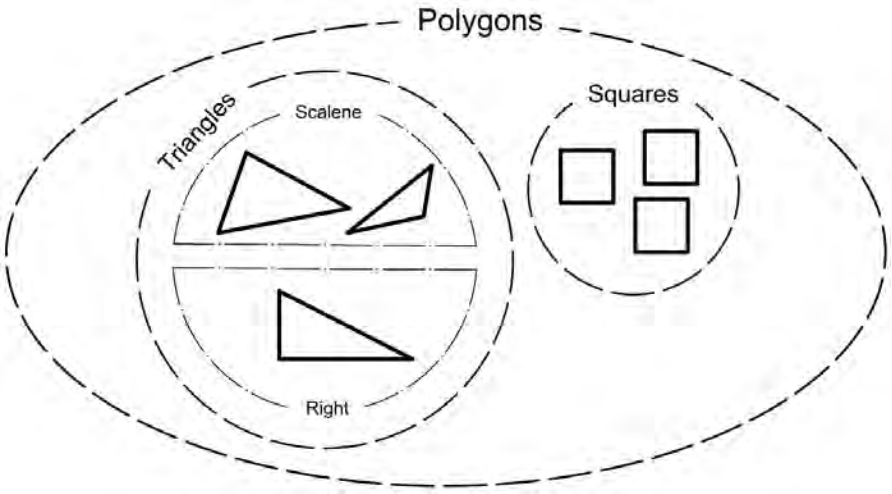

FIGURE 5 Homogeneity example.

many forms, including bootstrap sampling, subsampling of the observations, and/or subsampling of the variables (*16*). Boosting is one of the most powerful learning ideas introduced in the last 20 years. It was originally designed for classification problems, but it has been extended for regression purposes, as well. The motivation for boosting was a procedure that combines the outputs of many "weak" classifiers or predictions to produce a powerful "committee" (*12*). It repeatedly grows shallow trees to the residuals, and hence builds up an additive model consisting of a sum of trees. The basic mechanism in random forests is variance reduction by averaging. Each deep tree has a high variance, and the averaging bring the variance down. In boosting, the basic mechanism is bias reduction, although different flavors include some variance reduction, as well. Both methods inherit all the good attributes of trees, most notable of which is variable selection (*16*).

Artificial Neural Networks

In the mid-1980s, ANNs were first introduced, and they marked a shift of predictive modeling towards computer science and ML. An ANN is a highly parameterized model, inspired by the architecture of the human brain (*16*). The ANN takes data as inputs and attempts to classify that data by passing it through a series of hidden layers, which contain "neurons." The neurons are simply nodes with a certain weight that either amplifies or de-amplifies the corresponding input depending on how helpful it is for classification (the output). Figure 6a shows a simple example of a neural network diagram with a single hidden layer. Networks that are more complicated may have more than one hidden layer (Figure 6b).

Training of an ANN is accomplished by first identifying a set of input data and corresponding outputs. A learning algorithm is then used to adjust the weights in the network so that the network would give the desired output. There are many neural network training techniques, including back-propagation, quick propagation, conjugate gradient descent, projection operator, and Delta-Bar-Delta (*17*). The back-propagation algorithm is one of the most frequently used methods for training a multilayer network with onward connections. In this method, random values are used to set initial weights and biases. The ANN is then processed for the entire set of input data and known outputs, measuring the error or difference between the target output and the computed output. This error is then propagated backward to modify and update the weights and biases. The network is then processed with the new values to obtain a new error. This process is repeated until reaching a minimum error or until a maximum number of iterations is reached. At this point, the weights and biases are fixed, and the ANN can then be used to make predictions (*18*).

Support Vector Machines

SVMs are a ML algorithm that can be used for both classification and regression problems; however, it is mostly used for classification (*19*). The goal of SVMs algorithms is to find a separating

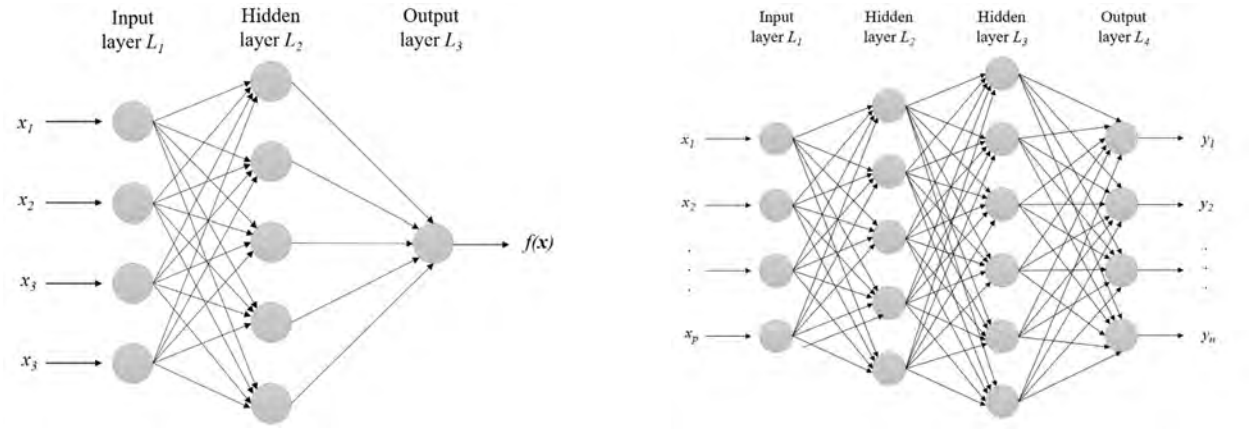

(a) **(b)**

FIGURE 6 (*a*) ANN diagram with a single hidden layer; and (*b*) ANN diagram with two hidden layers [adapted from (*16*)**].**

hyperplane among two or more classes in a high-dimensional space. The individual input data points are called vectors. The vectors closest to the separating hyperplane are called support vectors, and they define the hyperplane. Support vectors are like swing state voters in a tight election: they are the only vectors whose vote "counts". Thus, if the support vectors are altered, deleted, or replaced, the hyperplane will need to be altered, as well. A separating hyperplane is considered optimal when the distance from the support vectors to the plane (the margin) is maximized (*20*). Figure 7 shows that all the lines (*a*, *b*, *c*, *d*) are potential separating hyperplanes. In this example, line *b* is the best one since it maximizes the distance between support vectors and decision boundary. Besides the straight hyperplanes, SVMs can lead to a smooth curved boundary by remapping the raw data into a higher dimensional space (*21*).

SVMs have been shown to produce predictions, even with a small amount of training data (*22*). This is a significant advantage since collecting raw data is always expensive and time-consuming, and most ML approaches often require large datasets. Furthermore, SVMs are good at handling high-dimensional datasets (many inputs). This is valuable for geotechnical problems, which might involve several input parameters.

APPLICATIONS OF ML IN TRB, TRR, and NCHRP

Despite the increasing focus on ML and AI within the engineering community, applications within the realm of geotechnical engineering in NCHRP libraries are not found, currently. And, as of June 2020, only one paper has been published in TRR (*23*). The 2019 TRB annual meeting included a lectern session on ML for geotechnical design titled *Next Generation of Engineering Practice*, which shows the growing interest in ML in the geotechnical community. Transportation engineers associated with TRB and the TRR, on the other hand, have a long record of applications of ML. For instance, *Transportation Research Circular E-C113* (*24*) provides six articles describing five general AI areas, namely, knowledge-based systems, neural networks, fuzzy sets, genetic algorithms, and agent-based models. It was designed to serve as an informational resource for transportation practitioners and managers regarding AI tools within these general

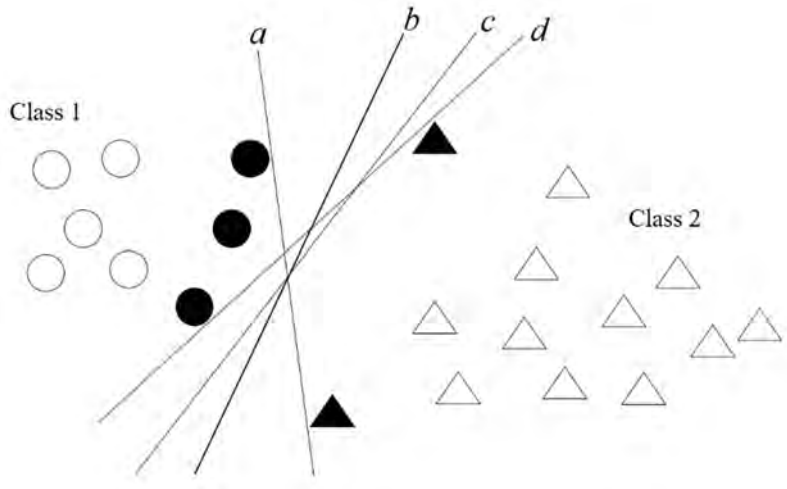

FIGURE 7 Margin maximization of SVM [adapted from (*20*)].

areas. *Transportation Research Circular E-C168* (*25*) describes five general AI applications: traffic operations, travel demand modeling, transportation safety, public transportation, and infrastructure design and construction. To demonstrate the capabilities of ML, a suit of selected successful applications found in TRB, TRR and NCHRP libraries is presented in Table 1.

Numerous additional applications of AI in transportation engineering can be found within the scope of the TRR: dynamic traffic routing (*30*), real-time traffic diversion (*31*), traffic prediction improvement (*32*), travel mode choice modeling (*33*), travel time prediction (*34*), work zone crash injury severity prediction (*35*), detection of railroad trespassing (*36*), etc. Examples of the integration of AI with other areas related to transportation infrastructure are available. The study presented by Karaaslan et al. (*37*) aims to create a smart, human-centered method for infrastructure inspection, maintenance, and management for the bridge owners by using AI and mixed reality systems. A traffic state estimation in heterogeneous networks with stochastic demand and supply is presented by Kavianipour et al. (*38*). And, the development of automatic detection of cracks for tunnels based on ML is shown by Daneshgaran et al. (*39*).

APPLICATIONS OF ML IN GEOTECHNICAL ENGINEERING

A number of wide-ranging applications of ML to geotechnical engineering problems can be found in the literature outside of the TRB, TRR, and NCHRP libraries. Two comprehensive reviews were found on the topic of AI and ML application to geotechnical engineering and related fields. Adeli (*40*) reviews neural network articles published in the fields of structural engineering, construction engineering and management, environmental and water resources engineering, traffic engineering, highway engineering, and geotechnical engineering between 1989 and 2000.

TABLE 1 Examples of Application of AI and ML in Transportation Engineering

Applications	AI or ML Technics	Reference
Structured selection problem. Condition assessment of utility cuts in flexible pavements. Dynamic traffic pattern classification. Modeling of driver anxiety during signal change intervals. Freeway incident management.	ANN and fuzzy set theory	TRR collection (*26*)
Diagnosis of malfunctioning transit railcar systems and subsystems.	Expert systems, case-based reasoning, model-based reasoning, ANN, computer vision, fuzzy logic, knowledge-based	Mulholland and Oren (*27*)
Freeway incident detection. Intelligent vehicle-highway systems Urban rail corridor control. Short-term traffic flow prediction.	ANN and fuzzy set theory	TRR collection (*28*)
Real-time arterial street incident detection. Waterway lock service times. Automatic bus vehicle location. Traffic signal control. Pavement maintenance strategies.	ANN, knowledge-based expert system, fuzzy logic, genetic algorithm	TRR collection (*29*)

The integration of neural networks with other computing paradigms to enhance the performance of neural network models is also presented. Shahin (*5*) discusses the strength and limitations of the selected AI techniques compared to other available modeling approaches. This review deals with three topics of pile foundations: bearing capacity prediction, settlement estimation, and modeling of load-settlement response. Shahin (*5*) concludes that AI techniques perform better than, or at least as good as the most traditional methods.

Several researchers have developed ANN models to predict axial bearing capacity of piles (*10*, *41*, *42*). Shahin et al. (*1*) indicate that ANN is a promising method for predicting settlement of shallow foundations on cohesionless soils, as they outperform the conventional methods. Tarawneh (*43*) developed an ANN model for predicting pipe pile setup which significantly outperforms other empirical formulas. Tarawneh (*9*) applied ANN for predicting SPT N-value from cone penetration test data. Ranasinghe (*44*) applied ANN for predicting the impact of rolling dynamic compaction, a popular and accepted soil compaction method, based on dynamic CPT results.

Samui (*2*) applied SVMs to the settlement of shallow foundations on cohesionless soils. Kordjazi et al. (*3*, *45*) developed SVMs models for predicting the ultimate axial load-carrying capacity of piles based on cone penetration test data, where the SVMs models developed in these papers outperform traditional methods. Goh (*46*) presented an overview of the SVMs and an example of its use to assess seismic liquefaction performance based on cone penetration test measurements. Samui (*11*) employed SVMs for prediction of liquefaction susceptibility of soil. Khan (*47*) developed prediction models for residual strength of clay based on functional networks, and compared the results with SVMs and ANN.

Correia (*48*) presented an overview of AI use in practical applications as compaction management and quality control aspects of embankments, pavement evaluation, and the mechanical behavior of jet grouting material. Goetz et al. (*4*) presented a comparison of traditional statistical approaches and ML models applied for regional-scale landslide susceptibility modeling. Similarly, Chen and Hoang (*49*) combined a ML learning algorithm with Bayesian probability for slope collapse prediction showing promising results.

AVAILABILITY OF DATA FOR FUTURE ML STUDIES

Expanding the use of ML in geotechnical and foundation engineering requires large, high-quality databases that can be used for training and validation of proposed models. For foundation engineering, these databases must contain information about the soil profile and properties, foundation dimensions and properties, loading, and observed response. Potential sources of this data are full-scale load tests, small-scale experiments, centrifuge modeling, and numerical studies. This data is often expensive to collect and so developing a separate database for each project is not practical. Fortunately, databases of foundation performance have been assembled by several researchers and institutions, which now are publicly available. Phoon and Tang (*50*) have compiled an exhaustive list of currently available load test databases for a variety of geo-structures. In recent years, free and low-cost data repositories have begun to grow in popularity, and technical journals have begun to require that data availability statements be included with published papers. Both of these trends are expected to lead to growth of available databases over time, which may also increase opportunities for applications of ML.

A significant number of load test databases have been compiled for deep foundations (*50*). One of the first modern databases of deep foundation load test data was created at the University of Texas in the early 1980s (*51*). Since that time, many other databases have been created and a brief history of this development process is discussed by Macharias et al (*52*). In the United States, available databases include state-specific databases (*45–49*) and the FHWA Deep Foundation Load Test Database (*58*). Databases of load testing on deep foundations have also been developed for other countries, including Ireland (*59*), Egypt (*60*), and the United Kingdom (*61*). In addition to these databases, some researchers have attempted to compile global databases of load test results (e.g., *52, 53*).

Multiple databases have also been developed to document the response of shallow foundations to loading. Whereas deep foundation databases have often been developed for specific regions, shallow foundation databases have tended to be more global in scope. Many results from earlier databases were combined into two global databases developed as part of NCHRP Project 24-31 (*64*) focused on bearing capacity of shallow foundations on granular soils and rock. Samtani and Allen (*65*) compiled a database on settlement of shallow foundations using field data from both the United States and Europe. In addition to field data, databases on shallow foundation behavior under earthquake loading have also been compiled from centrifuge test data (*58, 59*).

One significant challenge with using the databases listed above for ML applications is the lack of a standard format or structure for load test databases. Databases may also have incomplete information, which limits their usefulness. Desirable qualities for development of future load test databases have been summarized in (*68*) and (*69*), but these guidelines focus mostly on the content of the data and not the format or structure of the database itself. A lack of a standard format makes it difficult to combine data from multiple sources without a significant amount of user input. Attempts to create a standard format for geotechnical data, including the Data Interchange for Geotechnical and Geoenvironmental Specialists (DIGGS) project in the United States (*70*) and the AGS Format in the United Kingdom (*71*), may help with unifying geotechnical databases in the future. The database structure is equally important. Many current geotechnical databases are stored in static tables or spreadsheets, which limits the ability to update and analyze the databases using standard ML applications. Other databases have been developed to include user interfaces, which makes it easier to find and access single records but complicates automated analysis. For example, Macharias et al. (*52*) converted the FHWA Deep Foundation Load Test Database (*58*) to a relational database format in order to take advantage of Structured Query Language data analysis methods. Many database management systems are available that are compatible with common ML applications and should be considered for future database development.

DISCUSSION

ML-based methods have been applied to a large number of transportation engineering issues, as highlighted in this paper. The potential of big data, ML, AI, and other data-driven methods has been emphasized in recent important expert meetings (*7, 8*). Initiatives for using these technologies to improve traffic modeling and make safer roads are ongoing, as previously discussed. Hence, it is expected to see more and more applications in the next decades within the scope of TRB and TRR.

The extensive capabilities of ML-based methods have resulted in its broad application to several classical problems of geotechnical engineering, for example, estimation of soil properties, shallow foundation and deep foundation bearing capacity, settlement prediction, slope stability, liquefaction, and several more. As was shown, many researchers have found that data-driven models and ML methods can outperform traditional alternatives. Deployment of trained ML-based models is still a missing piece in the application of this technology to the daily practice of geotechnical engineers. The number of applications of AI and ML to transportation infrastructure problems, including bridges and bridge foundations, is likely to keep increasing as more data are available, and these techniques become accepted in the geotechnical engineering community.

The creation and maintenance of highly reliable geotechnical databases is a major challenge. The prediction capabilities of ML-based models are only as good as the data used to train them and so it is critical for the geotechnical community to continue creating and updating databases. Some of the difficulties with creating quality databases includes incomplete data, data formatting, and database structure. It is also important to expand the range of conditions covered by the databases. One significant limitation of ML-based models is extrapolation for predictions outside of the training data domain. Bridge foundation engineering and other geotechnical applications could see significant benefits from ML-based models and so continued investment in the development and standardization of databases is important.

CONCLUSIONS

With the availability of previously unseen amounts of data, cloud storing capabilities, and the continuity of increasing computing power, ML-based techniques have become a suitable tool for a number of applications in many areas of civil engineering. ML toolboxes and user-friendly software are now available to engineers to train their own models and make predictions from their collected data. Successful applications were shown in the fields of transportation engineering and geotechnical engineering. Multiple databases are available that can be used for development of ML-based approaches to foundation design, but the lack of a standard format or structure limits the usefulness of current databases. Future developments should focus on using standardized data formats, such as DIGGS or AGS format, and database management systems that are compatible with common ML toolboxes.

A number of studies within the scope of TRB and TRR publications related to ML were found in areas such as traffic operation, travel demand and mode choice modeling, travel time prediction, transportation safety, detection of railroad trespassing, work zone crash injury severity prediction, and others. Nevertheless, to the best of the authors' knowledge, as of June 2020, only one application ML in geotechnical engineering is published in TRR, and none was found in NCHRP libraries. Nevertheless, the lectern session on *Next Generation of Engineering Practice* held at the TRB 2019 Annual Meeting shows a growing interest in this topic. Given the fast-growing number of successful applications of ML that can be found in geotechnical engineering in other journals and scientific media, this topic could be a candidate for a NCHRP synthesis project. In addition, collaborations between the Standing Committees on Foundations of Bridges and Other Structures and on Artificial Intelligence and Advanced Computing could be highly beneficial for the field.

ACKNOWLEDGMENTS

The authors appreciate the feedback received from Dr. Nedret Billor (Department of Mathematics and Statistics at Auburn University) on the review of the ML techniques presented.

AUTHOR CONTRIBUTIONS

The authors confirm contribution to the paper as follows: study conception and design: Aguilar; data collection: Montgomery; analysis and interpretation of results: Wu; draft manuscript preparation: Aguilar, Wu, Montgomery. All authors reviewed the results and approved the final version of the manuscript.

REFERENCES

1. Shahin, M. A., M. B. Jaksa, and H. R. Maier. *Predicting the Settlement of Shallow Foundations on Cohesionless Soils Using Back-Propagation Neural Networks*. Publication R 167. Department of Civil and Environmental Engineering, University of Adelaide, 2000.
2. Samui, P. Support Vector Machine Applied to Settlement of Shallow Foundations on Cohesionless Soils. *Computers and Geotechnics*, Vol. 35, No. 3, 2008, pp. 419–427. https://doi.org/10.1016/j.compgeo.2007.06.014.
3. Kordjazi, A., F. Pooya Nejad, and M. B. Jaksa. Prediction of Ultimate Axial Load-Carrying Capacity of Piles Using a Support Vector Machine Based on CPT Data. *Computers and Geotechnics*, Vol. 55, 2014, pp. 91–102. https://doi.org/10.1016/j.compgeo.2013.08.001.
4. Goetz, J. N., A. Brenning, H. Petschko, and P. Leopold. Evaluating Machine Learning and Statistical Prediction Techniques for Landslide Susceptibility Modeling. *Computers & Geosciences*, Vol. 81, 2015, pp. 1–11. https://doi.org/10.1016/j.cageo.2015.04.007.
5. Shahin, M. A. State-of-the-Art Review of Some Artificial Intelligence Applications in Pile Foundations. *Geoscience Frontiers*, Vol. 7, No. 1, 2016, pp. 33–44. https://doi.org/10.1016/j.gsf.2014.10.002.
6. 6. Lu, P., S. Chen, and Y. Zheng. Artificial Intelligence in Civil Engineering. *Mathematical Problems in Engineering*, 2012.
7. National Academy of Sciences. *The Frontiers of Machine Learning: 2017 Raymond and Beverly Sackler U.S.-U.K. Scientific Forum.* National Academies Press, Washington, D.C., 2018.
8. Merrefield, C. *Transportation in the Age of Artificial Intelligence and Predictive Analytics*. John A. Volpe National Transportation Systems Center, 2019.
9. Tarawneh, B. Predicting Standard Penetration Test N-Value from Cone Penetration Test Data Using Artificial Neural Networks. *Geoscience Frontiers*, Vol. 8, No. 1, 2017, pp. 199–204. https://doi.org/10.1016/j.gsf.2016.02.003.
10. Harandizadeh, H., M. M. Toufigh, and V. Toufigh. *Different Neural Networks and Modal Tree Method for Predicting Ultimate Bearing Capacity of Piles*, 2018, p. 18.
11. Samui, P. Vector Machine Techniques for Modeling of Seismic Liquefaction Data. *Ain Shams Engineering Journal*, Vol. 5, No. 2, 2014, pp. 355–360. https://doi.org/10.1016/j.asej.2013.12.004.
12. Hastie, T., R. Tibshirani, and J. Friedman. *The Elements of Statistical Learning: Data Mining, Inference and Prediction*. Springer, Calif., 2017.
13. Song, Y.-Y., and L. U. Ying. Decision Tree Methods: Applications for Classification and Prediction. *Shanghai Jingshen Yixue*, Vol. 27, No. 2, 2015, p. 130.
14. Breiman, L., J. H. Friedman, R. A. Olshen, and C. J. Stone. Classification and Regression Trees. *International Group*, Vol. 432, 1984, pp. 151–166.

15. Breiman, L. Random Forests. *Machine Learning*, Vol. 45, No. 1, 2001, pp. 5–32. https://doi.org/10.1023/A:1010933404324.
16. Efron, B., and T. Hastie. *Computer Age Statistical Inference*. Cambridge University Press, 2016. https://doi.org/10.1017/CBO9781316576533.
17. Ishak, S., and F. Trifiro. Neural Networks. *Artificial Intelligence in Transportation*, 2007, pp. 17–32.
18. Aguilar, V., C. Sandoval, J. M. Adam, J. Garzón-Roca, and G. Valdebenito. Prediction of the Shear Strength of Reinforced Masonry Walls Using a Large Experimental Database and Artificial Neural Networks. *Structure and Infrastructure Engineering*, Vol. 12, No. 12, 2016, pp. 1661–1674. https://doi.org/10.1080/15732479.2016.1157824.
19. Boser, B. E., I. M. Guyon, and V. N. Vapnik. A Training Algorithm for Optimal Margin Classifiers. 1992. https://doi.org/10.1145/130385.130401.
20. Swan, B. *Adaptation and Comparison of Machine Learning Methods for Geomorphological Mapping and Terrace Prediction: A Case Study of the Buffalo River*. 2017.
21. Tso, B., and P. Mather. *Classification Methods for Remotely Sensed Data*. CRC Press, Boca Raton, Fla., 2009.
22. Foody, G. M., and A. Mathur. A Relative Evaluation of Multiclass Image Classification by Support Vector Machines. *IEEE Transactions on Geoscience and Remote Sensing*, Vol. 42, No. 6, 2004, pp. 1335–1343. https://doi.org/10.1109/TGRS.2004.827257.
23. Ahmed, A., S. Khan, S. Hossain, T. Sadigov, and P. Bhandari. Safety Prediction Model for Reinforced Highway Slope Using a Machine Learning Method. *Transportation Research Record: Journal of the Transportation Research Board*, No. 2674, 2020, pp. 761–773. https://doi.org/10.1177/0361198120924415.
24. *Transportation Research Circular E-C113: Artificial Intelligence in Transportation Information for Application*. Transportation Research Board, Washington, D.C., 2007.
25. *Transportation Research Circular E-C168: Artificial Intelligence Applications to Critical Transportation Issues*. Transportation Research Board, Washington, D.C., 2012.
26. Artificial Intelligence. *Transportation Research Record 1399*, Transportation Research Board, Washington, D.C., 1993.
27. Mulholland, I. P., and R. A. Oren. *Artificial Intelligence for Transit Railcar Diagnostics*. National Academy Press, Washington, D.C, 1994.
28. Intelligent Transportation Systems: Evaluation, Driver Behavior, and Artificial Intelligence. *Transportation Research Record 1453*, Transportation Research Board, Washington, D.C, 1994.
29. Artificial Intelligence and Geographical Information. *Transportation Research Record 1497*, Transportation Research Board, Washington, D.C., 1995.
30. Sadek, A. W., B. L. Smith, and M. J. Demetsky. Artificial Intelligence Search Algorithms for Dynamic Traffic Routing. *Transportation Research Record 1679*, 1999, pp. 87–94. https://doi.org/10.3141/1679-12.
31. Sadek, A. W., G. Spring, and B. L. Smith. Toward More Effective Transportation Applications of Computational Intelligence Paradigms. *Transportation Research Record: Journal of the Transportation Research Board*, No. 1836, 2003, pp. 57–63. https://doi.org/10.3141/1836-08.
32. Xiao, H., H. Sun, B. Ran, and Y. Oh. Fuzzy-Neural Network Traffic Prediction Framework with Wavelet Decomposition. *Transportation Research Record: Journal of the Transportation Research Board*, No. 1836, 2003, pp. 16–20. https://doi.org/10.3141/1836-03.
33. Zhang, Y., and Y. Xie. Travel Mode Choice Modeling with Support Vector Machines. *Transportation Research Record: Journal of the Transportation Research Board*, Vol. 2076, No. 1, 2008, pp. 141–150. https://doi.org/10.3141/2076-16.
34. Hou, Y., and P. Edara. Network Scale Travel Time Prediction Using Deep Learning. *Transportation Research Record: Journal of the Transportation Research Board*, Vol. 2672, No. 45, 2018, pp. 115–123. https://doi.org/10.1177/0361198118776139.
35. Mokhtarimousavi, S., J. C. Anderson, A. Azizinamini, and M. Hadi. Improved Support Vector Machine Models for Work Zone Crash Injury Severity Prediction and Analysis. *Transportation Research Record: Journal of the Transportation Research Board*, Vol. 2673, No. 11, 2019, pp. 680–692. https://doi.org/10.1177/0361198119845899.

36. Zaman, A., B. Ren, and X. Liu. Artificial Intelligence-Aided Automated Detection of Railroad Trespassing. *Transportation Research Record: Journal of the Transportation Research Board*, Vol. 2673, No. 7, 2019, pp. 25–37. https://doi.org/10.1177/0361198119846468.
37. Karaaslan, E., U. Bagci, and F. N. Catbas. Artificial Intelligence Assisted Infrastructure Assessment Using Mixed Reality Systems. *Transportation Research Record: Journal of the Transportation Research Board*, Vol. 2673, No. 12, 2019, p. 413–424. https://doi.org/10.1177/0361198119839988.
38. Kavianipour, M., R. Saedi, A. Zockaie, and M. Saberi. Traffic State Estimation in Heterogeneous Networks with Stochastic Demand and Supply: Mixed Lagrangian–Eulerian Approach. *Transportation Research Record: Journal of the Transportation Research Board*, Vol. 2673, No. 11, 2019, p. 114–126. https://doi.org/10.1177/0361198119850472.
39. Daneshgaran, F., L. Zacheo, F. D. Stasio, and M. Mondin. Use of Deep Learning for Automatic Detection of Cracks in Tunnels: Prototype-2 Developed in the 2017–2018 Time Period. *Transportation Research Record: Journal of the Transportation Research Board*, Vol. 2673, No. 9, 2019, p. 44–50. https://doi.org/10.1177/0361198119845656.
40. Adeli, H. Neural Networks in Civil Engineering: 1989–2000. *Computer-Aided Civil and Infrastructure Engineering*, Vol. 16, No. 2, 2001, pp. 126–142. https://doi.org/10.1111/0885-9507.00219.
41. Shahin, M. A. Load-Settlement Modeling of Axially Loaded Steel Driven Piles Using CPT-Based Recurrent Neural Networks. *Soil and Foundation*, Vol. 54, No. 3, 2014, pp. 515–522. https://doi.org/10.1016/j.sandf.2014.04.015.
42. Momeni, E., R. Nazir, D. Jahed Armaghani, and H. Maizir. Application of Artificial Neural Network for Predicting Shaft and Tip Resistances of Concrete Piles. *Earth Sciences Research Journal*, Vol. 19, No. 1, 2015, pp. 85–93. https://doi.org/10.15446/esrj.v19n1.38712.
43. Tarawneh, B. Pipe Pile Setup: Database and Prediction Model Using Artificial Neural Network. *Soil and Foundation*, Vol. 53, No. 4, 2013, pp. 607–615. https://doi.org/10.1016/j.sandf.2013.06.011.
44. Ranasinghe, R. A. T. M., M. B. Jaksa, Y. L. Kuo, and F. Pooya Nejad. Application of Artificial Neural Networks for Predicting the Impact of Rolling Dynamic Compaction Using Dynamic Cone Penetrometer Test Results. *Journal of Rock Mechanics and Geotechnical Engineering*, Vol. 9, No. 2, 2017, pp. 340–349. https://doi.org/10.1016/j.jrmge.2016.11.011.
45. Kordjazi, A., F. P. Nejad, and M. B. Jaksa. *Prediction of Load-Carrying Capacity of Piles Using a Support Vector Machine and Improved Data Collection*, 2016, p. 9.
46. Goh, A. T. C., and S. H. Goh. Support Vector Machines: Their Use in Geotechnical Engineering as Illustrated Using Seismic Liquefaction Data. *Computers and Geotechnics*, Vol. 34, No. 5, 2007, pp. 410–421. https://doi.org/10.1016/j.compgeo.2007.06.001.
47. Khan, S. Z., S. Suman, M. Pavani, and S. K. Das. Prediction of the Residual Strength of Clay Using Functional Networks. *Geoscience Frontiers*, Vol. 7, No. 1, 2016, pp. 67–74. https://doi.org/10.1016/j.gsf.2014.12.008.
48. Gomes Correia, A., P. Cortez, J. Tinoco, and R. Marques. Artificial Intelligence Applications in Transportation Geotechnics. *Geotechnical and Geological Engineering*, Vol. 31, No. 3, 2013, pp. 861–879. https://doi.org/10.1007/s10706-012-9585-3.
49. Cheng, M.-Y., and N.-D. Hoang. Slope Collapse Prediction Using Bayesian Framework with K-Nearest Neighbor Density Estimation: Case Study in Taiwan. *Journal of Computing in Civil Engineering*, Vol. 30, No. 1, 2016, p. 04014116. https://doi.org/10.1061/(ASCE)CP.1943-5487.0000456.
50. Phoon, K.-K., and C. Tang. Characterisation of Geotechnical Model Uncertainty. *Georisk: Assessment and Management of Risk for Engineered Systems and Geohazards*, Vol. 13, No. 2, 2019, pp. 101–130.
51. Dennis, N. D., and R. E. Olson. *Axial Capacity of Steel Pipe Piles in Sand*. 1983.
52. Machairas, N., G. A. Highley, and M. G. Iskander. Evaluation of FHWA Pile Design Method against the FHWA Deep Foundation Load Test Database Version 2.0. *Transportation Research Record: Journal of the Transportation Research Board*, Vol. 2672, No. 52, 2018, pp. 268–277. https://doi.org/10.1177/0361198118773196.
53. Anderson, J. B., and F. C. Townsend. A Laterally Loaded Pile Database. Deep Foundations. *An International Perspective on Theory, Design, Construction, and Performance*, Vol. 2002, 2002, pp. 262–273.

54. Roling, M. J., S. Sritharan, and M. T. Suleiman. *Development of LRFD Procedures for Bridge Pile Foundations in Iowa-Volume I: An Electronic Database for Pile Load Tests (PILOT)*. Iowa State University. Institute for Transportation, 2011.
55. Rauser, J., and C. Tsai. *Beneficial Use of the Louisiana Foundation Load Test Database*. 2016.
56. Moghaddam, R. B., P. W. Jayawickrama, W. D. Lawson, J. G. Surles, and H. Seo. Texas Cone Penetrometer Foundation Design Method: Qualitative and Quantitative Assessment. *DFI Journal-The Journal of the Deep Foundations Institute*, Vol. 12, No. 2, 2018, pp. 69–80. https://doi.org/10.1080/19375247.2018.1536409.
57. Garder, J., K. Ng, S. Sritharan, and M. Roling. *An Electronic Database for Drilled SHAft Foundation Testing (DSHAFT)*. InTrans Project 10-366. Iowa Department of Transportation, 2012.
58. Petek, K., R. Mitchell, and H. Ellis. *FHWA Deep Foundation Load Test Database Version 2.0 User Manual*. Federal Highway Administration, U.S. Department of Transportation, 2016.
59. Galbraith, A. P., E. R. Farrell, and J. J. Byrne. Uncertainty in Pile Resistance from Static Load Tests Database. *Geotechnical Engineering*, Vol. 167, No. 5, 2014, pp. 431–446. https://doi.org/10.1680/geng.12.00132.
60. AbdelSalam, S. S., F. A. Baligh, and H. M. El-Naggar. A Database to Ensure Reliability of Bored Pile Design in Egypt. *Geotechnical Engineering*, Vol. 168, No. 2, 2015, pp. 131–143. https://doi.org/10.1680/geng.14.00051.
61. Voyagaki, E., J. Crispin, C. Gilder, P. Nowak, N. O'Riordan, D. Patel, and P. J. Vardanega. *Analytical Approaches to Predict Pile Settlement in London Clay*, 2018.
62. Favaretti, C., A. Lemnitzer, A. W. Stuedlein, and J. Turner. Recent Discussions of Py Formulations for Lateral Load Transfer of Deep Foundations Based on Experimental Studies. *IFCEE 2015*, pp. 388–399.
63. Yang, Z. X., R. J. Jardine, W. B. Guo, and F. Chow. A New and Openly Accessible Database of Tests on Piles Driven in Sands. *Géotechnique Letters*, Vol. 5, No. 1, 2015, pp. 12–20. https://doi.org/10.1680/geolett.14.00075.
64. Paikowsky, S. G. Canniff, M. C; Lesny, K.; Kisse, A.; Amatya, S.; Muganga, R. *NCHRP Research Report 651: LRFD Design and Construction of Shallow Foundations for Highway Bridge Structures*. Transportation Research Board, 2010. https://trid.trb.org/view/919389.
65. Samtani, N. C., and T. M. Allen. *Implementation Report – Expanded Database for Service Limit State Calibration of Immediate Settlement of Bridge Foundation on Soil*. Publication FHWA-HIF-10-008. Federal Highway Administration, U.S. Department of Transportation, 2018.
66. Allmond, J., B. L. Kutter, J. Bray, and C. Hayden. New Database for Foundation and Ground Performance in Liquefaction Experiments. *Earthquake Spectra*, Vol. 31, No. 4, 2015, pp. 2485–2509. https://doi.org/10.1193/072814EQS120.
67. Gavras, A. Kutter, B. Hakhamaneshi, S. Gajan, A. Tsatsis, K. Sharma, T. Kouno, L. Deng, I. Anastasopoulos, G. Gazetas, and K. Variam. *FoRDy: Rocking Shallow Foundation Performance in Dynamic Experiments*. https://datacenterhub.org/resources/14666.
68. Abu-Hejleh, N. M., M. Abu-Farsakh, M. T. Suleiman, and C. Tsai. Development and Use of High-Quality Databases of Deep Foundation Load Tests. *Transportation Research Record: Journal of the Transportation Research Board*, Vol. 2511, 2015, pp. 27–36. https://doi.org/10.3141/2511-04.
69. Lesny, K. Evaluation and Consideration of Model Uncertainties in Reliability Based Design. Presented at the Joint ISSMGE TC 205/TC 304 Working Group on "Discussion of Statistical/Reliability Methods for Eurocodes, London, UK: International Society for Soil Mechanics and Geotechnical Engineering, 2017.
70. Cadden, A., and B. Keelor. *Implementation and Transition of Data Interchange for Geotechnical and Geoenvironmental Specialists (DIGGS v2. 0)*. Ohio Deptartment of Transportation, 2017.
71. Association of Geotechnical and Geoenvironmental Specalists. *Electronic Transfer of Geotechnical and Geoenvironmental Data*, Edition 4.0.4, Bromley, Kent. 2017

A Compatible Swarm Intelligence Model and Construction Method to Satisfy Bridge Design and Load Rating Requirements and Considering Geotechnical Variability

CHAD WILLIAM HARDEN
ANDRES LOZANO
Michael Baker International

This paper details the novel combination of a population-based swarm intelligence algorithm, structure mechanics, geotechnical variability, and a specific construction staging methodology, to propose an autonomous construction system which can erect a bridge over arbitrary crossing geometry while satisfying project constraints and conventional design code requirements (the Proposal). The fields of metaheuristic applications in structures, unmanned aerial systems (UAS), and additive manufacturing are each independent innovations in the transportation industry. The Proposal brings these fields together, with a vision that independent drone robots with very basic programming could construct a bridge with no user interruption and without performing a conventional structural design. A simulation as proof-of-concept is compared to a modern bridge design; the result is a modest increase in materials with an anticipated dramatic savings in labor. The paper also studies the effects of geotechnical variability for insight into preparation for possible future construction methodologies and algorithms. The Proposal has promise where socio-economic issues may be a factor, such as construction of infrastructure in remote locations or developing nations, and emergency repair or replacement of bridges. With recent U.S. policy supporting a permanent lunar presence and expanding Moon to Mars exploration through the Artemis program, the Proposal may also assist infrastructure development in advance of human missions.

INTRODUCTION AND MOTIVATION

Bridge construction and capacity enhancement in modern transportation networks is complicated by a number of geometric, environmental, and economic constraints. Urban development and right-of-way limit improvement and work areas (geometric constraint), biological resources or user interruption may preclude construction work areas over streams, channels, or in existing travelled ways (environmental constraint), and limited resources reduce the number of bridges which may be constructed and maintained (economic constraint). At the same time, the schedule for design and investigation (time constraint) is compressed by the need for capacity enhancement, urgency of improving deteriorated bridges, and increased sensitivity of the public toward delays and traffic impacts.

Any or all aforementioned project-specific constraints may be addressed and overcome in a real-time construction environment, with limited planning, and while satisfying structural design criteria, by combining the fields of metaheuristic applications in structures (MAS), UAS, or drone robotics, and additive manufacturing (or precision concrete placement). This paper proposes a basic population-based swarm intelligence algorithm, combined with current and developing technological capabilities, and following a specific construction staging methodology,

which can construct a bridge over a complicated and previously unknown crossing geometry while satisfying the Proposal.

The Proposal is robust in its simplicity to apply to a range of bridge types and crossing geometries, and to the various components of a bridge project. The Proposal provides solutions where socioeconomic issues may be a factor, such as construction of infrastructure in remote locations or developing nations, and emergency repair or replacement of bridges.

On a new and developing transportation front, recent U.S. policy increased funding to return American astronauts to the moon by 2024 and establish a lunar presence (*8*), as well as to expand to exploration from "Moon to Mars" with commercial and international partners as part of the long-term Artemis program (*9*). Successful collaboration and proof of innovation was accomplished between SpaceX and NASA on May 30, 2020 with the Demo-2 mission piloted by U.S. astronauts to the International Space Station (*10*).Combined with additive manufacturing technologies for future off-world settlements (*1, 2*), the Proposal may assist infrastructure improvement in advance of human missions.

A case study for comparison to conventional design is developed in the OpenSees platform (*1*), with graphical visualization in Sketchup and LumenRT. This simulation implementing the Proposal serves as proof-of-concept; construction of a bridge over a four-lane highway is possible with no user interruption, while accommodating required design vehicle loadings. Observations on the simulation are provided along with recommendations for future research into the methodology and necessary development of supporting overlapping technologies.

LITERATURE REVIEW

The Proposal is essentially the novel combination of swarm intelligence and structural mechanics as a proof-of-concept for the design and construction of a bridge with limited human direction. Swarm intelligence and the larger umbrella of MAS are reviewed here, as well as a review of current technologies required to support the Proposal, including the fields of UAS and automated concrete delivery.

Metaheuristic Applications in Structures

MAS algorithms are tools which employ exploration and randomization to discover the optimum solutions within a search space (*2*). The field of MAS has provided research into such problems as structure and bridge member optimization (Talatahari and Kaveh, 2013; Descamps and Coelho, 2013), structure layout optimization (*3*), and bridge maintenance scheduling (*4*) to name a few applications. The solution framework for each problem varies widely and may be based on real systems or on artificial systems or criteria. Examples of real systems include the behavior of social insects or "swarm intelligence" (*5*) and genetic algorithms (*2*). Therefore, swarm intelligence is a subfield of MAS, and the remarkable observation on swarm intelligence is that simple, local behaviors or processes on a micro-scale can produce effective solutions on a macro-scale (*5*). The Proposal suggests that independent drone robots with very basic programming could construct a bridge without performing a conventional design, while solving project-specific contraints and geometry not known a priori.

Form Finding

Form Finding (FF) is a field of research which aims to find the most economical and appropriate form for the final design of a structure or element using iterative optimization algorithms, or topology optimization. Such applications to bridges include optimization of shell-supported bridge structures (*6*) and optimizing solutions for suspension bridge installation analysis (*7*). While both FF and MAS may use iteration, FF uses iteration to optimize a design, while MAS applies a natural or arbitrary algorithm to perform the design. As a point of clarification, though seemingly similar in the use of algorithms to MAS, the approach or field of FF is not used in this paper.

Emerging Construction Technologies

Drones are currently being used in the bridge industry to provide bridge inspection in difficult areas (*8*) as well as mapping of bridges in disaster areas (*9, 10*). Precision placement of concrete with contour crafting (or 3D printing) techniques are also developing (*11*) for automated construction of whole structures and housing developments. This technology is envisioned as perhaps one of few feasible construction methods for off-world construction for human colonization on other planets. The NASA is actively investigating technologies to revolutionize space exploration: from research on application of swarm intelligence features of self-configuration, self-optimization, self-healing and self-protecting to support deep space missions systems (*12*), to supporting design challenges for students and industry to innovate cooperative robotics and 3-D printing for off-world habitats and settlements (NASA, 2018a and b).

Experimental Architecture

A fascinating experimental architecture research collaborative is leading the industry in visualizing the possibilities of self-organizing construction behavior. Through computation, visualization, and prototype construction, Snooks (2013) studies experimental architecture and the potential application for robotics as part of the design process. As highlighted in Mortice (2015), Stuart-Smith, et al. (2015) explores the possibility of adaptive construction using drone technologies to erect pre-designed structures which may adjust to accommodate weather and other site challenges.

THE PROPOSAL: ALGORITHM AND SUBROUTINES

While these technologies currently require human guidance and control, a logical trajectory combines these fields for the unified and elevated purpose of autonomous assembly of structures.

The Proposal suggests that an autonomous construction system (drones and ground-based construction) can assemble a bridge using smart materials to overcome project constraints. The algorithm architecture is designed to be very limited at the drone level, requiring only basic hardware and software requirements conducive for mass production. The actions of the individual drones, acting on basic rules of logic, will achieve a grander solution with benefits of reduced user interruption and reduced cost. The algorithm is also basic in the few requirements that need to be met, generally:

- Elements need to be added to ultimately achieve a bridge;
- Elements cannot be overstrained; and
- The bridge during its course of construction cannot impede traffic or encroach into prespecified “no-build” zones.

The algorithm is not based on a current, living system, but rather is formulated from the basic needs above and in a logical order. As indicated by Bonabeau, Dorigo and Theraulaz (1999), algorithms need not follow true biological systems, but they must be efficient and flexible. For these reasons, the Proposal is a population-based swarm intelligence algorithm. It is intended the model would not run before construction as is typical of current design practice; rather, the algortihm would act within individual, automated drones and other machines for construction in real time. The subroutines as described are also processed in the following order and as shown graphically in Figure 1.

Subroutine: “DL Check”

Here DL refers to dead load, or the response to the structure’s self-weight only. In this stage each element reports if strains or displacements exceed a maximum value. As an element’s allowable strain is exceeded, the element width is increased or additional elements are added to increase the overall section depth. If displacement exceeds a maximum value, a column is added to provide support, provided the location in question is not over a predefined no-build zone such as a highway or right-of-way boundary.

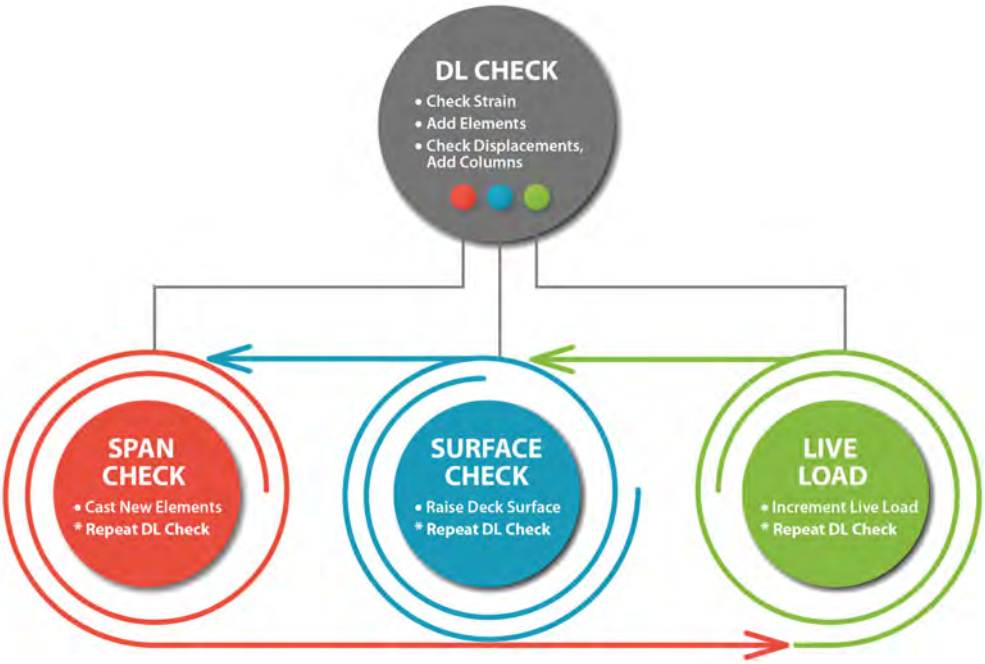

FIGURE 1 Construction algorithm for the Proposal.

Applicable technologies to this subroutine include intelligent materials to report strains within the materials, an autonomous system to coordinate transport and placement of concrete and rebar materials as well as foundations, and a positioning system to preclude construction within no-build zones or above the finished surface. It is envisioned that foundation elements would be installed either through UAS or land-based vehicles.

Subroutine: "Span Check"

In this stage a nominal number of new elements are added at the leading end of the bridge to further the progression toward the required bridge length. The DL check subroutine is repeated. Applicable technologies required for this subroutine are similar to those above, except specific detailing in algorithms to progress construction in the necessary direction(s) of the bridge.

Subroutine: "Surface Check"

In this stage new elements are created to raise the structure to the required profile grade of the finished bridge surface. Note that in the previous DL check, the algorithm does not allow the addition of new elements to exceed the final required profile grade. Any elements at the driving surface are widened to the width of the bridge, or that required for strain, whichever is greater. The DL check subroutine is repeated.

Subroutine: "Live Load"

Once the bridge has grown to the required length, design vehicles are applied to further grow the individual bridge elements as needed to support both the bridge self-weight and live loading. It is necessary that the first vehicle is incrementally increased in loading, or "stepped," to the full weight to allow the elements to grow uniformly across the bridge. Once the first vehicle has passed and the bridge is bolstered in strength due to growth and addition of new elements, the remaining vehicles may be applied without stepping the load. However, at each load step as the partial or whole vehicle is progressed across the bridge, the DL check subroutine is repeated.

As the vehicles are gradually increased in weight, conventional construction equipment of various classes could be employed to step up loading. The vehicles could be controlled under human direction either actively, remotely, or under autonomous control, perhaps even repurposing the use of any land-based construction equipment from previous stages. The use of several types of specialized equipment would likely be required, not unlike anatomical differences in social insects, which can organize division of labor (*5*).

The DL check, span check and surface check subroutines are repeated in a loop until the bridge has reached its required length. The DL check and LL subroutines are repeated in a loop until all vehicles have passed the bridge, at which time the bridge is completed. The bridge satisfies the necessary bridge design and load rating requirements through field load testing.

COMPARISON TO CONVENTIONAL DESIGN

Using the algorithm described above (the Proposal), a numerical simulation is performed to serve as a proof-of-concept. The simulation is compared to a project site where a bridge has been designed according to conventional design methods but not yet constructed. Herein, these results are either described as “simulation” (for the Proposal algorithm), or according to the “comparison structure” (conventional design).

Comparison Structure (Conventional Design)

The bridge comparison structure at the project site carries two lanes, shoulders and sidewalk for a total width of 14.45 m (47ft-5 in.), over a major arterial highway with four lanes in each direction and separated by a wide unpaved median. The bridge has ample minimum vertical clearance of approximately 8.2 m (27 ft). The details for the comparison bridge are shown in Figure 2.

The bridge is a cast-in-place two-span post-tensioned box girder bridge, with a total length of 105.8 m (347ft-0 in.), and individual spans of 54.7 and 51.1 m (179 ft-6 in. and 167 ft-6 in.). The bridge typical section consists of four webs with a superstructure depth of 2.2 m (7 ft-3 in.). The bent is constructed with a single 2.13 by 3.2 m (7 ft-0 in. by 10 ft-6 in.) oblong column, supported on a footing and 76 cm (30 in.) diameter cast-in-drilled-hole (CIDH) concrete piles.

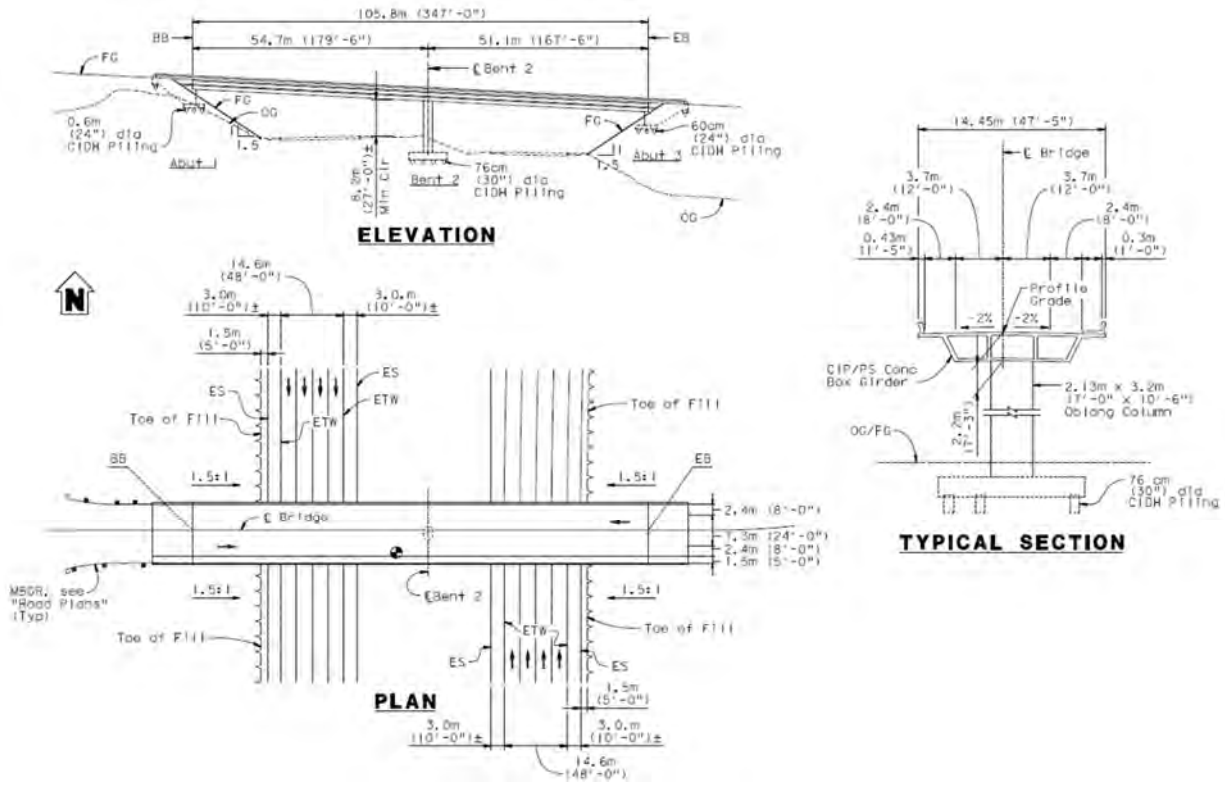

FIGURE 2 Plan, elevation and typical section of the conventional bridge design at sample project site.

The site offers flexibility of possible solutions. For example, in many overcrossing situations, the median (or median barrier) of the road below is narrow, such that possible substructure support locations are few or pre-defined. While the wide median provided between each highway direction of travel allows for freedom of results of the algorithm, the span over four lanes of traffic and shoulders is challenging. As the bridge grows through each span, it will require initial strength as a cantilever, followed by beam action as spans are completed and boundary conditions change.

Simulation

A general representation of the Proposal algorithm is incorporated into the TCL scripting language for analysis in the OpenSees structural engineering platform (*1*). The geometry of the project site is set as constraints, including the required profile grade of the completed bridge, the site terrain, and the no-build zone for columns over the highway lanes. The subroutines were configured to create two-dimensional (2-D), four-node quadrilateral element using physically stabilized single-point (SSP) integration, denoted as "SSPquad" elements in the OpenSees documentation. SSP quadrilateral elements eliminate the possibility of volumetric and shear locking (*13*).

The following simplifying assumptions were incorporated into the solution architecture:

- Reinforcing is not modeled explicitly. Quadrilateral elements, in general, were chosen to (1) more closely mimic a real system where discrete amounts of concrete would be placed in three dimensions, and (2) avoid the complication of locating reinforcing in this first proof-of-concept.
- The model is restricted to two planes: the primary axis along the proposed bridge centerline, and the vertical (elevation) axis. However, three dimensions were represented in the analysis. In the simulation, if an element's allowable strain is exceeded, additional elements are added to the perimeter of the element if possible, and the element width is increased proportional to the magnitude of the strain exceedence.
- When an element crosses the boundary of the existing terrain, the subject nodes are pinned. The assumption is that a foundation could be placed (autonomously) just prior to the placement of the element.

In keeping with the intention of swarm intelligence, model elements communicate with each other in a very limited fashion. Elements only record if they are connected to another element in either the *X* or *Z* axis, which is necessary for the algorithm to decide if the element should grow in width, have additional elements added on un-attached sides, or both. Therefore, as envisioned, smart materials with embedded strain transducers may be fabricated without excessive complexity. Note the system as a whole is not engineered nor is the geometry or result guided.

Specific modeling parameters are a 0.6 m (2 ft) square element production. In the span check mode, elements are projected out from the leading edge at least two forward and two in the vertical direction. Input model parameters were a concrete compressive strength of 34.5 MPa (5.0 ksi), elastic modulus of 47,350 MPa (6867 ksi), and max allowed strain of 0.001. The unit weight of concrete is modeled as approximately 6.4 kN/m^3 (41 pcf), allowing for a cellular structure in the concrete which is similar to the comparison structure effective unit weight when comparing the superstructure cross sectional area to the gross section area.

Allowable strain in the elements is limited to 0.001 to avoid excessive cracking. This value is estimated from the provisions controlling spacing of mild steel reinforcement for control of cracking in AASHTO LRFD Bridge Design Criteria (2014), and generally consistent with ranges published in other literature.

Following the completion of the bridge span from the specified begin to the specified end of the bridge, design vehicle loading (AASHTO, 2014) is applied to the structure. These vehicles generally included a design truck with maximum axle load of 142.3 kN (32 kips) at variable spacing, a design tandem with two axle loads of 111.2 kN (25 kips) at 1.2 m (4 ft) apart, and lane loading with two axle loads of 80 kN (18 kips) at variable spacing combined with a uniform load of 9.3 kN/m (0.64 kip/ft) in each lane. The first design truck vehicle is increased in weight in five increments until the full weight of the vehicle is applied to the bridge. At each increment in loading, the vehicle is moved at a regular spacing along the bridge after Scott and Kidarsa (2006), and the DL check algorithm is repeated to check appropriate element widths or thicknesses.

The final completed bridge is shown in Figure 3, and Figure 4 shows a video of the bridge model data during its growth and is also available online at https://youtu.be/DUOGRk-Bxj7M.

Observations (Qualitative)

The algorithm erected a bridge with a maximum span of approximately 26.2 m (86 ft). At this span a conventional reinforced concrete box girder bridge would have a depth-to-span ratio of 0.055 (*14*), resulting in a depth of approximately 1.4 m (4.7 ft). At anticipated negative moment locations, the simulation bridge depth is generally consistent with a depth of approximately 1.2 m (4 ft). The simulation provided the greatest section depths of 3 m (10 ft) at predictable locations of maximum mid-span moments. At the ends of each span, the section remains relatively thicker than at the beginning of the span, suggesting a high degree of redistribution in loading as the support conditions of the bridge change from a cantilever to multiple supports.

One insight from writing the simulation architecture is the possibility of allowing the algorithm to choose construction starting points and growth directions, rather than starting at the begin

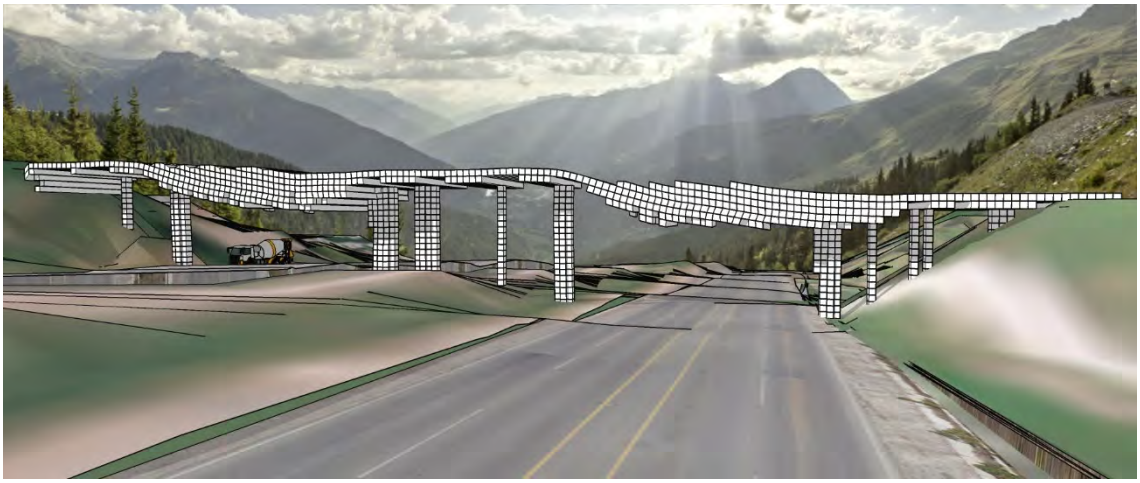

FIGURE 3 Visualization of the completed bridge analysis.

FIGURE 4 Video of model data though all stages of the bridge simulation. A higher resolution video is available online at https://youtu.be/DUOGRkBxj7M.

bridge as a constraint. This improvement may further speed construction and reduce necessary cantilever lengths of the bridge over the highway. For example, the algorithm could start bridge growth either from extreme ends toward the middle, or from an arbitrary center column and outward. However, for this first study, the goal is to explore the results of the simplest algorithm.

In terms of "Structural Art" as defined by Billington (1983), the bridge is an honest expression of the algorithm and the process of growth. Strain and deflection demands change with varying boundary conditions, bridge stiffness and weight, and vehicle loading as the bridge grows from beginning to end. These demands define column locations and shape beam and column section depths and thickness, resulting in a unique, appropriate, unguided solution.

Observations (Quantitative)

In the design comparison, the conventional bridge is designed with a total weight, including superstructure and columns, of 22,600 kN (5080 kips). This weight does not include the weight of the abutments or the bent column below grade, which is not modeled in the simulation. The simulation resulted in a total weight of 24,600 kN (5,530 kips), or an increase of 9% in concrete material over the conventional bridge. The simulation indicates the Proposal would initially result in bridges that are relatively more in terms of material cost; however, far greater savings in construction duration, labor force, and user delay costs would be realized.

Savings in construction duration and user delay have been realized using Accelerated Bridge Construction (ABC) - a recent innovation which requires significant investment by the bridge construction industry (*15*). Savings in required labor force are a speculation by the author, based on the Proposal of using autonomous UAS to install materials. Material costs would eventually decline as industry further develops the technology, refines algorithms, and contractors become more familiar and efficient in delivery. Further study of real biological algorithms, such as climbing plants (*16*) or cost–benefit analysis of the living bridges of army ants (*17*), may improve efficiency of the completed bridge. The variables within the swarm intelligence algorithm may also be optimized within a MAS study.

GEOTECHNICAL SENSITIVITY

The variable of foundation flexibility was introduced into the model to study its effects on model results and its interaction with the algorithm; this also provides insight on other processes or modification that may be required for future construction methodologies.

The algorithm was modified such that when a column is created or if a node crosses the theoretical original ground line, a boundary condition is created to apply a vertical spring "boundary element" at each of the two bottom nodes of the column quadrilateral element (Figure 5a). The boundary element is constructed of a zero-length element fixed against horizontal and vertical translation at one end, and connected to one of the bottom two nodes of the column quadrilateral element on the other end; these connected ends are also "released" in the vertical direction. The area and elastic modulus of the boundary element is calculated to achieve an effective spring stiffness of 58,400 (4,000), 87,500 (6,000), and 131,300 kN/m (9,000 kip/ft). These spring stiffnesses can be roughly correlated to spread footing and pile group stiffnesses. Considering a 40.6 cm (16 in.) and 61 cm (24 in.) pile typically have a nominal resistance of 890 kN (200 kip) and 1,780 kN (400 kip) (*18*), respectively; this results in a pile stiffness of 315 kN/cm (180 kip/in.) and 701 kN/cm (400 kip/in.) if these capacities are mobilized at a 1.3 cm (1/2 in.) displacement. Therefore, in the case of 40.6 cm (16 in.) and 61 cm (24 in.) piles, only two piles tributary to each 0.61 m (2 ft) square quadrilateral element equates to 58,400 kN / m and 131,300 kN/m (4,000 and 9,000 kip/ft), respectively. It is envisioned two piles per quadrilateral element would be constructed in a row perpendicular to the bridge centerline (Figure 5b). Similarly, for a spread footing, assuming a 0.61 m (2 ft) wide (parallel to bridge centerline) by 3 m (10 ft) wide (perpendicular to bridge centerline) footing is constructed at each quadrilateral column element (Figure 5c), the comparative subgrade modulus can be back-calculated and are within typical ranges of weak to strong granular soil types (*19*). The resulting comparison of foundation stiffness is provided in Table 1.

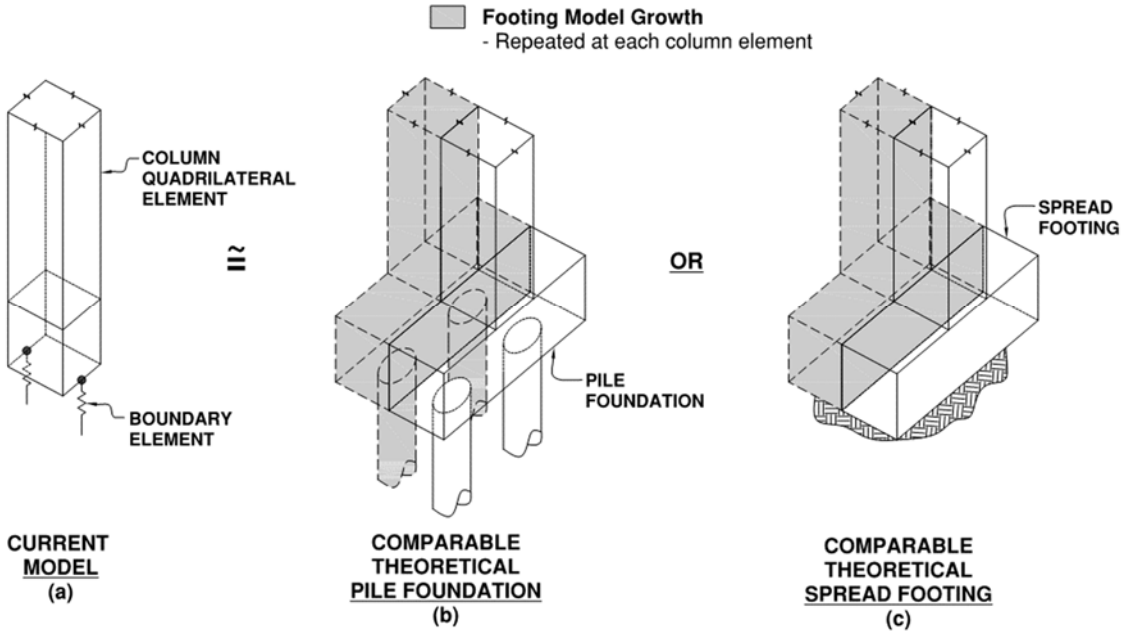

FIGURE 5 Diagram of equivalent column quadrilateral element.

TABLE 1 Range of Comparable Foundation Stiffnesses

Spring Stiffness kN/m (kip/ft)	Comparable Pile Type (2 Pile Row)	Pile Capacity at 1.3 cm (½ in.) Displacement kN (kip)	Comparable subgrade modulus for 0.61 x 3 m (2 x 10 ft) Spread Footing kN/m^3 (pci)
58,400 (4,000)	40.6 cm (16") CIDH	400 (90)	32,000 (115)
87,500 (6,000)	--	--	48,700 (175)
131,300 (9,000)	61 cm (24") CIDH	890 (200)	72,300 (260)

Using the variation of stiffnesses described, Figure 6 presents the result on model output. It is observed that foundation flexibility has a significant impact and influence on the model progression. Figure 6(a) presents the output based on a 58,400 kN/m (4,000 kip/ft) spring stiffness. Large deflections and rotations of the superstructure are evident from the shape of the bridge, especially at the right end where the last span is constructed. The authors also note that generally weaker stiffnesses resulted in model instability, thus indicating that sufficient confidence in pile capacity and construction practices are essential to future success of real-world construction.

Figure 6b presents the model output based on the mid-range 87,500 kN/m (6,000 kip/ft) spring stiffness. As the bridge grows and develops columns, those columns displace differentially. Differential displacement induces strain in the superstructure; this is counteracted by the algorithm placing more material in the bridge superstructure in overstrained regions. Therefore, this model output has a larger superstructure than observed in Figures 6a and c.

Finally, Figure 6c presents the model output based on the relatively largest 131,300 kN/m (9,000 kip/ft) spring stiffness. As anticipated, the larger spring capacity results in less displacement of the columns. The reduced differential displacements between columns requires a thinner superstructure between columns, indicating reduction in element strain. As the bridge grows with a reduced section, it is less "prepared" for the growing cantilever spans. Larger displacements and secondary column displacement are observed in Figure 6c as opposed to Figure 6b.

SUMMARY AND FUTURE RESEARCH

This paper details a basic population-based swarm intelligence algorithm, with the novel addition of structural mechanics, to suggest an autonomous construction system (drones and ground-based equipment) can assemble a bridge using smart materials to overcome project constraints. The Proposal has promise for infrastructure in developing countries, emergency repair and even off-world situations. A simulation as proof-of-concept is compared to a conventional bridge design; the result is a modest increase in materials with an anticipated dramatic savings in labor. Mimicking real biological algorithms, such as climbing plants or army ants, may improve efficiency of completed bridges.

The simplifying assumptions of the simulation provide direction for future research. The growth of the simulation is based on strains in homogeneous concrete elements. The effect of the necessary reinforcement, possible post-tensioning, and how this would be detailed in an algorithm and placed in construction requires study. Research would also need to address how humans or an independent autonomous system would be involved in quality control.

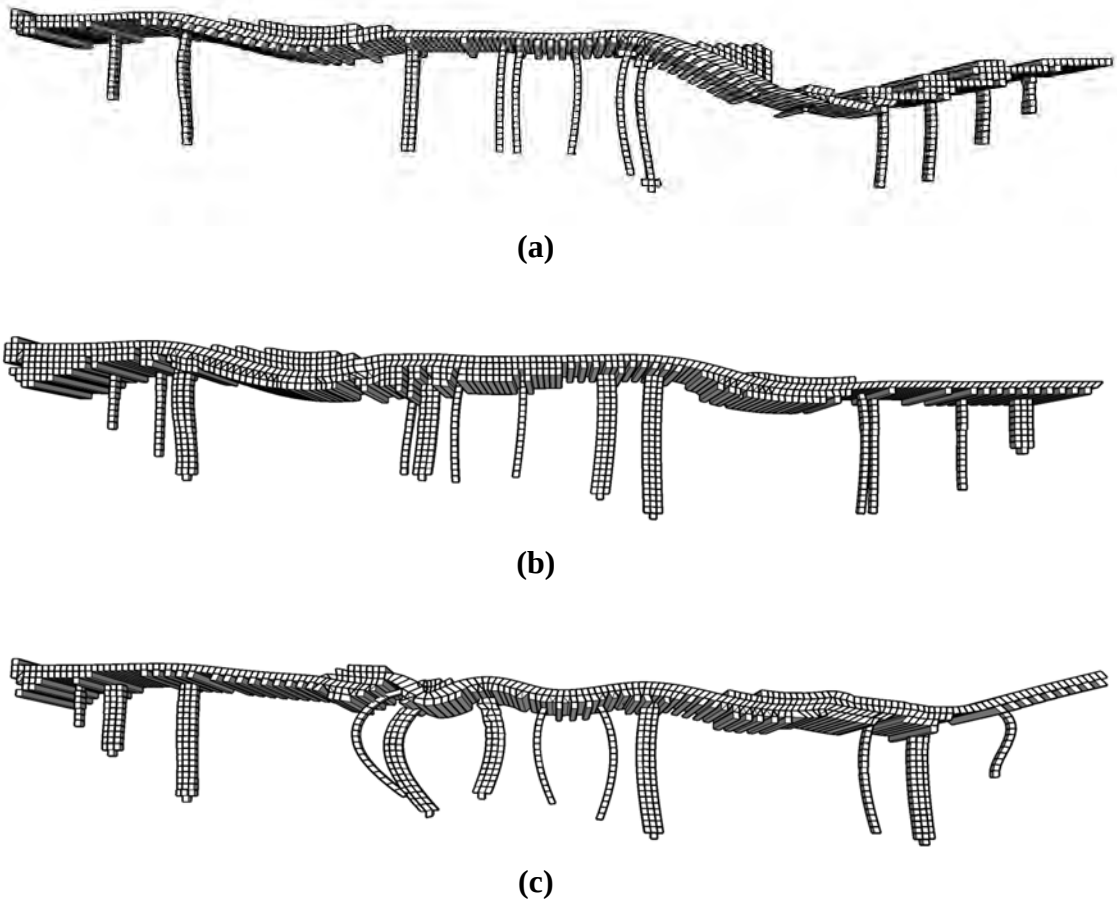

(a)

(b)

(c)

FIGURE 6 Visualization of the completed bridge analysis: (*a*) stiffness of 58,400 kn/m (4,000 kip/ft); (*b*) stiffness of 87,500 kn/m (6,000 kip/ft); and (*c*) stiffness of 131,300 kn/m (9,000 kip/ft).

The simulation grew in three dimensions by allowing element widths to be increased. However, addition of elements in all three dimensions would provide more insight into solutions in the physical world for column placement and cross-section shapes in response to out-of-plane bending, asymmetric span requirements, or curved horizontal alignments.

Strain is limited to a reasonable value in the simulation, and the result is coupled with the structure self-weight and design vehicles applied. Further calibration is needed to equate the combination of limiting strain values and anticipated LL construction vehicles applied, to probabilistic load factor and design vehicles. Further research is required to advance smart materials with embedded inexpensive devices to record and report strains with the controlling algorithm. Drone technology should be advanced in parallel to improve capabilities of placing the appropriate materials and devices where needed. Implementing of forward reconnaissance by UAV in the algorithm may be useful in guiding construction for long span lengths and to avoid excessive downward displacements.

Seismic performance and necessary detailing would need to be more fully understood for regions where this is a risk. The concepts of capacity protection in the superstructure and hinging in columns would be coordinated with more detailed algorithms that also control rebar placement.

The study of geotechnical variability applied soil springs, or boundary elements, at boundary conditions. This study assumes a foundation or pile element can be constructed autonomously, similar to the structural elements. Future technologies for autonomous vehicles and construction methods need to be advanced to support this idea as a reality. In addition, long-term foundation phenomena such as consolidation settlement, pile setup, and creep, etc., was not considered in the analysis and likely would never be sensed at the time of construction. Future research may consider the sensitivity or impacts if such effects are ignored; or alternatively, a cost–benefit comparison would be valuable to consider if overly conservative foundation types are pre-selected and implemented to generally account for these effects.

The algorithm could be expanded to explicitly model foundation elements, such as spread footings, micropiles, or other foundation types. Spread footings may apply to a greater number of sites through soil improvement; this improvement may be accomplished through conventional methods as well as semi-autonomous methods using microorganisms within the field of biogeotechnics (*20*). Biogeotechnics could lead improvements on site and ahead of bridge construction.

As detailed in this paper, several fields and technologies would require advancement or coordination in parallel, including algorithms for MAS, UAS or drone robotics, autonomous control and positioning systems for UAS and ground-based construction such as autonomous earth movers, additive manufacturing, and smart materials. The trajectory of overlapping developing technologies will only increase original solutions for the transportation industry. The Proposal is an exciting combination of swarm intelligence, structural mechanics, and new construction methods to autonomously assemble a bridge, satisfy design code requirements, and overcome project challenges.

ACKNOWLEDGMENTS AND DEDICATION

The author would like to express gratitude to those who have helped meet the challenge of this investigation. A sincere thank you to John Dietrick and Kyle Turner for their quality review and constructive comments. I have the great fortune to work with Michael Baker librarian Gina Hart, who is always so helpful and resourceful. Thank you to Faye Stroud and Christine Zeimer for preparing the illustrative figure for the algorithm.

REFERENCES

1. NASA. *New Space Policy Directive Calls for Human Expansion Across Solar System*, National Aeronautics and Space Administration, 2017. https://www.nasa.gov/press-release/new-space-policy-directive-calls-for-human-expansion-across-solar-system.
2. NASA. *What is Artemis?* National Aeronautics and Space Administration, 2019. https://www.nasa.gov/what-is-artemis.
3. NASA. National Aeronautics and Space Administration, 2020. https://www.nasa.gov/specials/dm2/.
4. Khoshnevis, B. Automated Construction By Contour Crafting—Related Robotics and Information Technologies. *Journal of Automation in Construction Special Issue: The Best of ISARC* 2002, Vol. 13, No. 1, pp. 5–19, 2004. https://doi.org/10.1016/j.autcon.2003.08.012.
5. David, L. *Mars: Our Future on the Red Planet*. National Geographic, Washington, D.C., 2016.
6. The Regents of the University of California. T*he Open System for Earthquake Engineering Simulation (OpenSees)*, 2016. http://opensees.berkeley.edu/.

7. Gandomi, A. H., X.-S. Yang, S. Talatahari, and A. H. Alavi. Metaheuristic Algorithms in Modeling and Optimization. *Metaheuristic Applications in Structures and Infrastructures* (A. H. Gandomi, X. Yang, S. Talatahari, and A. H. Alavi, eds.), Elsevier, London, 2013, pp. 1–24.
8. Nanakorn, P., and A. Nimtawat. Layout Design of Beam–Slab Floors by a Genetic Algorithm. *Metaheuristic Applications in Structures and Infrastructures* (A. H. Gandomi, X. Yang, S. Talatahari, and A. H. Alavi, eds.), Elsevier, London, 2013, pp. 147–171. https://doi.org/10.1016/B978-0-12-398364-0.00007-3.
9. Jha, M. K., M. Head, and S. P. Gar. Metaheuristic Applications in Bridge Infrastructure Maintenance Scheduling Considering Stochastic Aspects of Deteriorization. *Metaheuristic Applications in Structures and Infrastructures* (A. H. Gandomi, X. Yang, S. Talatahari, and A. H. Alavi, eds.), Elsevier, London, 2013, pp. 539–556.
10. Bonabeau, E., M. Dorigo, and G. Theraulaz. *Swarm Intelligence: From Natural to Artifical Systems*. Oxford University Press, New York, 1999. https://doi.org/10.1093/oso/9780195131581.001.0001.
11. Briseghella, B., L. Fenu, Y. Feng, C. Lan, E. Mazzarolo and T. Zordan. Optimization Indexes to Identify the Optimal Design Solution of Shell-Supported Bridges. *Journal of Bridge Engineering*, Vol. 21, No. 3, 2016. https://doi.org/10.1061/(ASCE)BE.1943-5592.0000838.
12. Chen, Z., H. Cao, K. Ye and H. Zhu. Improved Particle Swarm Optimization-Based Form-Finding Method for Suspension Bridge Installation Analysis. *Journal of Computing in Civil Engineering*, Vol. 29, No. 3, 2015. https://doi.org/10.1061/(ASCE)CP.1943-5487.0000354.
13. Yoder, L., and S. Sebastian. Autonomous Exploration for Infrastructure Modeling with a Micro Aerial Vehicle. *Field and Service Robotics*, 2015.
14. Christ, G. *Ohio Turnpike preparing to use drones*, 2016. http://www.cleveland.com/metro/index.ssf/2016/08/ohio_turnpike_preparing_to_use.html.
15. Shipman, M. *NCSU tech enables drones, insect biobots to map disaster areas*, 2016. http://wraltechwire.com/ncsu-tech-enables-drones-insect-biobots-to-map-disaster-areas/16250725/. Accessed December 14, 2016.
16. Vassev, E., R. Sterritt, C. Rouff, and M. Hinchey. Swarm Technology at NASA: Building Resilient Systems. *IT Professional*, Vol. 14, No. 2, 2012, pp. 36–42. https://doi.org/10.1109/MITP.2012.18.
17. McGann, C. R., P. Arduino, and P. Mackenzie-Helnwein. Stabilized Single-Point 4-Node Quadrilateral Element for Dynamic Analysis of Fluid Saturated Porous Media. *Acta Geotechnica*, Vol. 7, No. 4, 2012, pp. 297–311. https://doi.org/10.1007/s11440-012-0168-5.
18. California Department of Transportation. Comparative Bridge Costs, 2016. http://www.dot.ca.gov/hq/esc/estimates/COMP_BR_COSTS_2015-eng.pdf. Accessed July 12, 2017.
19. Oliva, W. Systematic Development, Implementation, and Deployment of Pre-Fabricated Bridge Elements. Presented at 94th Annual Meeting of Transportation Research Board, Washington D.C., 2015.
20. Gianoli, E. The behavioural ecology of climbing plants. *AoB Plants*, Vol. 7, No. plv013, 2015. https://doi.org/10.1093/aobpla/plv013.
21. Reid, C. R., M. J. Lutz, S. Powell, A. B. Kao, I. D. Couzin, and S. Garnier. Army Ants Dynamically Adjust Living Bridges in Response to a Cost–Benefit Trade-Off. *Proceedings of the National Academy of Sciences*, Vol. 112, No. 49, 2015, pp. 15113–15118. https://doi.org/10.1073/pnas.1512241112.
22. California Department of Transportation. *Standard Plans*. California Department of Transportation, Sacramento, 2015.
23. Bowles, J. E. *Foundation Analysis and Design*, 5th ed. Mcgraw-Hill Higher Education, 1995.
24. Dejong, J. T., K. Soga, E. Kavazanjian, S. Burns, L. A. Van Paassen, A. Al Qabany, A. Aydilek, S. S. Bang, M. Burbank, L. F. Caslake, C. Y. Chen, X. Cheng, J. Chu, S. Ciurli, A. Esnault-Filet, S. Fauriel, N. Hamdan, T. Hata, Y. Inagaki, S. Jefferis, M. Kuo, L. Laloui, J. Larrahondo, D. A. C. Manning, B. Martinez, B. M. Montoya, D. C. Nelson, A. Palomino, P. Renforth, J. C. Santamarina, E. A. Seagren, B. Tanyu, M. Tsesarsky, and T. Weaver. Biogeochemical Processes and Geotechnical Applications: Progress, Opportunities, and Challenges. *Geotechnique*, Vol. 63, No. 4, 2013, pp. 287–301. https://doi.org/10.1680/geot.SIP13.P.017.
25. AASHTO. *AASHTO LRFD Bridge Design Specifications*, 7th ed. American Association of State Highway and Transportation Officials, Washington, D.C., 2014.
26. Descamps, B., and R. F. Coelho. Graph Theory in Evolutionary Truss Design Optimization. *Metaheuristic Applications in Structures and Infrastructures* (A. H. Gandomi, X. Yang, S. Talatahari, and A.

H. Alavi, eds.), Elsevier, London, 2013, pp. 241–268. https://doi.org/10.1016/B978-0-12-398364-0.00010-3.
27. Mohammad, R., and M. Rais-Rohani. Element Exchange Method for Stochastic Topology Optimization. *Metaheuristic Applications in Structures and Infrastructures* (A. H. Gandomi, X. Yang, S. Talatahari, and A. H. Alavi, eds.), Elsevier, London, 2013, pp. 269–294.
28. Talatahari, S., and A. Kaveh. Optimum Design of Skeletal Structures via Bing Bang–Big Crunch Algorithm. *Metaheuristic Applications in Structures and Infrastructures* (A. H. Gandomi, X. Yang, S. Talatahari, and A. H. Alavi, eds.), Elsevier, London, 2013, pp. 173–205.
29. Mortice, Z. 4 Ways a Robot or Drone 3D Printer Will Change Architecture and Construction. *Redshift*, 2015.
30. Kelly, M. Army Ants' 'Living' Bridges Span Collective Intelligence, 'Swarm' Robotics. *Proceedings of the National Academy of Science*, 2015. https://blogs.princeton.edu/research/2015/11/24/army-ants-living-bridges-span-collective-intelligence-swarm-robotics-pnas/. Accessed April 4, 2017.
31. Scott, H. M., and A. Kidarsa. *Rating of Highway Bridges Using OpenSees and TCL*. Naperville, IL, 2006.
32. Snooks, R. *Behavioral Composites and Robotic Fabrication*. RMIT University, Monash University and The University of Melbourne, Australia, 2013.
33. Billington, D. *The Tower and the Bridge: The New Art of Structural Engineering*. Princeton University Press, New Jersey, 1983.
34. Stuart-Smith, R., T. Hosmer, M. Matsis, D. Chen, L. Xiao, S. Krishnasreni, and Y. Chen. *kokkugia: AADRL Swarm Printing: Aerial Robotic Bridge Construction*, AA School of Architecture, London, 2015.
35. NASA. NASA Swarmathon. National Aeronautics and Space Administration Minority University Research Program and The Moses Biological Computation Lab at the University of New Mexico (UNM), 2018b. http://nasaswarmathon.com/. Accessed July 1, 2018.
36. NASA. *NASA's Centennial Challenges: 3D-Printed Habitat Challenge*. National Aeronautics and Space Administration, 2018a. https://www.nasa.gov/directorates/spacetech/centennial_challenges/3DPHab/about.html. Accessed July 1, 2018.

Application of Unmanned Aerial Technologies for Inspecting Pavement and Bridge Infrastructure Asset Condition

SURYA SARAT CHANDRA CONGRESS
ANAND J. PUPPALA
MD ASHRAFUZZAMAN KHAN
NRIPOJYOTI BISWAS
Texas A&M University

Infrastructure in the United States was graded with "C–" in the 2021 ASCE report card. Frequent monitoring of the infrastructure assets is key to ensure the serviceability of the assets and safety to the public users. Advancements in aerial technologies, compact sensors, computer processing, and image analysis software have given rise to various engineering applications of the sensor-mounted aerial platforms. Unmanned aerial platforms with different sensors such as visible range, infrared, multispectral, and hyperspectral cameras are being used to obtain a more comprehensive perspective of infrastructure conditions than a simple visual examination by an experienced inspector. Many DOT agencies in the United States have been using unmanned aerial platforms for monitoring applications ranging from the research stage to using them for their regular inspection activities. These applications are mainly focused on inspecting infrastructure assets like pavements, bridges, railways, and others. The current research summarized the literature and discussed the approach followed to conduct aerial condition monitoring of pavements and bridges using sensors mounted on unmanned aerial platforms. This study was successful in capturing geotagged images and building 3D mapping products to conduct qualitative and quantitative inspections of the transportation infrastructure assets. The navigable three-dimensional models help to provide a virtual field-like visualization and enhance the experience of the engineers/practitioners. Overall, the rich visualization, safety, flexibility, and ease of handling offered by these technologies are expected to transform the way of conducting infrastructure performance monitoring inspections in the future.

INTRODUCTION

Growth in infrastructure can relate to the development of any nation. Agencies around the world are challenged to maintain infrastructure assets in good condition. Transportation infrastructure includes assets such as pavements, bridges, rail corridors, and other structures. The condition of these infrastructure assets is influenced by various factors including soil type, frequency and magnitude of loading, weather, environmental conditions, and monitoring frequency. The ASCE 2021 Infrastructure Report Card is the first of its kind as many new criteria were considered to evaluate and grade 17 infrastructure categories. Those criteria include capacity, condition, funding, future need, operation and maintenance, public safety, resilience, and innovation. In the United States, 43% of the public roadways are in poor or mediocre condition because of the growing, and unaddressed, wear and tear caused by increased traffic and environmental loads. Around 42% of the bridges that connect transportation corridors in the United States are over 50 years old (*1*).

The ASCE 2021 report card graded the overall infrastructure in the United States with a C–. Most infrastructure categories, barring railways, were graded C or worse. Even though these are the best grades received in the last 20 years, a C grade denotes that the infrastructure system or network is in fair to good condition but requires attention as it shows general signs of impending deterioration. Moreover, some elements may even exhibit conditional and functional deficiencies, with increasing vulnerability to risk (*1*). This highlights the need to adopt proactive monitoring techniques for preventive maintenance strategies. Pavement foundations within the transportation infrastructure are continuously exposed to various loading conditions in a variety of natural environments including extreme weather events such as prolonged droughts and hurricane-like events (*2*). Thousands of miles of pavements and many bridges have been built over problematic or expansive soils that create problems like uneven deformation, excessive cracking, and other infrastructure-related distress (*3–5*). The monitoring and timely maintenance of these infrastructure assets require a robust, reliable, fast, and efficient technology that can be used to conduct frequent inspections. Moreover, the increasing economic impact of highway and bridge closures due to frequent rehabilitation works has given impetus to adopting innovative monitoring technologies.

Remote sensing methods typically collect data without making any physical contact with the infrastructure asset under inspection. Modern-day remote sensing and recent inventions include the use of technologies ranging from smart cameras to advanced satellite mounted sensors for data capture, collection, and analyses related to the construction and functional performance of the assets. The authors collaborated with the Texas DOT on a research study to conduct infrastructure condition monitoring and assessments using unmanned aerial vehicles coupled with close-range photogrammetry (UAV-CRP) technology. Different pavements, bridges, rail corridors, and construction material sites were inspected using this innovative technology. This paper focuses on the use of a visible range camera mounted on UAVs or UASs for monitoring pavement and bridge infrastructure asset conditions. The last section of the paper discusses the futuristic scope of this innovative technology in transportation-related fields.

BACKGROUND

Unmanned Aerial Vehicles

Different types of aerial platforms such as rotary-wing and fixed-wing UAVs are available for infrastructure inspection. Rotary UAVs are preferred when inspecting enclosed and tight areas, whereas fixed-wing UAVs are more suitable for inspecting and mapping large areas (*6*). Various sensors including visible range cameras, infrared cameras, multispectral, and hyperspectral cameras, and light detection and ranging (lidar) can be mounted on UAV platforms for monitoring different infrastructure elements (*7*, *8*). The application of using UAVs for the infrastructure monitoring sector has recently gained considerable attention owing to the advancement of aerial platforms paralleled with the development of sophisticated sensors.

Data Collection Sensors

There are different sensors such as visible, infrared, multispectral, and hyperspectral cameras that are used for remotely collecting data. This paper includes a few case studies on using visible range camera sensors for infrastructure condition monitoring. In addition, the importance of infrared cameras for bridge inspection has also been acknowledged. Photogrammetry is a science that can measure and provide a 3D view of infrastructure using two or more images and can be considered as a part of remote sensing technologies. Remote collection of these images within a range of 1,000 ft is termed close-range photogrammetry (CRP) (*8*, *9*). UAV systems have become a popular means of gathering localized information and assessing infrastructure conditions. Images captured using UAV–CRP technology can generate high-quality dense point cloud models, orthomosaics, digital elevation models (DEMs), and digital terrain models. Analysis of these UAV–CRP collected data models can provide infrastructure health conditions that will assist in asset management strategies, planning and performing proactive rehabilitation strategies, quick assessment of stockpile volumetrics, and monitoring of infrastructure located at inaccessible conditions. All these will provide tremendous value to engineers and practitioners in the transportation and infrastructure sectors.

Factors Influencing the Quality of Aerial Data

Many previous studies have acknowledged the importance of considering different factors influencing the quality of aerial data collection and mapping products (*8*, *10–14*). The quality of the images depends upon various camera characteristics such as focal length, sensor size, focus, ISO, shutter type, and availability of digital or optical zoom. It also depends upon external factors such as the lighting conditions, flight speed and elevation, and the type of gimbal which offers a stable platform to mount the sensor. At a minimum, these images can be used to make qualitative inspections. Three-dimensional models can also be built from these images to make quantitative inspections. However, the accuracy of the 3D mapping products is governed by the quality of aerial images, longitudinal and lateral overlap, mapping type, ground control points (GCPs), and availability of real-time kinematic (RTK) or post-processing kinematic global navigation satellite system (GNSS) data (*10*). By using visible sensors, lidar, RTK GNSS, and GCPs, 3D models can achieve survey-grade accuracy and be used to make engineering assessments. However, these additional accessories are currently cost-intensive and are expected to become more affordable with widespread use in the future.

Federal Aviation Administration Rules for UAVS

In the United States, the FAA had released a new set of guidelines for the safe operation of small unmanned aerial vehicle systems in 2016 that are still effective (*15*). These guidelines are instrumental in safely conducting commercial operations using UAV platforms. Some of the highlights of the FAA part 107, rules for flying small drones (less than 55 lbs), are provided below:

1. All the UAVs must be registered, and the registration number needs to be attached to the aircraft before field operations.
2. Pilots should have FAA certification to perform the commercial operation of a single UAV at a time.

3. Airspace charts are provided to check if the site location falls within class G airspace if not, an authorization request is submitted to FAA for approval. The FAA sectional chart also details other potential hazards such as intense glider activity, military exercise area, and many others for pilots to exercise caution.
4. Without an approved waiver/authorization, the aircraft must remain within visual line of sight, only fly during the daytime, and under 400 feet above ground level.
5. The drone should always yield right-of-way to a manned aircraft and fly at or below 100 mph.
6. Any aerial operation that results in serious injury, loss of consciousness, or property damage of at least $500 must be reported to FAA within 10 days of the incident.
7. The pilot must not fly over people or moving vehicles without a waiver approved by FAA.

Some of the data collection scenarios require the submission of a waiver outlining the safety protocols and data collection methods followed in the field. These applications will be thoroughly reviewed by the FAA who then provides its decision regarding the waiver. The FAA has been proactive in handling the waivers and introduced low altitude authorization and notification capability to facilitate quick processing of waivers in restricted airspace. In addition, FAA is also introducing the remote identification rule for effective integration of UAVs into the national airspace system. At the end of April 2021, it is expected that part 107 rules will permit routine operations of small unmanned aircraft over moving vehicles, people, or nighttime, without the need for a waiver, by taking an online course. All these new changes are expected to help in conducting infrastructure inspections safely.

Infrastructure Applications of UAVS

Previous research was conducted using these unmanned aerial platforms owing to their ability to carry compact sensors to remote locations with a quick turnaround and safety. Bridge inspection, asset inventories and maintenance monitoring, pre-construction survey, construction monitoring, automated asphalt pavement inspection, traffic monitoring, law enforcement, avalanche monitoring, rail corridor monitoring, and airport monitoring are some of the transportation applications of unmanned aerial platforms (*8, 16–21*). Some of the previous transportation-related research conducted using drones are provided below.

Doherty et al. (*22*) used a vertical takeoff and landing systems mounted with either digital or infrared cameras to collect traffic patterns involving overtaking and U-turns. Shastry and Schowengerdt (*23*) developed a methodology to extract parameters of traffic flow from the aerial data. Washington State DOT explored the capabilities of UAV as an avalanche condition identification tool, especially over the slopes near state highways located on mountainous terrains (*16*). Kaaniche et al. (*24*) collected aerial videos of traffic to obtain various traffic characteristics such as vehicle counts, speed, flow rate, and density. Rathinam et al. (*25*) conducted fixed-wing UAV-based monitoring of linear structures such as roads, pipelines, bridges, and canals. Linear structures were detected by visual recognition techniques controlled by a closed-loop algorithm.

Irizarry et al. (*26*) used a small-scale drone equipped with a video camera that used image capturing as well as real-time videos at a construction site. Braut et al. (*27*) researched using airborne videos for developing origin and destination matrices at complex intersections. Pereira and Pereira (*28*) demonstrated embedded image processing systems for automatic crack recognition

using UAVs. Marinelli et al. (*29*) presented work on identifying the horizontal alignment from the road data images collected from mobile terrestrial and aerial remote sensing platforms. Zeng et al. (*30*) developed a hybrid approach for microscopic models to simulate pedestrian behavior at signalized intersections using aerial video data collected in Beijing, China. Congress et al. (*10*) conducted a comprehensive calibration analysis of the drone and the camera accessories to understand their compatibility to obtain accurate data. Moreu et al. (*18*) demonstrated the use of drones in monitoring railroad bridges and prioritizing maintenance. Puppala et al. (*31*) used UAV platforms to identify the pavement heaving caused due to high sulfate soils and provided 3-dimensional visualization of infrastructure conditions. Congress and Puppala (*19*) used unmanned aerial vehicles for different applications during pavement construction projects. Congress et al. (*32*) identified hazardous obstructions within an intersection using unmanned aerial data analysis. All these studies demonstrate the versatility of UAVs for monitoring transportation infrastructure aspects.

INFRASTRUCTURE MONITORING

In a research study conducted for the Texas DOT, the authors studied UAV-CRP technology to conduct infrastructure health condition monitoring and assessments. A multirotor Hexacopter UAV mounted with a visible camera was utilized in this study. The methodology adopted towards infrastructure monitoring using unmanned aerial platforms is as follows. First, a comprehensive calibration check was conducted on the acquired UAV and various accessories to assess the influence of system compatibility and environmental conditions on the model errors. Imagery data was collected and evaluated for different effects of geo-referencing methods, camera focal length and resolution, flight altitude and overlap, and ambient temperatures prevailing in the field conditions (*10*). This unique calibration analysis ensured the accuracy of the models required for making engineering interpretations and judgments. The authors followed Texas DOT's Flight Operations Manual as a guide for the safe operation of unmanned aerial vehicles on its assets (*33*).

The team comprising of an FAA-certified remote pilot in command and visual observer inspected several infrastructure sites including material stockpiles, pavements, rail corridor, and bridge sites. The collected images were geotagged with the help of high accuracy RTK GNSS data and used in conjunction with GCPs in building the three-dimensional mapping products. The geotagged aerial images were aligned and stitched to process the point cloud generation, mesh and texture rendering, and ortho-rectification. A fully navigable DEM was then generated along with the three-dimensional dense point clouds, mesh, and orthomosaic. Checkpoints were used to evaluate the accuracy of the generated models. The actual checkpoint coordinates were imported to mark the position of each checkpoint on the 3D model depending upon the respective latitude, longitude, and altitude values of each checkpoint. The accuracy of the generated 3D model was inferred from the root mean square error values calculated between latitude, longitude, and altitude values of the original checkpoint coordinates arranged on the model and their respective locations identified manually on the generated 3D model (*8*). The dense point cloud model and orthomosaic of the infrastructure were overlaid together to address different application areas, varying from evaluating infrastructure condition assessments to estimating construction material stockpile volumes. Aerial measurements made on these infrastructure assets were verified by collecting points using traditional data collection methods including mobile RTK

GNSS system and terrestrial LiDAR. Photogrammetry models of pavements and bridges built from the visible images were helpful in identifying and quantifying the distress characteristics in a quick, efficient, and accurate manner. The UAV-CRP studies on stockpile volumetric computations yielded results that agree with ground truth measurements from on-field survey results.

Pavement Monitoring

UAV–CRP based pavement monitoring studies showed that the data could provide pavement distress information including longitudinal and transverse cracks, permanent deformations, and pavement features such as longitudinal and cross-slope characteristics, as well as sight distances at intersections and/or crossings (*32*, *34*). Aerial images of the pavement can be collected in nadir as well as oblique viewpoints, as shown in Figure 1a. The images can be processed to build three-dimensional mapping products to assess the condition of the pavement as shown in Figure 1b. The distress parameters such as area and depth can be observed in Figure 1b. The photogrammetry-based analyses, with the help of additional accessories outlined in the above sections, yielded measurement results that agree with other traditional methods.

Bridge Monitoring

UAV–CRP studies performed on bridge sites used both top and bottom gimbals of the UAV to provide a complete 360° inspection of the bridge. The “substructure elements” and “superstructure elements” of a rail bridge were monitored with the sensor mounted on both gimbals, during separate flights, as shown in Figure 2a. During the inspection, the camera view was relayed continuously to a digital video display unit viewed by the subject matter expert. UAV–CRP results can provide assessments on joint width, approach slab settlements; movements and cracks in abutments, wing walls, bridge foundation conditions, and columns; and under-bridge deck as well as

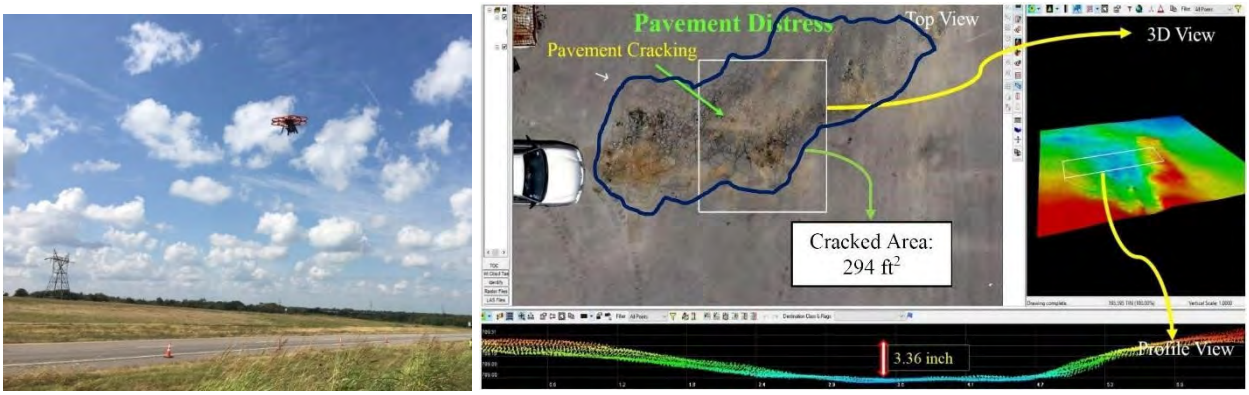

(a) (b)

FIGURE 1 Aerial inspection of roads (*a*) data collection and (*b*) measuring distress from 3D models viewed in multiple views (*34*).

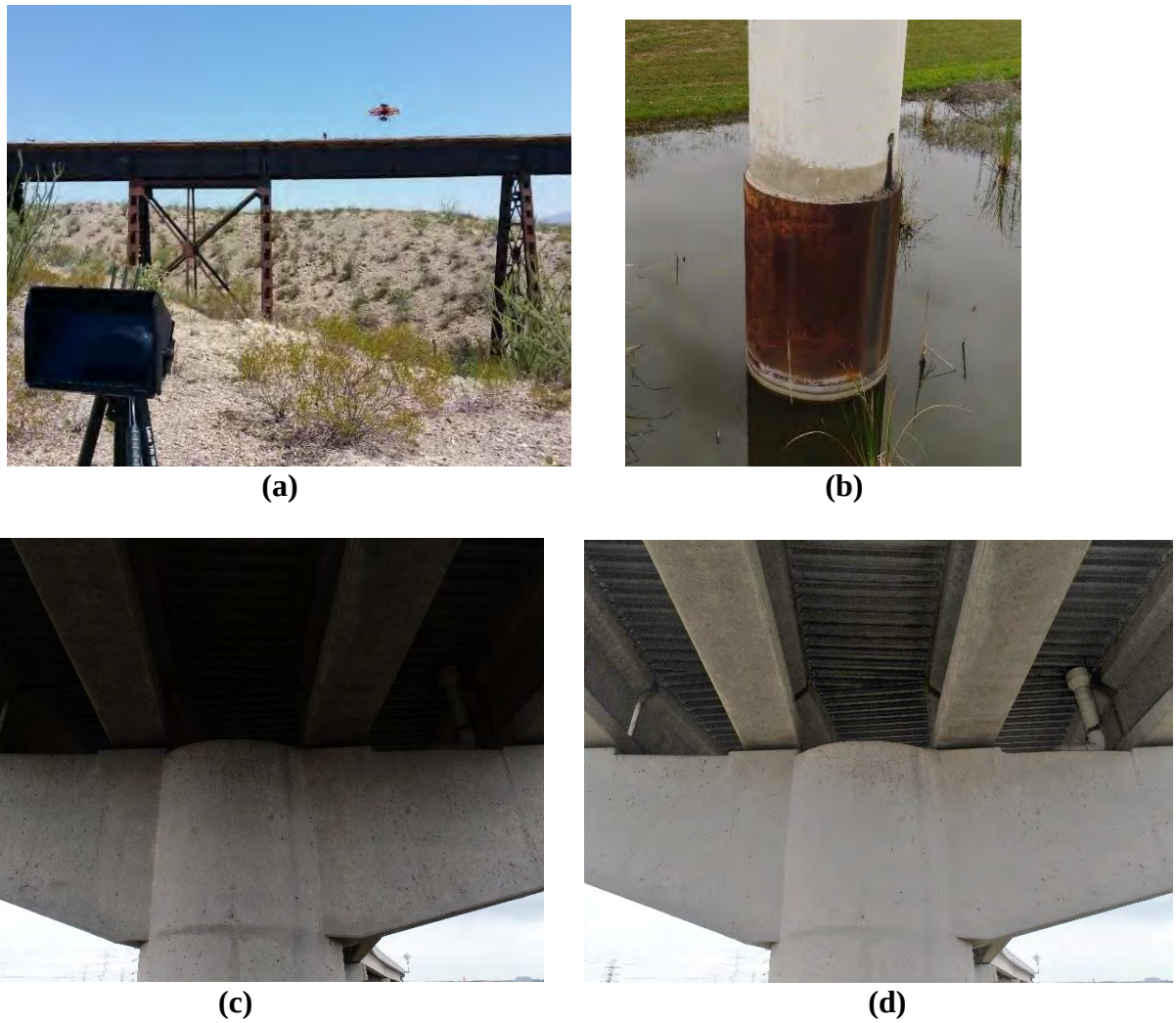

FIGURE 2 Bridge inspection using unmanned aerial platform (*a*) inspection viewed on a display screen; (*b*) accessing hard-to-reach areas; (*c*) original image collected underneath the bridge; and (*d*) processed image with enhanced lighting conditions.

upper deck condition assessments. On another project, aerial images were collected to access hard-to-reach areas shown in Figure 2b and c. These aerial images were used to build the dense point cloud models with location and color information. The bridge elements can be quantitatively assessed since each point had *X*, *Y*, and *Z* locations associated with respective RGB values.

Recorded videos of the bridge provided ample time for the bridge inspector to investigate and find any bridge element condition. Sometimes, the weather conditions may not be favorable for capturing high-quality images. Especially, underneath the bridge, the lighting conditions may not be optimal, as shown in Figure 2c. Collecting images in raw format and enhancing the quality, as shown in Figure 2d, is found to be effective in identifying the condition of the elements underneath the bridge deck. These enhanced images can be used for qualitative analysis. However, it is recommended that the original images be used for conducting quantitative assessments through photogrammetry-based three-dimensional model building techniques. Many other stud-

ies also highlighted and demonstrated the importance of using infrared imagery to quickly identify problematic areas on the bridge including spalling, cracks, rusting, and other defects based on temperature gradient (*17*, *20*, *35*).

All the procedures, analyses, and results indicate that the UAV–CRP technology provides a quick, efficient, and reproducible method of assessing infrastructure health conditions. These novel tools and methodologies will be inexpensive and safer to monitor transportation infrastructure when compared to conventional surveys and management tools.

FUTURISTIC AREAS

The dense point cloud models obtained from UAV data collection can be used for Building Information Modeling and incorporated with virtual reality to create a whole new experience of visualizing the infrastructure asset condition. The navigable 3D models help to provide a virtual real field-like visualization and enhance the experience of the engineers and practitioners. Another area that is being researched is the use of aerial data for the 3D printing of infrastructure assets and structural elements. The 3D printed model gives the engineers and decision-makers a field perspective of the infrastructure asset's condition. In the future, this technology can be further used to print prefabricated structural elements of infrastructure using additive manufacturing in order to replace a distressed element of the infrastructure asset.

AI and ML techniques are being applied to aerial data to automate the processing and analysis of infrastructure data for various distress. The development of algorithms that automatically feed these data into the different infrastructure maintenance database systems will be helpful to perform infrastructure asset management studies. There is a desire to explore the benefits of UAV data collection beyond what is currently allowed by FAA by flying beyond visual line of sight, nighttime flying, and flying over people, as the future readies for preprogramming flight plan and launching UAVs remotely. However, this needs further development and integration with unmanned aerial traffic management. This can support the deployment of drone swarms in assessing infrastructure conditions before and after a disaster in an efficient manner.

ACKNOWLEDGMENTS

The authors would like to thank the Texas DOT for granting the funds for research project 06944. The authors would like to acknowledge Harris County Toll Road Authority for their support. The authors would also like to acknowledge our RT members for their help during data collection. The authors gratefully acknowledge the support and generosity of the National Science Foundation (NSF) Industry-University Cooperative Research Center (I/UCRC) program funded 'Center for Integration of Composites into Infrastructure' site at TAMU (NSF PDs: Dr. Prakash Balan), for its partial support towards this work.

AUTHOR CONTRIBUTION STATEMENT

The authors confirm contribution to this paper as follows: study conception and design: Surya S. C. Congress and Anand J. Puppala; data collection: Surya S. C. Congress and Anand J. Puppala;

analysis and interpretation of results: Surya S. C. Congress and Anand J. Puppala; draft manuscript preparation: Surya S. C. Congress, Anand J. Puppala, Md Ashrafuzzaman Khan and Nripojyoti Biswas. All authors reviewed the results and approved the final version of the manuscript.

REFERENCES

1. ASCE. America's Infrastructure Report Card 2021. https://infrastructurereportcard.org/. Accessed March 7, 2021.
2. Asphalt Institute. *Asphalt Pavement Construction*. http://www.asphaltinstitute.org/engineering/frequently-asked-questions-faqs/asphalt-pavement-construction/. Accessed July 22, 2018.
3. Puppala, A. J., S. S. C. Congress, N. Talluri, and E. Wattanasanthicharoen. Sulfate-Heaving Studies on Chemically Treated Sulfate-Rich Geomaterials. *Journal of Materials in Civil Engineering*, Vol. 31, No. 6, 2019, p. 04019076. https://doi.org/10.1061/(ASCE)MT.1943-5533.0002729.
4. Little, D. N., S. Nair, and B. Herbert. Addressing Sulfate-Induced Heave in Lime Treated Soils. *Journal of Geotechnical and Geoenvironmental Engineering*, Vol. 136, No. 1, 2010, pp. 110–118. https://doi.org/10.1061/(ASCE)GT.1943-5606.0000185.
5. Talluri, N., A. J. Puppala, S. S. C. Congress, and A. Banerjee. Experimental Studies and Modeling of High-Sulfate Soil Stabilization. *Journal of Geotechnical and Geoenvironmental Engineering*, Vol. 146, No. 5, 2020, p. 04020019. https://doi.org/10.1061/(ASCE)GT.1943-5606.0002240.
6. Atkins. *The Use of Unmanned Aerial Systems for Road Infrastructure*. 2018. https://www.piarc.org/en/order-library/29470-en-TheUseofUnmannedAerialSystemsforRoadInfrastructure.htm. Accessed March 8, 2018.
7. Puppala, A. J., S. S. C. Congress, T. V. Bheemasetti, and S. R. Caballero. Visualization of Civil Infrastructure Emphasizing Geomaterial Characterization and Performance. *Journal of Materials in Civil Engineering*, Vol. 30, No. 10, 2018, p. 04018236. https://doi.org/10.1061/(ASCE)MT.1943-5533.0002434.
8. Congress, S. S. C. *Novel Infrastructure Monitoring Using Multifaceted Unmanned Aerial Vehicle Systems–Close Range Photogrammetry (UAV–CRP) Data Analysis*. Doctoral thesis. University of Texas at Arlington, 2018. Available from: https://rc.library.uta.edu/uta-ir/handle/10106/27746
9. Siebert, S., and J. Teizer. Mobile 3D Mapping for Surveying Earthwork Projects Using an Unmanned Aerial Vehicle (UAV) System. *Automation in Construction*, Vol. 41, 2014, pp. 1–14. https://doi.org/10.1016/j.autcon.2014.01.004.
10. Congress, S. S. C., A. J. Puppala, and C. L. Lundberg. Total System Error Analysis of UAV-CRP Technology for Monitoring Transportation Infrastructure Assets. *Engineering Geology*, Vol. 247, 2018, pp. 104–116. https://doi.org/10.1016/j.enggeo.2018.11.002.
11. Puppala, A. J., and S. S. C. Congress. A Holistic Approach for Visualization of Transportation Infrastructure Assets Using UAV-CRP Technology. *Information Technology in Geo-Engineering. ICITG 2019. Springer Series in Geomechanics and Geoengineering* (A. Correia, J. Tinoco, P. Cortez, and L. Lamas, eds.), Springer, Cham, 2020. https://doi.org/10.1007/978-3-030-32029-4_1.
12. Morgenthal, G., and N. Hallermann. Quality Assessment of Unmanned Aerial Vehicle (UAV) Based Visual Inspection of Structures. *Advances in Structural Engineering*, Vol. 17, No. 3, 2014, pp. 289–302. https://doi.org/10.1260/1369-4332.17.3.289.
13. Yao, H., R. Qin, and X. Chen. Unmanned Aerial Vehicle for Remote Sensing Applications—A Review. *Remote Sensing (Basel)*, Vol. 11, No. 12, 2019, p. 1443. https://doi.org/10.3390/rs11121443.
14. Hayat, S., E. Yanmaz, and R. Muzaffar. Survey on Unmanned Aerial Vehicle Networks for Civil Applications: A Communications Viewpoint. *IEEE Communications Surveys and Tutorials*, Vol. 18, No. 4, 2016, pp. 2624–2661. https://doi.org/10.1109/COMST.2016.2560343.
15. FAA. *FAA-G-8082-22 Remote Pilot-Small Unmanned Aircraft Systems Study Guide*. Flight Standards Service, Washington, D.C., 2016. https://www.faa.gov/regulations_policies/handbooks_manuals/aviation/media/remote_pilot_study_guide.pdf

16. McCormack, E. D., and T. Trepanier. *The Use of Small Unmanned Aircraft by the Washington State Department of Transportation*. No. WA-RD 703.1. Washington State Department of Transportation, 2008.
17. Wells, J., B. Lovelace, and C. Engineers. *Unmanned Aircraft System Bridge Inspection Demonstration Project Phase II Final Report.* Minnesota Deptartment of Transportation. 2017.
18. Moreu, F., and M. R. Taha. *Railroad Bridge Inspections for Maintenance and Replacement Prioritization Using Unmanned Aerial Vehicles (UAVs) with Laser Scanning Capabilities*. Rail Safety IDEA Project 32, 2018.
19. Congress, S. S. C., and A. J. Puppala. Novel Methodology of Using Aerial Close Range Photogrammetry Technology for Monitoring the Pavement Construction Projects. *Airfield and Highway Pavements*, 2019, pp. 121–130. https://doi.org/10.1061/9780784482476.014.
20. Brooks, C., R. J. Dobson, D. M. Banach, D. Dean, T. Oommen, R. E. Wolf, T. C. Havens, T. M. Ahlborn, and B. Hart. *Evaluating the Use of Unmanned Aerial Vehicles for Transportation Purposes.* Report No. RC-1616. Michigan Department of Transportation, 2015.
21. Duque, L., J. Seo, and J. Wacker. Synthesis of Unmanned Aerial Vehicle Applications for Infrastructures. *Journal of Performance of Constructed Facilities*, Vol. 32, No. 4, 2018, p. 04018046. https://doi.org/10.1061/(ASCE)CF.1943-5509.0001185.
22. Doherty, P., G. Granlund, K. Kuchcinski, E. Sandwall, K. Nordberg, and E. Skarman. The WITAS Unmanned Aerial Vehicle Project. *Proceedings of the 14th European Conference on Artificial Intelligence*, 2000, pp. 747–755. https://doi.org/10.1.1.224.4052..
23. Shastry, A., and R. Schowengerdt. Airborne Video Registration and Traffic-Flow Parameter Estimation. *IEEE Transactions on Intelligent Transportation Systems*, Vol. 6, No. 4, 2005, pp. 391–405. https://doi.org/10.1109/TITS.2005.858621.
24. Kaaniche, K., B. Champion, C. Pégard, and P. Vasseur. A Vision Algorithm for Dynamic Detection of Moving Vehicles with a UAV. *Proceedings of the 2005 IEEE International Conference on Robotics and Automation*, Barcelona, Spain, 2005, pp. 1878–1883. https://doi.org/10.1109/ROBOT.2005.1570387..
25. Rathinam, S., Z. W. Kim, and R. Sengupta. Vision-Based Monitoring of Locally Linear Structures Using an Unmanned Aerial Vehicle. *Journal of Infrastructure Systems*, Vol. 14, No. 1, 2008, pp. 52–63. https://doi.org/10.1061/(ASCE)1076-0342(2008)14:1(52).
26. Irizarry, J., M. Gheisari, and B. N. Walker. Usability Assessment of Drone Technology as Safety Inspection Tools. *Journal of Information Technology in Construction*, Vol. 17, No. 12, 2012, pp. 194–212.
27. Braut, V., M. Čuljak, V. Vukotić, S. Šegvić, M. Ševrović, and H. Gold. Estimating OD Matrices at Intersections in Airborne Video-a Pilot Study. *Proceedings of the 35th International Convention MIPRO*, Opatija, Croatia, 2012, pp. 977–982.
28. Pereira, F. C., and C. E. Pereira. Embedded Image Processing Systems for Automatic Recognition of Cracks Using UAVs. *IFAC-PapersOnLine*, Vol. 48, No. 10, 2015, pp. 16–21. https://doi.org/10.1016/j.ifacol.2015.08.101.
29. Marinelli, G., M. Bassani, M. Piras, and A. M. Lingua. Mobile Mapping Systems and Spatial Data Collection Strategies Assessment in the Identification of Horizontal Alignment of Highways. *Transportation Research Part C, Emerging Technologies*, Vol. 79, 2017, pp. 257–273. https://doi.org/10.1016/j.trc.2017.03.020.
30. Zeng, W., P. Chen, G. Yu, and Y. Wang. Specification and Calibration of a Microscopic Model for Pedestrian Dynamic Simulation at Signalized Intersections: A Hybrid Approach. *Transportation Research Part C, Emerging Technologies*, Vol. 80, 2017, pp. 37–70. https://doi.org/10.1016/j.trc.2017.04.009.
31. Puppala, A. J., N. Talluri, S. S. C. Congress, and A. Gaily. Ettringite Induced Heaving in Stabilized High Sulfate Soils. *Innovative Infrastructure Solutions*, Vol. 3, No. 1, 2018, p. 72. https://doi.org/10.1007/s41062-018-0179-7.
32. Congress, S. S. C., A. J. Puppala, A. Banerjee, and U. D. Patil. Identifying Hazardous Obstructions Within an Intersection Using Unmanned Aerial Data Analysis. *International Journal of Transportation Science and Technology*, 2021. https://doi.org/10.1016/j.ijtst.2020.05.004.

33. Texas Department of Transportation. *Unmanned Aircraft System (UAS) Flight Operations and User's Manual TxDOT Flight Services* (0-6944 Operations Manual). Texas Department of Transportation, Austin, 2018. https://web.archive.org/web/20180920160854/ftp.dot.state.tx.us/pub/txdot-info/avn/uas/user-manual.pdf
34. Congress, S. S. C., and A. J. Puppala. Evaluation of UAV–CRP Data for Monitoring Transportation Infrastructure Constructed over Expansive Soils. *Indian Geotechnical Journal*, 2020, pp. 1–13. https://doi.org/10.1007/s40098-019-00384-4.
35. Azari, H., D. O'Shea, and D. Constable. Reaching New Heights. *Public Roads*, Vol. 83, No. 4, 2020.

The National Academies of
SCIENCES • ENGINEERING • MEDICINE

The **National Academy of Sciences** was established in 1863 by an Act of Congress, signed by President Lincoln, as a private, non-governmental institution to advise the nation on issues related to science and technology. Members are elected by their peers for outstanding contributions to research. Dr. Marcia McNutt is president.

The **National Academy of Engineering** was established in 1964 under the charter of the National Academy of Sciences to bring the practices of engineering to advising the nation. Members are elected by their peers for extraordinary contributions to engineering. Dr. John L. Anderson is president.

The **National Academy of Medicine** (formerly the Institute of Medicine) was established in 1970 under the charter of the National Academy of Sciences to advise the nation on medical and health issues. Members are elected by their peers for distinguished contributions to medicine and health. Dr. Victor J. Dzau is president.

The three Academies work together as the **National Academies of Sciences, Engineering, and Medicine** to provide independent, objective analysis and advice to the nation and conduct other activities to solve complex problems and inform public policy decisions. The National Academies also encourage education and research, recognize outstanding contributions to knowledge, and increase public understanding in matters of science, engineering, and medicine.

Learn more about the National Academies of Sciences, Engineering, and Medicine at **www.nationalacademies.org**.

The **Transportation Research Board** is one of seven major programs of the National Academies of Sciences, Engineering, and Medicine. The mission of the Transportation Research Board is to provide leadership in transportation improvements and innovation through trusted, timely, impartial, and evidence-based information exchange, research, and advice regarding all modes of transportation. The Board's varied activities annually engage about 8,000 engineers, scientists, and other transportation researchers and practitioners from the public and private sectors and academia, all of whom contribute their expertise in the public interest. The program is supported by state transportation departments, federal agencies including the component administrations of the U.S. Department of Transportation, and other organizations and individuals interested in the development of transportation.

Learn more about the Transportation Research Board at **www.TRB.org**.

TRB

TRANSPORTATION RESEARCH BOARD
500 Fifth Street, NW
Washington, DC 20001

The National Academies of
SCIENCES • ENGINEERING • MEDICINE

The nation turns to the National Academies of Sciences, Engineering, and Medicine for independent, objective advice on issues that affect people's lives worldwide.

www.national-academies.org